REMARKS

Claims 69-73, 102, 106, 108-110 and 112-122 are pending in this application.

Applicants have amended claims 69 and 112 to delete the recitation of "BMP-4."

None of the amendments constitutes new matter.

THE REJECTIONS

35 U.S.C. § 102(b): Claims 69, 71, 106-112, 114 and 115

The Examiner has maintained the rejection of claims 69, 71, 106-108, 112, 114 and 115 under 35 U.S.C. § 102(b) as being anticipated by U.S. Patent 5,166,058 ("Wang"). The Examiner states that Wang intends the designation "BMP-2" to encompass both BMP-2A and BMP-2B and further, that BMP-2s may be combined with IGF-I. The Examiner contends that the designation BMP-2B is an alternative designation for BMP-4.

Applicants have amended claim 69 and 112 (and therefore, claims dependent therefrom) to cancel the recitation

of BMP-4. Accordingly, applicants request that the Examiner withdraw the novelty rejection.

35 U.S.C. § 103(a)

Claims 69 and 102: Wang in view of Kuberasampath I

The Examiner has maintained the rejection of claims 69 and 102 under 35 U.S.C. § 103(a) as being obvious over Wang in view of WO 91/18558 ("Kuberasampath I"). The Examiner asserts that the only disclosure of a heparin carrier in the present application is in the context of Kuberasampath I, which is the reference cited in the present rejection, and that heparin can be crosslinked to the collagen. The Examiner therefore concludes that the heparin carrier in the claimed method and the heparin carrier disclosed by Kuberasampath I are the same. The Examiner contends that Wang teaches BMP-2s, such as BMP-2A and BMP-2B may be combined with IGF-I and that BMP-2B is an alternative designation for BMP-4.

First, as described above, applicants have amended claim 69 (and therefore, claim 102) to cancel the recitation of BMP-4. Second, applicants have unexpectedly demonstrated that

IGF-I, hydrocortisone, insulin and PTH synergistically stimulate morphogenic proteins to induce tissue formation.

Wang discloses the use of BMP-2 and the growth factor IGF-I for treating bone, cartilage and periodontal diseases. Wang does not disclose that IGF-I synergizes BMP-2 and BMP-4. It only discloses that BMP-2 and BMP-4 "may act...perhaps synergistically with other related proteins and growth factors." The skilled worker would not have a reasonable expectation that any and all growth factors, more specifically IGF-I would act synergistically with BMP-2 and BMP-4. Wang does not disclose which of the numerous related proteins and growth factors would act synergistically. Therefore, the disclosure in Wang amounts to no more than an "obvious to try" rationale. It is well established that "obvious to try" is not the standard.

Kuberasampath I discloses a collagen-glycosaminoglycan porous matrix, wherein the glycosaminoglycan may be heparin. As described above, applicants have demonstrated that certain morphogenic protein stimulatory factors (IGF-I, hydrocortisone, insulin and PTH) act synergistically with BMPs to induce tissue formation. Nothing in the combination of Wang and Kuberasampath

I teaches or suggests the invention recited in the claims of the instant application.

Accordingly, applicant requests that the Examiner withdraw this obviousness rejection.

Claims 69 and 116: Wang

The Examiner has maintained his rejection of claims 69 and 116 under 35 U.S.C. § 103(a) as being obvious over Wang. The Examiner states that Wang teaches that the designation "BMP-2" is intended to encompass both BMP-2A and BMP-2B and that BMP-2s may be combined with IGF-I. The Examiner further states that BMP-2B is an alternative designation for BMP-4.

As discussed above, applicants have amended claim 69 (and therefore, claim 116) to cancel the recitation of BMP-4. Applicants have demonstrated that IGF-I, hydrocortisone, insulin and PTH surprisingly synergistically stimulate morphogenic proteins to induce tissue formation.

Wang only discloses that BMP-2 may act in concert or perhaps synergistically with other related proteins and growth factors. Wang does not teach or suggest that teaches or suggests

that IGF-I synergizes the tissue inductive ability of any of BMP-5, BMP-6, BMP-7 (OP-1), BMP-8, BMP-9, BMP-10, BMP-11, BMP-12, BMP-13, Dpp, Vg-1, COP-5 and COP-7, as claimed in the instant application. Furthermore, nothing in Wang teaches or suggests that hydrocortisone, insulin or parathyroid hormone can synergize the tissue inductive ability of the claimed morphogenic proteins. Accordingly, applicants request that the Examiner withdraw this obviousness rejection.

Claims 69, 113 and 117: Wang in view of the Kuberasampath II and Reddi

The Examiner has maintained the rejection of claims 69, 113 and 117 under 35 U.S.C. § 103(a) as being obvious over Wang in view of U.S. Patent 5,674,844 ("Kuberasampath II") and Reddi, A. H. et al., "Bone induction by osteogenin and bone morphogenic proteins", Biomaterials, 11: pp. 33-34 (1990) ("Reddi"). The Examiner states that Wang intends the designation of "BMP-2" to encompass both BMP-2A and BMP-2B, which may be combined with IGF-I, and further, that BMP-2B is an alternative designation for BMP-4. The Examiner states there would be reasonable expectation that the combination of OP-1 and IGF-I is synergistic given that

BMP-2 may act in concert with or perhaps synergistically with a growth factor such as IGF-I, and given that the initiation of bone formation by BMPs is promoted by IGF-I, which may have a beneficial effect on bone remodeling. The Examiner also contends that the present specification only shows the induction of alkaline phosphatase ("A.P.") activity and that AP is not the sole determinant of bone induction *in vivo* and that although all combinations of BMPs and growth factors may not synergistically enhance A.P. activity, the claims are not limited to the synergistic enhancement of A.P. activity.

As stated by the Examiner, Wang discloses that BMP-2 and BMP-4 may be used with IGF-I. Wang does not disclose that IGF-I synergizes BMP-2 or BMP-4. Wang merely discloses that growth factors "may act ... perhaps synergistically" with BMP-2 and BMP-4. As discussed above, applicants have amended the claims to delete the recitation of "BMP-4".

Kuberasampath II discloses that BMPs may be administered with cofactors known to have a beneficial effect on bone modeling, such as PTH, vitamin D3, prostaglandins, dexamethasone, IGF-I and IGF-II. Like Wang, Kuberasampath II

does not teach or suggest that the cofactors and BMP act synergistically to induce tissue formation.

Similarly, Reddi discloses that the initiation of bone induction by BMPs may be promoted by PDGF, TGF-β, IGF-I, IGF-II and FGF. Reddi does not teach or disclose that BMPs and IGF-I synergistically induce tissue formation. Nothing in Wang in combination with Kuberasampath II and Reddi would provide the skilled worker in the art with a reasonable expectation that IGF-I, hydrocortisone, insulin and parathyroid hormone would synergistically stimulate the ability of a morphogenic protein selected from the group consisting of BMP-5, BMP-6, BMP-7 (OP-1), BMP-8, BMP-9, BMP-10, BMP-11, BMP-12, BMP-13, Dpp, Vg-1, COP-5 and COP-7, to induce tissue formation as recited in the amended claims of the instant application. Accordingly, applicant requests that the Examiner withdraw this rejection.

35 U.S.C. § 112, first paragraph

Claims 69, 71, 102, 106, 108-110, 112-117

The Examiner has maintained the rejection of claims 69, 71, 102, 106, 108-110 and 112-117 under 35 U.S.C. § 112, first

paragraph for lack of enablement. The Examiner contends that although the results with various animal models of bone induction may be reasonably predictive of bone induction in vivo, the present specification only demonstrates an enhancement of AP activity *in vitro* and that the use of *in vitro* assay systems are not predictive of bone formation *in vivo*. The Examiner states in vitro assay of AP activity is not predictive of synergistic enhancement of bone formation in vivo based on the present application's disclosure that TGF-β is not an MPSF in combination with OP-1 in the AP activity assay in FRC cells in vitro which contrasts with Ogawa's teaching that TGF-β and BMP synergize in promoting formation of endochondral bone *in vivo*. The Examiner relies on the *in vitro* and *in vivo* results of TGF-β to conclude that the use of *in vitro* assay systems have proven not to be predictive of bone formation *in vivo*. Applicants traverse.

Applicants respectfully submit that contrary to the Examiner's contention, AP activity does correlate with the induction of bone *in vivo*. This is evidenced by the *in vivo* and *in vitro* results of the various BMP's recited in the amended claims. For example, Ebisawa et al., "Characterization of bone

morphogenetic protein-6 signaling pathways in osteoblast differentiation", J Cell Sci, 112: pp. 3519-3527 (1999) ("Ebisawa"), submitted herewith as Exhibit A, discloses that BMP-6 strongly induces AP activity in cells of the osteoblast lineage (see, e.g., Abstract on page 3519; Figure 1 on page 3521). Similarly, Gruber et al., "Porcine sinus mucosa holds cells that respond to bone morphogenetic protein (BMP)-6 and BMP-7 with increased osteogenic differentiation in vitro", Clin Oral Implants Res, 15: pp. 575-580 (2004) ("Gruber"), submitted herewith as Exhibit B, discloses that BMP-6 increases AP activity in mucosa-derived cells (see, e.g., Figure 4). The *in vitro* AP activity observed for BMP-6 is predictive of its ability to induce bone formation *in vivo* as confirmed by Gitelman et al., "Recombinant Vgr-1/BMP-6-expressing tumors induce fibrosis and endochondral bone formation in vivo", J Cell Biol, 126: 1595-1609 (1994) ("Gitelman"), submitted herewith as Exhibit C, which discloses that introduction of BMP-6-expressing CHO cells directly into the subcutaneously tissue of athymic nude mice resulted in the surrounding host mesenchymal cells developing along the endochondral bone pathway (see, e.g., Abstract at page

1595; Figure 6 at page 1603; Figure 8 at page 1605; Figure 9 at page 1606).

This correlation between the AP activity and the ability to induce bone formation *in vivo* is also observed for other morphogenic proteins, including but not limited to: OP-1, BMP-9, BMP-12, and BMP-13. For example, Yeh et al., "Osteogenic protein-1 (OP-1, BMP-7) induces osteoblastic cell differentiation of the pluripotent mesenchymal cell line C2C12", J Cell Biochem, 87: pp. 292-304 (2002) ("Yeh"), submitted herewith as Exhibit D, demonstrates that total AP activity was stimulated in C2C12 cell cultures when grown in the presence of OP-1 (see, e.g., Figure 2 at page 297). Similarly, OP-1 was able to stimulate AP activity in the rat osteosarcoma cell line, ROS 17/2.8, and was also able to induce new bone formation at bone defect sites in baboons (see, e.g., Figure 3 at page 1801; page 1803 at column 2; Figure 8 on page 1806), as demonstrated by Ripamonti et al., "Long-term evaluation of bone formation by osteogenic protein 1 in the baboon and relative efficacy of bone-derived bone morphogenic proteins delivered by irradiated xenogeneic collagenous matrices", J Bone Miner Res, 15: pp. 1798-1809 (2000) ("Ripamonti") (submitted herewith as Exhibit E).

Cheng et al., "Osteogenic activity of the fourteen types of human bone morphogenic proteins (BMPs)", J Bone Joint Surg Am, 85-A: pp. 1544-1552 (2003) ("Cheng"), submitted herewith as Exhibit F, demonstrates that the ability of BMP-9 to induce AP activity (see, e.g., Figure 1 at page 1546; Table 1 at page 1548) is correlative with it's ability to induce bone formation *in vivo*, as demonstrated by Kang et al., "Characterization of the distinct orthotopic bone-forming activity of 14 BMPs using recombinant adenovirus-mediated gene delivery", Gene Ther, 11: pp. 1312-1320 (2004) ("Kang"), submitted herewith as Exhibit G (see, e.g., page 1315, column 2 to page 1316, column 1).

BMP-12 also displayed both AP activity and the ability to induce bone formation *in vivo*. Furuya et al., "Effects of GDF7/BMP12 on proliferation and alkaline phosphatase expression in rat osteoblastic osteosarcoma ROS 17/2.8 cells", J Cell Biochem, 72: pp. 177-180 (1999) ("Furuya"), submitted herewith as Exhibit H, illustrates that BMP-12 enhanced AP activity in ROS 17/2.8 cells (see, e.g., Figure 3 at page 179; page 179, column 2), while Wikesjo et al., "Periodontal repair in dogs: effect of recombinant human bone morphogenetic protein-12 (rhBMP-12) on regeneration of alveolar bone and periodontal attachment", J Clin

Periodontol, 31: pp. 662-670 (1992) ("Wikesjo"), submitted herewith as Exhibit I, illustrates the ability of BMP-12 implants to induce bone regeneration in dogs with alveolar bone defects (see, e.g., Figure 2 at page 666).

Finally, Erlacher et al., "Cartilage-derived morphogenetic proteins and osteogenic protein-1 differentially regulate osteogenesis", J Bone Miner Res, 13: pp. 383-392 (1998) ("Erlacher"), submitted herewith as Exhibit J, describes the AP-inducing activity of BMP-13/CDMP-2 on the osteoblastic cell line, MC3T3-EI, and the rat osteoprogenitor-like cell line, ROB-C26 (see, e.g., Figure 5 at page 387) as well as the ability of BMP-13/CDMP-2 to induce bone formation in an *in vivo* subcutaneous implantation assay (see, e.g., Figure 2 at page 385).

In view of applicants' above remarks, the Examiner's contention that AP activity is not correlative of *in vivo* bone activity is clearly unsubstantiated. Applicants have provided the Examiner with ample support that the AP activity of many of the recited morphogenic proteins is correlated with *in vivo* bone inductive activity.

Finally, the Examiner's reliance on the teachings of Ogawa is misplaced. First, the present application discloses that IGF-I, hydrocortisone, insulin and parathyroid hormone would synergistically stimulate the ability of a morphogenic protein selected from the group consisting of BMP-5, BMP-6, BMP-7 (OP-1), BMP-8, BMP-9, BMP-10, BMP-11, BMP-12, BMP-13, Dpp, Vg-1, COP-5 and COP-7, as recited in the amended claims. As recited, TGF-β is not one of the specified MPSFs in the claims. Second, contrary to Ogawa's teaching that TGF-β may synergize with BMP to induce bone formation *in vivo*, applicants have discovered that TGF-β does not induce bone formation *in vivo*, as suggested by the absence of AP activity *in vitro*. This may be attributed to the use of different signaling mechanisms between TGF-β and BMPs. As described by Miyazono et al., "Divergence and convergence of TGF-β/BMP signaling," J. Cell. Physiol., 187: pp. 265-276 (2001) ("Miyazono"), submitted herewith as Exhibit K, the TGF-β superfamily ligands, which include TGF-β and BMPs, bind to type II and type I serine/threonine kinase receptors and transduce signals via Smad proteins. Smad proteins can be classified into three groups, i.e., receptor-regulated Smads (R-Smads), common-

mediator Smads (Co-Smads) and inhibitory Smads (I-Smads). There are two subclasses of R-Smads, i.e., those activated by activin and TGF-β signaling pathways (AR-Smads), and those activated by bone morphogenetic protein (BMP) pathways (BR-Smads). TGF-β and BMPs utilize divergent signaling pathways to exhibit a wide variety of biological activities and can elicit diverse effects on target cells. Thus, the ability of TGF-β to induce bone formation does not necessarily correlate with the ability of BMPs to induce the same activity.

Applicants respectfully submit that the present application provides sufficient enablement for one skilled in the art to make and use the invention without undue experimentation. Accordingly, applicants request that the Examiner withdraw the rejection.

Obviousness-Type Double Patenting

Claims 69, 71, 102, 106, 108-110, 112-117

The Examiner has maintained the rejection of claims 69, 71, 102, 106, 108-110, 112-117 under the judicially created doctrine of obviousness-type double patenting as being

unpatentable over claims 1-15 of United States patent 6,048,964 and claim 30 of United States patent 5,948,428.

Applicants acknowledge with appreciation the Examiner's acknowledgement that applicants are ready to submit a terminal disclaimer in compliance with 37 C.F.R. § 1.321(c) when the present claims are found allowable.

CONCLUSION

In view of the above, applicants respectfully request consideration and early allowance of the pending claims in this application.

Respectfully submitted,

James F. Haley, Jr. (Reg. No. 27,794)
Karen Mangasarian (Reg. No. 43,772)
Attorneys for Applicants
Connie Wong (Limited Recognition)
Agent for Applicants
c/o FISH & NEAVE LLP
1251 Avenue of the Americas
New York, New York 10020
Tel.: (212) 596-9000

Exhibit A

Journal of Cell Science

VOLUME 112 (20) OCTOBER 1999

biology

Contents

Volume 112 (20) October 1999

iv **In this issue**

Sticky wicket

3413 **Mentoring - a security blanket or a cover up?** Caveman

Commentary

3415 **Syndecan-4 and integrins: combinatorial signaling in cell adhesion.** Couchman, J. R. and Woods, A.

3421 **Control of morphology, cytoskeleton and migration by syndecan-4.** Longley, R. L., Woods, A., Fleetwood, A., Cowling, G. J., Gallagher, J. T. and Couchman, J. R.

3433 **Syndecan-4 core protein is sufficient for the assembly of focal adhesions and actin stress fibers.** Echtermeyer, F., Baciu, P. C., Saoncella, S., Ge, Y. and Goetinck, P. F.

3443 **A dynamic connection between centromeres and ND10 proteins.** Everett, R. D., Earnshaw, W. C., Pluta, A. F., Sternsdorf, T., Ainsztein, A. M., Carmena, M., Ruchaud, S., Hsu, W.-L. and Orr, A.

3455 **Distribution of thimet oligopeptidase (E.C. 3.4.24.15) in human and rat testes.** Pineau, C., McCool, S., Glucksman, M. J., Jégou, B. and Pierotti, A. R.

3463 **Dynamics of the nuclear lamina as monitored by GFP-tagged A-type lamins.** Broers, J. L. V., Machiels, B. M., van Eys, G. J. J. M., Kuijpers, H. J. H., Manders, E. M. M., van Driel, R. and Ramaekers, F. C. S.

3477 **Studies on the inhibition of endosome fusion by GTPγS-bound ARF.** Jones, A. T., Spiro, D. J., Kirchhausen, T., Melançon, P. and Wessling-Resnick, M.

3487 **Interaction of the universal mRNA-binding protein, p50, with actin: a possible link between mRNA and microfilaments.** Ruzanov, P. V., Evdokimova, V. M., Korneeva, N. L., Hershey, J. W. B. and Ovchinnikov, L. P.

3497 **Overexpression of protein kinase C-α in the epidermis of transgenic mice results in striking alterations in phorbol ester-induced inflammation and COX-2, MIP-2 and TNF-α expression but not tumor promotion.** Wang, H. Q. and Smart, R. C.

3507 **Overexpression of normal and mutant Arp1α (centractin) differentially affects microtubule organization during mitosis and interphase.** Clark, I. B. and Meyer, D. I.

3519 **Characterization of bone morphogenetic protein-6 signaling pathways in osteoblast differentiation.** Ebisawa, T., Tada, K., Kitajima, I., Tojo, K., Sampath, T. K., Kawabata, M., Miyazono, K. and Imamura, T.

3529 **Evidence for the presence of an NF-κB signal transduction system in *Dictyostelium discoideum*.** Traincard, F., Ponte, E., Pun, J., Coukell, B. and Veron, M.

3537 **A fraction of mouse sperm chromatin is organized in nucleosomal hypersensitive domains enriched in retroposon DNA.** Pittoggi, C., Renzi, L., Zaccagnini, G., Cimini, D., Degrassi, F., Giordano, R., Magnano, A. R., Lorenzini, R., Lavia, P. and Spadafora, C.

3549 **Fibrillin assembly: dimer formation mediated by amino-terminal sequences.** Ashworth, J. L., Kelly, V., Wilson, R., Shuttleworth, C. A. and Kielty, C. M.

3559 **VAMP (synaptobrevin) is present in the plasma membrane of nerve terminals.** Taubenblatt, P., Dedieu, J. C., Gulik-Krzywicki, T. and Morel, N.

3569 ***Schizosaccharomyces pombe* protein kinase C homologues, pck1p and pck2p, are targets of rho1p and rho2p and differentially regulate cell integrity.** Arellano, M., Valdivieso, M. H., Calonge, T. M., Coll, P. M., Duran, A. and Perez, P.

3579 **High affinity Rab3 binding is dispensable for Rabphilin-dependent potentiation of stimulated secretion.** Joberty, G., Stabila, P. F., Coppola, T., Macara, I. G. and Regazzi, R.

The Company of Biologists Limited, Bidder Building, 140 Cowley Road, Cambridge CB4 0DL, UK
ISSN: 0021-9533

Journal of Cell Science 112, 3519-3527 (1999)
Printed in Great Britain © The Company of Biologists Limited 1999
JCS0682

Characterization of bone morphogenetic protein-6 signaling pathways in osteoblast differentiation

Takanori Ebisawa[1,2], Keiichiro Tada[1], Isao Kitajima[3], Katsuyoshi Tojo[2], T. Kuber Sampath[4], Masahiro Kawabata[1], Kohei Miyazono[1,*] and Takeshi Imamura[1]

[1]Department of Biochemistry, The Cancer Institute of JFCR, and Research for the Future Program, Japan Society for the Promotion of Science, 1-37-1 Kami-ikebukuro, Toshima-ku, Tokyo 170-8455, Japan [2]Department of Internal Medicine (II), Jikei University School of Medicine, 3-25-8 Nishishinbashi, Minato-ku, Tokyo 105-8461, Japan
[3]Department of Laboratory Medicine, Faculty of Medicine, Kagoshima University, 8-35-1 Sakuragaoka, Kagoshima 890-8520, Japan, and [4]Creative BioMolecules, Inc., 45 South Street, Hopkinton, MA 01748, USA
*Author for correspondence (e-mail: miyazono-ind@umin.ac.jp)

Accepted 21 July; published on WWW 30 September 1999

SUMMARY

Bone morphogenetic protein (BMP)-6 is a member of the transforming growth factor (TGF)-β superfamily, and is most similar to BMP-5, osteogenic protein (OP)-1/BMP-7, and OP-2/BMP-8. In the present study, we characterized the endogenous BMP-6 signaling pathway during osteoblast differentiation. BMP-6 strongly induced alkaline phosphatase (ALP) activity in cells of osteoblast lineage, including C2C12 cells, MC3T3-E1 cells, and ROB-C26 cells. The profile of binding of BMP-6 to type I and type II receptors was similar to that of OP-1/BMP-7 in C2C12 cells and MC3T3-E1 cells; BMP-6 strongly bound to activin receptor-like kinase (ALK)-2 (also termed ActR-I), together with type II receptors, i.e. BMP type II receptor (BMPR-II) and activin type II receptor (ActR-II). In addition, BMP-6 weakly bound to BMPR-IA (ALK-3), to which BMP-2 also bound. In contrast, binding of BMP-6 to BMPR-IB (ALK-6), and less efficiently to ALK-2 and BMPR-IA, together with BMPR-II was detected in ROB-C26 cells. Intracellular signalling was further studied using C2C12 and MC3T3-E1 cells. Among the receptor-regulated Smads activated by BMP receptors, BMP-6 strongly induced phosphorylation and nuclear accumulation of Smad5, and less efficiently those of Smad1. However, Smad8 was constitutively phosphorylated, and no further phosphorylation or nuclear accumulation of Smad8 by BMP-6 was observed. These findings indicate that in the process of differentiation to osteoblasts, BMP-6 binds to ALK-2 as well as other type I receptors, and transduces signals mainly through Smad5 and possibly through Smad1.

Key words: BMP-6, Osteoblast differentiation, Serine/threonine kinase receptor, Smad

INTRODUCTION

Members of the transforming growth factor-β (TGF-β) superfamily are structurally related proteins which include TGF-βs, activins, and bone morphogenetic proteins (BMPs) (Kawabata et al., 1998a). BMPs were originally identified as proteins in bone that induce ectopic bone and cartilage formation in vivo, but are now known as multifunctional regulators of cell growth, differentiation, and apoptosis, and to play important roles during development (Reddi, 1994; Hogan, 1996). More than a dozen proteins belong to the BMP family, which can be divided into several subgroups based on their structural similarities. *Drosophila decapentaplegic* gene product (DPP), BMP-2, and BMP-4 form one subgroup, *Drosophila* 60A, BMP-5, BMP-6/Vgr-1, osteogenic protein (OP)-1/BMP-7, and OP-2/BMP-8 form another subgroup, and growth/differentiation factor (GDF)-5, -6, and -7 yet another. In vitro studies have revealed that BMPs have various biological effects on different cell types, e.g. stimulation of proteoglycan synthesis in chondroblasts, synthesis of collagen and alkaline phosphatase during chondrogenic and osteogenic differentiation, and induction of differentiation in neural cells (Katagiri et al., 1994; Shukunami et al., 1996; Paralkar et al., 1992).

BMP-6 was originally isolated from a murine embryonic cDNA library and was named Vgr-1, based on its homology to *Xenopus* Vg-1 (Lyons et al., 1989). The human and bovine homologues of Vgr-1 were subsequently isolated from bone and named BMP-6 (Celeste et al., 1990). Expression of the BMP-6 mRNA in mammals was demonstrated in various cell types of the nervous system, growth plate chondrocytes, and epidermis (Lyons et al., 1989; Jones et al., 1991). BMP-6 protein is predominantly expressed in mature chondrocytes during endochondral ossification (Gitelman et al., 1994). BMP-6 stimulates expression of chondrogenic and osteogenic phenotypes in vitro (Gitelman et al., 1995; Yamaguchi et al., 1996), and induces cartilage and bone formation in vivo

(Gitelman et al., 1994). These findings suggest that BMP-6 plays a pivotal role in endochondral bone formation.

BMPs transduce their effects through binding to two different types of serine/threonine kinase receptors, like other members of the TGF-β superfamily. Both type I receptors and type II receptors are required for signaling. In contrast to the TGF-β and activin receptors, BMP type I and type II receptors bind ligands independently, but binding affinity is up-regulated in the presence of both receptor types (Rosenzweig et al., 1995; Liu et al., 1995; Nohno et al., 1995). Three type I receptors have been shown to bind BMPs, i.e. activin receptor-like kinase (ALK)-2 (also termed ActR-I), BMP type IA receptor (BMPR)-IA (also termed ALK-3), and BMPR-IB (also termed ALK-6) (ten Dijke et al., 1994b; Koening et al., 1994; Macías-Silva et al., 1998), and three type II receptors have been identified, i.e. activin type II receptor (ActR)-II, ActR-IIB, and BMPR-II (Yamashita et al., 1995; Rosenzweig et al., 1995; Liu et al., 1995; Nohno et al., 1995). BMPR-IA and BMPR-IB were reported to bind BMP-2/4 and transduce certain BMP signals. ALK-2 was initially identified as an activin type I receptor because of its ability to bind activin in concert with ActR-II or ActR-IIB. However, recent studies demonstrated that ALK-2 activates Smad1-dependent pathways and mediates OP-1/BMP-7 signaling (ten Dijke et al., 1994b; Macías-Silva et al., 1998).

Intracellular signals of members of the TGF-β superfamily are transduced by Smad proteins (Heldin et al., 1997; Attisano and Wrana, 1998; Derynck et al., 1998; Massagué, 1998). Eight different Smad proteins have been identified in mammals, and are classified into three subgroups, i.e. receptor-regulated Smads (R-Smads), common-partner Smads (Co-Smads), and inhibitory Smads. R-Smads transiently and directly interact with activated type I receptors, and become phosphorylated at SSXS motifs at their C-termini. R-Smads then form heteromeric complexes with Co-Smad, Smad4, and translocate into the nucleus where they activate transcription of various target genes. Smad2 and Smad3 act in the TGF-β/activin pathway, and Smad1, Smad5, and presumably Smad8 are thought to act as specific R-Smads for BMPs. Among specific R-Smads for BMPs, Smad1 and Smad5 have been well-characterized and implicated in BMP-2 and BMP-4 signaling in mammals (Hoodless et al., 1996; Yamamoto et al., 1997; Nishimura et al., 1998) and in *Xenopus* (Graff et al., 1996; Thomsen, 1996; Suzuki et al., 1997). Smad8 is closely related to Smad1 and Smad5 in amino acid sequence, and was shown to be regulated by constitutively activated ALK-2 (Chen et al., 1997). Smad8 has thus been thought to act downstream of BMP receptors. However, it has not been demonstrated that Smad8 acts as a specific R-Smad for BMP signaling under physiological conditions.

In this study, we investigated the biological effects of BMP-6 on cell lines in the process of differentiation to osteoblasts, and identified physiological receptors for BMP-6. We also demonstrated the activation of various R-Smads by BMP-6 in osteoprogenitor cells.

MATERIALS AND METHODS

Cell culture

Mouse undifferentiated mesenchymal cells (C2C12), mink lung epithelial cells (Mv1Lu), and COS-7 cells were obtained from American Type Culture Collection (Rockvillle, MD). Mouse osteoblastic cells (MC3T3-E1) were obtained from Dr H. Kodama (Ohu Univ.), rat osteoprogenitor-like cells (ROB-C26) were from Dr A. Yamaguchi (Nagasaki Univ.), and mouse embryonal carcinoma cells (P19) were from Dr T. Momoi (National Institute of Neuroscience). MC3T3-E1, ROB-C26, and P19 cells were cultured in α-minimal essential medium containing 10% fetal bovine serum (FBS) and 100 units/ml penicillin. C2C12 cells were cultured in Dulbecco's modified Eagle's medium (Gibco) containing 20% FBS and antibiotics. Mv1Lu cells and COS-7 cells were cultured in Dulbecco's modified Eagle's medium (Sigma) containing 10% FBS and 100 units/ml penicillin. The cells were kept in a 5% CO_2 humid atmosphere at 37°C.

cDNA constructs and DNA transfection

pcDNA3-HA and pcDNA3-FLAG, which add HA- and FLAG-epitope tags, respectively, to inserted cDNAs, were prepared by inserting annealed oligonucleotides between the *Xho*I and *Xba*I sites of pcDNA3 (Invitrogen) (Imamura et al., 1997; Oeda et al., 1998; Kawabata et al., 1998b). The original constructions of ALK-1 to 6 were as reported (ten Dijke et al., 1994a). ALK-7 was obtained from Dr K. Tsuchida (Tokushima Univ.). ActR-II was a gift from Drs L. S. Mathews and W. W. Vale (Salk Inst.), and ActR-IIB was from Dr J. Massagué (Memorial Sloan-Kettering Inst.). BMPR-II cDNA was previously described (Kawabata et al., 1995). The receptor cDNAs were amplified by polymerase chain reaction (PCR), and subcloned into pcDNA3-HA for type I receptors and pcDNA3-FLAG for type II receptors. The integrity of the products was confirmed by sequencing. In order to obtain efficient expression levels of proteins, some inserts were subcloned into another expression vector, pcDEF3 (Kawabata et al., 1998b). These plasmids were transfected into COS-7 cells with FuGENE6 transfection reagent (Boehringer Mannheim) following the manufacturer's protocol.

Preparation of polyclonal antisera

Antisera against type I receptors, ActR-II (ARC-2) and BMPR-II (SMN and NRR) were previously reported (Franzén et al., 1993; Ichijo et al., 1993; ten Dijke et al., 1994a; Rosenzweig et al., 1995). In addition, an antiserum to ActR-IIB (RKP) was raised against a synthetic peptide corresponding to the intracellular juxtamembrane part of ActR-IIB (RHRKPPYGHVDIHE). The peptide was coupled to keyhole limpet hemocyanin (Calbiochem-Behring) with glutaraldehyde, mixed with Freund's adjuvant, and used to immunize rabbits. Antisera to Smad1 (TFP), Smad5 (SSN), and Smad8 (BSP) were described previously (Tamaki et al., 1998).

Alkaline phosphatase (ALP) staining

For histochemical analysis of ALP activity, cells were fixed for 10 minutes with 3.7% formaldehyde at room temperature. After washing with phosphate-buffered saline (PBS), the cells were incubated for 20 minutes with a mixture of 0.1 mg/ml of naphthol AS-MX phosphate (Sigma), 0.5% N, N-dimethylformamide, 2 mM $MgCl_2$, and 0.6 mg/ml of fast blue BB salt (Sigma) in 0.1 M Tris-HCl, pH 8.5, at room temperature. Cells were examined by phase-contrast microscopy.

Growth inhibition assay

Effects of BMP-6 on cell growth were examined by determining the rate of [^{3}H]thymidine incorporation into acid-insoluble DNA. Cells were plated on 24-well plates and cultured in medium containing 10% or 20% FBS for 15 hours. Then, various concentrations of ligands were added to the medium containing 0.1% FBS and cultured for 24 hours. Cells were labeled with 0.6 μCi/ml of [^{3}H]thymidine (Amersham) for 1 hour. The radioactive DNA in the cell layer was precipitated by 5% trichloroacetic acid, solubilized with 1 N NaOH, and quantitated by liquid scintillation counting.

Affinity cross-linking, immunoprecipitation and western blotting

Recombinant human BMP-6 and BMP-2 were iodinated using the Chloramine T method as described (ten Dijke et al., 1994a,b). Cells were incubated on ice for 3 hours with 0.2-0.5 nM of ^{125}I-labeled ligands in binding buffer (PBS containing 0.9 mM $CaCl_2$, 0.49 mM $MgCl_2$, and 1 mg/ml bovine serum albumin). After incubation, the cells were washed with the binding buffer without bovine serum albumin, and cross-linking was performed in the same buffer containing 0.27 mM of disuccinimidyl suberate (Pierce) for 15 minutes on ice. The cells were washed once with PBS, lysed for 30 minutes in lysis buffer (20 mM Tris-HCl, pH 7.5, 150 mM NaCl, 1% Triton X-100, 1% sodium deoxycholate) containing 1% aprotinin (Bayer) and 1 mM phenylmethylsulfonyl fluoride (PMSF), and clarified by centrifugation. Cross-linked materials were then incubated with antisera against ActR-II (ARC-2) and ActR-IIB (RKP), anti-FLAG antibody (M2) to BMPR-II, or anti-HA antibody (12CA5; Boehringer Mannheim) to type I receptors for 2-15 hours at 4°C. Immune complexes were bound to Protein A-Sepharose or Protein G-Sepharose (Kabi-Pharmacia) for 30 minutes at 4°C, washed twice with buffer containing 20 mM Tris-HCl, pH 7.5, 500 mM NaCl, 1% Triton X-100, 1% sodium deoxycholate, 0.2% SDS, followed by washing with the lysis buffer. The immune complexes were boiled for 3 minutes in SDS sample buffer (100 mM Tris-HCl, pH 8.8, 0.01% bromophenol blue, 36% glycerol, 4% SDS) containing 10 mM dithiothreitol and analyzed by SDS-8.5% polyacrylamide gel electrophoresis. The gels were fixed, dried, and subjected to analysis using a Fuji BAS 2500 Bio-Imaging Analyzer (Fuji Photo Film).

^{35}S-metabolic labeling and in vivo phosphorylation

For ^{35}S-metabolic labeling, cells were washed and incubated with methionine and cysteine-free medium containing 50 μCi/ml [^{35}S]methionine and cysteine (Amersham) for 4-12 hours at 37°C. Cells were then lysed and subjected to immunoprecipitation with specific Smad antisera. For [^{32}P]orthophosphate labeling, cells were washed and preincubated with phosphate-free medium for 1 hour. The cells were then incubated in a medium containing 1 mCi/ml [^{32}P]PO_4 for 3 hours at 37°C. After stimulation with 300 ng/ml BMP-6, the cells were washed and lysed in a buffer (20 mM Tris-HCl, pH 7.5, 150 mM NaCl, 10 mM EDTA, 1% Triton X-100, 1% deoxycholate) containing 1% aprotinin, 1 mM PMSF, 500 μM Na_3VO_4, and 100 mM NaF, and then subjected to immunoprecipitation with specific Smad antisera.

Nuclear translocation

C2C12 and MC3T3-E1 cells were grown on 8-well Lab-Tek chamber slides and stimulated with 500 ng/ml BMP-6. The cells were then fixed with a cold acetone/methanol (1:1) solution. Each slide was treated with CAS block (Zymed) for 7 minutes and then incubated with polyclonal anti-rabbit Smad1, Smad5, or Smad8 antibodies at 4°C for 15 hours. Immunohistochemical staining was performed with fluorescein isothiocyanate (FITC)-labeled goat anti-rabbit IgG (Cappel) at 1:400 dilution for 40 minutes at room temperature. Negative control samples were treated without the primary antibody. Intracellular localization was determined by confocal laser scanning microscopy. Following immunofluorescence staining, the percentage of cells with Smads staining predominantly in the nucleus was determined. In all cases, 200 stained cells were scored.

RESULTS

ALP activity induction and growth inhibition by BMP-6

To study the signal transduction by BMP-6, we first attempted to find cell lines that respond to BMP-6 using enzyme

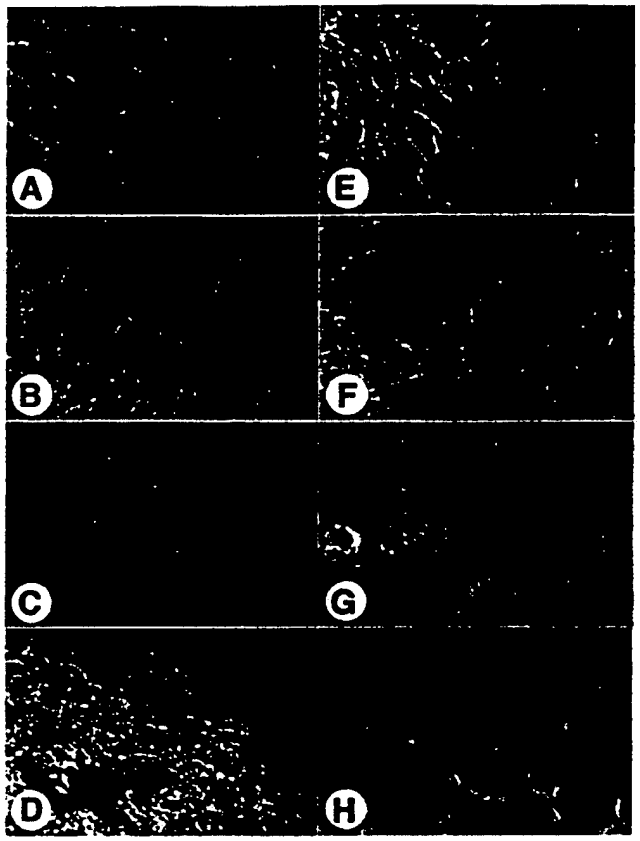

Fig. 1. Histochemical analysis of ALP activity in C2C12 cells. ALP staining in C2C12 cells without stimulation (A) and with stimulation by OP-1/BMP-7 (B-D) or BMP-6 (E-H). The concentrations of ligands are 30 ng/ml (E), 100 ng/ml (B,F), 300 ng/ml (C, G), and 1000 ng/ml (D,H).

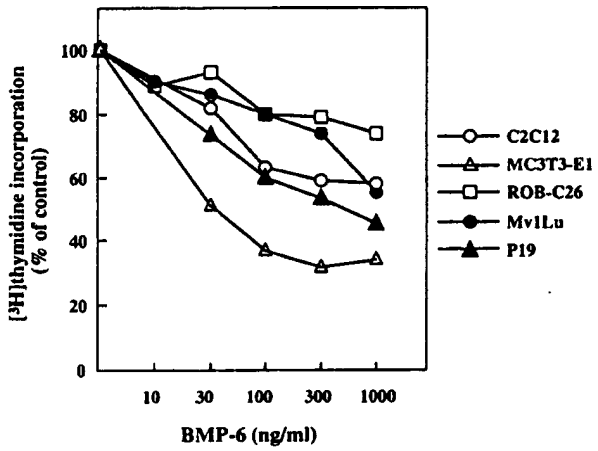

Fig. 2. Growth inhibitory effects of BMP-6 on various cell lines. Effects of various doses of BMP-6 on the growth of C2C12 cells (open circles), MC3T3-E1 cells (open triangles), ROB-C26 cells (open squares), Mv1Lu cells (solid circles), and P19 cells (solid triangles) were examined by [^{3}H]thymidine incorporation assay.

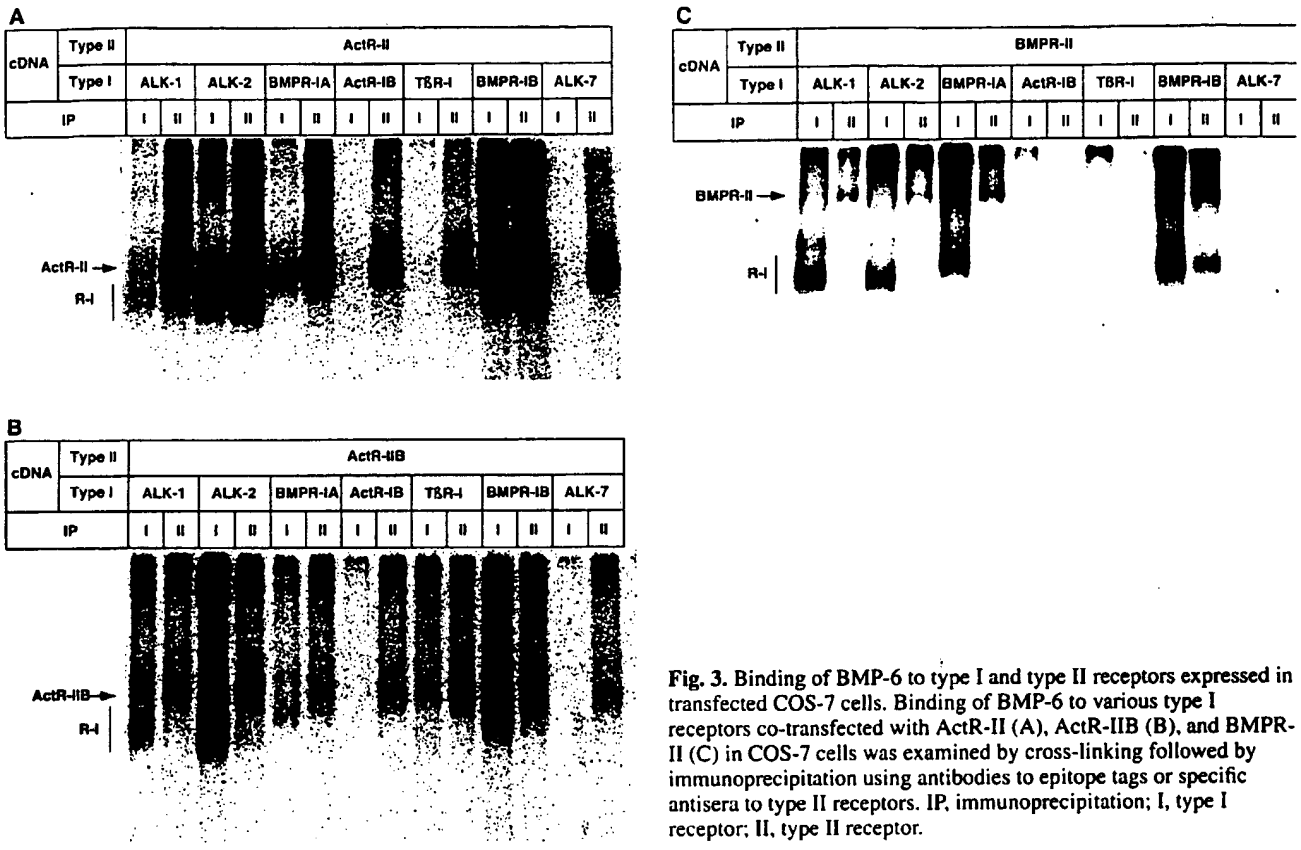

Fig. 3. Binding of BMP-6 to type I and type II receptors expressed in transfected COS-7 cells. Binding of BMP-6 to various type I receptors co-transfected with ActR-II (A), ActR-IIB (B), and BMPR-II (C) in COS-7 cells was examined by cross-linking followed by immunoprecipitation using antibodies to epitope tags or specific antisera to type II receptors. IP, immunoprecipitation; I, type I receptor; II, type II receptor.

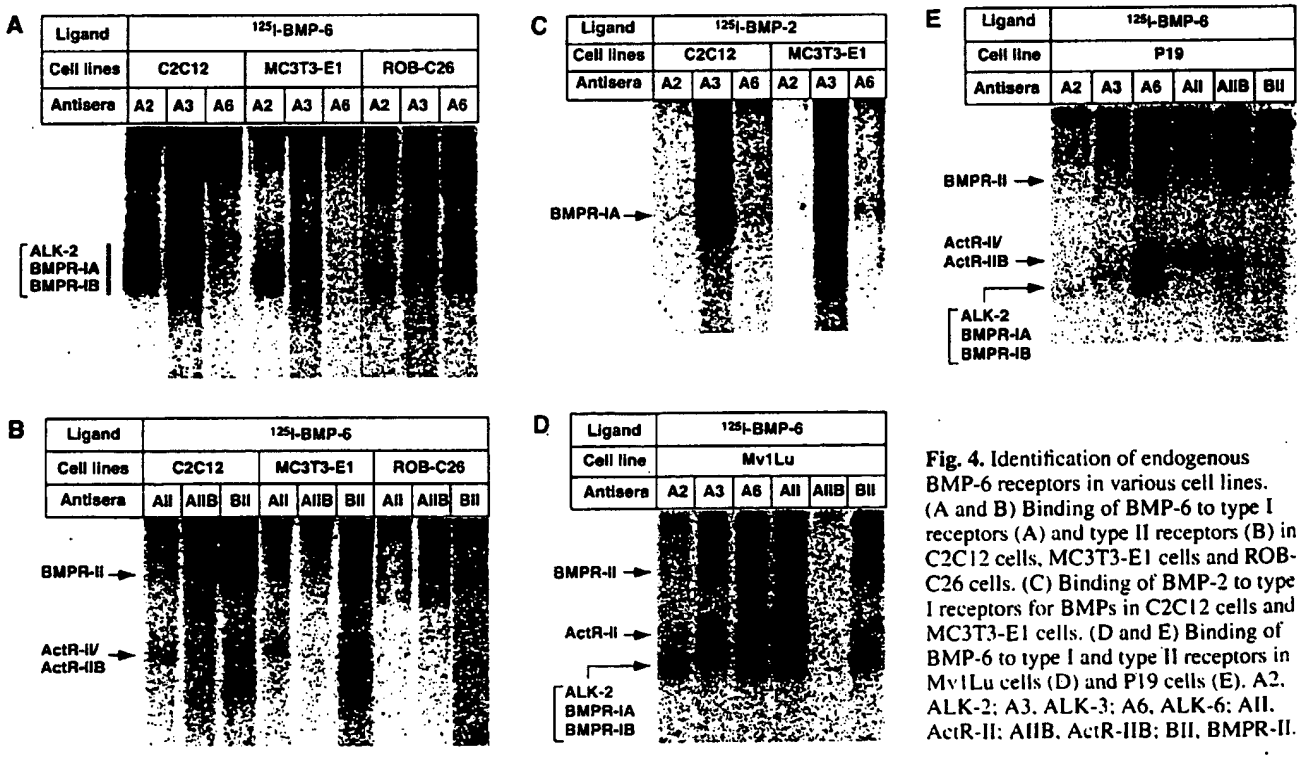

Fig. 4. Identification of endogenous BMP-6 receptors in various cell lines. (A and B) Binding of BMP-6 to type I receptors (A) and type II receptors (B) in C2C12 cells, MC3T3-E1 cells and ROB-C26 cells. (C) Binding of BMP-2 to type I receptors for BMPs in C2C12 cells and MC3T3-E1 cells. (D and E) Binding of BMP-6 to type I and type II receptors in Mv1Lu cells (D) and P19 cells (E). A2, ALK-2; A3, ALK-3; A6, ALK-6; AII, ActR-II; AIIB, ActR-IIB; BII, BMPR-II.

histochemical analysis of ALP activity, a typical osteoblast phenotype (Fig. 1). For C2C12 cells, 100 ng/ml of BMP-6 increased the number of ALP-positive cells. The number of ALP-positive cells was increased in a dose-dependent manner by stimulation with BMP-6. In contrast, the efficiency of OP-1/BMP-7 on the ALP activity was 10-fold less than that of BMP-6. Similar findings were obtained using MC3T3-E1 cells and ROB-C26 cells (data not shown).

We next examined the growth inhibitory activity of BMP-6 (Fig. 2). Growth inhibitory activities of BMP-6 were compared for various cell lines. [^{3}H]thymidine incorporation into C2C12 cells, MC3T3-E1 cells, ROB-C26 cells, and P19 cells, as well as Mv1Lu cells, was found to be inhibited by BMP-6 in a dose-dependent manner. The effect of BMP-6 on MC3T3-E1 cells was strongest, and about 10-fold stronger than that on the other cell types. The effect on ROB-C26 cells was less than that on any of the other cell types, with only a 20% decrease in [^{3}H]thymidine incorporation obtained with 1000 ng/ml of BMP-6.

Binding of BMP-6 to type I and type II receptors expressed in COS-7 cells

To determine which serine/threonine kinase receptors can serve as type I and type II receptors for BMP-6, binding of ^{125}I-BMP-6 was tested using COS-7 cells transfected with cDNAs for known serine/threonine kinase receptors. When the type I receptors were singly transfected, only weak binding of BMP-6 to BMPR-IB was observed (data not shown). When the type II receptors were singly transfected, we observed binding of BMP-6 to ActR-II and ActR-IIB, and less efficiently to BMPR-II (data not shown). When type I receptor cDNAs were co-transfected with the ActR-II, ActR-IIB or BMPR-II cDNA, BMP-6 bound to various type I receptors, and affinities of binding varied among the different combinations of type I and type II receptors. In the presence of either ActR-II or ActR-IIB, BMP-6 efficiently bound to ALK-2 and BMPR-IB, and weakly to ALK-1 and BMPR-IA (Fig. 3A and B). In the presence of BMPR-II, BMP-6 bound to ALK-1, ALK-2, BMPR-IA, and BMPR-IB (Fig. 3C). Binding of BMP-6 to BMPR-II was also increased in the presence of BMP type I receptors. Weak bands were observed after immunoprecipitation of TβR-I (ALK-5), but not reproducibly.

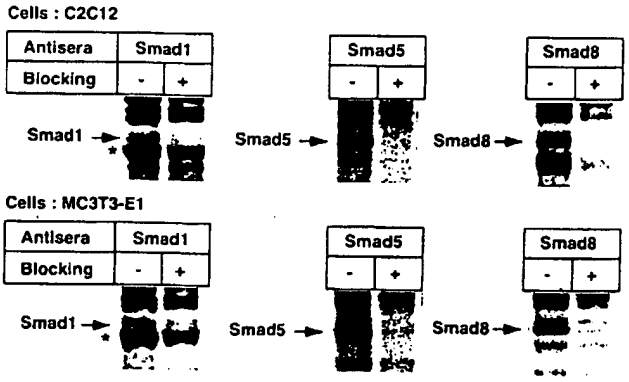

Fig. 5. Endogenous expression of Smad1, Smad5, and Smad8 in C2C12 cells and MC3T3-E1 cells. Asterisk indicates a nonspecific component immunoprecipitated with the Smad1 antiserum.

Identification of BMP-6 receptors in nontransfected cell lines

In order to determine which serine/threonine kinase receptors act endogenously as type I and type II receptors for BMP-6, C2C12, MC3T3-E1, and ROB-C26 cells were tested for binding of BMP-6. The cells were affinity-labeled using ^{125}I-BMP-6, and the cross-linked ligand-receptor complexes were analyzed by immunoprecipitation using the antisera against each of the type I and type II receptors, followed by SDS-gel electrophoresis under reducing conditions.

When C2C12 cells were affinity-labeled using ^{125}I-BMP-6, cross-linked complexes were immunoprecipitated by the ALK-2 antiserum and less efficiently by the BMPR-IA antiserum (Fig. 4A). In addition to these type I receptor antisera, ^{125}I-BMP-6-receptor complexes were also immunoprecipitated by the antisera against the type II receptors, ActR-II and BMPR-II, in these cells (Fig. 4B). In certain experiments, co-immunoprecipitation of type II receptors could be detected by antisera to type I receptors, and vice versa. In MC3T3-E1 cells, cross-linked complexes with ^{125}I-BMP-6 were precipitated by an antiserum to ALK-2, and less efficiently by that to BMPR-IA. The ActR-II and BMPR-II antisera also immunoprecipitated the cross-linked complexes. In contrast,

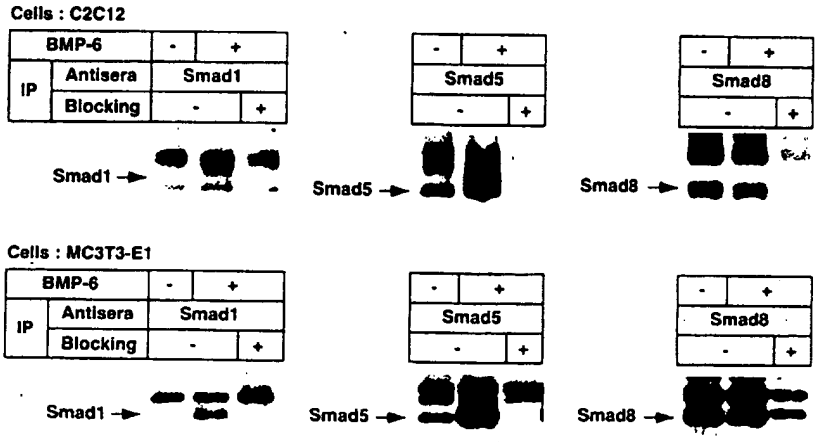

Fig. 6. Phosphorylation of Smad1, Smad5, and Smad8 in C2C12 cells and MC3T3-E1 cells. IP, immunoprecipitation.

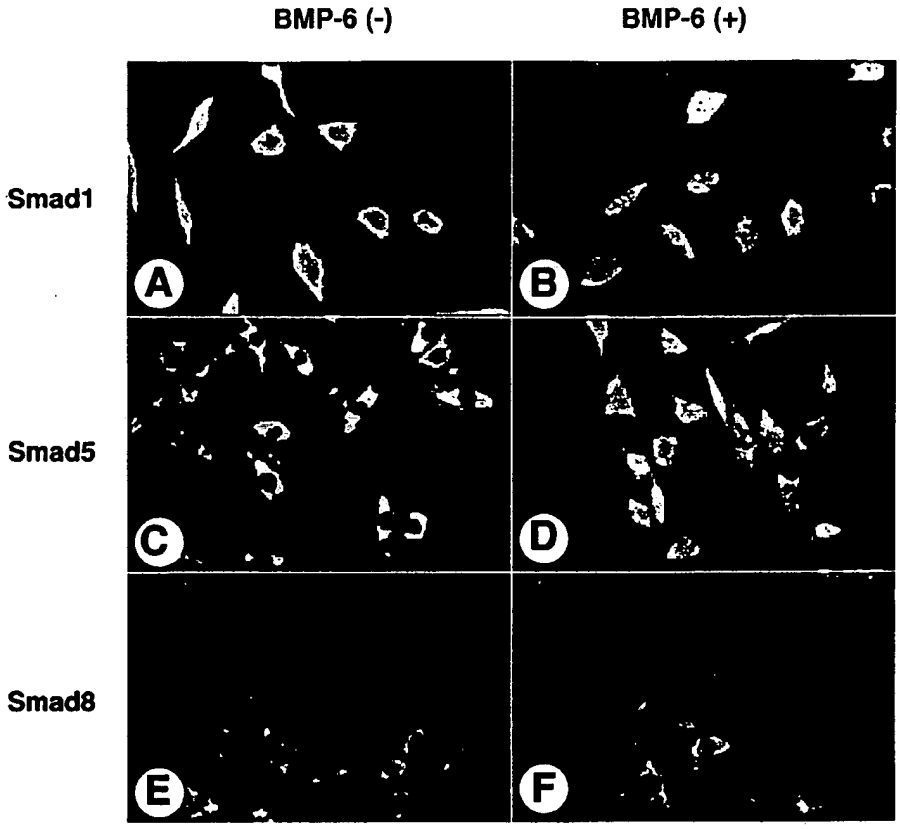

Fig. 7. Subcellular distribution of Smad1, Smad5, and Smad8 without or with stimulation by BMP-6 in C2C12 cells. (A-F) Smad1, Smad5, and Smad8 were detected by immunofluorescence using antisera against each Smad. Subcellular localizations of Smad1 (A,B), Smad5 (C,D), and Smad8 (E,F) without (A,C,E) or with (B,D,F) stimulation by BMP-6 are shown. (G) Quantitative analysis of nuclear cell staining for Smad1, Smad5, and Smad8 without or with stimulation by BMP-6. At least 200 cells were counted.

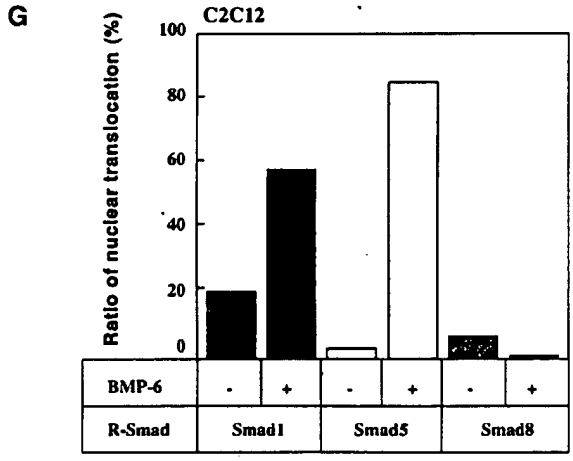

^{125}I-BMP-6-cross-linked complexes in ROB-C26 cells were immunoprecipitated by antisera to BMPR-IB and BMPR-II, and less efficiently by those to ALK-2 and BMPR-IA.

C2C12 cells and MC3T3-E1 cells were also affinity-labeled using ^{125}I-BMP-2, and cross-linked complexes were immunoprecipitated with different type I receptor antisera (Fig. 4C). Only the antiserum to BMPR-IA, but not those to ALK-2 or BMPR-IB, immunoprecipitated the BMP-2 cross-linked complex.

To identify the endogenous receptors for BMP-6 in other cell types, we tested Mv1Lu and P19 cells for binding of BMP-6. Cross-linked complexes obtained using ^{125}I-BMP-6 in Mv1Lu cells were immunoprecipitated by the antisera to all three type I receptors for BMPs, and by those to ActR-II and BMPR-II (Fig. 4D). Cross-linking of ^{125}I-BMP-6 to P19 cells, an embryonic carcinoma cell line, yielded complexes immunoprecipitated by antisera against each of the six BMP type I and type II receptors (Fig. 4E).

Endogenous expression of R-Smads in C2C12 and MC3T3-E1 cells

Intracellular signalling was further studied using C2C12 and MC3T3-E1 cells. We used antisera specific to various Smads to elucidate which Smads are endogenously expressed in C2C12 cells and MC3T3-E1 cells. Cells were metabolically labeled and cell lysates were immunoprecipitated with antisera to BMP-specific Smads (Fig. 5). Each antiserum recognized a 55-60 kDa component, which disappeared when an excess amount of blocking peptide was added together with the antiserum. Immunoprecipitation with antisera against Smads revealed that these three cell lines expressed all of Smad1, Smad5, and Smad8.

BMP-6 leads to specific phosphorylation of Smad1 and Smad5, but not Smad8 in nontransfected cell lines

The effect of BMP-6 on the phosphorylation of Smad1, Smad5, and Smad8 was analyzed using [^{32}P]orthophosphate-labeled cells (Fig. 6). In the absence of ligand, Smad1 and Smad5 were

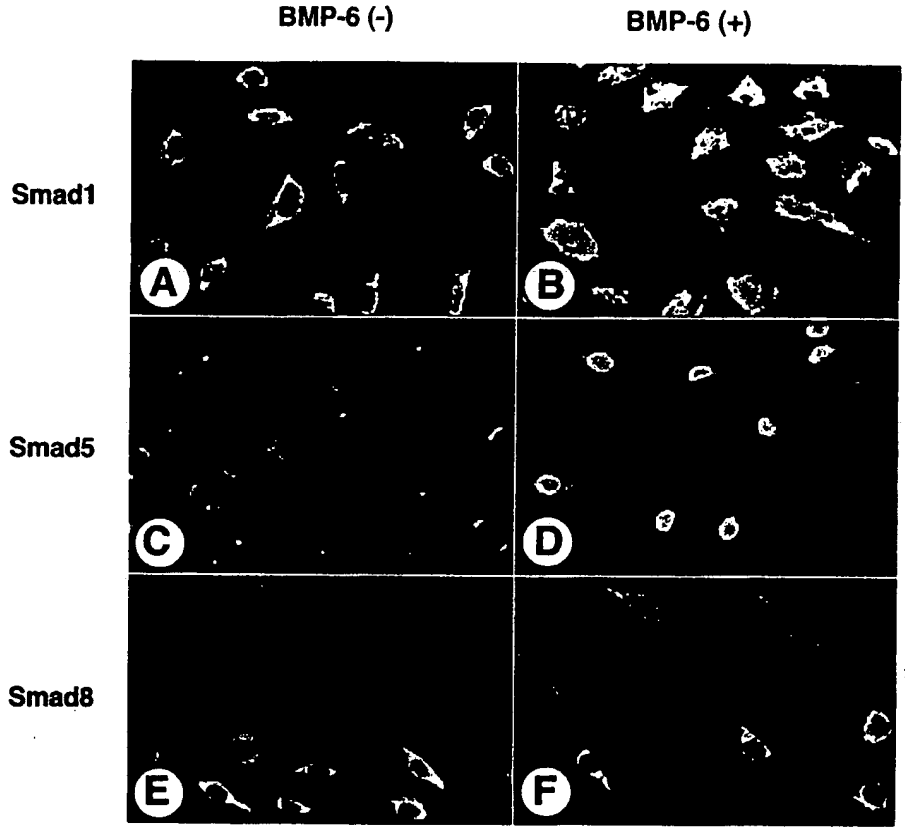

Fig. 8. Subcellular distribution of Smad1, Smad5, and Smad8 without or with stimulation by BMP-6 in MC3T3-E1 cells. (A-F) Smad1, Smad5, and Smad8 were detected by immunofluorescence using antisera against each Smad. Subcellular localizations of Smad1 (A,B), Smad5 (C,D), and Smad8 (E,F) without (A,C,E) or with (B,D,F) stimulation by BMP-6 are shown. (G) Quantitative analysis of nuclear cell staining for Smad1, Smad5, and Smad8 without or with stimulation by BMP-6. At least 200 cells were counted.

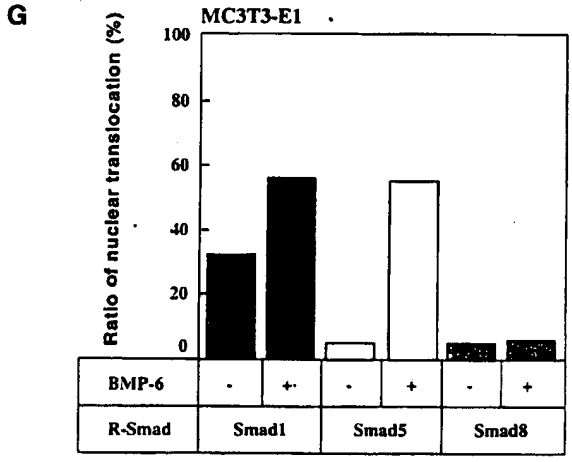

very weakly or not at all phosphorylated, but Smad8 was constitutively phosphorylated. Phosphorylation of Smad5 was induced by the addition of BMP-6. Smad1 was less efficiently phosphorylated by BMP-6, but there was no induction of Smad8 phosphorylation by BMP-6.

BMP-6-induced nuclear translocation of R-Smads

The effect of BMP-6 on the intracellular localization of Smads was studied (Fig. 7A-F and 8A-F). Following immunofluorescence staining, the percentage of cells stained predominantly in the nucleus by the Smad antisera was determined without or with BMP-6 stimulation (Fig. 7G and 8G).

In the absence of ligand, Smad1 was diffusely distributed, and Smad5 and Smad8 were predominantly localized in the cytoplasm in C2C12 cells (Fig. 7A,C,E). In the same cells, BMP-6 induced nuclear accumulation of Smad1 and Smad5, but not Smad8 (Fig. 7B,D,E). Very similar results were obtained in MC3T3-E1 cells (Fig. 8A-G).

DISCUSSION

The process of differentiation of osteoblasts can be divided into at least two stages. One is the commitment of undifferentiated mesenchymal cells to osteoblast progenitors, and the other is the maturation of osteoblast progenitors into osteoblasts. C2C12 cells are undifferentiated mesenchymal cells which differentiate into osteoblasts on stimulation by BMPs, and MC3T3-E1 cells and ROB-C26 cells are osteoblastic or osteoprogenitor cell lines which mature into osteoblasts on stimulation by BMPs. Use of these cells of osteoblast lineage may be ideal for investigating the physiological signaling components for BMP-6 in osteoblast differentiation.

In the present study, we first tested whether these three cell lines respond to BMP-6. Recombinant human BMP-6 efficiently induced ALP activity, a typical osteoblast phenotype, in all of the three cells of osteoblast lineage. The efficiency of BMP-6 in inducing ALP activity in these cell lines was 10-fold greater than that of OP-1/BMP-7. These findings suggest that, similar to BMP-2 and OP-1/BMP-7 (Katagiri et al., 1994; Takeda et al.,

1998), BMP-6 converts the differentiation pathway of myoblastic cell lines into that of osteoblast lineage, and induces osteoblast differentiation and maturation in osteoprogenitor and osteoblastic cell lines. We also examined the growth inhibitory activity of BMP-6 using various cells. BMP-6 inhibited growth of various cell types including those of osteoblast lineage. In addition, growth inhibitory effect of BMP-6 was observed in Mv1Lu cells, in which BMP-6 failed to induce ALP activity. Mv1Lu cells probably have the signaling components required for growth inhibition, but not those for osteoblast differentiation.

Next, we identified the endogenous receptors for BMP-6 in these cell lines using antibodies to known BMP receptors. Among the members of the BMP family, binding abilities to the receptors differ. For example, in MC3T3-E1 cells, which were previously shown to endogenously express ALK-2 and BMPR-IA, BMP-4 binds to BMPR-IA but not to ALK-2, whereas OP-1/BMP-7 binds to ALK-2 but not to BMPR-IA (ten Dijke et al., 1994b). Interestingly, we found that BMP-6 bound to ALK-2 as well as BMPR-IA in MC3T3-E1 cells and C2C12 cells. In the same two cell types, we confirmed that BMP-2 bound only BMPR-IA efficiently (Fig. 4C), as previously described (ten Dijke et al., 1994b). This observation is supported by the findings obtained using transfected COS-7 cells; BMP-6 bound to ALK-2 and BMPR-IB with ActR-II or ActR-IIB, while in the presence of BMPR-II, BMP-6 bound to ALK-2 and BMPR-IB, as well as BMPR-IA. It is thus likely that, in MC3T3-E1 cells and C2C12 cells, the major OP-1/BMP-7 type I receptor is ALK-2, while the type I receptor for BMP-2 is BMPR-IA, and that BMP-6 binds to ALK-2 as well as BMPR-IA. We also examined the profile of type I receptors for BMP-6 in ROB-C26 cells. Previous studies have shown that ROB-C26 cells predominantly express BMPR-IB rather than the other type I receptors, and that BMPR-IB, BMPR-II, and to a lesser extent, ActR-II serve as OP-1/BMP-7 receptors in this cell type (Tamaki et al., 1998). We have observed a similar binding profile of BMP-6 to type I and type II receptors in ROB-C26 cells. However, in addition to BMPR-IB, ALK-2 and BMPR-IA bound BMP-6 weakly in the same cells in our experiments. These findings together suggest that ALK-2 may be a principal type I receptor for BMP-6, but that different cell types express differing cell-type specific type I and II receptors for BMP-6, and that different type II receptors recruit different type I receptors into the BMP-6-receptor complex.

The specificity of the signals by type I receptors is determined by a specific region in the serine/threonine kinase domain, termed the L45 loop (Feng and Derynck, 1997). The L45 loop of ALK-1, the physiological ligands of which have not yet been determined, is identical to that of ALK-2. It is interesting to note that, in the present study, ALK-1 was observed to bind BMP-6 in concert with type II receptors when overexpressed in COS-7 cells. Previous studies showed that when type I receptors were overexpressed in COS cells together with TβR-II or ActR-II, almost all type I receptors formed complexes with TGF-β or activin, respectively (ten Dijke et al., 1994a). This suggested that ligand binding to receptors expressed in very large numbers in COS cells may not indicate physiologically significant interaction. We therefore tested the binding of BMP-6 to HUVEC cells which express ALK-1 abundantly (Attisano et al., 1993), and found that endogenous ALK-1 did not bind BMP-6 in this cell type (data not shown). This indicated that ALK-1 is not a physiological receptor for BMP-6.

Intracellular signals of BMPs are transduced by Smad proteins. Smad1 and/or Smad5 have been implicated in BMP-2/4 and OP-1/BMP-7 signaling (Hoodless et al., 1996; Nishimura et al., 1998; Macías-Silva et al., 1998; Tamaki et al., 1998). Smad8 is closely related to Smad1 and Smad5 in amino acid sequence, and has been shown to be regulated by a constitutively active form of ALK-2 (Chen et al., 1997). Thus, Smad1, Smad5, and presumably Smad8 are thought to act downstream of BMP receptors. Metabolic labeling of the cells revealed that, among R-Smads in the BMP pathways, Smad5 was more strongly detected than Smad1 and Smad8, when specific antisera to each Smad were used. Analysis by in vivo phosphorylation showed that Smad5 and, to lesser extent, Smad1 were phosphorylated by stimulation with BMP-6 in MC3T3-E1 cells and C2C12 cells. This may, however, have been due to differences in the levels of expression of Smad5 and Smad1 in these cells, or a difference in affinities of the antisera. In contrast, Smad8 was constitutively phosphorylated, and no further phosphorylation of Smad8 by BMP-6 was observed. To confirm this result, we further examined the subcellular distribution of R-Smads in the absence or presence of BMP-6. Since R-Smads act as transcriptional factors in the nucleus, nuclear translocation of R-Smads upon ligand stimulation is a critical event for signal transduction. In the present study, nuclear accumulation of Smad5 and Smad1 was observed following stimulation by BMP-6, and was correlated with the phosphorylation of these proteins. Smad8, however, was constitutively phosphorylated in both the presence and absence of BMP-6. Moreover, Smad8 was detected in the cytoplasm, and accumulation of Smad8 was not observed following stimulation by BMP-6. We concluded that Smad5 is a principal R-Smad for BMP-6, and that Smad1 may also act downstream of BMP-6 signaling. In contrast, Smad8 may act in other signaling pathways at least in the cell types examined here.

In the present study, we demonstrated BMP-6 signaling pathways in osteoblast differentiation. Future studies, including comparisons of receptor binding and activation of Smads with the other members of the BMP family, will be needed to more fully determine the in vivo functions of BMPs.

We thank Drs Peter ten Dijke and Carl-Henrik Heldin for the Smads antisera, Dr Kunihiro Tsuchida for ALK-7 cDNA, Dr Akira Yamaguchi for ROB-C26 cells, Dr Takashi Momoi for P19 cells, and Yasufumi Yuuki, Yuri Inada and Aki Hanyu for technical assistance. This study was supported by Grants-in-aid for scientific research from the Ministry of Education, Science, Sports, and Culture of Japan and special coordination funds for promoting science and technology from the Science and Technology Agency. T.I. was supported by The Mochida Memorial Foundation for Medical and Pharmaceutical Research.

REFERENCES

Attisano, L., Cárcamo, J., Ventura, F., Weis, F. M. B., Massagué, J. and Wrana, J. L. (1993). Identification of human activin and TGFβ type I receptors that form heteromeric kinase complexes with type II receptors. *Cell* **75**, 671-680.

Attisano, L. and Wrana, J. L. (1998). Mads and Smads in TGFβ signalling. *Curr. Opin. Cell Biol.* **10**, 188-194.

Celeste, A. J., Iannazzi, J. A., Taylor, R. C., Hewick, R. M., Rosen, V., Wang, E. A. and Wozney, J. M. (1990). Identification of transforming growth factor-β family members present in bone-inductive protein purified from bovine bone. *Proc. Nat. Acad. Sci. USA* **86**, 9843-9847.

Chen, Y., Bhushan, A. and Vale, W. (1997). Smad8 mediates the signaling

of the ALK-2 receptor serine kinase. *Proc. Nat. Acad. Sci. USA* **94**, 12938-12943.

Derynck, R., Zhang, T. and Feng, X.-H. (1998). Smads: Transcriptional activators of TGF-β responses. *Cell* **95**, 737-740.

Feng, X.-H. and Derynck, R. (1997). A kinase subdomain of transforming growth factor-β (TGF-β) type I receptor determines the TGF-β intracellular signaling specificity. *EMBO J.* **16**, 3912-3923.

Franzén, P., ten Dijke, P., Ichijo, H., Yamashita, H., Schulz, P., Heldin, C.-H. and Miyazono, K. (1993). Cloning of a TGFβ type I receptor that forms a heteromeric complex with the TGFβ type II receptor. *Cell* **75**, 681-692.

Gitelman, S. E., Kobrin, M. S., Ye, J.-Q., Lopez, A. R., Lee, A. and Derynck, R. (1994). Recombinant Vgr-1/BMP-6-expressing tumors induce fibrosis and enchondral bone formation in vivo. *J. Cell Biol.* **126**, 1595-1609.

Gitelman, S. E., Kirk, M., Ye, J.-Q., Filvaroff, E. H., Kahn, A. J. and Derynck, R. (1995). Vgr-1/BMP-6 induces osteoblast differentiation of pluripotential mesenchymal cells. *Cell Growth Differ.* **6**, 827-836.

Graff, J. M., Bansal, A. and Melton, D. A. (1996). *Xenopus* Mad proteins transduce distinct subsets of signals for the TGF-β superfamily. *Cell* **85**, 479-487.

Heldin, C.-H., Miyazono, K. and ten Dijke, P. (1997). TGF-β signalling from cell membrane to nucleus through SMAD proteins. *Nature* **390**, 465-471.

Hogan, B. L. (1996). Bone morphogenetic proteins: multifunctional regulators of vertebrate development. *Genes Dev.* **10**, 1580-1594.

Hoodless, P. A., Haerry, T., Abdollah, S., Stapleton, N., O'Connor, M. B., Attisano, L. and Wrana, J. L. (1996). MADR1, a MAD-related protein that functions in BMP-2 signaling pathways. *Cell* **85**, 489-500.

Ichijo, H., Yamashita, H., ten Dijke, P., Eto, Y., Heldin, C.-H. and Miyazono, K. (1993). Characterization of in vivo phosphorylation of activin type II receptor. *Biochem. Biophys. Res. Commun.* **194**, 1508-1514.

Imamura, T., Takase, M., Nishihara, A., Oeda, E., Hanai, J.-i., Kawabata, M. and Miyazono, K. (1997). Smad6 inhibits signalling by the TGF-β superfamily. *Nature* **389**, 622-626.

Jones, C. M., Lyons, K. M. and Hogan, B. L. M. (1991). Involvement of bone morphogenetic protein-4 (BMP-4) and Vgr-1 in morphogenesis and neurogenesis in mouse. *Development* **111**, 531-542.

Katagiri, T., Yamaguchi, A., Komaki, M., Abe, E., Takahashi, N., Ikeda, T., Rosen, V., Wozney, J. M., Fujisawa-Sehara, A. and Suda, T. (1994). Bone morphogenetic protein-2 converts the differentiation pathway of C2C12 myoblasts into the osteoblast lineage. *J. Cell Biol.* **127**, 1755-1766.

Kawabata, M., Chytil, A. and Moses, H. L. (1995). Cloning of a novel type II serine/threonine kinase receptor through interaction with the type I transforming growth factor-β receptor. *J. Biol. Chem.* **270**, 5625-5630.

Kawabata, M., Imamura, T. and Miyazono, K. (1998a). Signal transduction by bone morphogenetic proteins. *Cytokine Growth Factor Rev.* **9**, 49-61.

Kawabata, M., Inoue, H., Hanyu, A., Imamura, T. and Miyazono, K. (1998b). Smad proteins exist as monomers *in vivo* and undergo homo- and hetero-oligomerization upon activation by serine/threonine kinase receptors. *EMBO J.* **17**, 4056-4065.

Koening, B. B., Cook, J. S., Wolsing, D. H., Ting, J., Tiesman, J. P., Correa, P. E., Olson, C. A., Pecquet, A. L., Ventura, F., Grant, R. A., Chen, G.-X., Wrana, J. L., Massagué, J. and Rosenbaum, J. S. (1994). Characterization and cloning of a receptor for BMP-2 and BMP-4 from NIH 3T3 cells. *Mol. Cell. Biol.* **14**, 5961-5974.

Liu, F., Ventura, F., Doody, J. and Massagué, J. (1995). Human type II receptor for bone morphogenetic proteins (BMPs): extension of two-kinase receptor model to the BMPs. *Mol. Cell. Biol.* **15**, 3479-3486.

Lyons, K. M., Pelton, R. W. and Hogan, B. L. M. (1989). Patterns of expression of murine Vgr-1 and BMP-2 RNA suggest that transforming growth factor-β-like genes coordinately regulate aspects of embryonic development. *Genes Dev.* **3**, 1657-1668.

Macías-Silva, M., Hoodless, P. A., Tang, S. J., Buchwald, M. and Wrana, J. L. (1998). Specific activation of Smad1 signaling pathways by the BMP7 type I receptor, ALK2. *J. Biol. Chem.* **273**, 25628-25636.

Massagué, J. (1998). TGF-β signal transduction. *Annu. Rev. Biochem.* **67**, 753-791.

Nohno, T., Ishikawa, T., Saitoh, T., Hosokawa, K., Noji, S., Wolsing, D. H. and Rosenbaum, J. S. (1995). Identification of a human type II receptor for bone morphogenetic protein-4 that forms differential heteromeric complexes with bone morphogenetic protein type I receptors. *J. Biol. Chem.* **270**, 22522-22526.

Nishimura, R., Kato, Y., Chen, D., Harris, S. E., Mundy, G. R. and Yoneda, T. (1998). Smad5 and DPC4 are key molecules in mediating BMP-2-induced osteoblastic differentiation of the pluripotent mesenchymal precursor cell line C2C12. *J. Biol. Chem.* **273**, 1872-1879.

Oeda, E., Oka, Y., Miyazono, K. and Kawabata, M. (1998). Interaction of *Drosophila* inhibitors of apoptosis with thick veins, a type I serine/threonine kinase receptor for Decapentaplegic. *J. Biol. Chem.* **273**, 9353-9356.

Paralkar, V. M., Weeks, B. S., Yu, Y. M., Kleinman, H. K. and Reddi, A. H. (1992). Recombinant human bone morphogenetic protein 2B stimulates PC12 cell differentiation: potentiation and binding to type IV collagen. *J. Cell Biol.* **119**, 1721-1728.

Reddi, A. H. (1994). Bone and cartilage differentiation. *Curr. Opin. Genet. Dev.* **4**, 737-744.

Rosenzweig, B. L., Imamura, T., Okadome, T., Cox, G. N., Yamashita, H., ten Dijke, P., Heldin, C.-H. and Miyazono, K. (1995). Cloning and characterization of a human type II receptor for bone morphogenetic proteins. *Proc. Nat. Acad. Sci. USA* **92**, 7632-7636.

Shukunami, C., Shigeno, C., Atsumi, T., Ishizeki, K., Suzuki, F. and Hiraki, Y. (1996). Chondrogenic differentiation of clonal mouse embryonic cell line ATDC5 in vivo: differentiation-dependent gene expression of parathyroid hormone (PTH)/PTH-related peptide receptor. *J. Cell Biol.* **133**, 457-468.

Suzuki, A., Chang, C., Yingling, J. M., Wang, X.-H. and Hemmati-Brivanlou, A. (1997). Smad5 induces ventral fates in *Xenopus* embryo. *Dev. Biol.* **184**, 402-405.

Tamaki, K., Souchelnytskyi, S., Itoh, S., Nakao, A., Sampath, K., Heldin, C.-H. and ten Dijke, P. (1998). Intracellular signaling of osteogenic protein-1 through Smad5 activation. *J. Cell. Physiol.* **177**, 355-363.

Takeda, K., Ichijo, H., Fujii, M., Mochida, Y., Saitoh, M., Nishitoh, H., Sampath, T. K. and Miyazono, K. (1998). Identification of a novel bone morphogenetic protein-responsive gene that may function as a noncoding RNA. *J. Biol. Chem.* **273**, 17079-17085.

ten Dijke, P., Yamashita, H., Ichijo, H., Franzén, P., Laiho, M., Miyazono, K. and Heldin, C.-H. (1994a). Characterization of type I receptors for transforming growth factor-β and activin. *Science* **264**, 101-104.

ten Dijke, P., Yamashita, H., Sampath, T. K., Reddi, A. H., Estevez, M., Riddle, D. L., Ichijo, H., Heldin, C.-H. and Miyazono, K. (1994b). Identification of type I receptors for osteogenic protein-1 and bone morphogenetic protein-4. *J. Biol. Chem.* **269**, 16985-16988.

Thomsen, G. H. (1996). *Xenopus* mothers against *decapentaplegic* is an embryonic ventralization agent that acts downstream of BMP-2/4 receptor. *Development* **122**, 2359-2366.

Yamaguchi, A., Ishizuya, T., Kintou, N., Wada, Y., Katagiri, T., Wozney, J. M., Rosen, V. and Yoshiki, S. (1996). Effect of BMP-2, BMP-4, and BMP-6 on osteoblastic differentiation of bone marrow-derived stromal cell lines, ST2 and MC3T3-G2/PA6. *Biochem. Biophys. Res. Commun.* **220**, 366-371.

Yamamoto, N., Akiyama, S., Katagiri, T., Namiki, M., Kurokawa, T. and Suda, T. (1997). Smad1 and Smad5 act downstream of intracellular signaling of BMP-2 that inhibits myogenic differentiation and induces osteoblast differentiation in C2C12 myoblasts. *Biochem. Biophys. Res. Commun.* **238**, 574-580.

Yamashita, H., ten Dijke, P., Huylebroeck, D., Sampath, T. K., Andries, M., Smith, J. C., Heldin, C.-H. and Miyazono, K. (1995). Osteogenic protein-1 binds to activin type II receptors and induces certain activin-like effects. *J. Cell Biol.* **130**, 217-226.

Exhibit B

[CAL ORAL IMPLANTS RESEARCH

Official Publication of the European Association for Osseointegration

Clinical Research
Tissue Physiology
Wound Healing
Microbiology
Material Sciences
Prosthodontic Research
Occlusion of Oral Implants

Volume 15 · Issue No. 5 · October 2004 · Blackwell Munksgaard

Available online at: www.dentistry.blackwellmunksgaard.com/clr

CLINICAL
ORAL IMPLANTS
RESEARCH

Volume 15 · Number 5 · October 2004

Contents

Original articles

Titanium release from implants prepared with different surface roughness. An *in vitro* and *in vivo* study — 505 *A. Wennerberg, A. Ide-Ektessabi, S. Hatkamata, T. Sawase, C. Johansson, T. Albrektsson, A. Martinelli, U. Södervall & H. Odelius*

Morphologic, functional and behavioral effects of titanium dioxide exposure on nerves. An experimental study on rats — 513 *M. A. Onur, Z. Taş, A. Gürpinar, S. Şahin & M. C. Çehreli*

Predicting osseointegration by means of implant primary stability. A resonance-frequency analysis study with delayed and immediately loaded ITI SLA implants — 520 *R. Nedir, M. Bischof, S. Szmukler-Moncler, J.-P. Bernard & J. Samson*

Implant stability measurement of delayed and immediately loaded implants during healing. A clinical resonance-frequency analysis study with sandblasted-and-etched ITI implants — 529 *M. Bischof, R. Nedir, S. Szmukler-Moncler, J.-P. Bernard & J. Samson*

Histological evidence of osseointegration in human retrieved fractured hydroxyapatite-coated screw-type implants: a case report — 540 *T. Uehara, K. Takaoka & K. Ito*

Correlation of peri-implant health and myeloperoxidase levels: a cross-sectional clinical study — 546 *S. Liskmann, M. Zilmer, T. Vihalemm, O. Salum & K. Fischer*

Immunohistochemical analysis of soft tissues in implants with healthy and peri-implantitis condition, and aggressive periodontitis — 553 *P. Bullon, M. Fioroni, G. Goteri, C. Rubini & M. Battino*

Mandibular two-implant telescopic overdentures. 10-year clinical and radiographical results — 560 *S. M. Heckmann, A. Schrott, F. Graef, M. G. Wichmann & H.-P. Weber*

Measurement accuracy of reconstructed 2-D images obtained by multi-slice helical computed tomography — 570 *M. Naitoh, A. Katsumata, E. Nohara, C. Ohsaki & E. Ariji*

Porcine sinus mucosa holds cells that respond to bone morphogenetic protein (BMP)-6 and BMP-7 with increased osteogenic differentiation *in vitro* — 575 *R. Gruber, B. Kandler, G. Fuerst, M. B. Fischer & G. Watzek*

Effects of platelet lysates on select bone cell functions — 581 *E. Soffer, J.-P. Ouhayoun, C. Dosquet, A. Meunier & F. Anagnostou*

Tissue-engineered injectable bone regeneration for osseointegrated dental implants — 589 *Y. Yamada, M. Ueda, T. Naiki & T. Nagasaka*

Reconstruction of maxillary and mandibular defects using prefabricated microvascular fibular grafts and osseointegrated dental implants – a prospective study — 598 *C. Jaquiéry, D. Rohner, C. Kunz, P. Bucher, F. Peters, R. K. Schenk & B. Hammer*

Extensive augmentation of the alveolar ridge using autogenous calvarial split bone grafts for dental rehabilitation — 607 *T. Iizuka, W. Smolka, W. Hallermann & R. Mericske-Stern*

Anterior tooth replacement with implants in grafted alveolar cleft sites: a case series — 616 *M. S. Cune, G. J. Meijer & R. Koole*

Clinical Oral Implants Research is covered by Current Contents®/Clinical Medicine, the Science Citation Index®, and SciSearch®.

0905-7161(200410)15:05;1-K

Printed in Denmark by P.J.Schmidt A/S, Vojens
ISSN: 0905-7161

Reinhard Gruber
Barbara Kandler
Gabor Fuerst
Michael B. Fischer
Georg Watzek

Porcine sinus mucosa holds cells that respond to bone morphogenetic protein (BMP)-6 and BMP-7 with increased osteogenic differentiation *in vitro*

Authors' affiliations:
Reinhard Gruber, Barbara Kandler, Gabor Fuerst, Georg Watzek, Department of Oral Surgery, Dental School, University of Vienna, Vienna, Austria
Reinhard Gruber, Gabor Fuerst, Georg Watzek, Ludwig Boltzmann Institute of Oral Implantology, Vienna, Austria
Michael B. Fischer, Department of Transfusion Medicine, University of Vienna, Vienna, Austria

Correspondence to:
Reinhard Gruber
Department of Oral Surgery
Dental School
University of Vienna
Waehringerstraße 25a
A-1090 Vienna
Austria
Tel.: +43-4277-67010
Fax: +43-1-4277-67019
e-mail: reinhard.gruber@akh-wien.ac.at

Date:
Accepted 12 December 2003

To cite this article:
Gruber R, Kandler B, Fuerst G, Fischer MB, Watzek G. Porcine sinus mucosa holds cells that respond to bone morphogenetic protein (BMP)-6 and BMP-7 with increased osteogenic differentiation *in vitro*. *Clin. Oral Impl. Res.* 15, 2004; 575–580
doi: 10.1111/j.1600-0501.2004.01062.x

Key words: sinus mucosa, sinus augmentation, mesenchymal progenitor cells, osteogenic differentiation, alkaline phosphatase, osteocalcin, BMP-6, BMP-7

Abstract: The aim of this *in vitro* study was to determine whether the sinus mucosa holds cells with an osteogenic potential. Frozen sections of sinus mucosa from three adult pigs were investigated for the expression of STRO-1, a marker of mesenchymal progenitor cells, and alkaline phosphatase activity, an enzyme expressed by cells committed to the osteogenic lineage and by mature osteoblasts. To determine their osteogenic potential, mucosa-derived cells were incubated with bone morphogenetic protein (BMP)-6 and BMP-7, and alkaline phosphatase activity, osteocalcin expression, and mineralization of the extracellular matrix was measured. We found sinus mucosa cells staining positive for STRO-1 and alkaline phosphatase activity. When sinus mucosa tissue was placed in culture, alkaline phosphatase positive cells grew out from the explants and further increased alkaline phosphatase activity in response to BMP-6 and BMP-7. The expression level of the osteoblast-specific extracellular matrix protein osteocalcin, and the amount of calcium accumulation within the extracellular matrix was also increased in response to BMPs. We conclude that the sinus mucosa holds mesenchymal progenitor cells and cells committed to the osteogenic lineage that can respond to BMP-6 and BMP-7 by an increase of their osteogenic differentiation.

Sinus lift surgery is a common technique where grafting materials are placed between local host bone and the sinus mucosa to allow stable placement of dental implants (Boyne & James 1980; Tatum 1986; Misch 1987; van den Bergh et al. 1998). The long-term success rate of dental implants is increased when grafting materials are replaced or encompassed by newly formed bone, which starts growing from local host bone into the augmented area (Haas et al. 1998; van den Bergh et al. 1998; Schlegel et al. 2003). Bone formation requires osteoblasts, which are derived from progenitor cells of the mesenchymal lineage (Bruder et al. 1994; Ducy et al. 2000; Bianco et al. 2001). Mesenchymal progenitor cells can originate from various sources such as the bone marrow, the cambium layer of periosteum, and from pericytes surrounding blood capillaries (Bruder et al. 1994; Doherty et al. 1998; Bianco et al. 2001). The question whether the sinus mucosa, which covers approximately half of the augmentation material, contains cells with an osteogenic potential remains a matter of debate (Haas et al. 1998; Terheyden et al. 1999; Watzek & Haas 2001).

Mesenchymal progenitor cells can be characterized by their expression of STRO-1, a trypsin-resistant, cell-surface antigen progressively lost during the process of osteogenic differentiation (Simmons & Torok-Storb 1991; Gronthos et al. 1994; Stewart et al. 1999). Antibodies that recognize STRO-1-positive cells can be used to detect

potential mesenchymal progenitor cells *in situ* (Bianco et al. 2001; Shi & Gronthos 2003). Mesenchymal progenitor cells that have entered the osteogenic lineage express alkaline phosphatase, the matrix protein osteocalcin, and mineral salts accumulate within their extracellular matrix (Pittenger et al. 1999).

Differentiation of mesenchymal progenitor cells into bone forming osteoblasts is a multistep process, which can be stimulated by local growth factors (Bruder et al. 1994; Reddi 1998; Bianco et al. 2001; Lieberman et al. 2002; Gerstenfeld et al. 2003). Members of the bone morphogenetic protein (BMP) family are likely candidates to be involved in this process as they are expressed during bone repair, and have the potential to induce bone formation at ectopic sites (Bostrom 1998; Reddi 1998; Sakou 1998; Lieberman et al. 2002). Among the BMP superfamily, BMP-2 and BMP-7 have been tested for their potential to support bone formation in sinus lift surgery, giving first evidence that the application of BMPs can support this process of bone formation in an augmented area (Boyne et al. 1997; Margolin et al. 1998; McAllister et al. 1998; Groenveld et al. 1999; Terheyden et al. 1999; van den Bergh et al. 2000; Wada et al. 2001; Wikesjo et al. 2001). It remains however unknown whether osteogenic cells that initiate bone formation in the augmented area can solely be derived from the local host bone.

In this *in vitro* study, we investigated whether the sinus mucosa holds cells that can develop an osteogenic phenotype when cultured in the presence of the osteoinductive growth factors BMP-6 and BMP-7 (both R&D Systems, Minneapolis, MN, USA).

Material and methods

Preparation of porcine sinus mucosa

Sinus mucosa was harvested 6–8 h post mortem from three pigs (*Sus scrofa domestica*). The bony facial wall was exposed and a window of approximately 2 × 2 cm was cut by standard procedures (Haas et al. 1998). The facial sinus membrane was carefully elevated from the underlying bone tissue using appropriate surgical instruments (Friatec, Friedrichsfeld, Germany). Sinus mucosa of approximately 2 × 2 cm was harvested from each of six sinuses and placed into plastic tubes filled with sterile growth medium, which is an alpha modification of Eagle's medium (αMEM, Gibco/Life Technologies, Grand Island, NY, USA) supplemented with 10% fetal calf serum (FCS; Gibco), antibiotics, and antimycotics (Gibco).

Histochemical staining of alkaline phosphatase activity in frozen sections of sinus mucosa

Freshly prepared porcine sinus mucosa was washed in phosphate-buffered saline (PBS), cut into pieces of approximately 5 × 5 mm, embedded in optimum cutting temperature tissue compound (OCT compound; Miles Laboratories, Elkhart, IN, USA), and stored at −80°C. Frozen sections (7 µm) mounted on poly-D-lysine-coated slides were fixed with ice-cold acetone for 1 min and allowed to air dry. The slides were washed with PBS and subsequently incubated with the substrate solution for alkaline phosphatase activity containing 4 mg of naphthol AS-TR phosphate in 0.15 ml of *N,N'*-dimethylformamide and 12 mg of fast blue BB salt (all Sigma, St Louis, MO, USA) in 15 ml of 100 mM Tris-HCl (pH 9.6). After rinsing with distilled water, slides were counterstained with hematoxylin–eosin, embedded into water-soluble resin, and photographed.

Immunohistochemical determination of STRO-1-positive cells in frozen sections of mucosa

Frozen sections (7 µm) were fixed with cold acetone for 1 min and washed in PBS. The slides were placed into PBS containing 0.3% of hydrogen peroxide for 15 min to quench endogenous peroxidase, washed, and blocked with 2% bovine serum albumin in PBS for 1 h at room temperature. Sections were incubated with a 1:50 dilution of the STRO-1 antibody (mouse monoclonal antibody, IgM subclass; Developmental Studies Hybridoma Bank, University of Iowa, IA, USA) in blocking solution overnight at 4°C. For detection of STRO-1-positive cells, slides were incubated with a biotinylated goat anti-mouse IgM (1:100, An der Grub, Vienna, Austria) and a streptavidin–peroxidase conjugate (BioFX Laboratories, Inc., MD, USA) each at room temperature for 45 min. The peroxidase-containing complex was visualized by DAB substrate (Dako, Glostrup, Denmark) and counterstained with hematoxylin. The sections were embedded into water-soluble resin and photographed.

Explant cultures of sinus mucosa

Sinus mucosa tissue was washed twice with PBS and minced with a sterile scissor into pieces of approximately 5 × 5 mm. Following mincing, sinus mucosa was placed into T75-tissue culture flasks (Corning Glass Inc., Corning, NY, USA) containing αMEM supplemented with 10% FCS, antibiotics, and antimycotics. The flasks were placed into a humidified atmosphere at 37°C in 5% CO_2. Culture medium was replaced twice a week. After 2 weeks, cells that grew out from the explants, were released from the culture dish by trypsin (Gibco) and further expanded at an initial seeding density of 1 × 10^4 cells/cm^2. Mucosa-derived cells of the first and the second passage were used for further experiments.

Alkaline phosphatase activity and *in vitro* mineralization

Mucosa-derived cells were plated at 5 × 10^4 cells/cm^2 in 24-well plates (Corning Glass Inc.) in αMEM containing 10% FCS, antibiotics, and antimycotics. The next day, growth medium was replaced by serum-free medium supplemented with 10, 30, 100, and 300 ng/ml BMP-6 and BMP-7, and cells were cultured for another 72 h. Alkaline phosphatase activity was determined in cell lysates containing 0.2% Triton X-100 (Sigma). Aliquots of each sample were incubated with alkaline phosphatase substrate (20 mM diethanolamine, 150 mM NaCl, 2 mM $MgCl_2$, and 5 µM *p*-nitrophenylphosphate) for 5–30 min at room temperature. Total cellular protein was measured using the BCA-kit as recommended by the manufacturer (Pierce Chemical Co., Rockford, IL, USA). Alkaline phosphatase activity is given as the release of 1 nmol *p*-nitrophenol/minute/µg total cellular protein. For histochemical staining of alkaline phosphatase, cells were fixed with 10% neutral-buffered formaline for 15 min at room temperature and incubated with the same substrate solution as described for histochemistry of frozen sections. After rinsing with distilled water, cultures were photographed.

For detection of the mineralized matrix, cells were stimulated with BMPs as described above for 24 h and further cul-

tured in growth medium supplemented with β-glycerophosphate at 10 mM and ascorbic acid-2 phosphate at 50 μM for another week. Cells were fixed with ice-cold methanol, stained with 40 mM alizarin red (all Sigma), and photographs were taken.

Reverse transcription-polymerase chain reaction (RT-PCR) analysis of osteocalcin expression

Mucosa-derived cells were plated at 5×10^4 cells/cm² in six-well plates (Corning) in αMEM containing 10% FCS, antibiotics, and antimycotics. The next day, growth medium was replaced by serum-free medium supplemented with 300 ng/ml BMP-6 and BMP-7, and cells were cultured for another 72 h. Total RNA was extracted from the cultured cells with TRIzol reagent (Gibco). Aliquots of 2 μg total RNA were primed by random hexamers and converted into cDNA using a kit following the instructions of the manufacturer (MBI Fermentas, St. Leon – Rot, Germany). One microliter of cDNA was used for the amplification reaction in a total volume of 20 μl. The primer set for osteocalcin (accession number AY150038, position 15–229 bp) was 5′-cagatcctctggagccagg-3′ and 5′-cttacacttgccgggcaggg-3′ with an annealing temperature of 60°C, and 5′-tgaactgctatgtatctggg-3′ and 5′-cataatctctgtgatgccg-3′ for β2-microglobulin (accession number L13854, position 185–434 bp) with an annealing temperature of 57°C. For semi-quantitative RT-PCR analysis, we performed 21–36 cycles to determine the linear range of amplification. Amplified PCR products were subjected to gel electrophoresis and the intensity of the bands was determined by densitometry (Bio-Rad Laboratories, Hercules, CA, USA).

Statistical analysis

Statistical analysis was performed by ANOVA, with significance assigned at the $P < 0.05$ level. Experiments were performed with sinus mucosa and mucosa-derived cells from three different individuals.

Results

Histochemical staining of alkaline phosphatase activity in frozen sections of sinus mucosa and in mucosa-derived cells

Histochemical analysis showed cells staining positive for alkaline phosphatase in frozen sections of sinus mucosa. Alkaline phosphatase positive cells were randomly distributed throughout the connective tissue, and in perivascular regions (Fig. 1A, B). Positive staining for alkaline phosphatase was also observed in cells that grew out from mucosa tissue in explant cultures. The majority of mucosa-derived cells did not express alkaline phosphatase activity (Fig. 2A, B).

Immunohistochemical determination of STRO-1-positive cells in frozen sections of mucosa

Immunohistochemical studies of frozen sections from porcine sinus mucosa showed STRO-1-positive cells in the submucosal layer of the lamina propria. STRO-1-positive cells mainly appeared in cluster-like structures that were randomly distributed within the stroma. The cluster-like staining pattern of STRO-1-positive cells was observed in frozen sections of sinus mucosa from all investigated individuals (Fig. 3).

Effects of BMP-6 and BMP-7 on alkaline phosphatase activity in mucosa-derived cells

Mucosa-derived culture-expanded cells contain a subset of cells that stain positive for alkaline phosphatase. Incubation of the cells with either BMP-6 or BMP-7 for 72 h under serum-free conditions dose-dependently increased alkaline phosphatase activity. Addition of BMP-6 at the highest investigated concentration of 300 ng/ml led to a fourfold stimulation of the enzymatic activity when compared with control cultures, which did not receive the growth factors ($P < 0.01$). Similarly, BMP-7 at 300 ng/ml increased alkaline phosphates

Fig. 1. Staining of alkaline phosphatase-positive cells in porcine sinus mucosa. Frozen sections of freshly prepared porcine sinus mucosa were fixed with ice-cold acetone and incubated with a substrate solution for alkaline phosphatase. Alkaline phosphatase-positive cells stain blue (perivascular tissue; black arrow; connective tissue, white arrow). Slides were counterstained with hematoxylin–eosin, embedded into water-soluble resin, and photographed. (A) × 10 magnification, (B) × 20 magnification.

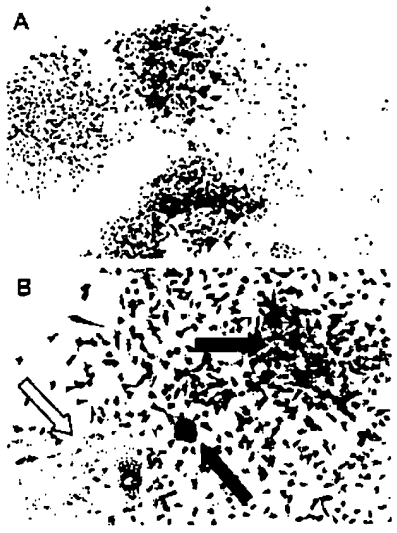

Fig. 2. Detection of alkaline phosphatase in cells that grew out from explants of sinus mucosa. Porcine sinus mucosa was minced and placed into tissue culture flasks containing growth medium. Cells that grew out from the explants were fixed with neutral-buffered formaline and incubated with a substrate solution for alkaline phosphatase. Alkaline phosphatase positive cells stain blue (black arrows). White arrows show cells that are negative for alkaline phosphatase activity. Slides were counterstained with hematoxylin and photographed. (A) × 10 magnification, (B) × 20 magnification.

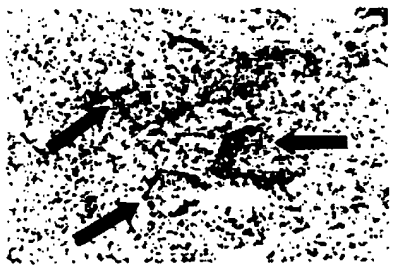

Fig. 3. Immunohistochemical detection of STRO-1-positive cells in porcine sinus mucosa. Immunohistochemical detection of STRO-1 was performed on frozen sections of freshly prepared porcine sinus mucosa as described in the method section. STRO-1-positive cells stain brown. Slides were counterstained with hematoxylin, embedded into water-soluble resin, and photographed. × 20 magnification.

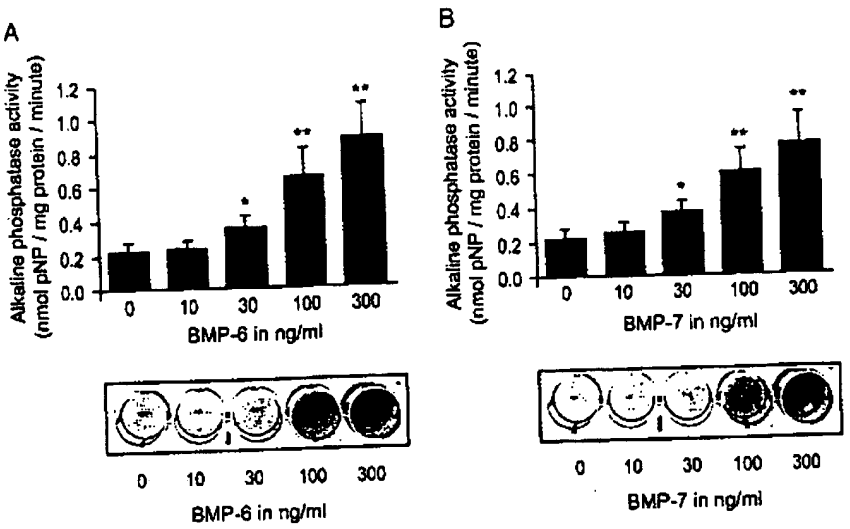

Fig. 4. Effects of bone morphogenetic protein (BMP)-6 and BMP-7 on alkaline phosphatase activity of mucosa-derived cells. Mucosa-derived cells were seeded at an initial density of $5 \times 10^4/cm^2$ into 24-well plates. The next day, cells were subjected to serum-free medium with and without the addition of BMP-6 and BMP-7, both at 300 ng/ml for 72 h. (A) Alkaline phosphatase activity was determined in cell lysates and normalized to total cellular protein. Data are means + standard deviation from quadruplicates of three donors; $^*P<0.05$ and $^{**}P<0.01$ vs. medium control. (B) In parallel, cells were fixed in neutral-buffered formalin before the addition of substrate solution for alkaline phosphatase. Alkaline phosphatase-positive cells are given in blue.

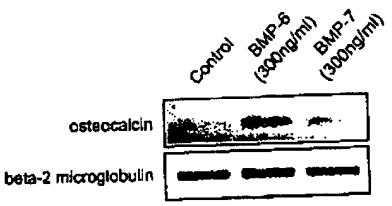

Fig. 5. Osteocalcin expression levels of mucosa-derived cells that were cultured in the presence of bone morphogenetic protein (BMP)-6 and BMP-7. Mucosa-derived cells were seeded at an initial density of $5 \times 10^4/cm^2$ into six-well plates. The following day the growth medium was changed to serum-free medium with and without the addition of BMP-6 and BMP-7 at 300 ng/ml for 72 h. Total RNA was isolated, transcribed into cDNA, and subjected to PCR. Product specific bands were within the linear range of amplification.

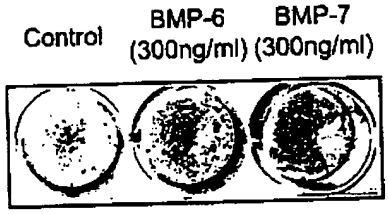

Fig. 6. Effects of bone morphogenetic protein (BMP)-6 and BMP-7 on *in vitro* mineralization of mucosa-derived cells. Mucosa-derived cells were plated at 5×10^4 cells/cm^2 in 24-well plates. The next day, growth medium was replaced by serum-free medium supplemented with BMP-6 and BMP-7 both at 300 ng/ml and cells were cultured for 24 h. Cells were cultured in growth medium supplemented with ascorbic acid and beta-glycerophosphate for another week. The formation of mineralized extracellular matrix was determined in cells that were fixed with ice-cold methanol and stained with alizarin red.

activity in mucosa-derived cells 3.5-fold ($P<0.01$) (Fig. 4A, B).

Effects of BMP-6 and BMP-7 on osteocalcin expression of mucosa-derived cells

Semi-quantitative RT-PCR analysis showed higher expression levels of osteocalcin at the expected size in mucosa-derived cells that were cultured in the presence of BMP-6 or BMP-7, both at 300 ng/ml, when compared with unstimulated controls (Fig. 5).

Effect of BMP-6 and BMP-7 on *in vitro* mineralization of mucosa-derived cells

Mucosa-derived cells form a mineralized matrix when cultured in the presence of ascorbic acid and beta-glycerophosphate. The accumulation of mineral salts in the extracellular matrix was more prominent in cells pre-stimulated with BMP-6 and BMP-7 (Fig. 6).

Discussion

The present study indicates that porcine sinus mucosa holds cells that stain positive for STRO-1 and alkaline phosphatase activity, and respond to the osteoinducive growth factors BMP-6 and BMP-7 by an increase of osteogenic differentiation, e.g. alkaline phosphatase activity, osteocalcin expression, and accumulation of mineral salts in their extracellular matrix. Tissue samples of sinus mucosa were prepared in analogy to the clinical procedure where the facial wall of the sinus was fenestrated and the mucosa carefully released from the underlying bone by blunt instruments (Haas et al. 1998). Histological analysis of the freshly prepared sinus mucosa revealed STRO-1-positive cells indicating the presence of mesenchymal progenitor cells (Simmons & Torok-Storb 1991; Gronthos et al. 1994; Stewart et al. 1999; Shi & Gronthos 2003). The sinus mucosa also holds cells that stain positive for the osteogenic differentiation marker alkaline phosphatase. We further assessed the osteogenic potential of culture-expanded cells under defined laboratory conditions. Cells were released from tissue explants by a technique that was described for the isolation of cells from other tissues such as bone (Gruber et al. 2002), gingiva (van der Pauw et al. 2002), periodontal ligament (van der Pauw et al. 2002), and periosteum (Gruber et al. 2003). These cells represent a mixed population of different cell types and stages of differentiation, as indicated by morphological criteria and the staining pattern of alkaline phosphatase. Mucosa-derived cells also expressed osteocalcin, a gene encoding for an extracellular matrix protein, which is specific for mature osteoblasts. These observations indicate that at least a small portion of cells that grew out from sinus mucosa explants express marker genes of the osteogenic lineage.

The expression of osteogenic differentiation markers was increased in mucosa-derived cells stimulated with either BMP-6 or BMP-7. Although alkaline phosphatase is an unspecific marker of early stages of osteogenic differentiation, its increase clearly indicates the presence of target cells for BMPs. Together with the enhanced expression of osteocalcin and accumulation of mineral salts these data support the assumption that the sinus mucosa holds target cells for BMPs that can respond to these growth factors by an increase of their osteogenic differentiation.

From the clinical point of view, our data support previous findings where bone formation was observed in close proximity to the sinus membrane when bovine bone

mineral grafts were combined with BMP-7/OP-1 (Terheyden et al. 1999). In contrast, no bone formation close to the sinus membrane was observed with bovine bone mineral alone (Haas et al. 1998; Terheyden et al. 1999). It can be speculated that cells with an osteogenic potential can originate from the sinus mucosa when grafts are supplemented with osteoinductive signaling molecules such as members of the BMP family.

Results from this *in vitro* study support the hypothesis that the sinus mucosa is a potential source of cells that can differentiate towards the osteogenic lineage in response to BMP-6 and BMP-7.

Acknowledgements: The work was supported by the Austrian Nationalbank Grant No. 9269. The authors want to acknowledge Manuela Pensch and Philipp Kleinrath for technical assistance.

Résumé

Le but de cette étude a été de déterminer si la muqueuse du sinus contenait des cellules ayant un potentiel ostéogénique. Des coupes congelées de la muqueuse du sinus de trois porcs adultes ont été analysées pour leur expression en STRO-1, un marqueur des cellules progénitrices mésenchymateuses, et pour l'activité de la phosphatase alcaline, une enzyme exprimée par les cellules ayant traits à la lignée ostéogénique et par les ostéoblastes mûrs. Afin de déterminer leur potentiel ostéogénique, des cellules dérivées de la muqueuse ont été incubées avec de la protéine morphogénétique osseuse (BMP)-6 et BMP-7; l'activité de la phosphatase alcaline, l'expression de l'ostéocalcine, et la minéralisation de la matrice extracellulaire ont été mesurées. Les cellules de la muqueuse du sinus se coloraient positivement pour le STRO-1 et l'activité de la phosphatase alcaline. Lorsque le tissu de la muqueuse du sinus était placé en culture les cellules positives à la phosphatase alcaline poussaient en s'éloignant des implants et augmentaient de plus l'activité de la phosphatase alcaline en réponse à BMP-6 et BMP-7. Le taux d'expression de l'ostéocalcine protéinique de la matrice extracellulaire spécifique à l'ostéoblaste et la quantité d'accumulation de calcium à l'intérieur de la matrice extracellulaire étaient également augmentés en réponse aux BMP. La muqueuse du sinus détient donc des cellules progénitrices mésenchymateuses et des cellules qui sont en rapport avec la lignée ostéogénique qui peuvent correspondre aux BMP-6 et BMP-7 par une augmentation de leur différenciation ostéogénique.

Zusammenfassung

Ziel dieser *in vitro* Studie was es, herauszufinden, ob Sinusmucosa Zellen mit einem osteogenen Potential enthält. Es wurden dazu Gefrierschnitte von Sinusmucosa dreier ausgewachsener Schweine auf die Expression von STRO-1, einem Marker mesenchymaler Vorläuferzellen untersucht. Zusätzlich wurde die alkalische Phosphataseaktivität bestimmt, ein Enzym, welches von Zellen, die bereits osteogen differenziert sind sowie von reifen Osteoblasten exprimiert wird. Um ihr osteogenes Potential zu analysieren, wurden mucosale Zellen mit den Bone morphogenetic protein (BMP)-6 und BMP-7 inkubiert und anschließend alkalische Phosphataseaktivität, Osteocalzinexpression und Mineralisation der extrazellulären Matrix gemessen. Wir fanden, dass Sinusmucosazellen positiv für STRO-1 und alkalische Phosphatase waren. Zellen mit alkalischer Phosphataseaktivität wuchsen in einem Explant-Kulturmodell aus Gewebestücken heraus. Die Enzymaktivität der ausgewachsenen Zellen konnte als Antwort auf BMP-6 und BMP-7 gesteigert werden. Ebenso kam es durch die beiden Wachstumsfaktoren zu einer Steigerung der Expression von Osteokalzin, einem osteoblastenspezifischen Matrixprotein und zu einer Steigerung der Akkumulation von Kalzium in der extrazellulären Matrix. Wir schließen daraus, dass die Sinusmucosa mesenchymale Vorläuferzellen sowie Zellen die bereits osteogen differenziert sind enthält, welche auf BMP-6 und BMP-7 mit einer Steigerung ihres osteogenen Phänotyps reagieren können.

Resumen

La intención de este estudio *in vitro* fue determinar si la mucosa del seno posee células con potencial osteogénico. Se investigaron secciones congeladas de la mucosa del seno de tres cerdos adultos para la emisión de STRO-1, un marcador de células progenitoras mesenquimales, y de fosfatasa alcalina, una enzima emitida por células comprometidas en la línea osteogénica y por osteoblastos maduros. Para determinar su potencial osteogénico, se incubaron células derivadas de la mucosa con proteína ósea morfogenética (BMP)-6 y BMP-7, y se midió la actividad de la fosfatasa alcalina, la emisión de osteocalcina, y la mineralización de la matriz extracelular. Encontramos células de la mucosa del seno con tinción positiva para el STRO-1 y la actividad de la fosfatasa alcalina. Al cultivar la mucosa del seno las células positivas a la fosfatasa alcalina se originaron de los explantes, y aumentaron aun más la actividad de la fosfatasa alcalina en respuesta a la BMP-6 y BMP-7. También se incrementó el nivel de emisión de la matriz de proteína osteocalcina extracelular específica, y la cantidad de acumulación de calcio entre la matriz extracelular en respuesta a las BMPs. Concluimos que la mucosa del seno contiene células progenitoras mesenquimales y células comprometidas con la línea osteogénica que pueden responder a BMP-6 y BMP-7 incrementando su diferenciación osteogénica.

要旨

本 in vitro 研究は、上顎洞粘膜が骨形成能を有する細胞を保持しているかどうかを調べた。既成豚3頭の上顎洞粘膜の凍結切片を、間葉前駆細胞のマーカーである STRO-1 の発現と、骨形成性細胞系統に属する細胞と成熟骨芽細胞によって発現される酵素、アルカリ・ホスホターゼの活性を調べた。骨形成能を調べるために、粘膜由来の細胞を骨形成蛋白 BMP－6 と BMP－7 で培養し、アルカリ・ホスホターゼ活性、オステオカルシンの発現、細胞外基質の石灰化を測定した。上顎洞粘膜の細胞は、STRO-1 とアルカリ・ホスホターゼ活性について陽性に染まった。上顎洞粘膜組織を培養した時、アルカリ・ホスホターゼ陽性細胞は外植片から外に増殖し、BMP-6 と BMP-7 に反応してさらにアルカリ・ホスホターゼ活性が増加した。骨芽細胞特異的な細胞外基質蛋白オステオカルシンの発現レベルと、細胞外基質内のカルシウム堆積量は BMP に反応して増加した。従って上顎洞粘膜は、間葉前駆細胞と、BMP-6 と BMP-7 に反応して骨形成性分化を促進する事ができる骨形成性細胞の系統に属した細胞を保持していると結論される。

References

van den Bergh, J.P., ten Bruggenkate, C.M., Groeneveld, H.H., Burger, E.H. & Tuinzing, D.B. (2000) Recombinant human bone morphogenetic protein-7 in maxillary sinus floor elevation surgery in 3 patients compared to autogenous bone grafts. A clinical pilot study. *Journal of Clinical Periodontology* 27: 627–636.

van den Bergh, J.P., ten Bruggenkate, C.M., Krekeler, G. & Tuinzing, D.B. (1998) Sinusfloor elevation and grafting with autogenous iliac crest bone. *Clinical Oral Implants Research* 9: 429–435.

Bianco, P., Riminucci, M., Gronthos, S. & Robey, P.G. (2001) Bone marrow stromal stem cells: nature, biology, and potential applications. *Stem Cells* 19: 180–192.

Bostrom, M.P. (1998) Expression of bone morphogenetic proteins in fracture healing. *Clinical Orthopaedics* 355 (Suppl.): S116–S123.

Boyne, P.J. & James, R.A. (1980) Grafting of the maxillary sinus floor with autogenous marrow and bone. *Journal of Oral Surgery* 38: 613–616.

Boyne, P.J., Marx, R.E., Nevins, M., Triplett, G., Lazaro, E., Lilly, L.C., Alder, M. & Nummikoski, P. (1997) A feasibility study evaluating rhBMP-2/absorbable collagen sponge for maxillary sinus floor augmentation. *International Journal of Periodontics & Restorative Dentistry* 17: 11–25.

Bruder, S.P., Fink, D.J. & Caplan, A.I. (1994) Mesenchymal stem cells in bone development, bone repair, and skeletal regeneration therapy. *Journal of Cell Biochemistry* 56: 283–294.

Doherty, M.J., Ashton, B.A., Walsh, S., Beresford, J.N., Grant, M.E. & Canfield, A.E. (1998) Vascular pericytes express osteogenic potential

in vitro and *in vivo*. *Journal of Bone and Mineral Research* 13: 828–838.

Ducy, P., Schinke, T. & Karsenty, G. (2000) The osteoblast: a sophisticated fibroblast under central surveillance. *Science* 289: 1501–1504.

Gerstenfeld, L.C., Cullinane, D.M., Barnes, G.L., Graves, D.T. & Einhorn, T.A. (2003) Fracture healing as a post-natal developmental process: molecular, spatial, and temporal aspects of its regulation. *Journal of Cell Biochemistry* 88: 873–884.

Groenveld, H.H., van den Bergh, J.P., Holzmann, P., ten Bruggenkate, C.M., Tuinzing, D.B. & Burger, E.H. (1999) Histological observations of a bilateral maxillary sinus floor elevation 6 and 12 months after grafting with osteogenic protein-1 device. *Journal of Clinical Periodontology* 26: 841–846.

Gronthos, S., Graves, S.E., Ohta, S. & Simmons, P.J. (1994) The STRO-1 + fraction of adult human bone marrow contains the osteogenic precursors. *Blood* 84: 4164–4173.

Gruber, R., Karreth, F., Frommlet, F., Fischer, M.B. & Watzek, G. (2003) Platelets are mitogenic for periosteum-derived cells. *Journal of Orthopaedic Research* 21: 941–948.

Gruber, R., Varga, F., Fischer, M.B. & Watzek, G. (2002) Platelets stimulate proliferation of bone cells: involvement of platelet-derived growth factor, microparticles and membranes. *Clinical Oral Implants Research* 13: 529–535.

Haas, R., Donath, K., Fodinger, M. & Watzek, G. (1998) Bovine hydroxyapatite for maxillary sinus grafting: comparative histomorphometric findings in sheep. *Clinical Oral Implants Research* 9: 107–116.

Lieberman, J.R., Daluiski, A. & Einhorn, T.A. (2002) The role of growth factors in the repair of bone. Biology and clinical applications. *Journal of Bone and Joint Surgery. American Volume* 84A: 1032–1044.

Margolin, M.D., Cogan, A.G., Taylor, M., Buck, D., McAllister, T.N., Toth, C. & McAllister, B.S. (1998) Maxillary sinus augmentation in the non-human primate: a comparative radiographic and histologic study between recombinant human osteogenic protein-1 and natural bone mineral. *Journal of Periodontology* 69: 911–919.

McAllister, B.S., Margolin, M.D., Cogan, A.G., Taylor, M. & Wollins, J. (1998) Residual lateral wall defects following sinus grafting with recombinant human osteogenic protein-1 or Bio-Oss in the chimpanzee. *International Journal of Periodontics & Restorative Dentistry* 18: 227–239.

Misch, C.E. (1987) Maxillary sinus augmentation for endosteal implants: organized alternative treatment plans. *International Journal of Oral Implantology* 4: 49–58.

van der Pauw, M.T., Everts, V. & Beertsen, W. (2002) Expression of integrins by human periodontal ligament and gingival fibroblasts and their involvement in fibroblast adhesion to enamel matrix-derived proteins. *Journal of Periodontal Research* 37: 317–323.

Pittenger, M.F., Mackay, A.M., Beck, S.C., Jaiswal, R.K., Douglas, R., Mosca, J.D., Moorman, M.A., Simonetti, D.W., Craig, S. & Marshak, D.R. (1999) Multilineage potential of adult human mesenchymal stem cells. *Science* 284: 143–147.

Reddi, A.H. (1998) Role of morphogenetic proteins in skeletal tissue engineering and regeneration. *Nature Biotechnology* 16: 247–252.

Sakou, T. (1998) Bone morphogenetic proteins: from basic studies to clinical approaches. *Bone* 22: 591–603.

Schlegel, K.A., Fichtner, G., Schultze-Mosgau, S. & Wiltfang, J. (2003) Histologic findings in sinus augmentation with autogenous bone chips vs. a bovine bone substitute. *International Journal of Oral & Maxillofacial Implants* 18: 53–58.

Shi, S. & Gronthos, S. (2003) Perivascular niche of postnatal mesenchymal stem cells in human bone marrow and dental pulp. *Journal of Bone and Mineral Research* 18: 696–704.

Simmons, P.J. & Torok-Storb, B. (1991) Identification of stromal cell precursors in human bone marrow by a novel monoclonal antibody, STRO-1. *Blood* 78: 55–62.

Stewart, K., Walsh, S., Screen, J., Jefferiss, C.M., Chainey, J., Jordan, G.R. & Beresford, J.N. (1999) Further characterization of cells expressing STRO-1 in cultures of adult human bone marrow stromal cells. *Journal of Bone and Mineral Research* 14: 1345–1356.

Tatum, H. Jr (1986) Maxillary and sinus implant reconstructions. *Dental Clinics of North America* 30: 207–229.

Terheyden, H., Jepsen, S., Moller, B., Tucker, M.M. & Rueger, D.C. (1999) Sinus floor augmentation with simultaneous placement of dental implants using a combination of deproteinized bone xenografts and recombinant human osteogenic protein-1. A histometric study in miniature pigs. *Clinical and Oral Implants Research* 10: 510–521.

Wada, K., Niiml, A., Watanabe, K., Sawai, T. & Ueda, M. (2001) Maxillary sinus floor augmentation in rabbits: a comparative histologic–histomorphometric study between rhBMP-2 and autogenous bone. *International Journal of Periodontics & Restorative Dentistry* 21: 252–263.

Watzek, G. & Haas, R. (2001) Internal augmentation of the alveolar crest with the sinus membrane for guided bone regeneration. An experimental study in sheep. *Oral Maxillofacial Surgery Clinics of North America* 13: 511–520.

Wikesjo, U.M., Sorensen, R.G. & Wozney, J.M. (2001) Augmentation of alveolar bone and dental implant osseointegration: clinical implications of studies with rhBMP-2. *Journal of Bone and Joint Surgery. American Volume* 83-A (Suppl. 1): S136–S145.

Exhibit C

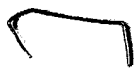

The Journal of

Cell Biology

Contents:
The Journal of Cell Biology

Volume 126, Number 6, September 1994

1331 An RNase-sensitive particle containing *Drosophila melanogaster* DNA topoisomerase II.
V. H. Meller, M. McConnell, and P. A. Fisher

1341 Inhibition of DNA topoisomerase II by ICRF-193 induces polyploidization by uncoupling chromosome dynamics from other cell cycle events.
R. Ishida, M. Sato, T. Narita, K. R. Utsumi, T. Nishimoto, T. Morita, H. Nagata, and T. Andoh

1353 Localization of HIV RNA in mitochondria of infected cells: Potential role in cytopathogenicity.
M. Somasundaran, M. L. Zapp, L. K. Beattie, L. Pang, K. S. Byron, G. J. Bassell, J. L. Sullivan, and R. H. Singer

1361 Regulation of mitochondrial morphology and inheritance by Mdm10p, a protein of the mitochondrial outer membrane.
L. F. Sogo and M. P. Yaffe

1375 *MMM1* encodes a mitochondrial outer membrane protein essential for establishing and maintaining the structure of yeast mitochondria.
S. M. Burgess, M. Delannoy, and R. E. Jensen

1393 Guanine nucleotide dissociation inhibitor is essential for Rab1 function in budding from the endoplasmic reticulum and transport through the Golgi stack.
F. Peter, C. Nuoffer, S. N. Pind, and W. E. Balch

1407 Microsomal aldehyde dehydrogenase is localized to the endoplasmic reticulum via its carboxyl-terminal 35 amino acids.
R. Masaki, A. Yamamoto, and Y. Tashiro

1421 Ponticulin is an atypical membrane protein.
A. L. Hitt, T. H. Lu, and E. J. Luna

1433 Ponticulin is the major high affinity link between the plasma membrane and the cortical actin network in *Dictyostelium*.
A. L. Hitt, J. H. Hartwig, and E. J. Luna

1445 Ezrin has a COOH-terminal actin-binding site that is conserved in the ezrin protein family.
O. Turunen, T. Wahlström, and A. Vaheri

1455 Microtubule dynamics in fish melanophores.
V. I. Rodionov, S.-S. Lim, V. I. Gelfand, and G. G. Borisy

1465 Human γ-tubulin functions in fission yeast.
T. Horio and B. R. Oakley

1475 *Drosophila* cytoplasmic dynein, a microtubule motor that is asymmetrically localized in the oocyte.
M. G. Li, M. McGrail, M. Serr, and T. S. Hays

1495 Mutations in the *SUP-PF-1* locus of *Chlamydomonas reinhardtii* identify a regulatory domain in the β-dynein heavy chain.
M. E. Porter, J. A. Knott, L. C. Gardner, D. R. Mitchell, and S. K. Dutcher

1509 Orientation of spindle axis and distribution of plasma membrane proteins during cell division in polarized MDCKII cells.
S. Reinsch and E. Karsenti

1527 Spatial changes in calcium signaling during the establishment of neuronal polarity and synaptogenesis.
C. Verderio, S. Coco, G. Fumagalli, and M. Matteoli

1537 CRAC, a cytosolic protein containing a pleckstrin homology domain, is required for receptor and G protein–mediated activation of adenylyl cyclase in *Dictyostelium*.
R. Insall, A. Kuspa, P. J. Lilly, G. Shaulsky, L. R. Levin, W. F. Loomis, and P. Devreotes

1547 The mouse ileal lipid-binding protein gene: A model for studying axial patterning during gut morphogenesis.
M. W. Crossman, S. M. Hauft, and J. I. Gordon

1565 Mitogen-activated protein kinases mediate changes in gene expression, but not cytoskeletal organization associated with cardiac muscle cell hypertrophy.
J. Thorburn, J. A. Frost, and A. Thorburn

Contents continued

Cover picture: Fluorescent image of mouse sperm binding to eggs. Sperm were prelabeled with two different lipophilic dyes. This technique was developed to assess the relative binding potential of genotypically distinct sperm populations. See related article in this issue by Youakim et al., 1573–1583.

1573 Overexpressing sperm surface β1,4-galactosyltransferase in transgenic mice affects multiple aspects of sperm–egg interactions.
A. Youakim, H. J. Hathaway, D. J. Miller, X. Gong, and B. D. Shur

1585 The role of protein tyrosine phosphorylation in integrin-mediated gene induction in monocytes.
T. H. Lin, A. Yurochko, L. Kornberg, J. Morris, J. J. Walker, S. Haskill, and R. L. Juliano

1595 Recombinant Vgr-1/BMP-6–expressing tumors induce fibrosis endochondral bone formation in vivo.
S. E. Gitelman, M. S. Kobrin, J.-Q. Ye, A. R. Lopez, A. Lee, and R. Derynck

1611 Parathyroid hormone–related peptide (PTHrP) depleted mice show abnormal epiphyseal cartilage development and altered endochondral bone formation.
N. Amizuka, H. Warshawsky, J. E. Henderson, D. Goltzman, and A. C. Karaplis

1625 ADDITIONS AND CORRECTIONS

1627 ADDITIONS AND CORRECTIONS

1629 AUTHOR INDEX FOR VOLUME 126

1637 SUBJECT INDEX FOR VOLUME 126

Recombinant Vgr-1/BMP-6–expressing Tumors Induce Fibrosis and Endochondral Bone Formation In Vivo

Stephen E. Gitelman,*‡ Michael S. Kobrin,** Jian-Qin Ye,*‡ Alfredo R. Lopez,¶ Angela Lee,** and Rik Derynck‡§‖

Departments of *Pediatrics, ‡Growth and Development, and §Anatomy, ‖Programs in Cell Biology and Developmental Biology, and ¶Hematology/Oncology Section at Veterans Administration Medical Center, University of California at San Francisco, San Francisco, California 94143; and **Genentech, Inc., South San Francisco, California 94080

Abstract. Members of the TGF-β superfamily appear to modulate mesenchymal differentiation, including the processes of cartilage and bone formation. Nothing is yet known about the function of the TGF-β–related factor vgr-1, also called bone morphogenetic protein-6 (BMP-6), and only limited studies have been conducted on the most closely related factors BMP-5, osteogenic protein-1 (OP-1) or BMP-7, and OP-2. Because vgr-1 mRNA has been localized in hypertrophic cartilage, this factor may play a vital role in endochondral bone formation. We developed antibodies to vgr-1, and documented that vgr-1 protein was expressed in hypertrophic cartilage of mice. To further characterize the role of this protein in bone differentiation, we generated CHO cells that overexpressed recombinant murine vgr-1 protein. Western blot analysis documented that recombinant vgr-1 protein was secreted into the media and was proteolytically processed to yield the mature vgr-1 molecule. To assess the biological activity of recombinant vgr-1 in vivo, we introduced the vgr-1–expressing CHO cells directly into the subcutaneous tissue of athymic nude mice. CHO-vgr-1 cells produced localized tumors, and the continuous secretion of vgr-1 resulted in tumors with a strikingly different gross and histological appearance as compared to the parental CHO cells. The tumors of control CHO cells were hemorrhagic, necrotic, and friable, whereas the CHO-vgr-1 tumors were dense, firm, and fibrotic. In contrast with control CHO tumors, the nests of CHO-vgr-1 tumor cells were surrounded by extensive connective tissue, which contained large regions of cartilage and bone. Further analysis indicated that secretion of vgr-1 from the transfected CHO tumor cells induced the surrounding host mesenchymal cells to develop along the endochondral bone pathway. These findings suggest that endogenous vgr-1 acts as an osteoinductive factor during endochondral bone formation.

During development, a variety of growth and differentiation factors influence cell proliferation, differentiation, and migration. Several secreted peptide growth factors have been shown to mediate these processes, exerting their activities locally in an autocrine or paracrine fashion (reviewed in reference 20). The TGF-β superfamily represents one group of such factors that is particularly important in modulating mesenchymal differentiation (reviewed in references 10, 41). This family of factors influences pluripotent progenitor cells to differentiate into fibroblasts, adipocytes, myoblasts, chondrocytes, or osteoblasts. Correctly coordinated differentiation of mesenchymal cells into such cell lineages may depend on a defined spatial and temporal expression pattern for specific TGF-β–related factors (for examples, see references 14, 31).

One aspect of mesenchymal differentiation that remains incompletely characterized includes endochondral bone formation, bone fracture healing, and ectopic bone formation, all of which proceed through a similar developmental cascade. In these processes, mesenchymal precursor cells first differentiate into chondrocytes and give rise to a cartilage template. Within the center of this template, the chondrocytes enter a proliferative phase, then mitosis arrests and the cells undergo hypertrophy. The hypertrophic cartilage mineralizes in the later stages of maturation, and is eventually invaded by blood vessels and replaced by a mineralized bone matrix. This bone matrix is deposited by osteoblasts, which also have differentiated from mesenchymal progenitor cells. Recent evidence implicates TGF-β superfamily members as playing a central role in this complex developmental process (reviewed in references 10, 55).

The TGF-β superfamily consists of a growing number of homologous, secreted, disulfide-bonded dimers (reviewed in

Address all correspondence to Stephen E. Gitelman, Department of Pediatrics, University of California at San Francisco, Box 0136, Millberry Union East, Room 405, San Francisco, CA 94143. Phone: (415) 476-3748; fax: (415) 476-1343. The present address for Michael S. Kobrin is Departments of Medicine and Biological Chemistry, University of California, Irvine, CA 94305-5487. The present address for Angela Lee is Department of Immunology, Stanford University School of Medicine, Palo Alto, CA 94305-5487.

references 10, 41). These proteins can be further subdivided into several groups, based on sequence homology. One of these groups consists of the three TGF-β isoforms, TGF-β1, -β2, and -β3. Other distinct groups include the activins, inhibins, and Müllerian inhibitory substance. However, by far the largest group comprises the bone morphogenetic proteins (BMPs)[1], *Xenopus* vg-1, *Drosophila* decapentaplegic (dpp), and the more recently cloned polypeptides nodal (59), dorsalin (3), vgr-2 (22), and growth/differentiation factors (GDF)-1 (27) and GDF-3 (33). This group has been referred to as the decapentaplegic/vg-1–related proteins (DVR) (30).

The TGF-β superfamily, and especially the DVR group, appears to be of considerable importance in bone and cartilage development. Several members of this superfamily have been localized during intramembranous and endochondral bone formation, and they are expressed in a spatially and temporally distinct but overlapping pattern in the differentiating tissue (for an example, see reference 31). The proteins that have been best characterized in terms of their osteoinductive activity are the subgroup consisting of BMP-2 and BMP-4 (reviewed in reference 55), which bear closest homology with the decapentaplegic complex protein dpp of *Drosophila* (38). BMP-2 and BMP-4 have the ability to induce osteoblastic differentiation in vitro and ectopic bone formation when injected intramuscularly (for examples, see references 6, 17, 18, 24, 49, 51, 56, 57), and are at least partially responsible for the osteoinductive activity originally purified from bone (40, 46).

The largest subgroup of DVR proteins consists of BMP-5 (5), vgr-1 (29) or BMP-6 (5), osteogenic protein-1 (OP-1) (36) or BMP-7 (5), and OP-2 (37), all of which have a high degree of homology to the ancestral 60A protein in *Drosophila* (12). Although BMP-7 has been shown in an initial study to induce bone formation in vivo (43) and osteoblastic and chondrocytic differentiation in vitro (1, 43), little is currently known about the functions of the other members of this subgroup and their expression patterns during mammalian development. To define the function of this subgroup in mesenchymal differentiation and especially during endochondral bone formation, we have selected vgr-1/BMP-6 as a prototype for our studies. This cDNA was originally isolated from a murine embryonic cDNA library and was named vgr-1, based on its homology with *Xenopus* vg-1 (29). The human and bovine homologues of vgr-1 were subsequently cloned from bone and were named BMP-6 (5), but no bone morphogenetic activity has been reported for this protein. Extensive in situ hybridization analyses have localized vgr-1 mRNA expression to the central nervous system, to various epithelial structures including the suprabasal layer of the epidermis, and, of most relevance to the current studies, to hypertrophic cartilage (21, 31). Notably, it is the only member of the TGF-β superfamily that has been localized to hypertrophic cartilage, and, as such, vgr-1 protein could be involved in the maturation of hypertrophic cartilage and/or stimulation of osteoblastic differentiation. However, in a recent immunohistochemical localization study, vgr-1 protein was not detected in hypertrophic cartilage, suggesting that there may be translational inhibition of vgr-1 expression in the latter tissue (50).

1. *Abbreviations used in this paper:* BMPs, bone morphogenic proteins; dhfr, dihydrofolate reductase; dpp, decapentaplegic; DVR, dpp/vg-1–related proteins; GDF, growth/differentiation factors; OP-1, osteogenic protein-1.

In this study, we developed antibodies to vgr-1, and showed that vgr-1 protein was indeed expressed in hypertrophic cartilage. Furthermore, we generated transfected CHO cells that produced recombinant vgr-1 protein, and showed that the protein was proteolytically processed and secreted by these cells. Injection of the vgr-1–expressing CHO cells into the subcutaneous tissue of nude mice resulted in tumors with fibrosis and regions of cartilage and bone. Further analysis indicated that vgr-1 secreted by the injected CHO cells induced the surrounding host mesenchymal cells to differentiate into chondrocytes and osteoblasts. Our data indicate that vgr-1 may represent a vital factor for differentiation along the endochondral bone cascade.

Materials and Methods

Construction of the vgr-1 Expression Vector

To obtain the vgr-1 gene, a 780-bp SmaI fragment from the 5' end of the vgr-1 cDNA was used as a probe to screen a mouse genomic library in λ Charon 4A under high stringency. The library was plated at 50,000 pfu/plate, and ~1 × 10^6 clones were screened. Candidate positive clones from duplicate filter lifts were purified through subsequent rounds of screening. Library plating, probe labeling, phage lifts, and filter hybridizations were carried out as described previously (11). Restriction fragments of one such phage were subcloned into pUC219 for further mapping, and subsequently sequenced in M13 through standard dideoxy sequencing (44) with Sequenase (United States Biochemical Corp., Cleveland, OH). This analysis led to the identification of the first coding exon of the vgr-1 gene.

For expression studies, the original vgr-1 cDNA (29) was subcloned into the BamHI-EcoRI site of the pRK7 expression vector (53). To generate the composite full-length vgr-1 cDNA expression vector, we replaced the 5' coding sequence of the original cDNA (29) with an 851-bp BamHI/BspHI genomic fragment that contained 5' flanking DNA and the first coding exon, and then performed a three-part ligation in which this fragment was ligated with the downstream 1551-bp BspHI/EcoRI 3' vgr-1 cDNA fragment and the pRK 7 expression vector that had been digested with BamHI and EcoRI. The resultant plasmid was named pRK7-vgr-1.

Cell Culture and Transfection

CHO cells deficient in the synthesis of dihydrofolate reductase (dhfr) (47) were propagated in F-12 Ham's nutrient mix (Gibco BRL, Gaithersburg, MD) and supplemented with 10% fetal calf serum (Hyclone Laboratories, Logan, UT), 100 U/ml penicillin, and 100 μg/ml streptomycin (both from Gibco BRL). Cells were transfected with 15 μg of the pRK7-vgr-1 expression vector and 300 ng of pSV-dhfr DNA (45) using the calcium-phosphate precipitation method (52). Cells were incubated for 4 h, the medium was removed, and the cells were exposed to a 15% glycerol shock for 1 min. After rinsing twice with PBS, the cells were incubated in supplemented media until they reached confluence, at which time they were split 1:8 and selected in media lacking glycine, hypoxanthine, and thymidine, and supplemented with 5% dialyzed fetal calf serum. Individual clones were selected after 3 wk, and, after expansion, were screened by Northern blot analysis for expression of vgr-1 mRNA. The integrated plasmid sequences of several positive clones were amplified through culturing in gradually increasing levels of methotrexate, up to 500 nM, thereby generating the CHO-vgr-1 cells.

Transient transfections of pRK7-vgr-1 into 293 cells were performed as described previously (15).

RNA Preparation and Northern Blot Analysis

Total RNA was prepared from cultured cells by lysis with guanidinium isothiocyanate, phenol extraction, and ethanol precipitation, according to standard protocols (7). The RNA was quantitated spectrophotometrically at 260 nm, and was stored at −70°C until use. For Northern blot analysis, 20 μg of total RNA was electrophoresed in a formaldehyde gel in MOPS buffer and transferred to nylon membranes (Gene Screen; New England Nuclear, Boston, MA). The vgr-1 cDNA probe corresponded to the 2.4-kb BamHI/EcoRI cDNA from the pRK7-vgr plasmid, and was radiolabeled using the [^{32}P]dCTP random primer labeling method (Oligolabeling Kit;

Pharmacia, Uppsala, Sweden). Hybridization, washing, and autoradiography were performed as described previously (14).

Cell Growth Rate

CHO or transfected CHO-vgr-1 cells were rinsed with PBS, trypsinized in 0.25% trypsin with 0.02% versene, and diluted in standard media. The cell number was determined using a Coulter counter (Coulter Corp., Hialeah, FL), and 10,000 cells were plated per well on 24-well plates. The cells were grown in standard media with 10% fetal calf serum. For analysis of growth rate in the presence of serum, the wells were rinsed, trypsinized, and counted at regular intervals starting 12 h after initial plating. For each time point, three separate wells of cells were individually counted three times, and the cell number was then averaged. For analysis of growth rate in the absence of serum, the freshly plated cells were grown in 10% fetal calf serum for 24 h, then the cells were rinsed three times with PBS and subsequently grown in media supplemented with insulin, transferrin, and selenium (GMS-G supplement; Gibco-BRL). The cells were again grown in triplicate for each time point, and were first counted 24 h after the serum had been withdrawn.

Antibody Production

Oligopeptides were synthesized corresponding to the deduced murine protein sequence at amino acids 141-157 for the pro region antibody and 392–407 for the mature region antibody (see Fig. 2). No similar sequences are present in BMP-5 and BMP-7, and therefore no crossreactivity was expected between the vgr-1 antibodies and these BMPs. An additional cysteine residue was added to the amino terminus of each oligopeptide. The peptides were coupled to keyhole limpet hemocyanin according to the method of Green et al. (16), and were then mixed in Freund's adjuvant and injected into rabbits (Caltag Laboratories, Inc., South San Francisco, CA). Two animals were injected with each antigen. The initial injection consisted of 150 μg in Freund's adjuvant with subsequent booster doses of 100 μg 3 and 4 wk from the initial injection. The first bleed occurred at 5 wk from the initial injection. A 100-μg injection was given after that bleed, and follow-up bleeds and injections were each performed at weekly intervals for the next 2 wk, and with a last bleed 1 wk later. There was a 2-wk rest period, then weekly booster injections for 2 wk, followed by a repetition of the above cycle. Antisera was stored at −20°C until use.

Whole antisera was used for Western blot analysis at the dilutions noted below. For immunohistochemistry, the antisera were first purified by passage over the appropriate antigen affinity column. The columns were constructed by coupling of the synthetic oligopeptides to Affigel-10 (Bio Rad, Laboratories, Richmond, CA) according to manufacturer's instructions. The antisera was purified by mixing with an equal volume of 0.1 M PBS (pH 7.2) and loading onto the appropriate affinity column that had been preequilibrated with this buffer. The column was washed with PBS until the eluant achieved a baseline reading at OD_{280nm}. The specific anti-vgr-1 antibodies were then eluted with 40 mM diethylamine (pH 11.4), and exchanged into PBS buffer by passage over a YM-10 membrane (Amicon Corp., Beverly, MA).

Western Blot Analysis

Conditioned media was collected from CHO or CHO-vgr-1 transfectants grown in media in the absence of serum for 24 h. 200-μl aliquots were lyophilized to dryness, and were resuspended in sample buffer under reducing conditions with 5% β-mercaptoethanol. After SDS-PAGE, the samples were transferred to nitrocellulose. Immunoblotting was performed with the enhanced chemiluminesence kit (Amersham Corp., Arlington Heights, IL) according to manufacturer's recommendations. Whole antisera directed against the precursor oligopeptide were used at a 1:1000 dilution, and that derived from the mature oligopeptide was used at a 1:250 dilution. Incubations with the antibodies were performed overnight at 4°C.

Injections into Nude Mice

Homozygous nude, athymic 30-g female mice were obtained from Charles River Laboratories (Wilmington, MA). 5×10^6 CHO or CHO-vgr-1 cells were injected into the right paraspinous area in the lower lumbar region. Cells were prepared for injection by trypsinization, multiple washes with PBS, and resuspension in 0.5 ml of serum-free media per sample. The animals were fed ad libitum and monitored three times per week for the appearance of solid tumors. When the tumors reached 4 cm in largest diameter, or by 4 wk, the animals were euthanized, and the tumors were resected. Portions of the tumors were fixed in 4% paraformaldehyde and embedded in paraffin. The remainder were placed in Tissue Tek OCT compound (Miles Inc., Elkhart, IN) and snap frozen in liquid N_2.

Histochemistry and Immunohistochemistry

5-μm paraffin sections were used for all histochemical analyses, and all staining was performed according to standard procedures (8).

For immunocytochemistry, cells were grown on tissue culture chamber slides (Nunc Inc., Naperville, IL) to 80% confluence, washed with PBS, fixed in methanol for 10 min, and then stored at −70°C. After several PBS rinses, endogenous peroxidase activity was quenched with 0.3% H_2O_2 in 10% methanol for 20 min. The slides were again rinsed in PBS and blocked with 3% BSA in PBS for 30 min at room temperature. The primary antibodies were then applied and incubated overnight at 4°C. The affinity-purified vgr-1 precursor antibody was used at a 1:50 dilution (8 μg/ml). After washes with PBS-0.1% Tween 20, anti-rabbit IgG horseradish peroxidase (Amersham Corp.) was applied at a 1:1000 dilution for 60 min at room temperature. After further washes, 3-amino-9-ethylcarbazole (AEC) substrate (Dako Co., Carpinteria, CA) was added for 5 to 10 minutes, and then the slides were washed in de-ionized H_2O, counterstained with hematoxylin, and washed with tap H_2O.

For analysis of vgr-1 expression in histological sections, we collected mice from gestational day 18.5 embryos, fixed the tissue in 4% paraformaldehyde for 30 minutes, and used 5 μm sections for immunostaining. The affinity-purified mature vgr-1 antibody was used at a 1:50 dilution (6 μg/ml). For analysis of the tumors, we used sections from tumors that had been snap frozen in liquid N_2 following embedding in Tissue Tek OCT Compound. The collagen type I antibody was an affinity purified goat antibody raised against human and bovine antigens, and the collagen type II antibody was an affinity-purified antibody directed against the bovine antigen (both antibodies from Southern Biotechnologies, Inc., Birmingham, AL). Both antibodies were used at dilutions of 1:1,500. The monoclonal murine osteocalcin antibody was purchased from Biomedical Technologies, Inc. (Stoughton, MA), and was used at a 1:200 dilution.

In Situ Hybridization

To evaluate the expression of dihydrofolate reductase, we used the 548-bp BamHI/BglII fragment from the 3′ untranslated region of the hepatitis B surface antigen gene, which had been incorporated into the 3′ region of the dihydrofolate reductase expression unit (45). This fragment was cloned into the Bluescript vector (Stratagene, La Jolla, CA), and sense and antisense riboprobes were generated with [^{35}S]UTP and T3 and T7 RNA polymerases, respectively, according to the supplier's protocols (Promega Corp., Madison, WI).

Frozen sections of 5 μm were cut onto "probe-on plus" microscope slides (Fisher Scientific, Pittsburgh, PA), and stored at −70°C. The sections were fixed in paraformaldehyde, acetylated, and prehybridized essentially as described previously (34). Prehybridization was performed at 50°C in hybridization buffer for 1 h, and then the solution was removed and replaced with the same buffer containing 1×10^6 cpm of riboprobe, and incubated for 16 h at 50°C. Posthybridization washes and RNase treatments were carried out as noted previously (34). After washes, the slides were dehydrated in increasing concentrations of ethanol with 0.3 M ammonium acetate, air dried, and dipped into Ilford Nuclear Research Emulsion (Cheshire, United Kingdom). Sections were exposed in light safe boxes at 4°C for 6 d, and then developed in D-19 developer (Eastman Kodak, Rochester, NY). The slides were counterstained in Harris' hematoxylin, and then analyzed under bright-field and dark-field microscopy.

Results

Vgr-1 Protein is Expressed in Hypertrophic Cartilage

Previous in situ hybridization studies have documented expression of vgr-1 mRNA in the central nervous system, various epithelial structures including the suprabasal layer of skin, and hypertrophic cartilage (21, 31). Wall et al. recently developed an antibody directed against the precursor region of the murine vgr-1 protein, and subsequent immunohistochemical analysis in the developing mouse confirmed the presence of vgr-1 protein in the central nervous system

and various epithelial structures (50). However, this antibody failed to detect vgr-1 protein expression in hypertrophic cartilage and in some cell lines that express vgr-1 mRNA, suggesting that there was translational control of vgr-1 expression. Thus, before proceeding with our studies on the role of vgr-1 in endochondral bone formation, we had to determine if vgr-1 protein was even present in hypertrophic cartilage. Towards this end, we developed polyclonal antibodies that specifically recognized both the precursor and mature portions of the murine vgr-1 protein.

No purified vgr-1 protein was yet available for antibody production. Instead, we synthesized two oligopeptides from the deduced murine vgr-1 cDNA sequence for use as immunogens. These peptides were selected from regions that have no similarity with the corresponding sequences of the most closely related factors BMP-5 and -7 (5), and thus the resultant antibodies should not cross-react with any related DVR-like factor. Oligopeptides corresponding to amino acids 141-157 in the precursor and 392-407 in the mature portion of the vgr-1 protein (see Fig. 2) were synthesized, coupled to keyhole limpet hemocyanin, and were then used as immunogens in rabbits. Antisera exhibited high titers in ELISA assays with these peptides, and reacted in Western blot assays with recombinant vgr-1 protein synthesized by transfected CHO cells (see below). The whole antisera were then affinity purified using the appropriate immunogenic oligopeptide coupled to Affigel as an affinity matrix, and they yielded antibodies suitable for immunohistochemical analyses of vgr-1 expression.

Immunostaining using the antibody raised against the mature, carboxy-terminal portion of the protein detected vgr-1 protein in the suprabasal layer of the epidermis (see Fig. 1, *A* and *B*), as described previously (50). In addition, and of importance to our study, we detected vgr-1 protein in hypertrophic cartilage (Fig. 1, *A* and *C*). This staining was predominantly in the extracellular matrix surrounding the hypertrophic chondrocytes. Furthermore, vgr-1 protein localized specifically to regions of hypertrophic cartilage that had undergone mineralization, as shown by corresponding von Kossa staining in an adjacent tissue section (Fig. 1 *D*). Thus, vgr-1 protein appeared in the latter stages of hypertrophic cartilage differentiation. The negative control, performed with substitution of rabbit IgG as the primary antibody, resulted in no such staining pattern, demonstrating the specificity of the vgr-1 immunostaining. When using the antibody raised against the precursor segment peptide, vgr-1 protein was again detected in skin, but only very weak immunostaining was apparent in hypertrophic cartilage (data not shown).

Expression of Recombinant Vgr-1 Protein by Transfected Cells

The expression of vgr-1 in the hypertrophic cartilage suggested that it may play a role in the maturation of the hypertrophic chondrocytes and/or may stimulate new bone formation. However, to date, no natural vgr-1 protein has been purified, and thus nothing is known about its physiological activities. Therefore, to determine the role of this factor in endochondral bone formation, it was necessary to first produce recombinant vgr-1 protein.

Initially, the published vgr-1 cDNA (29) was inserted downstream of the cytomegalovirus promoter in the expression vector pRK7. However, transfections of this expression vector into 293 cells did not result in detectable vgr-1 protein expression. Inspection of the predicted vgr-1 polypeptide sequence showed that the NH_2-terminal sequence did not comply well with the consensus rules of von Heijne for signal peptides (48), and we suspected that our cDNA clone was partial length. We subsequently screened a murine genomic library with a 5′ vgr-1 cDNA probe, and identified an upstream exon that contained the 5′ untranslated region, a translational initiation consensus sequence (26), and a canonical signal peptide sequence (48). Primer extension experiments, using RNA from PYS cells, verified that this sequence represented the 5′ end of the vgr-1 mRNA (Kobrin, M. S., unpublished data). Furthermore, the polypeptide sequence deduced from this genomic fragment now had a high degree of sequence similarity with the NH_2 terminus of bovine BMP-6 (5). In retrospect, we believe that the different 5′ end in the published mouse vgr-1 sequence (29) resulted from a cDNA artifact that is likely related to the high G-C content of this sequence. We then constructed a composite vgr-1 expression vector in pRK7 by ligating a 5′ 851-bp BamHI-BspHI genomic fragment onto the corresponding downstream vgr-1 cDNA fragment (29). Transient transfections of the pRK7-vgr-1 plasmid into 293 cells and metabolic labeling of the proteins now resulted in the appearance of an overexpressed protein consistent in size with the vgr-1 protein (data not shown). The full-length cDNA sequence encoding the 510–amino acid murine vgr-1 polypeptide is shown in Fig. 2.

To produce a stable source of recombinant vgr-1 protein, we cotransfected pRK7-vgr-1 and a dihydrofolate reductase expression plasmid into CHO cells, selected several clones expressing high levels of vgr-1 mRNA, and amplified its expression in the presence of increasing concentrations of methotrexate. As shown in Fig. 3 *A*, Northern blot analysis revealed a high level of vgr-1 mRNA in one such clone grown in 500 nM methotrexate. In contrast, CHO cells transfected with dihydrofolate reductase alone did not express vgr-1 mRNA. Immunostaining using the vgr-1 antiserum also showed specific staining of the vgr-1 mRNA–overproducing CHO-vgr-1 cells, indicating the synthesis of vgr-1 protein (Fig. 3 *C*). The parental CHO cells exhibited no such staining, again indicating lack of vgr-1 expression.

To assume biological activity, members of the TGF-β superfamily must enter the secretory pathway and undergo a proteolytic cleavage that separates the precursor region from the biologically active carboxy terminal domain. To determine if such processing occurs in the CHO-vgr-1 stable transfectants, we collected conditioned media produced by these cells and performed Western blot analyses using our vgr-1 antisera (Fig. 3 *B*). After denaturing gel electrophoresis under reducing conditions and Western analysis, each antiserum recognized two protein bands from the media of transfected cells, but not of the nontransfected cells. The larger protein band had a size of ~69 kD, and it reacted in Western blots with antisera raised against both the precursor and mature vgr-1 segments. This band most likely corresponded to the uncleaved vgr-1 precursor polypeptide, given its dual antibody reactivity and its size. Two lower protein bands were seen as well: a 46-kD protein that reacted only with the antibody specific for the vgr-1 precursor segment, and a 23-kD protein that reacted with the antibody for mature vgr-1. These proteins thus corresponded to the two

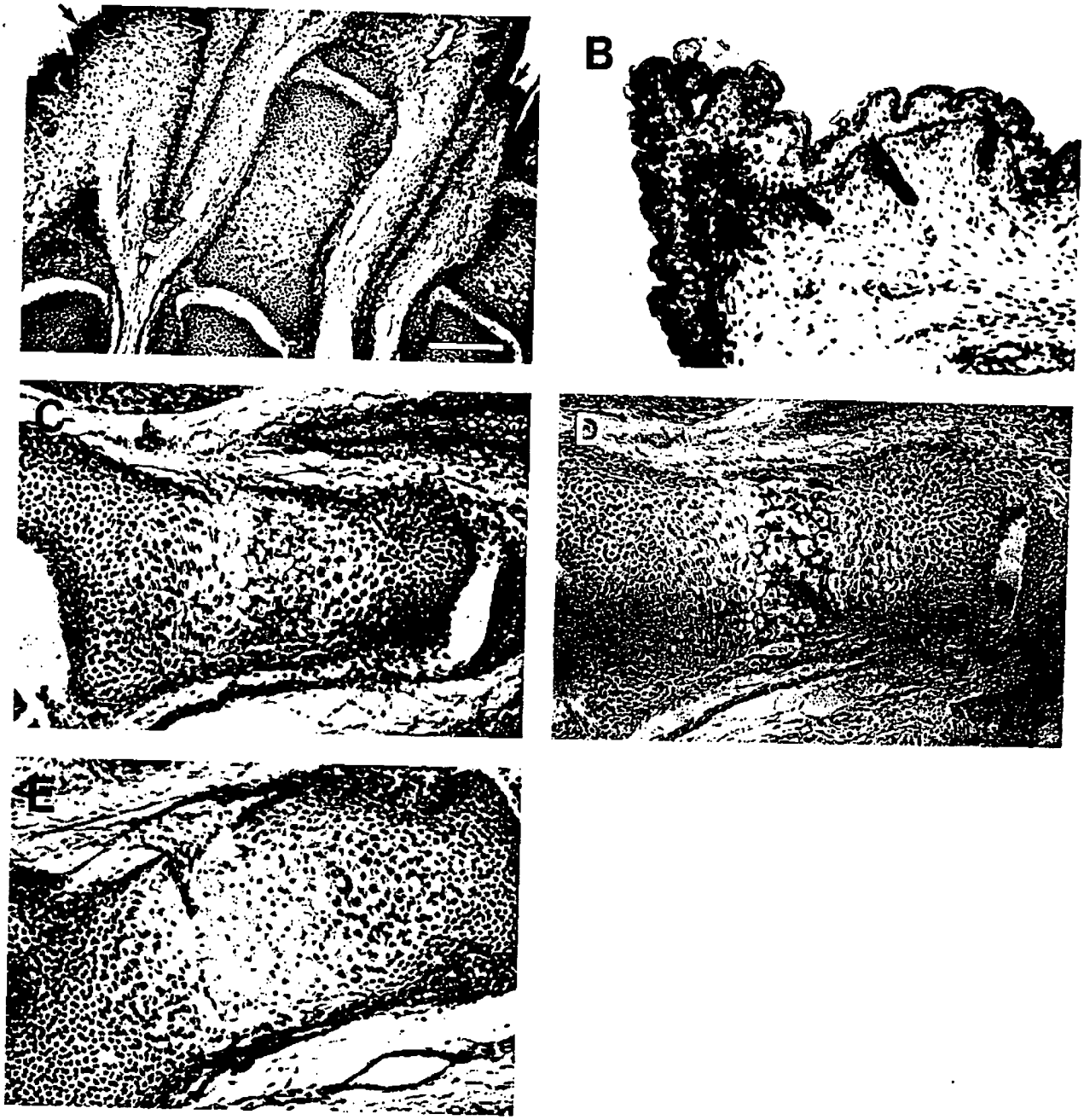

Figure 1. Vgr-1 protein expression in skin and hypertrophic cartilage. Forelimbs from 18.5-d gestation mice were stained with affinity-purified antibody directed against the mature portion of vgr-1. (*A*) ×10 view showing vgr-1 expression in both suprabasal layer of epithelium (*arrows*) and hypertrophic cartilage (*center of figure*). Bar, 200 μm (*B*) ×20 view of the skin showing localization of vgr-1 to suprabasal layer of epithelium. (*C*) ×20 view of vgr-1 expression in hypertrophic cartilage (*center*). (*D*) Section adjacent to that used for *C*, with von Kossa stain (*black*) indicating areas of mineralization, and counterstained with nuclear fast red. (*E*) Negative control, where nonspecific IgG is used as the primary antibody.

cleavage products expected after proteolytic processing of the vgr-1 precursor. These cells secreted ~2 μg/ml per 24 h of the recombinant factor, and based on these Western analyses, ~50% of the secreted protein had been proteolytically processed. The 69- and 46-kD bands each migrated as a subtle doublet (Fig. 3 *B*), which was most apparent in lower percentage polyacrylamide gels (data not shown). This may have been caused by variations in glycosylation.

Effects of vgr-1 on CHO Cells in Culture

To determine the effect of vgr-1 overexpression on these cells, we characterized changes in morphology, growth rate, and collagen synthesis. No significant difference in cell size, shape, or adherence was noted between CHO and CHO-vgr-1 cells (Fig. 3 *C*). However, in comparison with the parental CHO cells, CHO-vgr-1 cells had a significantly slower rate

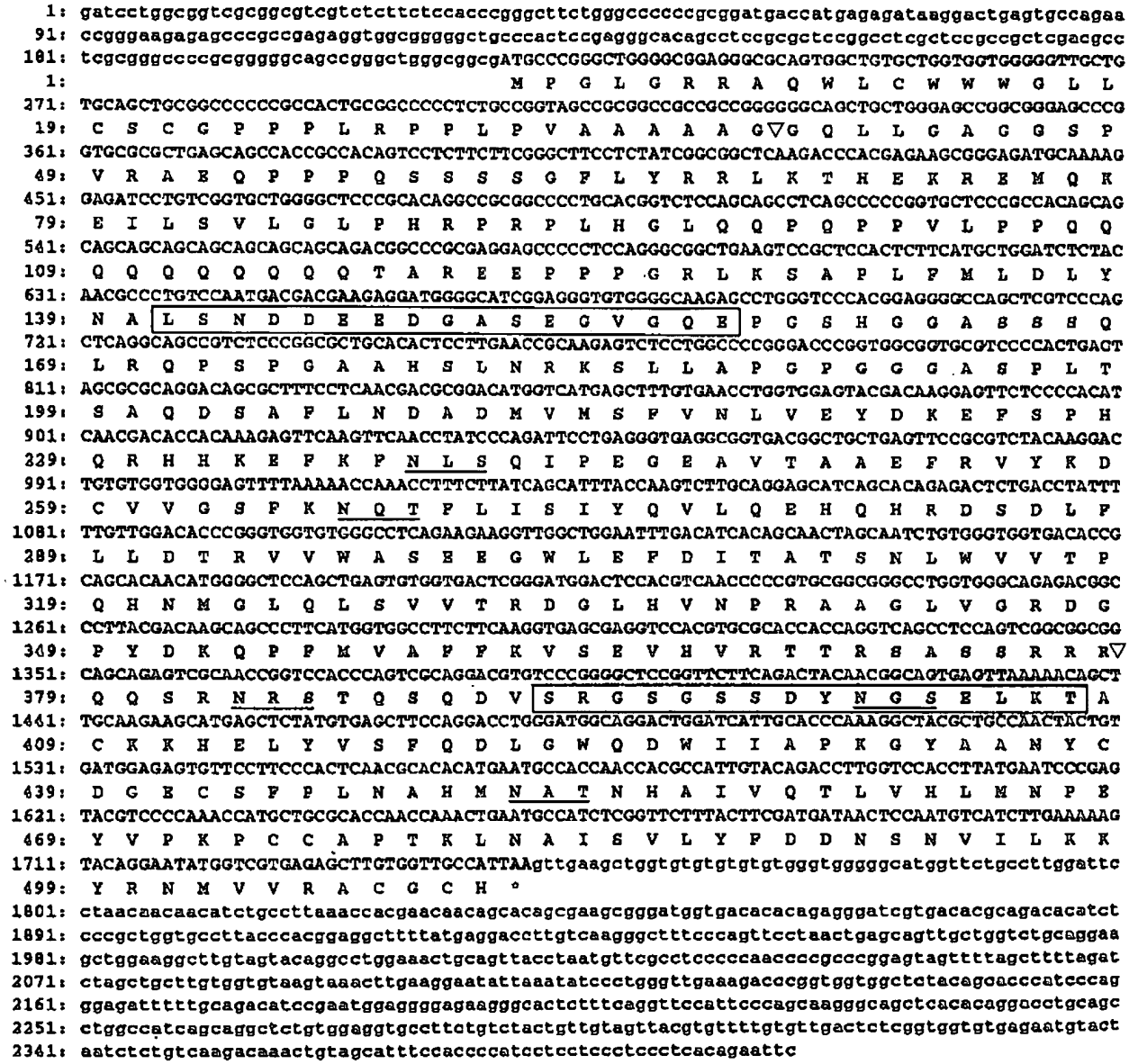

Figure 2. Nucleotide and deduced amino acid sequence of composite vgr-1 cDNA. The 5' 851 bp are derived from a BamHI/BspHI genomic fragment, and the downstream 1551 bp are from previous vgr-1 cDNA cloning (29). Nucleotide and amino acid numbering is shown in the left column. Untranslated nucleotides are in lowercase lettering. Oligopeptides used for antibody production are boxed, and potential N-linked glycosylation sites are underlined. Potential cleavage sites for eliminating the signal sequence (48) and for separating precursor from mature domains are marked with inverted arrowheads. The stop codon is marked with an asterisk. The nucleotide and protein sequence data reported in this paper will appear in the EMBL Database under the accession number X80992.

of cell proliferation both in the presence and absence of serum (Fig. 4). There were no differences in levels of expression of collagen I and II, as assessed by immunocytochemistry and Northern blot analysis (data not shown).

Vgr-1–expressing CHO Cells form Tumors with Altered Phenotype

To evaluate the effects of vgr-1 in vivo, we injected the vgr-1–expressing CHO cells subcutaneously into nude mice. Previous studies had shown that CHO cells form localized tumors when injected subcutaneously into nude mice (for an example, see reference 13), and we reasoned that the continuous release of recombinant vgr-1 by the tumor cells would allow us to evaluate the biological activity of vgr-1 in vivo. This approach would thus not necessitate the purification of recombinant vgr-1, but would rely on a continuous release of vgr-1 that was naturally activated and incorporated into the extracellular matrix. To this end, we injected CHO or CHO-vgr-1 cells into the right paraspinous area in the lower lumbar region of nude, athymic mice. Five animals were injected with the parental cells, and five with the stable transfected CHO-vgr-1 cells. One animal from each group

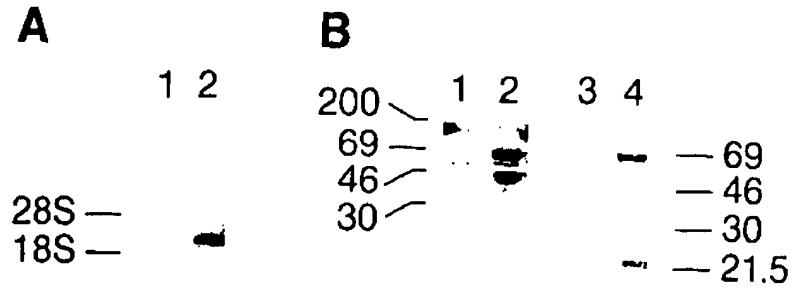

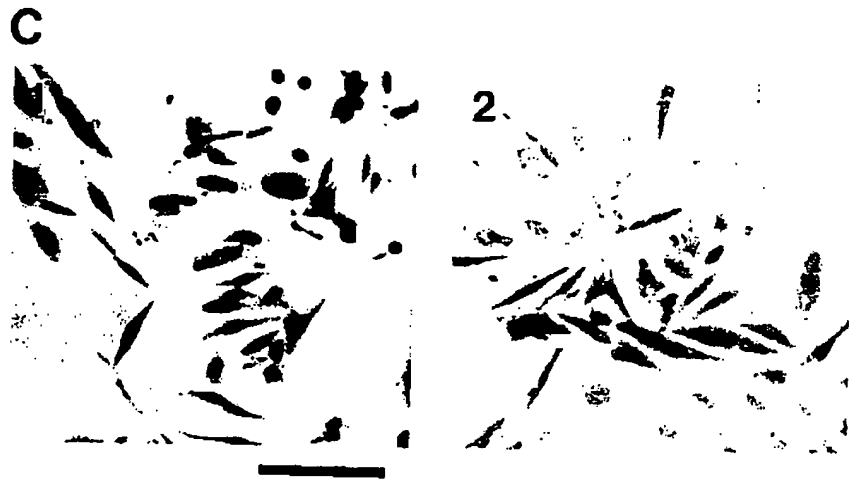

Figure 3. Characterization of CHO-vgr-1 stable transfectants. (*A*) Northern blot analysis of total RNA from CHO (lane *1*) and CHO-vgr-1 cells (lane *2*) after hybridization with vgr-1 cDNA and stringent washing. The positions of 28S and 18S ribosomal RNA are marked. (*B*) Western blot analysis of conditioned media from CHO (lanes *1* and *3*) and CHO-vgr-1 cells (lanes *2* and *4*) incubated with either antisera directed against the vgr-1 precursor segment (lanes *1* and *2*) or mature vgr-1 protein (lanes *3* and *4*). Protein standards are noted. (*C*) Immunostaining of (*1*) CHO and (*2*) CHO-vgr-1 transfectants with affinity-purified vgr-1 antibody directed against the precursor portion of the molecule. Bar, 100 μm.

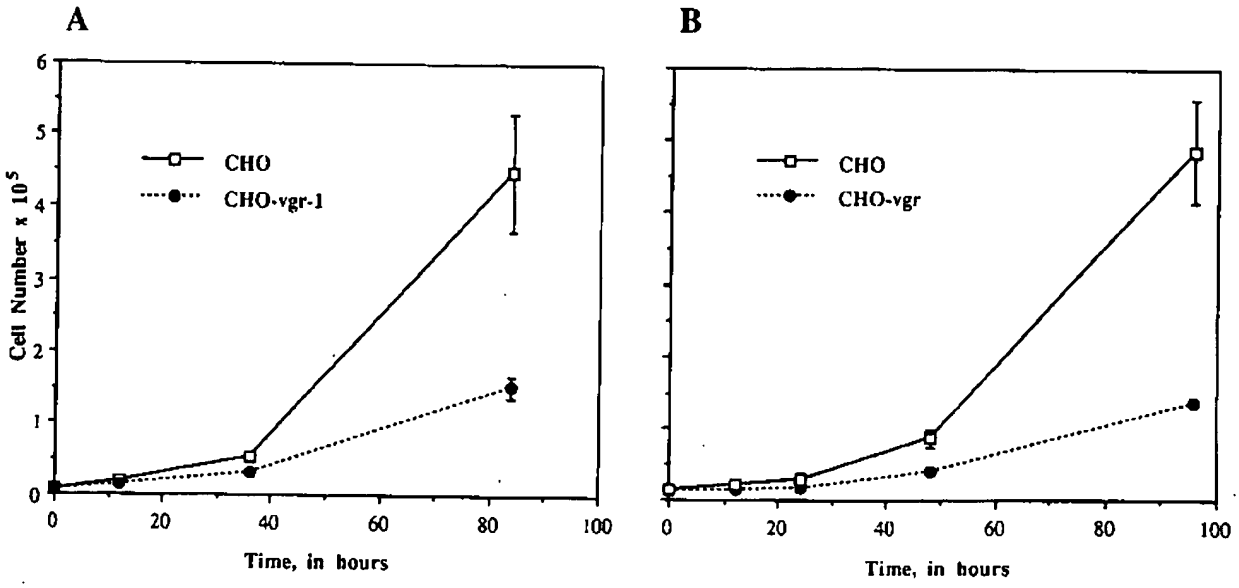

Figure 4. Growth rate of CHO vs CHO-vgr-1 transfectants. Cells were grown in either 10% fetal calf serum (*A*) or in insulin, transferrin, and selenium (*B*). The growth of CHO cells is represented by the full line with open symbols, and CHO-vgr-1 cells are noted by the dashed line with closed symbols. Three independent plates were grown for each cell type under each condition at each time point, and each plate was counted individually three times and then averaged. Each point on the graph represents the average of these readings, with standard deviation as noted by the error bars.

died from nonspecific causes before visible tumor growth occurred. After 2 wk, tumors were visible in all mice injected with either cell line. In concordance with the in vitro growth rate studies, the tumors produced by the parental cells grew faster than those from the vgr-1–transfected CHO cells (data not shown). After 1 mo, or by the time the tumors reached 4 cm in largest diameter, the animals were killed and autopsies were performed.

The tumors produced by both cell types were well localized and encapsulated. However, the tumors had striking differences in gross morphology (Fig. 5). The parental cells produced tumors with a convoluted surface, and they were hemorrhagic, necrotic, and friable (Fig. 5 *A*). In contrast, the CHO-vgr-1 tumors did not have a significant hemorrhagic component, had a smooth surface, and were quite dense, firm, and fibrotic (Fig. 5 *B*).

Histological examination of these tumors further highlighted the differences noted in the gross morphology. Hematoxylin and eosin staining of the CHO tumors showed nests of tumor cells surrounded by necrotic debris, as well as red and white blood cells (Fig. 6 *A*). Similar nests of tumor cells were also seen in the CHO-vgr-1 tumors, but there were no significant areas of necrosis. Moreover, the tumor cells were encompassed by regions of fibrosis, with significant expansion of surrounding connective tissue (Fig. 6 *B*). The tumors induced by the CHO-vgr-1 cells appeared to contain a well-developed vasculature, which in turn supported the growth and development of an organized tissue mass.

Bone and Cartilage Formation in vgr-1 Expressing CHO Tumors

Further histological examination of hematoxylin-eosin-stained tissue sections from CHO-vgr-1 revealed regions of cartilage and bone tissue within portions of the mesenchyme in and around the tumors, accounting for ~20% of the tumor mass (Fig. 6 *C*). These areas contained varying amounts of cartilage and bone, with some consisting solely of cartilage, others containing a mixture of both cartilage and bone, and finally, areas corresponding solely to bone. No bone and cartilage tissue was observed in any of the tumors derived from the parental CHO cells.

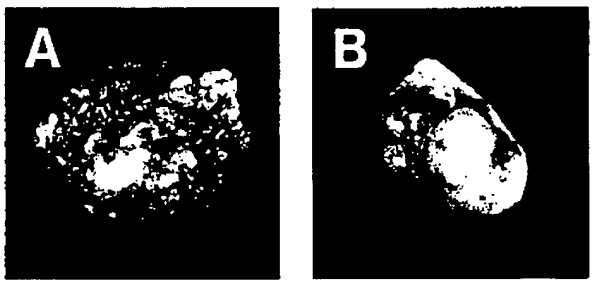

Figure 5. Gross morphology of tumors produced by CHO or CHO-vgr-1 cells. (*A*) A CHO tumor, with convoluted surface and significant hemorrhage, was friable and necrotic. (*B*) A CHO-vgr-1 tumor, with smooth surface and only limited hemorrhage, was firm, dense, and fibrotic. Scale bar indicates the size of the tumors.

To further characterize these areas of bone and cartilage formation, we performed several histochemical and immunohistochemical staining procedures. In Fig. 7, the tumor sections were stained with Alcian blue, which binds to mucopolysaccharides found in cartilage. The CHO tumor sections did not stain with Alcian blue, but only with the counterstain, whereas the CHO-vgr-1 tumors contained extensive regions of blue staining (Fig. 7, *A* and *B*). At higher magnification, these areas appeared morphologically as chondrocytes or hypertrophic chondrocytes (Fig. 7 *C*). An adjacent section was stained by the von Kossa method, and some of these same areas stained black, indicating regions of mineralization. Thus, such areas contained hypertrophic cartilage that had mineralized; if this tumor had been incubated longer in vivo, then this area would presumably have been replaced by bone.

To confirm areas of bone formation within the CHO-vgr-1 tumors, we analyzed different sections using the von Kossa and trichrome staining methods. As shown in Fig. 8, CHO-vgr-1 tumors, but not tumors derived from the parental CHO cells, had areas that stained positively in regions that appeared morphologically as trabecular bone. At a higher magnification, we noted the presence of osteoblasts, osteocytes, and osteoclasts within such areas of trabecular bone.

The regions of cartilage and bone were further defined with immunohistochemical analyses for collagen II, which is specifically deposited in cartilage, and for collagen I and osteocalcin, proteins associated with bone. Portions of the CHO-vgr-1 tumor stained specifically with the collagen II antibody, with such staining apparent in cartilage matrix, but not in areas of apparent bone formation (Fig. 9 *A*). No collagen II staining was detected in the CHO tumors. Other areas that appeared histologically as bone were stained with antibodies for both collagen I and osteocalcin (Fig. 9, *B* and *C*). No such dual collagen I and osteocalcin staining was seen in any region of the CHO tumors. Collagen I staining was not confined to bone in the CHO-vgr-1 tumors, but was also noted within areas of surrounding connective tissue; widespread staining was also noted within the CHO tumors in regions of necrotic debris. Finally, CHO-vgr-1 tumors also had regions that stained with all three antibodies, indicative of cartilage adjacent to bone tissue (Fig. 9 *D*). Collectively, these findings suggest that there had been a recapitulation of endochondral bone formation within these tumors, in which a cartilage template formed initially and was eventually replaced by bone.

We postulated that the vgr-1 secreted by the transfected CHO cells had induced mesenchymal cells of the host animal to differentiate into bone and cartilage. Indeed, mesenchymal cells are known to differentiate into chondroblasts and osteoblasts, whereas CHO cells are not known to differentiate. To prove this hypothesis, we designed a riboprobe for in situ hybridization to distinguish injected CHO cells from host mouse cells. Although both the host and transfected CHO cells expressed endogenous dhfr mRNA, the CHO cells also overexpressed an additional dhfr mRNA derived from the transfected expression vector (45). This latter transcript contained a unique 3′ untranslated region derived from the hepatitis B surface antigen gene. This region served as a riboprobe to specifically identify CHO cells within the tumor samples. As seen in Fig. 10 *A*, the antisense riboprobe hybridized intensely to the nests of CHO-

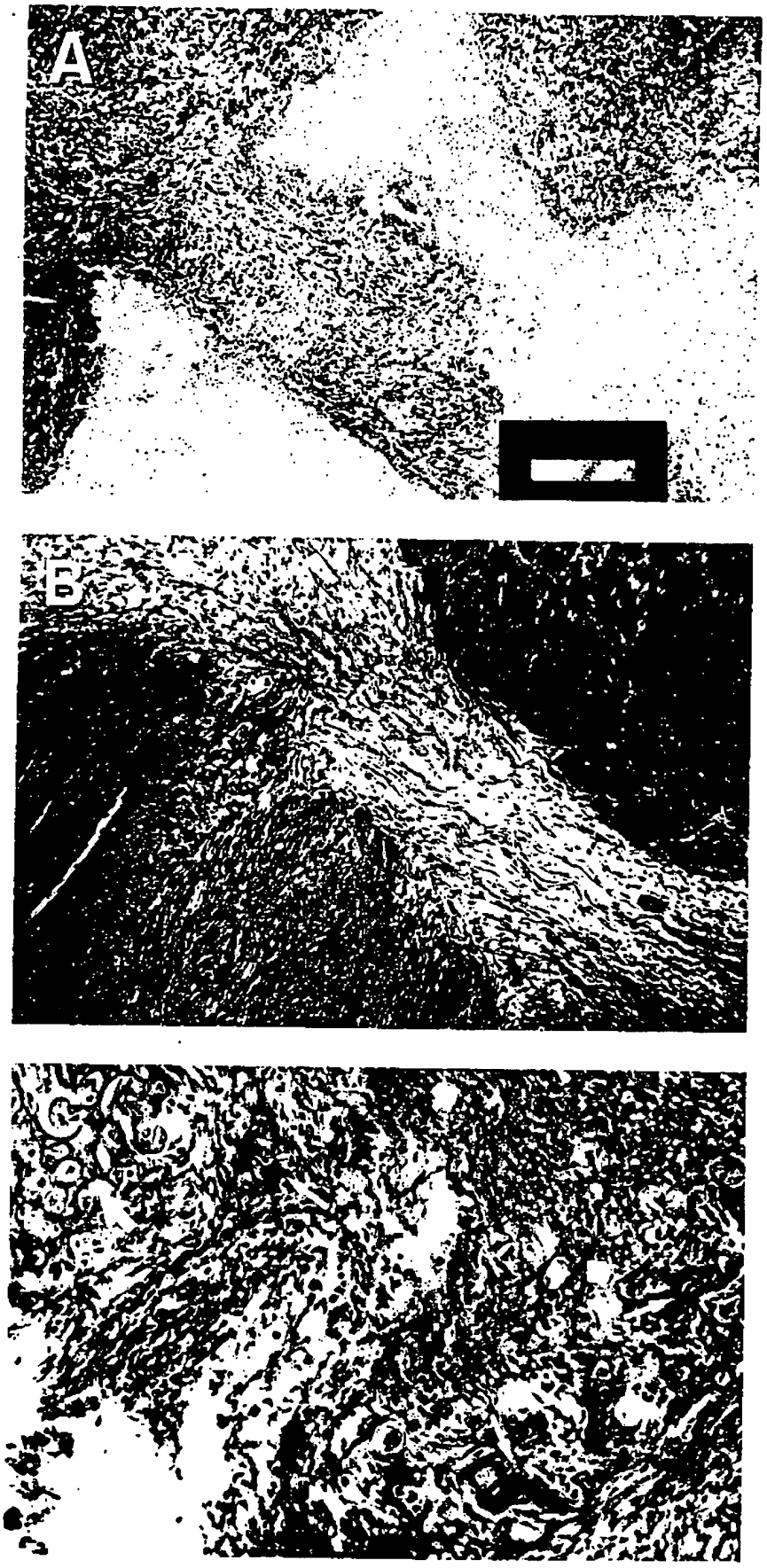

Figure 6. Haematoxylin and eosin staining of tumors. (*A*) Section from a CHO tumor, showing areas of darker stained tumor cells with surrounding hemorrhage (*orange*) and necrosis (*lighter stained pink areas*). Bar, 200 μm. (*B*) Section from a CHO-vgr-1 tumor, showing two regions of darker stained tumor cells separated by connective tissue. (*C*) Section of CHO-vgr-1 tumor showing areas of cartilage (*upper left corner of figure, large arrow*) and bone (*smaller arrows*). Magnification for *A* and *B* is ×10, and *C* is ×20.

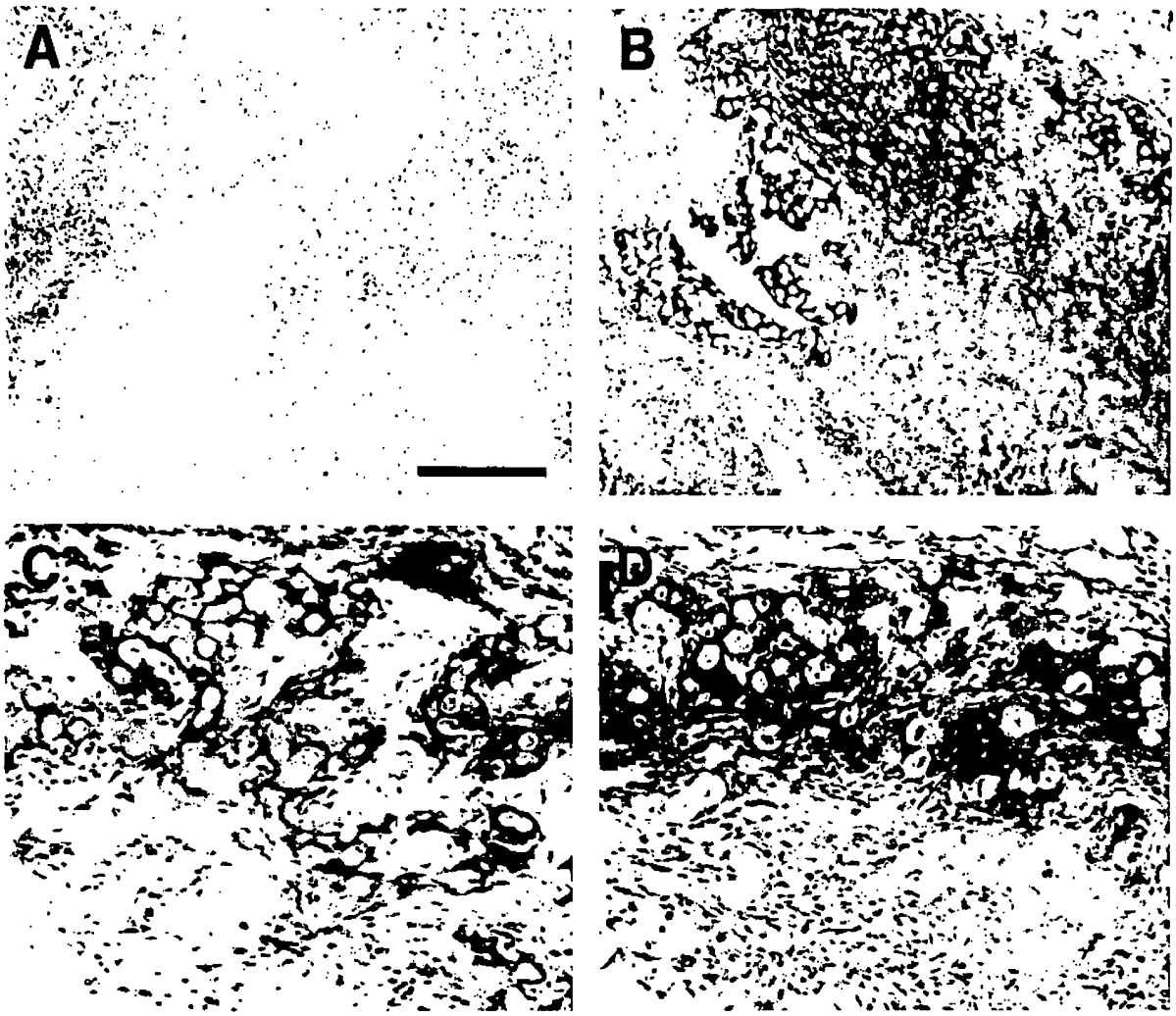

Figure 7. Regions of cartilage within the CHO-vgr-1 tumors. (*A*) CHO tumor stained with Alcian blue and nuclear fast red counterstain, with only the counterstain visualized. CHO cells are present in the upper left corner of the figure, with surrounding necrotic debris and red blood cells (*tan*). Image is seen at ×10. Bar, 200 μm. (*B*) ×10 view of CHO-vgr-1 tumor stained with Alcian blue, with marked areas of intense blue staining the matrix surrounding chondrocytes. (*C*) ×20 view of the Alcian blue staining region shown in *B*. Cell morphology corresponds to chondrocytes and hypertrophic chondrocytes. (*D*) von Kossa stain of an adjacent section, with black areas corresponding to mineralization of some portions of the cartilage.

vgr-1 tumor cells, but did not react with the cells in the cartilage and bone tissue and surrounding mesenchyme at the tumor periphery. Therefore, the cells within these tissues must have arisen from mesenchymal cells of the host animal that had been incorporated into the tumor. A low, uniform background of nonspecific hybridization was seen using the sense strand probe as a negative control (Fig. 10, *C* and *D*). This conclusion was further strengthened by the positive immunostaining for osteocalcin (Fig. 9). This antibody recognizes only mouse but not hamster osteocalcin, confirming that the bone tissue must have originated from mouse.

Discussion

Little is currently known about the function of a distinct subgroup of the TGF-β superfamily consisting of BMP-5, vgr-1/BMP-6, OP-1/BMP-7, and OP-2. We have focused on vgr-1/BMP-6 as a prototype member of this subgroup. The previous finding that vgr-1 mRNA is the only TGF-β superfamily member localized to hypertrophic cartilage suggests that it may play a pivotal role in the transition of cartilage to bone during endochondral bone formation. We report here the generation of vgr-1-specific antibodies and the subsequent immunohistochemical localization of vgr-1 protein to hypertrophic cartilage. Furthermore, we produced stably transfected CHO cells expressing recombinant vgr-1 protein at high levels. Finally, we injected the vgr-1-expressing CHO cells into mice to evaluate the effects of continuous release of vgr-1 in vivo. In contrast to the nontransfected cells, the tumors formed by vgr-1-expressing cells contained extensive areas of fibrosis, with bone and cartilage formation in a pattern that seemed to mimic endochondral bone formation.

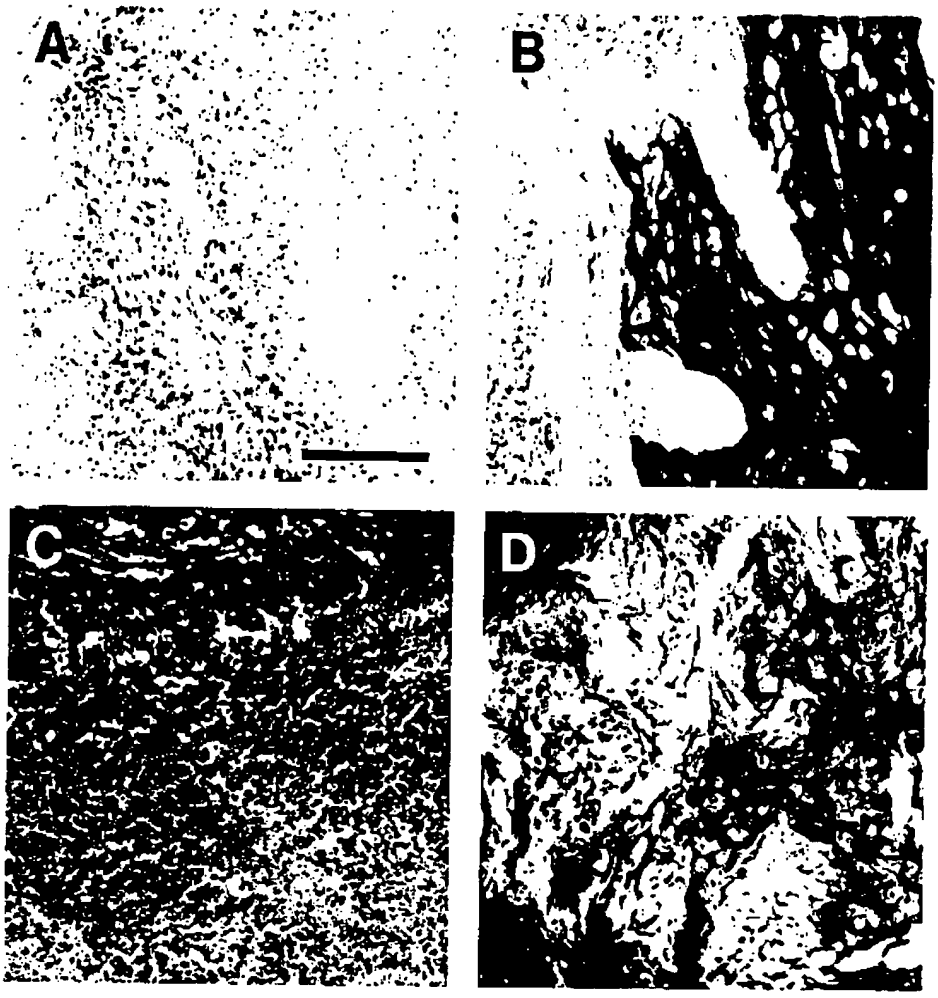

Figure 8. Regions of bone within the CHO-vgr-1 tumors. (*A*) von Kossa stain of CHO-tumor, with only background nuclear fast red stain visualized. CHO cells stain pink, and they are visualized in the left central portion of the figure surrounded by necrotic debris and red blood cells (*staining tan*). (*B*) von Kossa stain of CHO-vgr-1 tumor, with black areas corresponding to regions of trabecular bone. CHO-vgr-1 cells are the pink-stained cells on the left side of the figure. (*C*) Trichrome stain of CHO tumor with no positive staining, and only the Weigert hematoxylin counterstain is visualized. CHO cells are the magenta-stained regions on the upper portion of the figure. (*D*) Trichrome stain of CHO-vgr-1 tumor with intense blue staining of trabecular bone. CHO-vgr-1 cells are the magenta-stained regions in the upper left and lower left portions of the figure. All images are seen at ×20. Bar, 100 μm.

Vgr-1 Expression in Hypertrophic Cartilage

Previous studies have localized vgr-1 expression in the developing mouse using both in situ hybridization and immunohistochemistry (21, 29, 50). The former studies established the expression of vgr-1 mRNA in the central nervous system, suprabasal layer of the epidermis and other epithelial structures, and in hypertrophic cartilage. However, using immunohistochemistry, vgr-1 protein was found only in the central nervous system and epithelial structures, but not in hypertrophic cartilage, leading to the suggestion that the mRNA may not be translated in the latter tissue (50). We now report that vgr-1 mRNA is indeed translated into protein in hypertophic chondrocytes, as assessed by immunohistochemical staining using our vgr-1 antibody. The antibody staining is highly localized in the matrix surrounding the hypertrophic chondrocytes. This staining pattern strongly suggests that the secreted vgr-1 has a very limited diffusion range and that the hypertrophic cartilage matrix serves as a reservoir for this TGF-β superfamily member.

Vgr-1 was immunolocalized to hypertrophic cartilage solely using an antibody against the mature, carboxy-terminal portion of the protein. In contrast, both Wall et al. (50) and ourselves were unable to detect protein expression in this tissue using an antibody directed against the vgr-1 precursor segment. The reason for this inability remains unclear. One possibility is that the precursor region has acquired an altered conformation, either naturally or as a result of the treatment procedure, that renders it inaccessible to the antibody. If this were the case, then this modification must be different from that in epithelial structures and in the central nervous system, where the vgr-1 precursor antibody was used successfully. Alternatively, the vgr-1 precursor segment may be proteolytically degraded in hypertrophic cartilage. This would resemble the proteolytic activation of TGF-β1 in situ after irradiation, which is accompanied by a strong decrease in immunostaining using a precursor-specific antibody (2). Such vgr-1 precursor segment degradation could, in turn, provide higher accessibility of mature vgr-1 for its receptor, as in the case of TGF-β.

Recombinant Expression of vgr-1 Protein and Biological Activity In Vivo

To evaluate the biological functions of murine vgr-1, we generated an efficient expression plasmid to overexpress recombinant protein. CHO cells stably transfected with this vector synthesized and secreted high levels of recombinant vgr-1 protein, approximately half of which had undergone the predicted proteolytic cleavage. The transfected cells grew

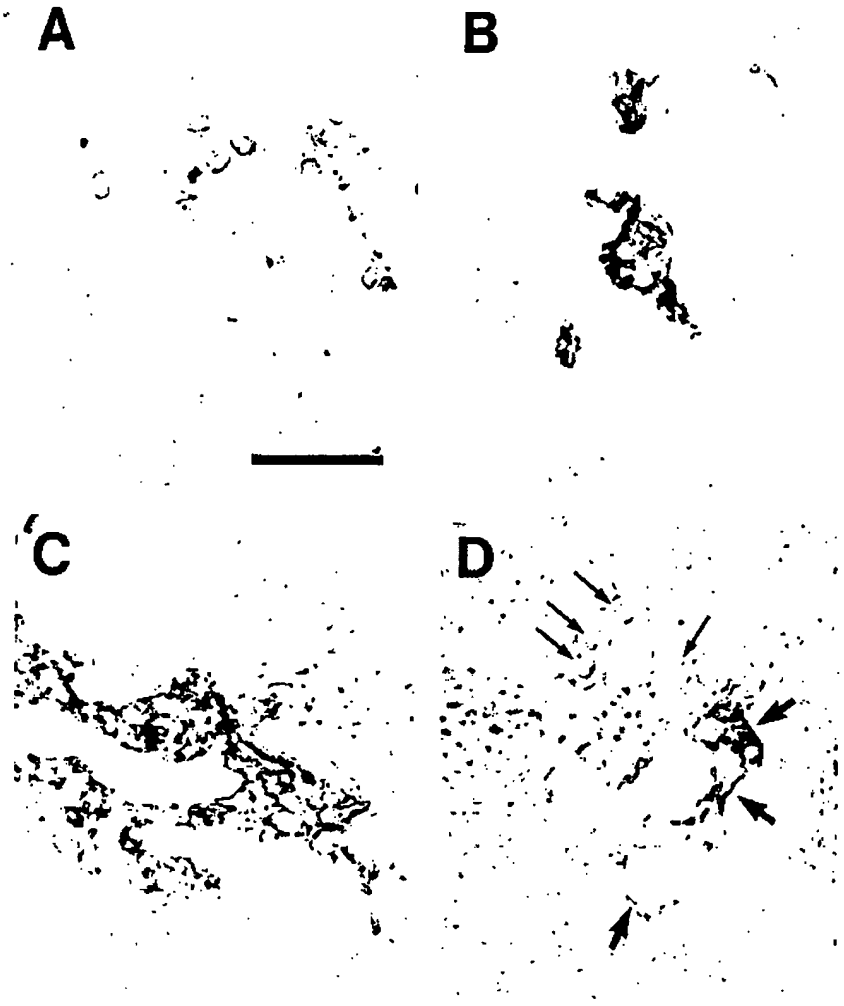

Figure 9. Immunohistochemistry of bone and cartilage in CHO- vgr-1 tumors. (*A*) CHO-vgr-1 tumor section stained with a collagen II antibody, identifying areas of cartilage formation (*brown*). (*B*) CHO-vgr-1 tumor section stained with a collagen I antibody, identifying regions corresponding to bone (*brown*). (*C*) CHO-vgr-1 tumor section stained with an osteocalcin antibody, identifying regions corresponding to bone (*brown*). (*D*) CHO-vgr-1 tumor section that contains an area that appears morphologically as bone (*large arrows*), and stained with collagen II antibody, identifying chondrocytes that are adjacent to bone tissue (*circular brown areas noted by smaller arrows*). All views are ×20. Bar, 100 μm.

slower than the parental cells, but otherwise exhibited no significant differences when characterized in vitro.

To assay the biological activity of vgr-1 in vivo, we introduced the CHO-vgr-1 transfectants directly into mice via a subcutaneous injection, rather than first purifying recombinant protein from conditioned media of the CHO-vgr-1 cells. Previous studies have documented that CHO cells form localized tumors when injected subcutaneously (13), and we reasoned that the transfected cells would act as a depot source of vgr-1 by continuously releasing the recombinant protein within the tumor. As expected, injection of the CHO-vgr-1 stable transfectants in nude mice induced tumor formation, as did the parental cells. However, the CHO-vgr-1 tumors showed a striking increase in surrounding connective tissue and exhibited bone and cartilage formation. Some areas showed only cartilage or trabecular bone; others contained bone intimately associated with adjacent areas of cartilage, or contained areas of mineralized cartilage. Taken collectively, these findings suggest recapitulation of endochondral bone formation, in which a cartilage template is first formed, and is later replaced by mineralized bone.

Another fundamental difference between the tumors induced by the CHO cells as opposed to the CHO-vgr-1 transfectants was that the parental cells produced tumors lacking any organized vascular supply. Thus, overgrowth of these cells resulted in hemorrhagic, necrotic debris, and the tumors were unable to support development of an organized tissue mass. By contrast, the CHO-vgr-1 cells formed tumors with a well-delineated vascular supply, and thereby supported development of well-organized tumor masses, with profusion of connective tissue and differentiation of cartilage and bone. During endochondral bone formation, angiogenesis in hypertrophic cartilage is critical for mineralization and subsequent bone formation. The endogenous localization of vgr-1 to the site of angiogenesis in hypertrophic cartilage suggests that this factor may mediate new vessel formation.

The cellular elements of fibrosis and endochondral bone formation within the CHO-vgr-1 tumors did not appear to have arisen directly from the CHO cells, but instead from the effects of secreted vgr-1 on surrounding host mesenchymal cells. Several lines of evidence support this hypothesis. First, the connective tissue, cartilage, and bone did not hybridize with a riboprobe that specifically identified the transfected CHO cells. Second, CHO cells are not known to differentiate

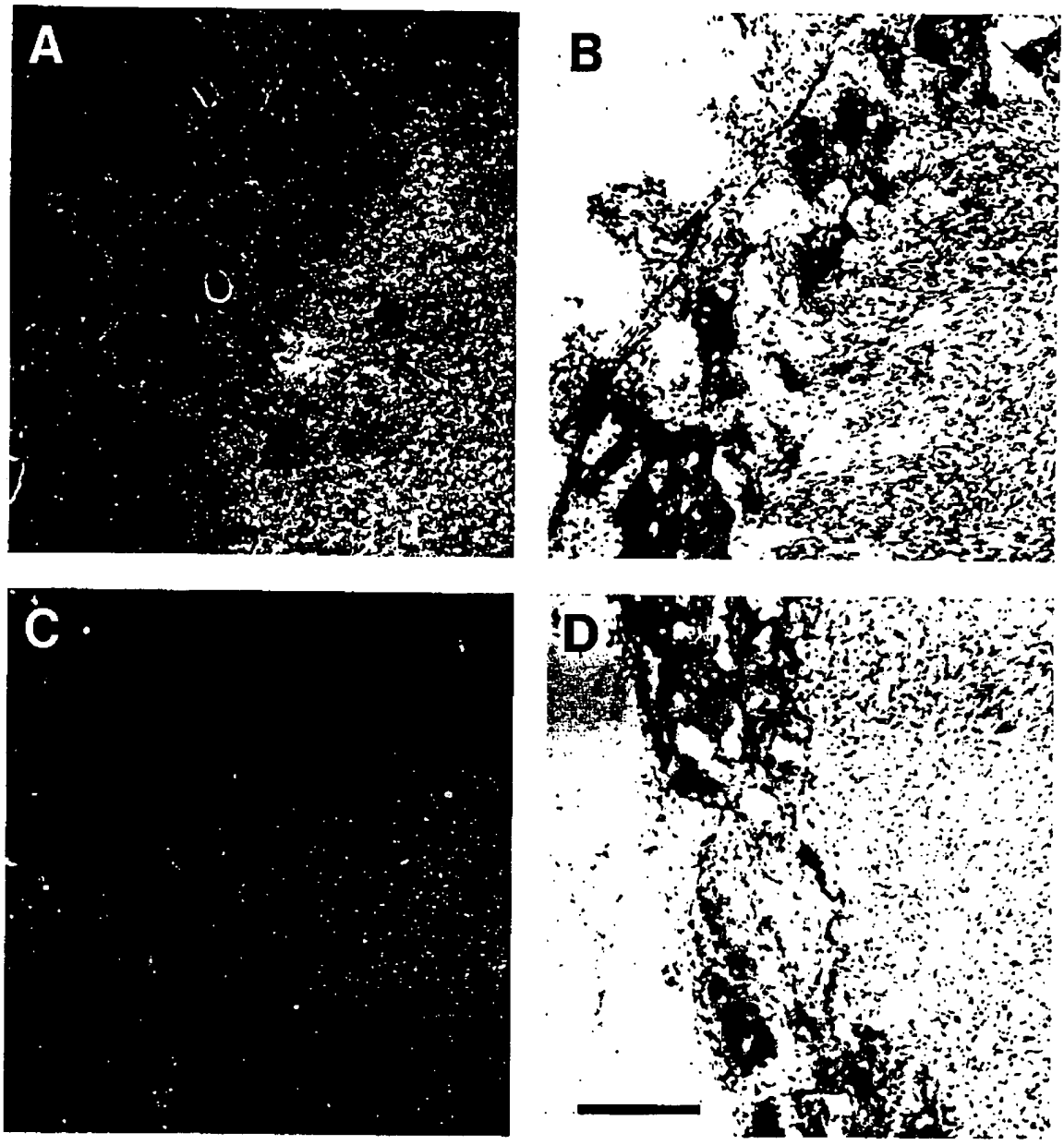

Figure 10. In situ hybridizations to define CHO cells within the tumors. (*A*) Dark-field microscopy of section from a CHO-vgr-1 tumor that has been hybridized with an antisense riboprobe directed against the 3′ untranslated region of hepatitis B surface antigen. This probe corresponds to part of the dhfr transcript generated from the expression vector transfected into the CHO cells, and most importantly, it identifies an mRNA specific to the CHO cells. White grains correspond to probe that has hybridized to CHO-vgr-1 cells. Note that the bone and surrounding mesenchyme lack significant hybridization. (*B*) Bright-field view of section shown in *A*. The darker staining regions correspond to trabecular bone. (*C*) Dark-field microscopy of section from a CHO-vgr-1 tumor that has been hybridized with a sense riboprobe to hepatitis B surface antigen, serving as a negative control. A low level of background hybridization is shown uniformly throughout the section. (*D*) Bright-field view of the section shown in *C*. All views are ×10. Bar, 200 μm.

in vitro or in vivo, making it unlikely that the vgr-1-transfected CHO cells differentiated into osteoblasts or chondrocytes. In fact, the transfected cells exhibited no such differentiation when evaluated in vitro. Third, the bone matrix within the CHO-vgr-1 tumors stained positively using a monoclonal antibody specific for mouse osteocalcin that does not cross-react with rat or hamster osteocalcin, further substantiating our conclusion that the ectopic bone did not originate from hamster cells. Finally, conditioned media from CHO-vgr-1 cells, but not from CHO cells, also induced ectopic bone formation when injected intramuscularly (Kirk, M., and S. E. Gitelman, unpublished results).

Vgr-1 secreted by the CHO-vgr-1 tumors appeared to have acted only locally within these animals. We have not devel-

oped an assay to measure serum levels of vgr-1, and thus have not formally tested if these animals contained significant circulating levels of this factor. However, analysis of long bones near the site of the tumor showed no changes as compared to those of the control animals, and extensive autopsies revealed no significant changes in any other major organs.

Possible Mechanisms of Vgr-1 Action

Our findings indicate that recombinant vgr-1 protein was sufficient to induce fibrosis and bone and cartilage formation in vivo. Yet, the complexity of such an in vivo study makes it difficult to pinpoint the specific primary actions directly attributable to vgr-1, as opposed to secondary actions mediated through other factors. One important function of vgr-1, at least in the context of this study, may be as a chemoattractant to bring various cell types to the tumor, including mesenchymal precursors. Alternatively, vgr-1 may act as a mitogen to increase the number of various host cells already present in or near the tumor. In fact, several other members of the TGF-β superfamily can serve as chemoattractants or mitogens for a variety of cell types, including mesenchymal cells, fibroblasts, osteoblasts, neutrophils, monocytes, epithelial cells, and endothelial cells (for examples, see references 19, 39, 42, 58). The most widely studied factor from this standpoint has been TGF-β1. Injection of recombinant TGF-β1 into newborn mice and chicken chorioallantoic membrane induces a granulation tissue response, with inflammation, fibrosis, and angiogenesis (42, 58). The hypercellular lesions in the chicken study resulted not from cellular proliferation, but from enhanced cell migration through chemotaxis (58). Only limited studies have been conducted with the BMPs, with BMP-3 and BMP-4 chemotactic for monocytes in vitro (9). Further studies are needed to determine if vgr-1 also serves as a chemoattractant and/or mitogen, and if vgr-1's actions in this regard are distinguishable from that of other members of the TGF-β superfamily. Vgr-1 does not alter the growth rate of two pluripotent mesenchymal cell lines in vitro, suggesting that it may not function as a mitogen in vivo (Gitelman, S. E., J. Q. Ye, and R. Derynck, unpublished results).

The influx of additional host cells into the tumor site adds another layer of complexity in characterizing the primary actions of vgr-1. Each of these cell types may release additional factors into the tumor area, such as other TGF-β superfamily members, local growth factors, cytokines, or various extracellular matrix proteins. Vgr-1 may act in a paracrine fashion to stimulate production and release of such factors from these neighboring host cells, and may also act in concert with these factors to induce the fibrotic changes and endochondral bone formation noted within the CHO-vgr-1 tumors.

Role of TGF-β Superfamily in Endochondral Bone Formation

Several members of the TGF-β superfamily have now been shown to induce endochondral bone formation when injected in vivo. TGF-β1 and TGF-β2 induce endochondral bone formation when introduced subperiosteally or at a fracture site, but not at a site that is not anatomically connected to bone (4, 23, 32, 35). In contrast, BMP-2, -3, -4, -7, and now vgr-1 have the ability to induce ectopic bone formation when injected intramuscularly or subcutaneously (17, 28, 43, 51, 54). Such findings suggest that these BMPs may act on a less differentiated mesenchymal precursor than TGF-β during endochondral bone formation. The findings also imply functional redundancy among these factors, yet specificity appears to reside in the spatially and temporally distinctive patterns of their expression (for an example, see reference 31).

In all other studies, a recombinant factor has been introduced in vivo as a purified protein delivered within an inert carrier. Our study is the first to have been conducted with direct injection of CHO cells that continuously release recombinant protein. As a result, comparison of vgr-1's potency with that of the other TGF-β related factors is not yet possible, and awaits purification of recombinant vgr-1 from conditioned media.

Definition of the specific role of individual TGF-β superfamily members in endochondral bone formation awaits more refined studies, both in vitro and in vivo. The present study entailed overexpression of vgr-1 in an ectopic location, and demonstrated that vgr-1 had the ability to initiate mesenchymal differentiation along the endochondral bone pathway. To further define the function of this factor during normal bone and cartilage development, it will be important to manipulate the expression of vgr-1 and its receptor within hypertrophic cartilage, vgr-1's endogenous site of production.

We thank Ilse Sauerwald for her assistance in fixation and sectioning of tissues and histological staining. We also acknowledge the generous help of Drs. Päivi Miettinen, Synthia Mellon, and Henry Rodriguez with the in situ hybridizations. We appreciate the interest and support of Arnold Kahn throughout the course of this work.

This work was supported by grants from the Lawson Wilkens Pediatric Endocrine Society (Genentech Clinical Scholar's Award) and National Institutes of Health (NIH) grant 1 K08 AR01897-01 to S. Gitelman, and NIH grants R01-AR41126 to R. Derynck, and P50DE10306 to the Research Center in Oral Biology.

Received for publication 5 January 1994 and in revised form 14 May 1994.

References

1. Asahina, I., T. K. Sampath, I. Nishimura, and P. V. Hauschka. 1993. Human osteogenic protein-1 induces both chondroblastic and osteoblastic differentiation of osteoprogenitor cells derived from newborn rat calvaria. *J. Cell Biol.* 123:921–933.
2. Barcellos-Hoff, M.-H., R. Derynck, M. L.-S. Tsang, and J. A. Weatherbee. 1994. Transforming growth factor-β activation in irradiated murine mammary gland. *J. Clin. Invest.* 93:892–899.
3. Basler, K., T. Edlund, T. M. Jessell, and T. Yamada. 1993. Control of cell pattern in the neural tube: regulation of cell differentiation by dorsalin-1, a novel TGF-β family member. *Cell.* 73:687–702.
4. Beck, L. S., L. Deguzman, W. P. Lee, Y. Xu, L. A. McFatridge, N. A. Gillett, and E. P. Amento. 1991. TGF-β1 induces bone closure of skull defects. *J. Bone Miner. Res.* 6:1257–1265.
5. Celeste, A. J., J. A. Iannazzi, R. C. Taylor, R. M. Hewick, V. Rosen, E. A. Wang, and J. M. Wozney. 1990. Identification of transforming growth factor β family members present in bone-inductive protein purified from bovine bone. *Proc. Natl. Acad. Sci. USA.* 87:9843–9847.
6. Chen, T. L., R. L. Bates, A. Dudley, R. G. Hammonds, and E. P. Amento. 1991. Bone Morphogenetic protein-2b stimulation of growth and osteogenic phenotypes in rat osteoblast-like cells: comparison with TGF-β1. *J. Bone Miner. Res.* 6:1387–1393.
7. Chomczynski, P., and N. Sacchi. 1987. Single-step method of RNA isolation by acid guanidium thiocyanate-phenol-chloroform extraction. *Anal. Biochem.* 162:156–159.
8. Clark, G. 1981. Staining Procedures. 4th ed. Williams and Wilkins, Baltimore.
9. Cunningham, N. S., V. Paralkar, and A. H. Reddi. 1992. Osteogenin and recombinant bone morphogenetic protein 2B are chemotactic for human monocytes and stimulate transforming growth factor β1 mRNA expression. *Proc. Natl. Acad. Sci. USA.* 89:11740–11744.
10. Derynck, R. 1994. Transforming growth factor β. *In* The Cytokine Handbook. 2nd ed. A. Thompson, editor. Academic Press, Boston. pp. 319–342.

11. Derynck, R., P. B. Lindquist, A. Lee, D. Wen, J. Tamm, J. L. Graycar, L. Rhee, A. J. Mason, D. A. Miller, R. J. Coffey, et al. A new type of transforming growth factor β, TGF-β3. *EMBO (Eur. Mol. Biol. Organ.) J.* 7:3737–3743.
12. Doctor, J. S., P. D. Jackson, K. E. Rashka, M. Visalli, and F. M. Hoffmann. 1992. Sequence, biochemical characterization, and developmental expression of a new member of the TGF-β superfamily in *Drosophila melanogaster*. *Dev. Biol.* 151:491–505.
13. Esko, J. D., K. S. Rostand, and J. L. Weinke. 1988. Tumor formation dependent on proteoglycan biosynthesis. *Science (Wash. DC).* 241:1092–1095.
14. Gazit, D., R. Ebner, A. J. Kahn, and R. Derynck. 1993. Modulation of expression and cell surface binding of members of the transforming growth factor-β superfamily during retinoic acid-induced osteoblastic differentiation of multipotential mesenchymal cells. *Mol. Endocrinol.* 7:189–198.
15. Gorman, C., R. Padmanabhn, and B. H. Howard. 1983. High efficiency DNA-mediated transformation of primate cells. *Science (Wash. DC).* 221:551–553.
16. Green, N., H. Alexander, A. Olson, S. Alexander, T. M. Shinnick, J. G. Sutcliffe, and R. A. Lerner. 1982. Immunogenic structure of the influenza virus hemagglutinin. *Cell.* 28:477–487.
17. Hammonds, R. G., R. Schwall, A. Dudley, C. Lai, L. Berkemeier, N. Cunningham, A. H. Reddi, W. I. Wood, and A. J. Mason. 1991. Bone-inducing activity of mature BMP-2b produced from a hybrid BMP-2a/2b precursor. *Mol. Endocrinol.* 4:149–155.
18. Hiraki, Y., H. Inoue, C. Shigeno, Y. Sanma, H. Benz, D. M. Rosen, A. Asada, and F. Suzuki. 1991. Bone Morphogenetic Proteins (BMP-2 and BMP-3) promote growth and expression of the differentiated phenotype of rabbit chondrocytes and osteoblastic MC3T3-E1 cells in vitro. *J. Bone Miner. Res.* 6:1373–1385.
19. Hughes, F. J., J. E. Aubin, and J. N. M. Heersche. 1992. Differential chemotactic responses of different populations of fetal rat calvaria cells to platelet-derived growth factor and transforming growth factor β. *Bone Miner.* 19:63–74.
20. Jessell, T. M., and D. A. Melton. 1992. Diffusible factors in vertebrate embryonic induction. *Cell.* 68:257–270.
21. Jones, C. M., K. M. Lyons, and B. L. M. Hogan. 1991. Involvement of bone morphogenetic protein-4 (BMP-4) and vgr-1 in morphogenesis and neurogenesis in the mouse. *Development (Camb.).* 111:531–542.
22. Jones, C. M., D. Simon-Chazottes, J.-L. Guenet, and B. L. M. Hogan. 1992. Isolation of Vgr-2, a novel member of the transforming growth factor-β-related gene family. *Mol. Endocrinol.* 6:1961–1968.
23. Joyce, M. E., A. B. Roberts, M. B. Sporn, and M. E. Bolander. 1990. Transforming growth factor-β and the initiation of chondrogenesis and osteogenesis in the rat femur. *J. Cell Biol.* 110:2195–2207.
24. Katagiri, T., A. Yamaguchi, T. Ikeda, S. Yoshiki, J. M. Wozney, V. Rosen, E. A. Wang, H. Tanaka, S. Omura, and T. Suda. 1990. The non-osteogenic mouse pluripotent cell line, C3H10T1/2, is induced to differentiate into osteoblastic cells by recombinant human bone morphogenetic protein-2. *Biochem. Biophys. Res. Commun.* 172:295–299.
25. Deleted in proof.
26. Kozak, M. 1987. An analysis of 5′-noncoding sequence from 699 vertebrate messenger RNAs. *Nucleic Acids Res.* 15:8125–8148.
27. Lee, S. J. 1990. Identification of a novel member (GDF-1) of the transforming growth factor-β superfamily. *Mol. Endocrinol.* 4:1034–1040.
28. Luyten, F. P., N. S. Cunningham, S. Ma, N. Muthukumaran, R. G. Hammonds, W. B. Nevins, W. I. Woods, and A. H. Reddi. 1989. Purification and partial amino acid sequence of osteogenin, a protein initiating bone differentiation. *J. Biol. Chem.* 264:13377–13380.
29. Lyons, K., J. L. Graycar, A. Lee, S. Hashmi, P. B. Lindquist, E. Y. Chen, B. L. M. Hogan, and R. Derynck. 1989. Vgr-1, a mammalian gene related to *Xenopus* Vg-1, is a member of the transforming growth factor beta gene superfamily. *Proc. Natl. Acad. Sci. USA.* 86:4554–4558.
30. Lyons, K. M., C. M. Jones, and B. L. M. Hogan. 1991. The DVR gene family in embryonic development. *Trends Genet.* 7:408–412.
31. Lyons, K. M., R. W. Pelton, and B. L. M. Hogan. 1989. Patterns of expression of murine Vgr-1 and BMP-2 RNA suggest that transforming growth factor-beta-like genes coordinately regulate aspects of embryonic development. *Genes & Dev.* 3:1657–1668.
32. Marcelli, C., A. J. Yates, and G. R. Mundy. 1990. In vivo effects of human recombinant transforming growth factor β on bone turnover in normal mice. *J. Bone Miner. Res.* 5:1087–1096.
33. McPherron, A. C., and S.-J. Lee. 1993. GDF-3 and GDF-9: two new members of the transforming growth factor-β superfamily containing a novel pattern of cysteines. *J. Biol. Chem.* 268:3444–3449.
34. Miettinen, P., and K. Heikinheimo. 1992. Transforming growth factor-alpha and insulin gene expression in human fetal pancreas. *Development (Camb.).* 114:833–840.
35. Noda, M., and J. J. Camilliere. 1989. In vivo stimulation of bone formation by transforming growth factor β. *Endocrinology.* 124:2991–2994.
36. Ozkaynak, E., D. C. Rueger, E. A. Drier, C. Corbett, R. J. Ridge, T. K. Sampath, and H. Opperman. 1990. OP-1 cDNA encodes an osteogenic protein in the TGF-β family. *EMBO (Eur. Mol. Biol. Organ.) J.* 9:2085–2093.
37. Ozkaynak, E., P. N. J. Schnegelsberg, D. F. Jin, G. M. Clifford, F. D. Warren, E. A. Drier, and H. Oppermann. 1992. Osteogenic protein-2. *J. Biol. Chem.* 267:25220–25227.
38. Padgett, R. W., R. D. Johnston, and W. M. Gelbart. 1987. A transcript from a *Drosophila* pattern gene predicts a protein homologous to the transforming growth factor-beta family. *Nature (Lond.).* 325:81–84.
39. Pfeilschifter, J., O. Wolf, A. Naumann, H. W. Minne, G. R. Mundy, and R. Ziegler. 1990. Chemotactic response of osteoblastlike cells to transforming growth factor β. *J. Bone Miner Res.* 5:825–830.
40. Reddi, A. H., and C. Huggins. 1972. Biochemical sequences in the transformation of normal fibroblasts in adolescent rats. *Proc. Natl. Acad. Sci. USA.* 69:1601–1605.
41. Roberts, A. B., and M. B. Sporn. 1990. The transforming growth factor-betas. *In* Handbook of Experimental Pharmacology. Peptide Growth Factors and their Receptors. Springer-Verlag, Heidelberg, Germany. M. B. Sporn and A. B. Roberts, editors. pp. 419–472.
42. Roberts, A. B., M. B. Sporn, R. K. Assoian, J. M. Smith, N. S. Roche, L. M. Wakefield, U. I. Heine, L. A. Liotta, V. Falanga, J. H. Kehrl, and A. S. Fauci. 1986. Transforming growth factor β: rapid induction of fibrosis and angiogenesis in vivo and stimulation of collagen formation in vitro. *Proc. Natl. Acad. Sci. USA.* 83:4167–4171.
43. Sampath, T. K., J. C. Maliakal, P. V. Hauschka, W. K. Jones, H. Sasak, R. F. Tucker, K. H. White, J. E. Coughlin, M. M. Tucker, R. H. L. Pang, et al. Recombinant human osteogenic protein-1 (hOP-1) induces new bone formation in vivo with a specific activity comparable with natural bovine osteogenic protein and stimulates osteoblast proliferation and differentiation in vitro. *J. Biol. Chem.* 267:20352–20362.
44. Sanger, F., S. Nicklen, and A. R. Coulson. 1977. DNA sequencing with chain-terminating inhibitors. *Proc. Natl. Acad. Sci. USA.* 74:5463–5467.
45. Simonsen, C. C., and A. D. Levinson. 1983. The isolation and expression of an altered mouse dihydrofolate reductase cDNA. *Proc. Natl. Acad. Sci. USA.* 80:2495–2499.
46. Urist, M. R. 1965. Bone: formation by autoinduction. *Science (Wash. DC).* 150:893–899.
47. Urlaub, G., and L. A. Chasin. 1980. Isolation of chinese hamster cell mutants deficient in dihydrofolate reductase activity. *Proc. Natl. Acad. Sci. USA.* 77:4216–4220.
48. von Heijne, G. 1986. A new method for predicting signal sequence cleavage sites. *Nucleic Acids Res.* 14:4683–4690.
49. Vukicevic, S., F. Luyten, and A. H. Reddi. 1989. Stimulation of the expression of osteogenic and chondrogenic phenotypes in vitro by osteogenin. *Proc. Natl. Acad. Sci. USA.* 86:8793–8797.
50. Wall, N. A., M. Blessing, C. V. E. Wright, and B. L. M. Hogan. 1993. Biosynthesis and in vivo localization of the decapentaplegic-Vg-related protein, DVR-6 (bone morphogenetic protein-6). *J. Cell Biol.* 120: 493–502.
51. Wang, E. A., V. Rosen, J. S. D'Alessandro, M. Bauduy, P. Cordes, T. Harada, D. I. Israel, R. M. Hewick, K. M. Kerns, P. LaPan, et al. Recombinant human bone morphogenetic protein induces bone formation. *Proc. Natl. Acad. Sci. USA.* 87:2220–2224.
52. Wigler, M., R. Sweet, G. K. Sim, B. Wold, A. Pellicer, E. Lacy, T. Maniatis, S. Silverstein, and R. Axel. 1979. Transformation of mammalian cells with genes from prokaryotes and eukaryotes. *Cell.* 16:777–785.
53. Wood, W. I., G. Cachianes, W. I. Henzel, J. A. Winslow, S. A. Spencer, R. Helmiss, J. L. Martin, and R. C. Baxter. 1988. Cloning and expression of the growth hormone-dependent insulin-like growth factor binding protein. *Mol. Endocrinol.* 2:1176–1185.
54. Wozney, J., V. Rosen, A. J. Celeste, L. M. Mitsock, M. J. Whitters, R. W. Kriz, R. M. Hewick, and E. A. Wang. 1988. Novel regulators of bone formation: molecular clones and activities. *Science (Wash. DC).* 242:1528–1534.
55. Wozney, J. M. 1992. The bone morphogenetic protein family and osteogenesis. *Mol. Reprod. Dev.* 32:160–167.
56. Yamaguchi, A., and A. J. Kahn. 1991. Clonal osteogenic cell lines express myogenic and adipocytic developmental potential. *Calcif. Tissue Int.* 49: 221–225.
57. Yamaguchi, A., T. Katagiri, T. Ikeda, J. M. Wozney, V. Rosen, E. A. Wang, A. J. Kahn, T. Suda, and S. Yoshiki. 1991. Recombinant human bone morphogenetic protein-2 stimulates osteoblastic maturation and inhibits myogenic differentiation in vitro. *J. Cell Biol.* 113:681–687.
58. Yang, E. Y., and H. L. Moses. 1990. Transforming growth factor β1-induced changes in cell migration, proliferation, and angiogenesis in the chicken chorioallantoic membrane. *J. Cell Biol.* 111:731–741.
59. Zhou, X., H. Sasaki, L. Lowe, B. L. Hogan, and M. R. Kuehn. 1993. Nodal is a novel TGF-beta-like gene expressed in the mouse node during gastrulation. *Nature (Lond.).* 361:543–547.

Exhibit D

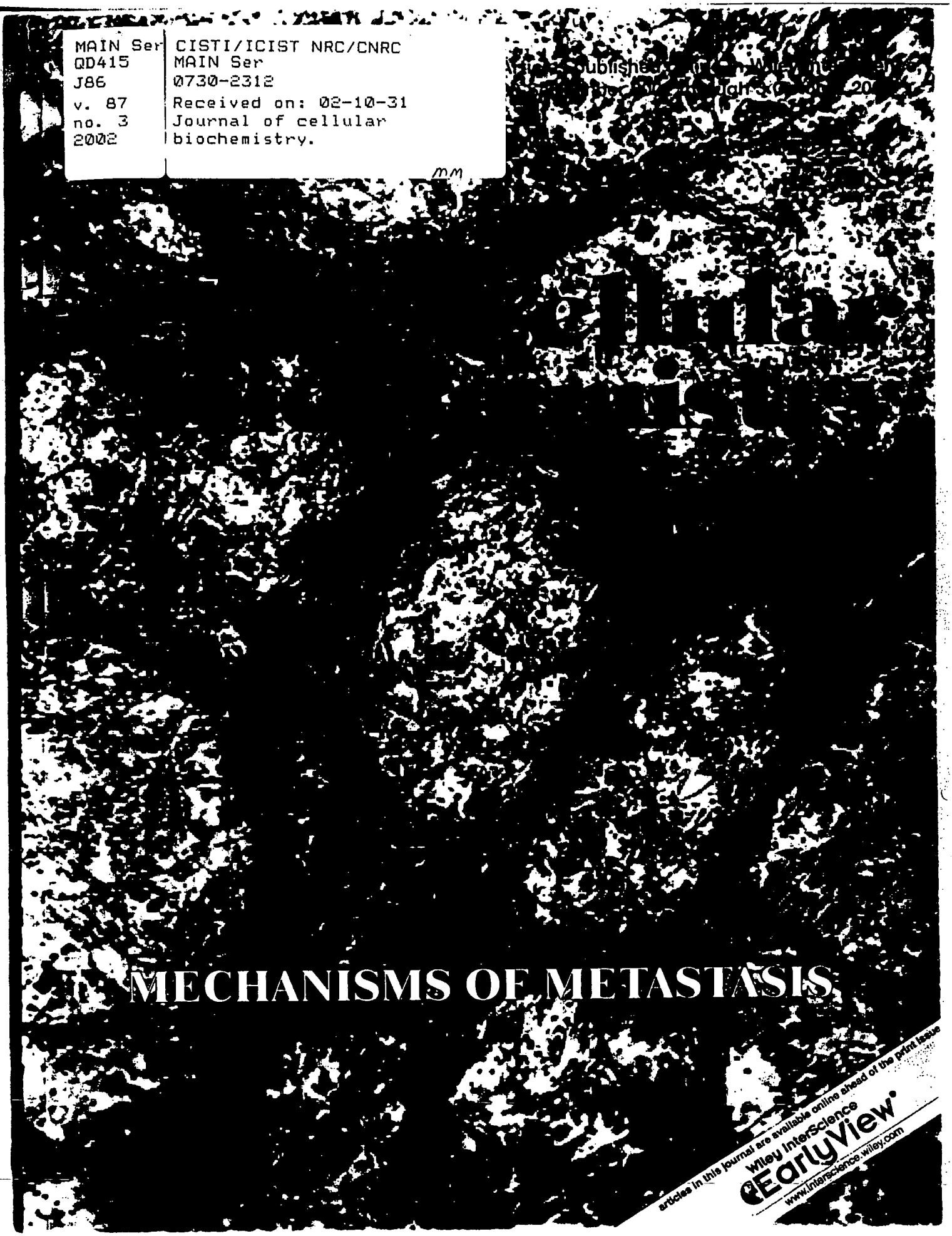

MECHANISMS OF METASTASIS

Journal of Cellular Biochemistry

Volume 87 • Number 3

MEETING REPORT

UICC Study Group on Basic and Clinical Cancer Research: Mechanisms of Metastasis
Max M. Burger 253
Published online 3 October 2002

PROSPECT

Roles for Cytoplasmic Polyadenylation in Cell Cycle Regulation
Rebecca L. Read and Chris J. Norbury 258
Published online 1 October 2002

ARTICLES

Hydrostatic Pressure Induces Apoptosis in Human Chondrocytes From Osteoarthritic Cartilage Through Up-Regulation of Tumor Necrosis Factor-α, Inducible Nitric Oxide Synthase, p53, c-myc, and bax-α, and Suppression of bcl-2
Najmul Islam, Tariq M. Haqqi, Karl J. Jepsen, Matthew Kraay, Jean F. Welter, Victor M. Goldberg, and Charles J. Malemud 266
Published online 1 October 2002

DNase I Sensitive Site in the Core Region of the Human β-globin Origin of Replication
Vera Djeliova, George Russev, and Boyka Anachkova 279
Published online 1 October 2002

Retinoid Signalling and Gene Expression in Neuroblastoma Cells: RXR Agonist and Antagonist Effects on CRABP-II and RARβ Expression
Quentin Campbell Hewson, Penny E. Lovat, Andrew D.J. Pearson, and Christopher P.F. Redfern 284
Published online 30 September 2002

Osteogenic Protein-1 (OP-1, BMP-7) Induces Osteoblastic Cell Differentiation of the Pluripotent Mesenchymal Cell Line C2C12
Lee-Chuan C. Yeh, Alicia D. Tsai, and John C. Lee 292
Published online 3 October 2002

BMP-2, BMP-4, and PDGF-bb Stimulate Chemotactic Migration of Primary Human Mesenchymal Progenitor Cells
Jörg Fiedler, Götz Röderer, Klaus-Peter Günther, and Rolf E. Brenner 305
Published online 30 September 2002

(continued on next page)

Cover shows bright-field microscopy of aggressive human melanoma cells on a three-dimensional type I collagen matrix stained with PAS (periodic acid-Schiff), forming vasculogenic-like networks. These tumor cells are engaged in vasculogenic mimicry and express multiple phenotypes illustrative of their plasticity, including endothelial-associated genes such as VE-cadherin. See Meeting Report in this issue by Dr. Max M. Burger, page 253. Photograph was provided by Dr. Angela Hess, The University of Iowa.

WILEY-LISS

A WILEY-LISS, INC., PUBLICATION

(continued from previous page)

TNF-α Suppresses Bone Sialoprotein (BSP) Expression in ROS17/2.8 Cells
Hiroshi Samoto, Emi Shimizu, Yuko Matsuda-Honjo, Ryoichiro Saito, Muneyoshi Yamazaki, Kazutaka Kasai, Shunsuke Furuyama, Hiroshi Sugiya, Jaro Sodek, and Yorimasa Ogata 313
Published online 1 October 2002

Evidence on the Operation of ATP-Induced Capacitative Calcium Entry in Breast Cancer Cells and Its Blockade by 17β-Estradiol
Ana M. Rossi, Gabriela Picotto, Ana R. de Boland, and Ricardo L. Boland 324
Published online 30 September 2002

Proliferation Marker pKi-67 Affects the Cell Cycle in a Self-Regulated Manner
Mirko H.H. Schmidt, Rainer Broll, Hans-Peter Bruch, and Michael Duchrow 334
Published online 30 September 2002

Alterations in the Spatiotemporal Expression Pattern and Function of N-Cadherin Inhibit Cellular Condensation and Chondrogenesis of Limb Mesenchymal Cells In Vitro
Anthony M. DeLise and Rocky S. Tuan 342
Published online 30 September 2002

Erratum 360

Erratum 361

Volume 87, Number 3, was mailed the week of October 28, 2002.

Journal of Cellular Biochemistry 87:292–304 (2002)

Osteogenic Protein-1 (OP-1, BMP-7) Induces Osteoblastic Cell Differentiation of the Pluripotent Mesenchymal Cell Line C2C12

Lee-Chuan C. Yeh,* Alicia D. Tsai, and John C. Lee

Department of Biochemistry, The University of Texas Health Science Center, San Antonio, Texas 78229-3900

Abstract The effects of Osteogenic Protein-1 (OP-1, BMP-7) on the differentiation of the pluripotent mesenchymal cell line, C2C12, were examined. OP-1 at 50 ng/ml partially inhibited myotube formation in C2C12 cells, while OP-1 at 200 ng/ml completely inhibited myotube formation and induced the formation of cells displaying osteoblastic morphology. High concentrations of OP-1 elevated the alkaline phosphatase (AP) activity dramatically, both as a function of time and OP-1 concentration. Osteocalcin (OC) mRNA expression was detected as early as 8 days in OP-1-treated cultures and subsequently increased considerably. Expression of bone sialoprotein (BSP) mRNA was low in control cultures and stimulated by OP-1. Collagen type I mRNA expression was enhanced by OP-1 during the early days in culture, but gradually decreased thereafter. MyoD mRNA expression, high in control cultures, was suppressed by OP-1 in a dose- and time-dependent manner. OP-1 enhanced ActR-I mRNA expression and significantly elevated the mRNA expressions of BMP-1, BMP-4, BMP-5, GDF-6, and GDF-8. The present results indicate that OP-1 is a potent inducer of C2C12 differentiation into osteoblastic cells. J. Cell. Biochem. 87: 292–304, 2002.

Key words: osteogenic protein-1; bone morphogenetic protein-7; osteoblastic cell differentiation; C2C12; gene expression; BMP expression; BMP receptor expression

Urist [1965] first reported that demineralized bone matrix could induce ectopic bone formation when implanted into muscular tissues and later attributed the activity to a factor(s) named bone morphogenetic protein (BMP) [Urist and Strates, 1971]. Subsequently, numerous BMPs have been discovered, purified, and their genes cloned. BMPs belong to the transforming growth factor-β (TGF-β) superfamily [Ozkaynak et al., 1990; Sampath et al., 1990; Kingsley, 1994; Wozney and Rosen, 1998; Reddi, 2000]. Based on the degree of their sequence homology, they can be further classified into several subfamilies: the BMP-2/BMP-4 subfamily, the BMP-3 subfamily, the BMP-5/BMP-6/BMP-7(OP-1)/BMP-8 subfamily, the BMP-9 subfamily, and the BMP-12(GDF-7, CDMP-3)/BMP-13(GDF-6, CDMP-2)/BMP-14 (GDF-5, CDMP-1) subfamily. Several BMPs exhibit multiple biological activities on different cell types [Dudley et al., 1995; Luo et al., 1995]. For example, Osteogenic Protein-1 (OP-1) [Asahina et al., 1993; Chen et al., 1995; Wu et al., 1997; Klein-Nulend et al., 1998], BMP-2, and BMP-4 [Paralkar et al., 1992; Katagiri et al., 1994; Hogan, 1996] induce bone and cartilage formation in vivo and stimulate expression of the osteoblast phenotype in osteoprogenitor cells in vitro [Thies et al., 1992; Kawasaki et al., 1998]. OP-1 also appears to be involved in the development/differentiation of different organs, such as the neural system, the heart, the kidney, the eye, and the oral tissues.

BMPs transduce their effects through the binding to two types of transmembrane serine/threonine kinase receptors: type I and type II. They are distinguishable by their amino acid sequences and functional features. Both type I and type II receptors bind ligands independently,

Grant sponsor: Stryker Biotech.

*Correspondence to: Lee-Chuan C. Yeh, PhD, Department of Biochemistry (MC7760), University of Texas Health Science Center, 7703 Floyd Curl Drive, San Antonio, TX 78229-3900. E-mail: carolyeh@biochem.uthscsa.edu

Received 23 July 2002; Accepted 24 July 2002

DOI 10.1002/jcb.10315

Published online 3 October 2002 in Wiley InterScience (www.interscience.wiley.com).

but the binding affinity is increased in the presence of both receptor types [Liu et al., 1995; Nohno et al., 1995; Rosenzweig et al., 1995]. Down-stream signaling also requires both type I and type II receptors. Three type I receptors have been shown to bind BMPs, i.e., activin receptor-like kinase (ALK-2, ActR-I), BMP type IA receptor (BMPR-IA, ALK-3), and BMPR-IB (ALK-6) [Koenig et al., 1994; ten Dijke et al., 1994; Macias-Silva et al., 1998]. Three type II receptors have also been identified, i.e., activin type II receptor (ActR-II), ActR-IIB, and BMPR-II [Liu et al., 1995; Nohno et al., 1995; Rosenzweig et al., 1995; Yamashita et al., 1995].

Previous studies have suggested that the pluripotent mesenchymal precursor cell line C2C12 may be a model to examine the early stage of osteoblast differentiation during bone formation in muscular tissues. For example, BMP-2 (300 ng/ml) inhibited myoblast differentiation of the C2C12 cells and promoted osteoblastic cell differentiation [Katagiri et al., 1994]. Similar results were obtained when C2C12 cells were transfected with a replication-deficient adenoviral vector expressing human BMP-2 [Okubo et al., 1999]. Subsequent studies showed that BMP-6 inhibited growth of C2C12 cells, reaching a maximum inhibition of about 40% at 1 μg/ml. The number of AP-positive cells in C2C12 cells increased in a BMP-6 dose-dependent manner, and BMP-6 appeared to be tenfold more potent than OP-1 in stimulating formation of AP-positive cells at the similar dosage [Ebisawa et al., 1999]. On the contrary, Inada et al. [1996] showed that BMP-12 and -13 inhibited myoblast cell differentiation without the induction of osteoblastic cell differentiation in C2C12 cells. These two BMPs were much less efficient in inhibiting myotube formation than BMP-2. TGF-β alone also inhibited myotube formation, but failed to induce the osteoblastic phenotype. TGF-β potentiated the inhibitory effect of BMP-2 on myotube formation, but also reduced the BMP-2-induced alkaline phosphatase (AP) activity and osteocalcin expression.

Here we report the effects of OP-1 on cell differentiation and gene expression in the pluripotent mesenchymal precursor C2C12 cells. Continuous exposure of C2C12 cells to OP-1 inhibited myotube formation and induced the formation of osteoblasts. Concomitantly, MyoD mRNA expression was suppressed, but the AP activity and the mRNA expression of osteocalcin (OC) as well as bone sialoprotein (BSP) were stimulated by OP-1. Northern blot analysis also showed detectable mRNA levels coding for ActR-I, BMPR-IA, BMPR-IB, and BMPR-II in control cells. OP-1 stimulated ActR-I mRNA expression, but did not appear to alter the expression of the others.

MATERIALS AND METHODS

Materials

Recombinant human OP-1 was provided by Stryker Biotech (Hopkinton, MA) and was dissolved in 47.5% ethanol/0.01% trifluoroacetic acid. Radioisotopes were purchased from ICN (Irvine, CA). Fetal bovine serum (FBS), Hank's Balanced Salt Solution (HBSS), Dulbecco's modified Eagle's medium (DMEM), penicillin/streptomycin, trypsin-EDTA, and collagenase were purchased from Life Technologies (Grand Island, NY). TRI Reagent was from Sigma (St. Louis, MO). All reagents were of molecular biology grade. All buffers were prepared with diethylpyrocarbonate-treated water.

Cell Culture and Microscopic Examination

The mouse pluripotent mesenchymal precursor cell line C2C12 was purchased from American Type Culture Collection (Rockville, MD). C2C12 cells were cultured in DMEM containing 10% FBS and penicillin/streptomycin at 37°C in a humidified 5% CO_2 atmosphere. For experimentation, C2C12 cells were subcultured in DMEM containing 5% FBS and in the absence or presence of various concentrations of OP-1. For the AP activity assay, cells were grown in 48-well plates. For isolation of total RNA, cells were grown in 100-mm culture dishes. Media were replenished every 3 days. Cell morphological changes were monitored with a phase contrast microscope, and the images were captured after 2, 4, 8, 12, and 16 days of treatment, using an Olympus CK2 inverted microscope equipped with a CCD camera.

Alkaline Phosphatase Activity Assay

After 2, 5, 8, 12, and 15 days of culturing in the presence of OP-1, cells were rinsed with PBS and lysed by sonication in 0.1% Triton X-100 in PBS (100 μl/well) for 5 min at room temperature. The total cellular AP activity in C2C12 cells was measured using a commercial assay

kit (Sigma Chemical Co.) as described previously [Yeh et al., 1996]. Reactions were terminated by the addition of 0.5N NaOH. Absorbance of the reaction mixture was measured at 405 nm using a MRX-II microplate reader (Dynex Technologies, Chantilly, VA). Protein was measured according to the method of Bradford [1976] using BSA as a standard. AP activity was expressed as nanomoles of p-nitrophenol liberated per microgram of total cellular protein.

Northern Blot Analysis

After 2, 4, 8, 12, and 16 days of culturing in the presence of 0, 50, or 200 ng/ml of OP-1, total RNA was isolated using the TRI reagent following the manufacturer's recommendation. The intactness of the RNA preparation was examined by agarose (1%) gel electrophoresis followed by ethidium bromide staining. Only RNA preparations showing intact species were used for subsequent analyses. The cDNA probe for the rat Cbfa1 gene was a 680-bp fragment isolated from the plasmid with EcoRI digestion. The plasmid contained the 680-bp fragment of the rat Cbfa1 gene cloned in the pCRII-TOPO vector (Invitrogen, Carlsbad, CA). The Cbfa1 sequence was generated by RT-PCR. The forward primer was (5′) ATG CTT CAT TCG CCT CAC AAA CAA CCA (3′); the reverse primer: (5′) GAA GGC CAC GGG CAG GGT CTT GTT GCA (3′). The cDNA probe for MyoD was a 440-bp fragment isolated from the plasmid with PstI digestion. The plasmid contained a 2.25 kb mouse MyoD cDNA cloned in the pT7T3D-Pac vector was obtained from ATCC (clone ID 1064620). The cDNA probes for OC, BSP, TIC, ActR-I, BMPR-IA, BMPR-IB, and BMPR-II were obtained by digestion of the corresponding plasmids with the appropriate restriction endonucleases as reported previously [Yeh et al., 2000]. The cDNA probes were labeled with ^{32}P α-dATP using the StripEZ DNA labeling kit from Ambion (Austin, TX).

Northern analyses were conducted as previously described [Yeh et al., 1997]. Briefly, total RNAs (20 μg) were denatured and analyzed on 2.2 M formaldehyde/1% GTG agarose gels. RNA standards (0.24–9.5 kb) from Life technologies were used as size markers. The fractionated RNA was transferred onto a "Nytran Plus" membrane using a Turboblot apparatus (Schleicher & Schuell, Inc., Keene, NH). The lane containing the standards was removed from the blot, and the RNA was covalently linked to the membrane using a UV Crosslinker (Stratagene, La Jolla, CA). The membranes were incubated overnight at 42°C with the cDNA probes. The radioactive signal was detected using the PhosphorImager, and the intensity of the signal was quantified using the ImageQuant Software from Molecular Dynamics (Sunnyvale, CA). Before probing with another DNA probe, the signal from the previous probe was stripped from the blot using Ambion's StripEZ Degradation and Reconstitution buffers following manufacturer's recommendation. The blots were also probed with an 18S rRNA oligonucleotide probe to correct for loading variations.

RNase Protection Assay

Twenty micrograms of total RNA were used to determine the mRNA levels for other BMPs and GDFs by RNase protection assay (RPA). The RiboQuant RPA kits with the mBMP-1 and the mGDF-1 Multi-Probe Template Sets were purchased from BD PharMingen (San Diego, CA) and used according to the manufacturer's instruction. The mBMP-1 kit allows detection of mRNAs for BMP-1, -2, -3, -4, -5, -6, -7, -8A and -8B with the protected fragment of 148, 160, 181, 226, 253, 283, 316, 353, and 133 nucleotides in length, respectively. The mGDF-1 kit allows detection of mRNAs for GDF-1, -3, -5, -6, -8, and -9 with the protected fragment of 148, 160, 181, 226, 283, and 316 nucleotides in length, respectively. Both kits also allow detection of mRNA for ribosomal protein L32 and GAPDH. Their mRNA levels were used for correcting sampling or technique errors. The protected RNA fragments were fractionated on 5% polyacrylamide gel containing 8 M urea. After electrophoresis, the gel was fixed in 10% acetic acid/10% methanol for 10 min, dried, and exposed to a Phosphorscreen. Radioactive bands were detected using the PhosphorImager and their intensities were quantified with the ImageQuant Software (Molecular Dynamics, Sunnyvale, CA).

Statistical Analysis

Data are presented as the mean ± SEM. Statistical differences between means were determined by one-way ANOVA, followed by post-hoc Least Significant Difference Multiple Comparisons in the SIMSTAT3 software package (Normand Peladeau, Provalis Research, Montreal, Canada). Differences at $P < 0.05$ were considered significant.

RESULTS

Conversion of C2C12 to Cells With Osteoblastic Morphology When Cultured in the Presence of OP-1

Figure 1 shows a time study of the morphology of cultures treated with solvent, 50 or 200 ng/ml of OP-1. In the control cultures, C2C12 cells were elongated in shape, resembling myoblastic cells. In the presence of low concentrations of OP-1, the cells began to change morphology around day 4 after treatment, but still maintained the elongated morphology. When incubated with OP-1 at 200 ng/ml, cells assumed a morphology that is more akin to that of osteoblastic cells, beginning about day 4. The osteoblastic cell morphology persisted thereafter and the cultures became quite confluent.

Total AP Activity was Stimulated in Cultures Grown in the Presence of OP-1

In the absence of OP-1, a very low level of AP activity was detected in the C2C12 cultures, for as long as 15 days. When C2C12 cells were cultured in the presence of various concentrations of OP-1, the total AP activity in the cell lysates changed as a function of both the time in culture (Fig. 2A) and the OP-1 concentration (Fig. 2B). In the presence of low concentrations of OP-1 (<100 ng/ml), the AP activity increased only slightly beyond the basal level, for as long as 15 days in culture. This observation is in agreement with the observed morphology (Fig. 1), i.e., most of the cells remained myoblastic. However, in the presence of higher concentrations of OP-1 (≥200 ng/ml), the AP activity was elevated significantly beyond the control, and increased dramatically as a function of time. Specifically, the total AP activity was not notably elevated prior to day 8 of treatment in all the cultures treated with the range of OP-1 concentrations tested (Fig. 2A). After 8 days, cells cultured in OP-1 at 200 ng/ml or higher concentrations showed significant elevation in AP activity. It is noteworthy that the magnitude of the response to OP-1 was more dramatic on day 12 than those on day 8 and 15. On day 8 and 15, the AP activity in cells treated with 400 ng/ml of OP-1 was about 27- and 40-fold higher than the control, respectively. On day 12, the AP activity was about 74-fold higher.

Effects of OP-1 on mRNA Expression of Selected Osteoblastic Cell Markers

To confirm further that the cells cultured in the presence of OP-1 became osteoblastic in nature, the mRNA level of several biochemical markers characteristic of osteoblastic cells was measured by Northern blot analysis. These included OC, BSP, and type I collagen (TIC). Figure 3 shows a representative PhosphorImage of the Northern blots and Figure 4 shows the quantitative data. No OC mRNA was detected in cultures treated with vehicle or OP-1 at 50 ng/ml for up to 16 days in culture (Fig. 4A). A significant increase in the OC mRNA level was detected at 8 days in OP-1-treated cultures (200 ng/ml) and its level continued to increase, reaching a 4- to 5-fold stimulation at 16 days.

A very low level of BSP mRNA was detected in cultures treated with vehicle or OP-1 at 50 ng/ml. The level remained low throughout the 16 days of culture (Fig. 3). In cultures treated with OP-1 at 200 ng/ml, a considerable increase in BSP mRNA was observed at 8 days and its level continued to increase, reaching a fivefold stimulation at 12 days, and remained elevated at 16 days in culture (Fig. 4B).

Figure 4C shows the quantitative data on type I collagen mRNA expression. The level was low but detectable in control cultures up to about 12 days and became undetectable afterwards (Fig. 3). In cultures treated with either the low or the high concentration of OP-1, the mRNA level increased by about 40% during the early stages (2–8 days), but dropped dramatically to the control level thereafter.

Effects of OP-1 on mRNA Expression of Selected Transcription Regulatory Factors

To assess whether the expression of regulator factors of myogeneic differentiation is inhibited by OP-1, MyoD mRNA expression was examined in C2C12 cells cultured in the absence and presence of two concentrations of OP-1 for varying time periods. Figure 3 shows that MyoD mRNA expression decreased both as a function of time of treatment and OP-1 concentration. At the low OP-1 concentration, MyoD mRNA expression was stimulated transiently from 4 to 8 days, reaching a peak at 8 days, but decreased thereafter to an almost non-detectable level on day 16 (Figs. 3 and 5A). At 200 ng/ml of OP-1, the MyoD mRNA level decreased as early as 4 days and became completely undetectable at 12 days

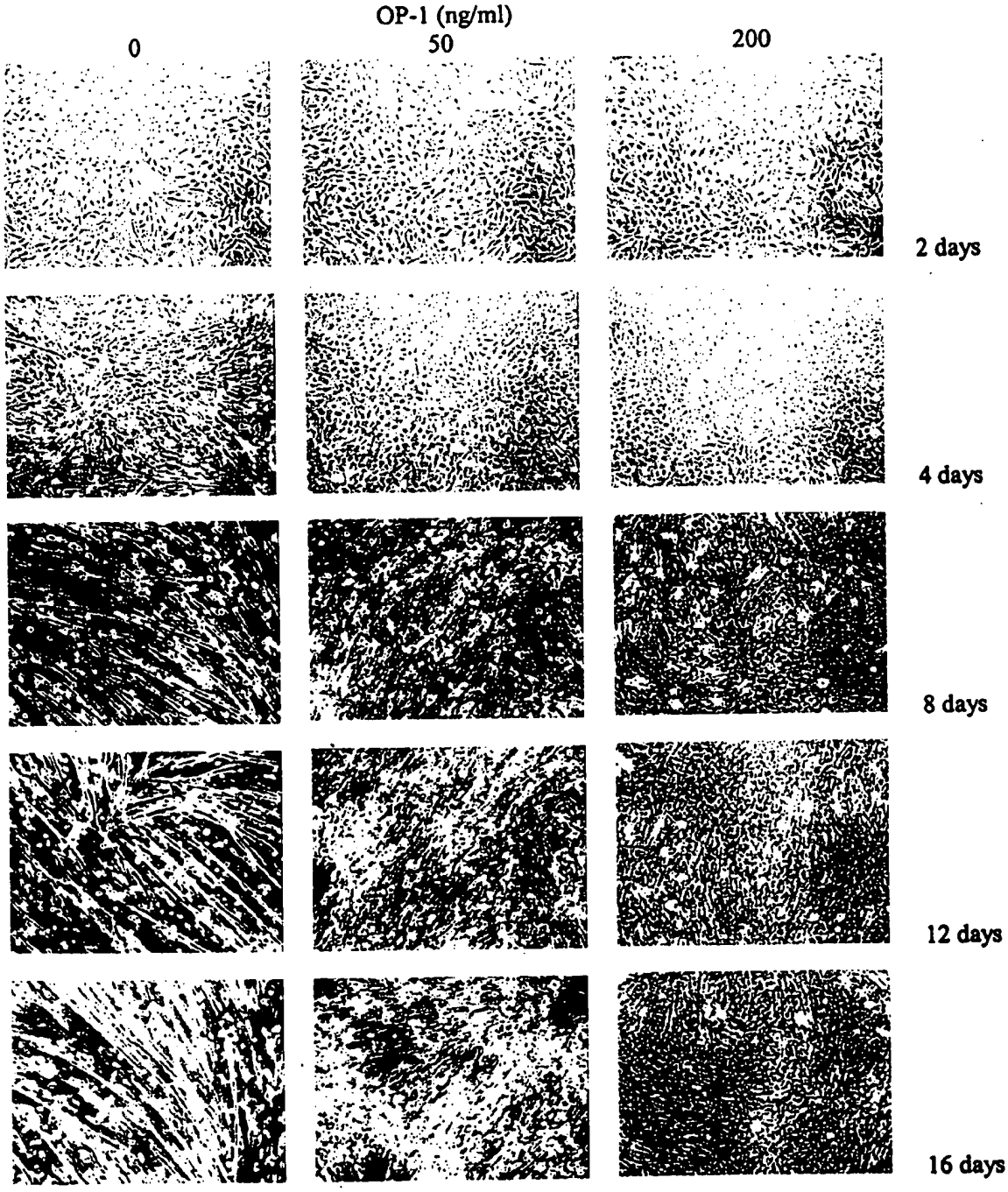

Fig. 1. Morphological changes in C2C12 cells cultured in the presence of OP-1. C2C12 cells were cultured in the absence or presence of 50 or 200 ng/ml of OP-1. Media were changed every 3 days. Cell morphology was monitored with a phase contrast microscope, and the images were captured with a CCD camera. Representative images (phase contrast with 100× magnification) are presented.

(Fig. 3). The expression of an osteoblast specific transcription factor, Runx2/Cbfa1, was also studied by Northern blot analysis. Figure 3 shows that a relatively high level of Runx2/Cbfa1 mRNA level was detected in control cultures. In cells cultured in the presence of a low concentration of OP-1, the Runx2/Cbfa1 mRNA level increased slightly (by about 20%

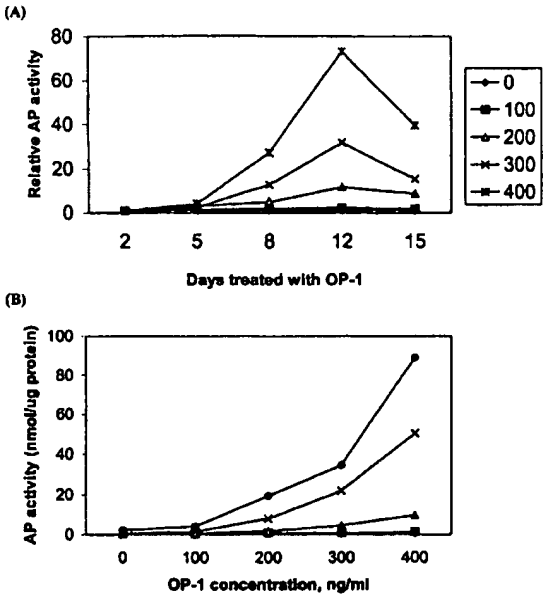

Fig. 2. Alkaline phosphatase activity in C2C12 cultures as a function of time of OP-1 treatment (A) and OP-1 concentration (B). Cells were grown in 48-well plates in the presence of OP-1. Control cultures were treated with equal amount of vehicle. At the indicated time, total cellular AP activity was measured and expressed as nanomoles of p-nitrophenol liberated per microgram of total cellular protein. Values represented mean ± SEM of three independent determinations. (A) ◆, 0; ■, 100; ▲, 200; ✖, 300; ✱, 400 ng/ml of OP-1. (B) ●, 15; X, 12; ▲, 8; ■, 5; ✱, 2 days of treatment.

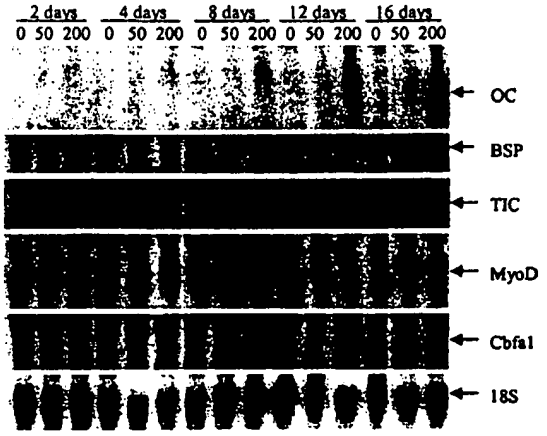

Fig. 3. Effects of continuous OP-1 treatment on bone sialoprotein (BSP), osteocalcin (OC), type I collagen (TIC), MyoD, Runx1/Cbfa1 mRNA expression in C2C12 cultures. C2C12 cells were grown in 100-mm dishes in the presence of vehicle or OP-1 (50 or 200 ng/ml) for 2, 4, 8, 12, and 16 days. Total RNA was isolated using the TRI reagent. Twenty micrograms of total RNA was fractionated on an agarose gel containing formaldehyde, and subsequently transferred to a Nytran Plus membrane. The mRNA expressions of OC and BSP, type I collagen (TIC), MyoD and Cbfa1 were measured by Northern analysis using ^{32}P-labeled cDNA probes. The blots were also hybridized with the oligonucleotide probe for 18S rRNA. Representative PhosphorImages are presented.

compared to the same day control) at day 4 and then dropped to the control level thereafter. In cells cultured in 200 ng/ml of OP-1, the Runx2/Cbfa1 mRNA level raised slightly by about 16–20% compared to the same day control throughout the remaining time in culture (Fig. 5B).

Effects of OP-1 on OP-1 Receptor Gene Expression

In light of the results described above and previous findings that OP-1 differentially regulated BMPR mRNA expression in osteoblastic cells derived from fetal rat calvaria [Yeh et al., 2000], we examined the expression of ActR-I, BMPR-IA, BMPR-IB, and BMPR-II by Northern blot analysis. Figure 6 shows a representative PhosphorImage and the quantitative data are shown in Figure 7. In control cultures, the steady-state mRNA levels for all four receptor types were detectable and remained unchanged throughout the 16 days of culture. Of the four receptor types studied, the ActR-I mRNA level increased most significantly (about 40% higher than the same day control) in cultures treated with the high OP-1 concentration (Fig. 7A). The increase began at day 4 and remained at the elevated level thereafter. The steady-state mRNA levels for BMPR-IA, BMPR-IB, and BMPR-II remained relatively unchanged throughout the 16 days in culture for both the control and the OP-1-treated cells (Fig. 7B–D).

Effects of OP-1 on BMP-1, -4, -5, -6, and -8A mRNA Expression

Effects of continuous OP-1 treatment on the mRNA expression of several BMPs as a function of culture time were examined by RPA. Figure 8 is a representative PhosphorImage showing the protected fragments for BMP-1, -4, -5, -6, and -8A in control and C2C12 cells treated with two concentrations of OP-1 up to 16 days. The mRNA expression level for each BMP was quantified and normalized to that of ribosomal protein L32. The relative levels of mRNA for the different BMPs as a function of time and OP-1 concentration are shown in Figure 9.

BMP mRNA Expression in Control Cultures

In control cultures, the BMP-1 mRNA level was detectable and remained unchanged throughout the 16 days in culture (Fig. 8). The BMP-4

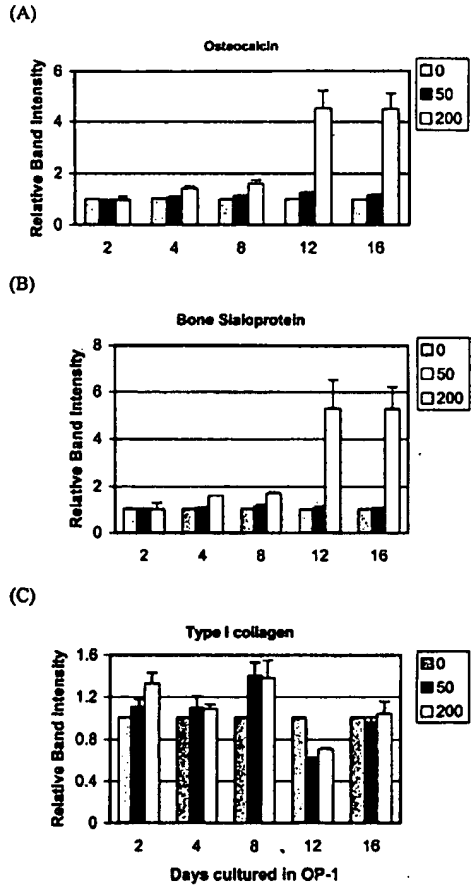

Fig. 4. Quantitative analysis of (A) OC, (B) BSP, and (C) TIC mRNA levels in long-term cultures of C2C12 cells in the presence of OP-1. The intensity of the hybridized RNA species on Northern blots, as shown in Figure 3, was analyzed by the ImageQuant software. The mRNA level was normalized to the 18S rRNA level. The normalized mRNA level was then compared to that in the same day control (as 1). Values represent mean ± SEM from 2 to 4 independent determinations.

mRNA expression was significantly lower than those of BMP-1 initially and changed during culture, reaching a maximum of threefold after 16 days. The BMP-5 and -6 mRNA expressions were very low initially, but increased gradually beginning at 12 days, reaching a maximum of about threefold at 16 days. BMP-8A mRNAs were not detectable initially, but became detectable about 12 days, reaching a maximum of about twofold at 16 days.

BMP mRNA Expression in OP-1-Treated Cultures

Figures 8 and 9 also show the effects of OP-1 on the mRNA expression of several BMP members. At both concentrations, OP-1 increased

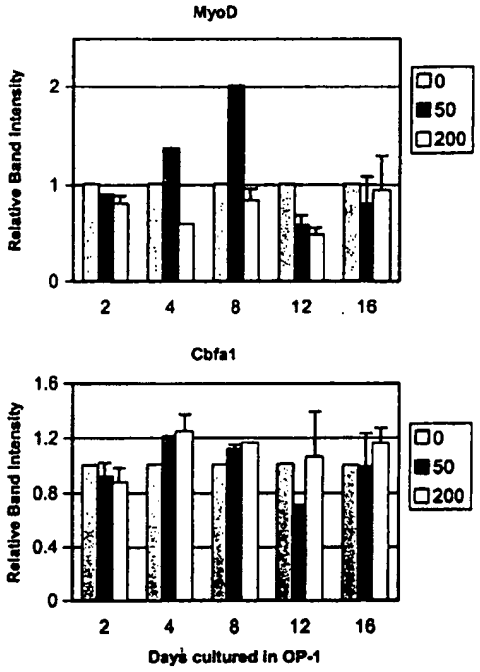

Fig. 5. Quantitative analysis of (A) MyoD, and (B) Runx1/Cbfa1 mRNA levels in long-term cultures of C2C12 cells grown in the presence of OP-1. See legend of Figure 4.

BMP-1 mRNA expression initially in an OP-1-dose-dependent manner, but reduced it to the initial control level after 12–16 days. The BMP-4 mRNA levels also increased in an OP-1-dose-dependent manner. In cells cultured in the

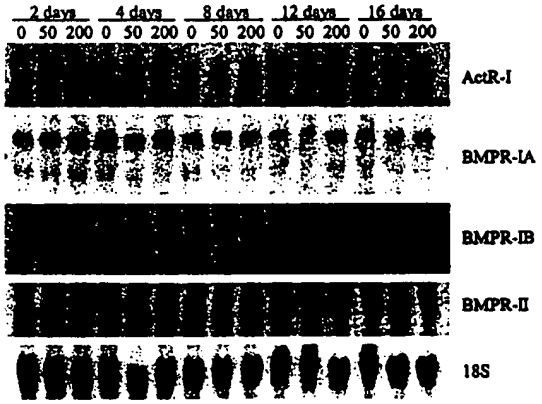

Fig. 6. Northern analysis of the effect of OP-1 on BMP receptor mRNA expression in long-term cultures of C2C12 cells grown in the presence of OP-1. C2C12 cells were treated for 2, 4, 8, 12, and 16 days with different concentrations of OP-1 (0, 50, or 200 ng/ml). Total RNA was isolated as described in Figure 3. The blots were hybridized with the cDNA probes for ActR-I, BMPR-IA, BMPR-IB, and BMPR-II sequentially, and finally the oligonucleotide probe for 18S rRNA. After washings, the blots were exposed to a PhosphorImage screen.

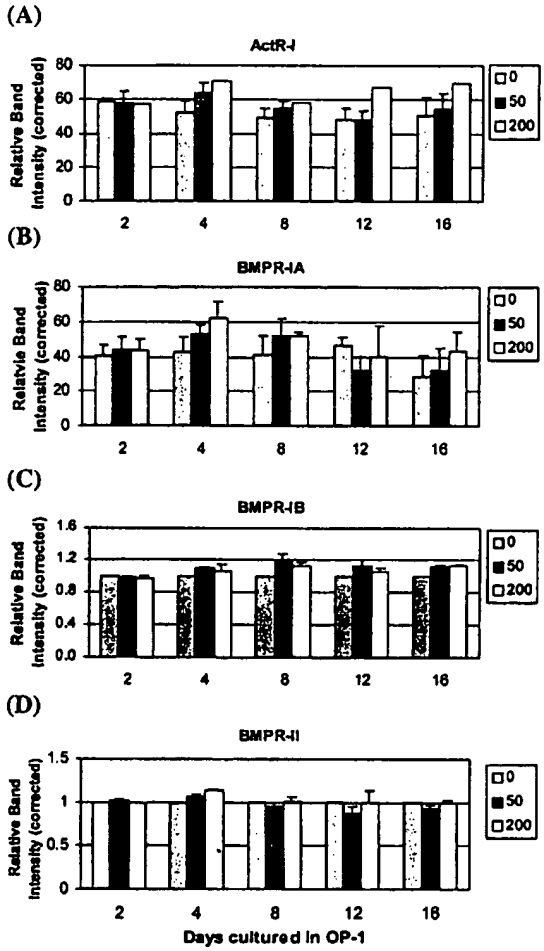

Fig. 7. Quantitative analysis of the BMP receptor mRNA level in long-term cultures of C2C12 cells grown in the presence of OP-1. The intensity of the hybridized RNA species on Northern blots, as shown in Figure 6, was analyzed by the ImageQuant software. The mRNA level was normalized to the 18S rRNA level. The normalized mRNA level was then compared to that in the same day control (as 1). Values represent mean ± SEM from 2 to 3 independent determinations. (A) ActR-I, (B) BMPR-IA, (C) BMPR-IB, and (D) BMPR-II.

presence of OP-1 at 50 ng/ml increased by about fivefold at day 4 but began to decline thereafter to the control level. The BMP-4 mRNA level increased by about 10-fold at 4 days and an additional 10-fold at 8 days in cells cultured in the presence of OP-1 at 200 ng/ml. However, the level dropped thereafter. The BMP-5 mRNA levels also increased in an OP-1-dose-dependent manner, reaching a maximum of about fourfold at 8 days. Both the BMP-6 and -8A mRNA levels were not changed significantly.

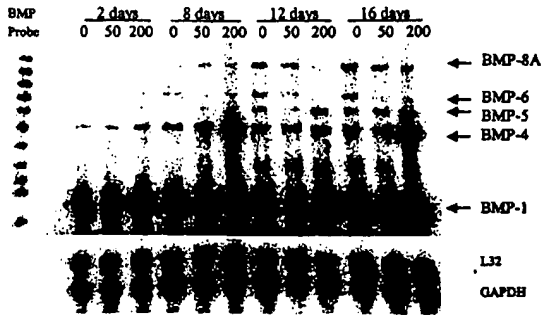

Fig. 8. RNase protection analysis of the effect of OP-1 on BMP mRNA expression in long-term cultures of C2C12 cells. Confluent cultures were treated with vehicle or OP-1 (50 or 200 ng/ml) for 2, 8, 12, and 16 days. Total RNA was isolated using the TRI reagent. Twenty micrograms of total RNA was used for the measurement of BMP mRNA expression by the RNase protection assay. The protected RNA fragments were fractionated on 5% polyacrylamide gels containing 8 M urea and detected by PhosphorImaging. Positions of labeled probes for the different BMPs and the two housekeeping gene controls (ribosomal protein L32 and GAPDH) are marked on the left of the image. The protected fragments are indicated on the right with arrows.

Effects of OP-1 on GDF mRNA Expression

Effects of continuous OP-1 treatment on the mRNA expression of several GDFs as a function of time in culture were examined by RPA.

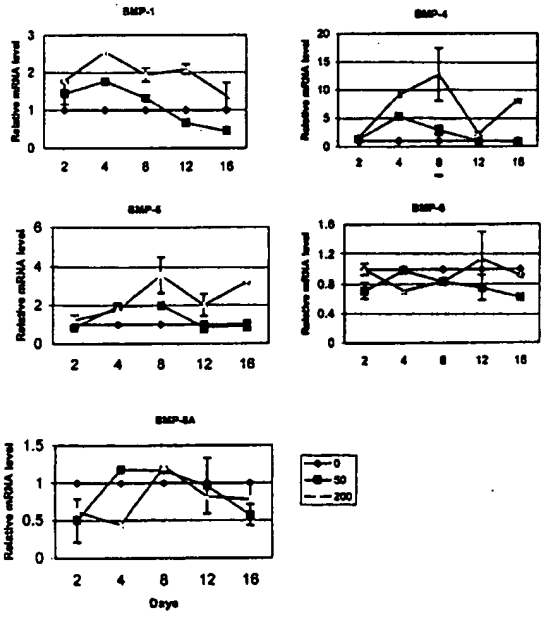

Fig. 9. Quantitative analysis of the BMP mRNA levels in C2C12 cells. The intensity of the protected fragments as shown in Figure 8 was analyzed, quantified using the PhospImageQuant Software, and normalized to the L32 expression level. Values represent mean ± SEM from two different determinations.

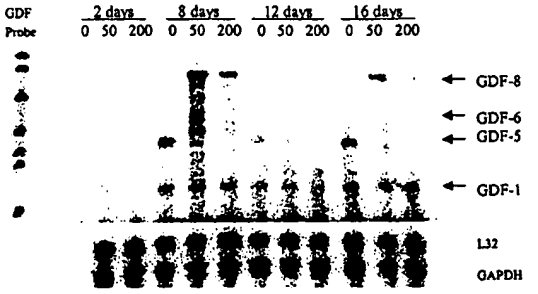

Fig. 10. RNase protection analysis of the effect of OP-1 on GDF mRNA expression in long-term cultures of C2C12 cells. Same as in Figure 8.

Figure 10 is a representative PhosphorImage showing the protected fragments for GDF-1, -5, -6, and -8A in C2C12 cells cultured in the presence of vehicle or two concentrations of OP-1 up to 16 days. The mRNA expression level for each GDF was quantified and normalized to the mRNA level of ribosomal protein L32. The relative levels of mRNA for the different GDFs as a function of time and OP-1 concentration are shown in Figure 11.

GDF mRNA Expression in Control Cultures

In control cultures, GDF-1 mRNA appeared to be the most abundant among the GDFs examined. The GDF-1 mRNA level increased gradually, reaching a maximum of about fivefold at 16 days compared to the value at day 2. GDF-5 mRNA expression also increased gradually, reaching a maximum of about eightfold at 16 days. GDF-6 and -8 mRNA expressions were relatively low and remained unchanged throughout the culture period examined.

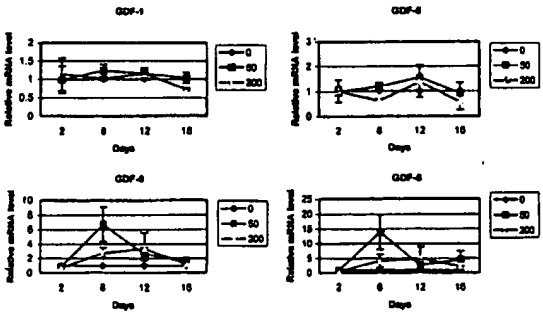

Fig. 11. Quantitative analysis of the GDF mRNA levels in C2C12 cells. The intensity of the protected fragments as shown in Figure 10 was analyzed and quantified as in Figure 9. Values represent mean ± SEM from two different determinations.

GDF mRNA Expression in OP-1-Treated Cultures

Figures 10 and 11 show the consequences of OP-1 treatment on the expression of several GDF members. In the presence of either OP-1 concentrations (50 or 200 ng/ml), the GDF-1 and -5 mRNA expressions remained unchanged compared to the control. OP-1 treatment (at 50 ng/ml) increased GDF-6 mRNA expressions significantly (about sixfold compared to the same-day control) at 8 days and declined thereafter to the control levels. At a higher OP-1 concentration (200 ng/ml), GDF-6 mRNA expression reached a peak at 12 days with an increase of about threefold (compared to the same-day control), but returned to the same-day control at 16 days. At 50 ng/ml, OP-1 treatment elevated the GDF-8 mRNA level by about 15-fold at 8 days and the level dropped subsequently. Similar to GDF-6, at a higher OP-1 concentration, GDF-8 mRNA expression reached a peak later at 12 days with an increase of about fivefold (compared to the same-day control).

DISCUSSION

In the present study, we demonstrated that continuous exposure of C2C12 cells to a moderate concentration (200 ng/ml) of OP-1 inhibits C2C12 cells from differentiating into myoblasts and induces these cells to differentiate into the osteoblast lineage. Previous studies indicated that several members of the BMP family also could inhibit myoblast differentiation but only a limited number could induce osteoblastic cell differentiation. Those that could induce osteoblastic cell differentiation also appeared to display different potencies.

The present data showed that a noticeable morphological change was observed when cells were treated for 4 days in the presence of 50 ng/ml of OP-1. In the presence of a higher OP-1 concentration (200 ng/ml), a complete conversion to osteoblastic cells occurred. Significant increases in total cellular AP were also detected in these cultures. Previous studies reported that incubation of C2C12 cells for 6 days with BMP-2 (300 ng/ml) inhibited myotube formation, and induced osteoblastic cell formation with >90% of the cells stained positive for AP [Katagiri et al., 1994]. Treatment of C2C12 cells with BMP-6 resulted in a dose-dependent increase in the number of AP-positive cells [Ebisawa et al., 1999].

Three other protein factors were reported to fail to induce osteoblastic cell formation. TGF-β1 (5 ng/ml) almost completely inhibited myotubes formation in C2C12 cells, but did not induce expression of AP activity and OC [Katagiri et al., 1994]. Incubation of C2C12 cells with 300 and 1000 ng/ml of BMP-12 (CDMP-3, GDF-7) or BMP-13 (CDMP-2, GDF-6) for 6 days inhibited myotube formation by about 25 and 30%, respectively, but did not stimulate AP activity in C2C12 cells [Inada et al., 1996]. Thus, BMP-12 and -13 could not induce C2C12 cells into the osteoblastic cell differentiation pathway.

The temporal sequence of gene expression in long-term, OP-1-treated cultures of C2C12 cells appears to be similar to that observed in the primary culture of osteoblastic cells. For example, previous reports showed that the primary culture of FRC cells undergoes distinct stages of cell differentiation and a temporal sequence of gene expression can be observed within each stage of differentiation [Owen et al., 1990; Lian and Stein, 1992; Yao et al., 1994; Yeh et al., 2000]. The AP activity and both BSP and TIC mRNA expressions begin to increase in cultures entering the matrix formation stage. OC mRNA expression occurs later in osteoblastic cell differentiation and coincides with the bone nodule mineralization stage. In C2C12 cells cultured in OP-1, OC and BSP mRNA expression as well as AP activity began to increase around day 8. Both the AP activity and BSP expression peaked at about day 12, whereas OC expression did not peak until about day 16. It is interesting to note that the increase in TIC mRNA expression occurred before that in OC and BSP mRNA, and then returned to the control level thereafter. Since TIC participates in mineralization, it is not clear at present why TIC expression returned to the control level after the transient increase. By comparison, in C2C12 cells treated with BMP-2, an increase in AP and OC mRNA was also observed but it occurred around day 2, much earlier than that observed for OP-1 [Katagiri et al., 1997]. The reason(s) for the difference between the two observations is not clear at present. Although BMP-6 also could induce AP activity in C2C12 cells [Ebisawa et al., 1999], the temporal sequence of the expression of these genes is not known.

The current study also showed that OP-1 at 200 ng/ml suppressed MyoD mRNA expression in C2C12 cells early during cell differentiation. However, at the low OP-1 concentration, MyoD mRNA expression was transiently stimulated at 4–8 days and then returned to the control level. MyoD mRNA expression was also transiently stimulated at 1–3 h by BMP-2 (300 ng/ml), but decreased thereafter [Katagiri et al., 1997]. On the other hand, TGF-β1 (5 ng/ml) inhibited MyoD mRNA expression as early as 3–6 h after treatment. Thus, even though all three protein factors inhibited MyoD mRNA expression in C2C12 cells, the timing of the event appeared to be different. The physiological significance, if any, of the difference in timing must await further experimentation.

The present study showed that Cbfa1 mRNA expression in C2C12 cultures was not significantly stimulated by OP-1 at 200 ng/ml. However, several published reports indicated that treatment of C2C12 cells with BMP-2 and TGF-β resulted in an induction of Runx2/Cbfa1 [Lee et al., 1999, 2000]. In particular, the type II/p57 isoform of Runx2/Cbfa1 was induced by BMP-2 [Banerjee et al., 2001]. In addition, treatment with a BMP4/7 heterodimer (100 ng/ml) enhanced Cbfa1 mRNA expression [Tsuji et al., 1998]. However, these authors also observed that overexpression of Cbfa1 resulted in a suppression of TIC and OC mRNA expression.

The current data indicate that significant levels of mRNA for ActR-I, BMPR-IA, BMPR-IB, and BMPR-II are present in control C2C12 cells. By Northern blot analysis, Akiyama et al. [1997] reported detection of BMPR-IA, and BMPR-II mRNA in C2C12 cells but not BMPR-IB mRNA. Namiki et al. [1997] also reported detection of BMPR-IA and TGF-β type I receptor but not BMPR-IB mRNA in C2C12 cells. However, the same authors demonstrated the presence of BMPR-IB protein on the cell surface of C2C12 cells by affinity binding assay followed by immunoprecipitation.

Previous studies suggested that BMPs may regulate their actions by affecting expression of individual BMP receptors. The present study revealed that the ActR-I mRNA expression was elevated in C2C12 cells cultured in the presence of OP-1. BMPR-IA, BMPR-IB, and BMPR-II mRNA expression levels were not significantly affected. Whether these observed changes in the steady-state mRNA levels are translated to the level of surface receptor proteins remains to be established experimentally. Relevant to the current data is the finding of Namiki et al. [1997] who, using a kinase-domain truncated

BMPR-IA, showed that the inductive effect of BMP-2 on converting the C2C12 cells into the osteoblastic cells is mediated via BMPR-IA. By comparison, OP-1 induces an increase in the mRNA expression of ActR-IA, BMPR-IA, and BMPR-II, but has little effect on the BMPR-IB mRNA expression in FRC cells [Yeh et al., 1998, 2000]. The same study also showed that, in the human SaOS-2 osteosarcoma cells, the ActR-I mRNA expression was increased by OP-1, whereas the BMPR-IA and BMPR-IB mRNA levels remained unchanged. The BMPR-II mRNA levels dropped after 24 h of treatment with OP-1. In contrast, in human TE85 osteosarcoma cells, the mRNA levels for ActR-I, BMPR-IA, BMPR-IB, and BMPR-II were significantly elevated following OP-1 treatment for 24 h. Taken together, it appears that the effects of OP-1 on BMP receptor expression in osteoblastic cells vary widely according to the physiological and differentiation stage of the cell.

It is noteworthy that control C2C12 cells expressed a high level of BMP-1 mRNA which is technically not a BMP. BMP-1 is a cysteine-rich zinc-peptidase that has been suggested to activate latent TGF-β [Sarras, 1996]. In C2C12 cells, cultured in the presence of the high concentration of OP-1, BMP-1 mRNA expression was elevated significantly during the entire culture period, suggesting that BMP-1 might play an important role in the conversion and differentiation of the C2C12 cells to osteoblastic cells.

The BMP-2 mRNA level in C2C12 cells was below detection and OP-1 did not stimulate its expression. On the other hand, OP-1 stimulated significantly the expression of the other member of this subgroup, BMP-4. By comparison, OP-1 did not alter the BMP-2 mRNA expression, but suppressed the BMP-4 mRNA expression in FRC cells [Yeh et al., 2000]. On the other hand, BMP-2 stimulated the BMP-2 mRNA expression but inhibited BMP-4 mRNA initially and stimulated BMP-4 expression during the mineralization phase [Chen et al., 1997].

We previously reported that OP-1 down-regulated the mRNA expressions of two (BMP-5, and -6) out of the three members of the subgroup consisting of BMP-5, -6, and -7, but did not change BMP-7 mRNA expression in primary cultures of FRC cells [Yeh et al., 2000]. In contrast to these observations, OP-1 treatment of C2C12 cells stimulated BMP-5 mRNA expression without affecting BMP-6 mRNA expression. BMP-7 mRNA level was below detection. In the U2 human osteosarcoma cell line, OP-1 treatment increased the BMP-6 mRNA level [Honda et al., 1997]. In another human osteosarcoma cell line, SaOS-2, OP-1 treatment resulted in a slightly different effect, that is, OP-1 decreased BMP-4 mRNA and increased BMP-6 mRNA, but had no effect on the BMP-2 mRNA level. Taken together, these observed differences in the response of the various osteoblastic cells to OP-1 suggest that the state of differentiation and perhaps the physiological state of the osteoblastic cells might play an important role in their responsiveness to the BMPs. The differential expression of the different BMP receptors might also contribute to the variation in responsiveness to the different BMPs.

The present study is the first to report detectable, but varying levels of mRNA coding for GDF-1, -5, -6, and -8 in C2C12 cells. Upon treatment of C2C12 cells with a high concentration of OP-1 (200 ng/ml) to induce osteoblastic cell formation and differentiation, the GDF-1 and -5 mRNA levels were not detectably changed, but the GDF-6 and -8 mRNA levels were elevated significantly. During distractal osteogenesis induced by mechanical-tension stress in rats, BMP-2, -4, but not BMP-6, BMP-7, and GDF-5 mRNA levels were elevated [Sato et al., 1999]. In vivo ectopic implantation studies with GDF-5 and -6 showed that both proteins induced de novo cartilage and bone formation [Erlacher et al., 1998]. They also stimulated osteogenesis in bone marrow-derived progenitor cells, although they were less potent than BMP-6 and OP-1 [Gruber et al., 2000]. Previously, GDF-8, also known as myostatin, was detected in cardiac muscle and its level was up-regulated in cardiomyocytes after infarct [Sharma et al., 1999]. Our observation that OP-1 inhibited myoblast differentiation in C2C12 cells agrees with the previous finding that GDF-8 (myostatin) is a negative regulator of skeletal muscle growth [Hamrick et al., 2000]. Whether GDF-8 plays a positive role in osteogenesis is not clear at present.

In conclusion, we demonstrate that OP-1 is a potent inducer of osteoblastic differentiation of the pluripotent mesenchymal cell C2C12. We have further indicated several molecules, such as ActR-I, as potential mediators via which OP-1 blocks myogenic differentiation and induces osteoblast differentiation in C2C12 cells. Future studies on these molecules and

other downstream signaling molecules, such as the Smads, will be needed to more fully determine the mechanism of action of OP-1 in this cell model. The current findings also reveal a complex interplay of several BMPs and GDFs as well as the BMP receptors. Thus, the current results should provide a molecular basis for future studies to further elucidate the actions of the different BMP members and the receptors.

ACKNOWLEDGMENTS

Support by Stryker Biotech is acknowledged.

REFERENCES

Akiyama S, Katagiri T, Namiki M, Yamaji N, Yamamoto N, Miyama K, Shibuya H, Ueno N, Wozney JM, Suda T. 1997. Constitutively active BMP type I receptors transduce BMP-2 signals without the ligand in C2C12 myoblasts. Exp Cell Res 235:362–369.

Asahina I, Sampath TK, Nishimura I, Hauschka PV. 1993. Human osteogenic protein-1 induces both chondroblastic and osteoblastic differentiation of osteoprogenitor cells derived from newborn rat calvaria. J Cell Biol 123:921–933.

Banerjee C, Javed A, Choi JY, Green J, Rosen V, van Wijnen AJ, Stein JL, Lian JB, Stein GS. 2001. Differential regulation of the two principal Runx2/Cbfa1 N-terminal isoforms in response to bone morphogenetic protein-2 during development of the osteoblast phenotype. Endocrinology 142:4026–4039.

Bradford M. 1976. A rapid and sensitive method for the quantitation of microgram quantities of protein utilizing the principle of protein-dye binding. Anal Biochem 72: 248–254.

Chen P, Vukicevic S, Sampath TK, Luyten FP. 1995. Osteogenic protein-1 promotes growth and maturation of chick sternal chondrocytes in serum-free cultures. J Cell Sci 108:105–114.

Chen D, Harris MA, Rossini G, Dunstan CR, Dallas SL, Feng JQ, Mundy GR, Harris SE. 1997. Bone morphogenetic protein 2 (BMP-2) enhances BMP-3, BMP-4, and bone cell differentiation marker gene expression during the induction of mineralized bone matrix formation in cultures of fetal rat calvarial osteoblasts. Calcif Tissue Int 60:283–290.

Dudley AT, Lyons KM, Robertson EJ. 1995. A requirement for bone morphogenetic protein-7 during development of the mammalian kidney and eye. Genes Dev 9:2795–2807.

Ebisawa T, Tada K, Kitajima I, Tojo K, Sampath TK, Kawabata M, Miyazono K, Imamura T. 1999. Characterization of bone morphogenetic protein-6 signaling pathways in osteoblast differentiation. J Cell Sci 112:3519–3527.

Erlacher L, McCartney J, Piek E, ten Dijke P, Yanagishita M, Oppermann H, Luyten FP. 1998. Cartilage-derived morphogenetic proteins and osteogenic protein-1 differentially regulate osteogenesis. J Bone Miner Res 13:383–392.

Gruber R, Mayer C, Schulz W, Graninger W, Peterlik M, Watzek G, Luyten FP, Erlacher L. 2000. Stimulatory effects of cartilage-derived morphogenetic proteins 1 and 2 on osteogenic differentiation of bone marrow stromal cells [in process citation]. Cytokine 12:1630–1638.

Hamrick MW, McPherron AC, Lovejoy CO, Hudson J. 2000. Femoral morphology and cross-sectional geometry of adult myostatin-deficient mice. Bone 27:343–349.

Hogan BL. 1996. Bone morphogenetic proteins in development. Curr Opin Genet Dev 6:432–438.

Honda Y, Knutsen R, Strong DD, Sampath TK, Baylink DJ, Mohan S. 1997. Osteogenic protein-1 stimulates mRNA levels of BMP-6 and decreases mRNA levels of BMP-2 and -4 in human osteosarcoma cells. Calcif Tissue Int 60:297–301.

Inada M, Katagiri T, Akiyama S, Namika M, Komaki M, Yamaguchi A, Kamoi K, Rosen V, Suda T. 1996. Bone morphogenetic protein-12 and -13 inhibit terminal differentiation of myoblasts, but do not induce their differentiation into osteoblasts. Biochem Biophys Res Commun 222:317–322.

Katagiri T, Yamaguchi A, Komaki M, Abe E, Takahashi N, Ikeda T, Rosen V, Wozney JM, Fujisawa-Sehara A, Suda T. 1994. Bone morphogenetic protein-2 converts the differentiation pathway of C2C12 myoblasts into the osteoblast lineage. J Cell Biol 127:1755–1766.

Katagiri T, Akiyama S, Namiki M, Komaki M, Yamaguchi A, Rosen V, Wozney JM, Fujisawa-Sehara A, Suda T. 1997. Bone morphogenetic protein-2 inhibits terminal differentiation of myogenic cells by suppressing the transcriptional activity of MyoD and myogenin. Exp Cell Res 230:342–351.

Kawasaki K, Aihara M, Honmo J, Sakurai S, Fujimaki Y, Sakamoto K, Fujimaki E, Wozney JM, Yamaguchi A. 1998. Effects of recombinant human bone morphogenetic protein-2 on differentiation of cells isolated from human bone, muscle, and skin. Bone 23:223–231.

Kingsley DM. 1994. The TGF-beta superfamily: New members, new receptors, and new genetic tests of function in different organisms. Genes Dev 8:133–146.

Klein-Nulend J, Louwerse RT, Heyligers IC, Wuisman PI, Semeins CM, Goei SW, Burger EH. 1998. Osteogenic protein (OP-1, BMP-7) stimulates cartilage differentiation of human and goat perichondrium tissue in vitro. J Biomed Mater Res 40:614–620.

Koenig BB, Cook JS, Wolsing DH, Ting J, Tiesman JP, Correa PE, Olson CA, Pecquet AL, Ventura F, Grant RA. 1994. Characterization and cloning of a receptor for BMP-2 and BMP-4 from NIH 3T3 cells. Mol Cell Biol 14:5961–5974.

Lee MH, Javed A, Kim HJ, Shin HI, Gutierrez S, Choi JY, Rosen V, Stein JL, van Wijnen AJ, Stein GS, Lian JB, Ryoo HM. 1999. Transient upregulation of CBFA1 in response to bone morphogenetic protein-2 and transforming growth factor beta1 in C2C12 myogenic cells coincides with suppression of the myogenic phenotype but is not sufficient for osteoblast differentiation. J Cell Biochem 73:114–125.

Lee KS, Kim HJ, Li QL, Chi XZ, Ueta C, Komori T, Wozney JM, Kim EG, Choi JY, Ryoo HM, Bae SC. 2000. Runx2 is a common target of transforming growth factor beta1 and bone morphogenetic protein 2, and cooperation between Runx2 and Smad5 induces osteoblast-specific gene expression in the pluripotent mesenchymal precursor cell line C2C12. Mol Cell Biol 20:8783–8792.

Lian JB, Stein GS. 1992. Concepts of osteoblast growth and differentiation: Basis for modulation of bone cell

development and tissue formation. Crit Rev Oral Biol Med 3:269–305.

Liu F, Ventura F, Doody J, Massague J. 1995. Human type II receptor for bone morphogenic proteins (BMPs): Extension of the two-kinase receptor model to the BMPs. Mol Cell Biol 15:3479–3486.

Luo G, Hofmann C, Bronckers AL, Sohocki M, Bradley A, Karsenty G. 1995. BMP-7 is an inducer of nephrogenesis, and is also required for eye development and skeletal patterning. Genes Dev 9:2808–2820.

Macias-Silva M, Hoodless PA, Tang SJ, Buchwald M, Wrana JL. 1998. Specific activation of Smad1 signaling pathways by the BMP7 type I receptor, ALK2. J Biol Chem 273:25628–25636.

Namiki M, Akiyama S, Katagiri T, Suzuki A, Ueno N, Yamaji N, Rosen V, Wozney JM, Suda T. 1997. A kinase domain-truncated type I receptor blocks bone morphogenetic protein-2-induced signal transduction in C2C12 myoblasts. J Biol Chem 272:22046–22052.

Nohno T, Ishikawa T, Saito T, Hosokawa K, Noji S, Wolsing DH, Rosenbaum JS. 1995. Identification of a human type II receptor for bone morphogenetic protein-4 that forms differential heteromeric complexes with bone morphogenetic protein type I receptors. J Biol Chem 270:22522–22526.

Okubo Y, Bessho K, Fujimura K, Iizuka T, Miyatake S. 1999. Expression of bone morphogenetic protein-2 via adenoviral vector in C2C12 myoblasts induces differentiation into the osteoblast lineage. Biochem Biophys Res Commun 262:739–743.

Owen TA, Aronow M, Shalhoub V, Barone LM, Wilming L, Tassinari MS, Kennedy MB, Pockwinse S, Lian JB, Stein GS. 1990. Progressive development of the rat osteoblast phenotype in vitro: Reciprocal relationships in expression of genes associated with osteoblast proliferation and differentiation during formation of the bone extracellular matrix. J Cell Physiol 143:420–430.

Ozkaynak E, Rueger DC, Drier EA, Corbett C, Ridge RJ, Sampath TK, Oppermann H. 1990. OP-1 cDNA encodes an osteogenic protein in the TGF-beta family. EMBO J 9:2085–2093.

Paralkar VM, Weeks BS, Yu YM, Kleinman HK, Reddi AH. 1992. Recombinant human bone morphogenetic protein 2B stimulates PC12 cell differentiation: Potentiation and binding to type IV collagen. J Cell Biol 119:1721–1728.

Reddi AH. 2000. Bone morphogenetic proteins and skeletal development: The kidney-bone connection [in process citation]. Pediatr Nephrol 14:598–601.

Rosenzweig BL, Imamura T, Okadome T, Cox GN, Yamashita H, ten Dijke P, Heldin CH, Miyazono K. 1995. Cloning and characterization of a human type II receptor for bone morphogenetic proteins. Proc Natl Acad Sci USA 92:7632–7636.

Sampath TK, Coughlin JE, Whetstone RM, Banach D, Corbett C, Ridge RJ, Ozkaynak E, Oppermann H, Rueger DC. 1990. Bovine osteogenic protein is composed of dimers of OP-1 and BMP-2A, two members of the transforming growth factor-beta superfamily. J Biol Chem 265:13198–13205.

Sarras MP, Jr. 1996. BMP-1 and the astacin family of metalloproteinases: a potential link between the extracellular matrix, growth factors and pattern formation. Bioessays 18:439–442.

Sato M, Ochi T, Nakase T, Hirota S, Kitamura Y, Nomura S, Yasui N. 1999. Mechanical tension-stress induces expression of bone morphogenetic protein (BMP)-2 and BMP-4, but not BMP-6, BMP-7, and GDF-5 mRNA, during distraction osteogenesis. J Bone Miner Res 14: 1084–1095.

Sharma M, Kambadur R, Matthews KG, Somers WG, Devlin GP, Conaglen JV, Fowke PJ, Bass JJ. 1999. Myostatin, a transforming growth factor-beta superfamily member, is expressed in heart muscle and is upregulated in cardiomyocytes after infarct. J Cell Physiol 180:1–9.

ten Dijke P, Yamashita H, Sampath TK, Reddi AH, Estevez M, Riddle DL, Ichijo H, Heldin CH, Miyazono K. 1994. Identification of type I receptors for osteogenic protein-1 and bone morphogenetic protein-4. J Biol Chem 269: 16985–16988.

Thies RS, Bauduy M, Ashton BA, Kurtzberg L, Wozney JM, Rosen V. 1992. Recombinant human bone morphogenetic protein-2 induces osteoblastic differentiation in W-20-17 stromal cells. Endocrinology 130:1318–1324.

Tsuji K, Ito Y, Noda M. 1998. Expression of the PEBP2alphaA/AML3/CBFA1 gene is regulated by BMP4/7 heterodimer and its overexpression suppresses type I collagen and osteocalcin gene expression in osteoblastic and nonosteoblastic mesenchymal cells. Bone 22:87–92.

Urist MR. 1965. Bone: formation by autoinduction. Science 150:893–899.

Urist MR, Strates BS. 1971. Bone morphogenetic protein. J Dent Res 50:1392–406.

Wozney JM, Rosen V. 1998. Bone morphogenetic protein and bone morphogenetic protein gene family in bone formation and repair. Clin Orthop 346:26–37.

Wu LN, Ishikawa Y, Genge BR, Sampath TK, Wuthier RE. 1997. Effect of osteogenic protein-1 on the development and mineralization of primary cultures of avian growth plate chondrocytes: modulation by retinoic acid. J Cell Biochem 67:498–513.

Yamashita H, ten Dijke P, Huylebroeck D, Sampath TK, Andries M, Smith JC, Heldin CH, Miyazono K. 1995. Osteogenic protein-1 binds to activin type II receptors and induces certain activin-like effects. J Cell Biol 130: 217–226.

Yao KL, Todescan R, Jr, Sodek J. 1994. Temporal changes in matrix protein synthesis and mRNA expression during mineralized tissue formation by adult rat bone marrow cells in culture. J Bone Miner Res 9:231–240.

Yeh LC, Adamo ML, Kitten AM, Olson MS, Lee JC. 1996. Osteogenic protein-1-mediated insulin-like growth factor gene expression in primary cultures of rat osteoblastic cells. Endocrinology 137:1921–1931.

Yeh LC, Adamo ML, Olson MS, Lee JC. 1997. Osteogenic protein-1 and insulin-like growth factor I synergistically stimulate rat osteoblastic cell differentiation and proliferation. Endocrinology 138:4181–4190.

Yeh LC, Betchel KP, Lee JC. 1998. Inhibition of BMP receptor synthesis by antisense oligonucleotides attenuates OP-1 action in primary cultures of fetal rat calvaria cells. J Bone Miner Res 13:1870–1879.

Yeh LC, Unda R, Lee JC. 2000. Osteogenic protein-1 differentially regulates the mRNA expression of bone morphogenetic proteins and their receptors in primary cultures of osteoblasts. J Cell Physiol 185:87–97.

Exhibit E

NAL OF D MINERAL RESEARCH

VOL. 15. NO. 9. SEPTEMBER 2000 PP. 1645-1866

www.jbmronline.org

JBMR

PUBLISHED MONTHLY BY
THE AMERICAN SOCIETY FOR BONE AND MINERAL RESEARCH

JOURNAL OF BONE AND MINERAL RESEARCH

VOLUME 15 NUMBER 9 SEPTEMBER 2000

PERSPECTIVE

Corticosteroid Osteoporosis: Practical Implications of Recent Trials — P.N. Sambrook — 1645

ORIGINAL ARTICLES

Type V Osteogenesis Imperfecta: A New Form of Brittle Bone Disease — F.H. Glorieux, F. Rauch, H. Plotkin, L. Ward, R. Travers, P. Roughley, L. Lalic, D.F. Glorieux, F. Fassier, and N.J. Bishop — 1650

Hedgehog Proteins Stimulate Chondrogenic Cell Differentiation and Cartilage Formation — M. Enomoto-Iwamoto, T. Nakamura, T. Aikawa, Y. Higuchi, T. Yuasa, A. Yamaguchi, T. Nohno, S. Noji, T. Matsuya, K. Kurisu, E. Koyama, M. Pacifici, and M. Iwamoto — 1659

Interleukin-1β Increases the Functional Expression of Connexin 43 in Articular Chondrocytes: Evidence for a Ca^{2+}-Dependent Mechanism — R. Tonon and P. D'Andrea — 1669

Congenital Hip Dysplasia and Bone Mineral Density of the Hip—a New Risk Factor for Osteoporotic Fracture? — B.M. Obermayer-Pietsch, D. Walter, S. Kotschan, M. Freigassner-Pritz, R. Windhager, and G. Leb — 1678

Coordinate Expression of Novel Genes During Osteoblast Differentiation — A. Seth, B.K. Lee, S. Qi, and C.P.H. Vary — 1683

Evidence for the Involvement of Two Pathways in Activation of Extracellular Signal-Regulated Kinase (Erk) and Cell Proliferation by Gi and Gq Protein–Coupled Receptors in Osteoblast-Like Cells — J. Caverzasio, G. Palmer, A. Suzuki, and J.-P. Bonjour — 1697

Effects of Glucocorticoids on Tumor Necrosis Factor α–Dependent Activation of Nuclear Factor κB and Expression of the Intercellular Adhesion Molecule 1 Gene in Osteoblast-Like ROS17/2.8 Cells — K. Kurokouchi, F. Kambe, T. Kikumori, T. Sakai, D. Sarkar, N. Ishiguro, H. Iwata, and H. Seo — 1707

Phosphatidylinositol 3-Kinase Translocates to the Nucleus of Osteoblast-Like MC3T3-E1 Cells in Response to Insulin-Like Growth Factor I and Platelet-Derived Growth Factor But Not to the Proapoptotic Cytokine Tumor Necrosis Factor α — A.M. Martelli, P. Borgatti, R. Bortul, M. Manfredini, L. Massari, S. Capitani, and L.M. Neri — 1716

Mechanically Strained Cells of the Osteoblast Lineage Organize Their Extracellular Matrix Through Unique Sites of $\alpha_V\beta_3$-Integrin Expression — M. Wozniak, A. Fausto, C.P. Carron, D.M. Meyer, and K. A. Hruska — 1731

Human Bone Cell Hyperpolarization Response to Cyclical Mechanical Strain Is Mediated by an Interleukin-1β Autocrine/Paracrine Loop — D.M. Salter, W.H.B. Wallace, J.E. Robb, H. Caldwell, and M.O. Wright — 1746

(Continued)

Particulate Wear Debris Activates Protein Tyrosine Kinases and Nuclear Factor κB, Which Down-Regulates Type I Collagen Synthesis in Human Osteoblasts	C. Vermes, K.A. Roebuck, R. Chandrasekaran, J.G. Dobai, J.J. Jacobs, and T.T. Glant	1756
Importance of Membrane- or Matrix-Assoicated Forms of M-CSF and RANKL/ODF in Osteoclastogenesis Supported by SaOS-4/3 Cells Expressing Recombinant PTH/PTHrP Receptors	K. Itoh, N. Udagawa, K. Matsuzaki, M. Takami, H. Amano, T. Shinki, Y. Ueno, N. Takahashi, and T. Suda	1766
Collagen Structure Regulates Fibril Mineralization in Osteogenesis as Revealed by Cross-Link Patterns in Calcifying Callus	M.H.M. Wassen, J. Lammens, J.M. Tekoppele, R.J.B. Sakkers, Z. Liu, A.J. Verbout, and R.A. Bank	1776
Evaluation of Changes in Trabecular Bone Architecture and Mechanical Properties of Minipig Vertebrae by Three-Dimensional Magnetic Resonance Microimaging and Finite Element Modeling	B. Borah, T.E. Dufresne, M.D. Cockman, G.J. Gross, E.W. Sod, W.R. Myers, K.S. Combs, R.E. Higgins, S.A. Pierce, and M.L. Stevens	1786
Long-Term Evaluation of Bone Formation by Osteogenic Protein 1 in the Baboon and Relative Efficacy of Bone-Derived Bone Morphogenetic Proteins Delivered by Irradiated Xenogeneic Collagenous Matrices	U. Ripamonti, B. Van Den Heever, J. Crooks, M.M. Tucker, T.K. Sampath, D.C. Rueger, and A.H. Reddi	1798
Effect of Vitamin K_2 on Three-Dimensional Trabecular Microarchitecture in Ovariectomized Rats	T. Mawatari, H. Miura, H. Higaki, T. Moro-Oka, K. Kurata, T. Murakami, and Y. Iwamoto	1810
Effect of Calcitriol on Bone Loss After Cardiac or Lung Transplantation	P. Sambrook, N.K. Henderson, A. Keogh, P. MacDonald, A. Glanville, P. Spratt, P. Bergin, P. Ebeling, and J. Eisman	1818
Immunosuppression with FK506 Increases Bone Induction in Demineralized Isogeneic and Xenogeneic Bone Matrix in the Rat	G. Voggenreiter, S. Assenmacher, E. Kreuzfelder, M. Wolf, M.-R. Kim, D. Nast-Kolb, and F.U. Schade	1825
Serum Estradiol and Sex Hormone–Binding Globulin and the Risk of Hip Fracture in Elderly Women: The EPIDOS Study	R.D. Chapurlat, P. Garnero, G. Bréart, P.J. Meunier, and P.D. Delmas, for the EPIDOS Study Group	1835
Effect of Deconditioning on Cortical and Cancellous Bone Growth in the Exercise Trained Young Rats	J. Iwamoto, J.K. Yeh, and J.F. Aloia	1842
Reconciling Quantitative Ultrasound of the Calcaneus with X-Ray–Based Measurements of the Central Skeleton	M. Ayers, M. Prince, S. Ahmadi, and D.T. Baran	1850
Hypovitaminosis D in a Sunny Country: Relation to Lifestyle and Bone Markers	M.-H. Gannagé-Yared, R. Chemali, N. Yaacoub, and G. Halaby	1856
Book Review *Atlas of Musculoskeletal Imaging.* T. L. Pope, Jr., S. Loehr (eds.) C. Hagenstad, Contributing Author. Thieme, New York, NY, U.S.A., 2000.	C.H. Chesnut III	1863
Announcements		1864

JOURNAL OF BONE AND MINERAL RESEARCH
Volume 15, Number 9, 2000

Long-Term Evaluation of Bone Formation by Osteogenic Protein 1 in the Baboon and Relative Efficacy of Bone-Derived Bone Morphogenetic Proteins Delivered by Irradiated Xenogeneic Collagenous Matrices

U. RIPAMONTI,[1] B. VAN DEN HEEVER,[1] J. CROOKS,[1] M.M. TUCKER,[2] T.K. SAMPATH,[2] D.C. RUEGER,[3] and A.H. REDDI[4]

ABSTRACT

To investigate the long-term efficacy of irradiated recombinant human osteogenic protein 1 (hOP-1) in bone regeneration and morphogenesis, hOP-1 was combined with a bovine collagenous matrix carrier (0, 0.1, 0.5, and 2.5 mg hOP-1/g of matrix), sterilized with 2.5 Mrads of γ-irradiation, and implanted in 80 calvarial defects in 20 adult baboons (*Papio ursinus*). The relative efficacy of partially purified bone-derived baboon bone morphogenetic proteins (BMPs), known to contain several osteogenic proteins, was compared with the recombinant hOP-1 device in an additional four baboons. Histology and histomorphometry on serial undecalcified sections prepared from the specimens harvested on day 90 and day 365 showed that γ-irradiated hOP-1 devices induced regeneration of the calvarial defects by day 90, although with reduced bone area compared with a previous published series of calvarial defects treated with nonirradiated hOP-1 devices. One year after application of the irradiated hOP-1 devices, bone and osteoid volumes and generated bone tissue areas were comparable with nonirradiated hOP-1 specimens. Moreover, 365 days after healing regenerates induced by 0.5 mg and 2.5 mg of irradiated hOP-1 devices showed greater amounts of bone and osteoid volumes when compared with those induced by nonirradiated hOP-1 devices. On day 90, defects treated with 0.1 mg and 0.5 mg of bone-derived baboon BMPs, combined with irradiated matrix, showed significantly less bone compared with defects receiving irradiated devices containing 0.1 mg and 0.5 mg hOP-1; 2.5 mg of partially purified BMPs induced bone and osteoid volumes comparable with the 0.1-mg and 0.5-mg hOP-1 devices. Control specimens of γ-irradiated collagenous matrix without hOP-1 displayed a nearly 2-fold reduction in osteoconductive bone repair when compared with nonirradiated controls. These findings suggest that the reduction in bone volume and bone tissue area on day 90 may be caused by a reduced performance of the irradiated collagenous matrix substratum rather than to a reduction in the biological activity of the irradiated recombinant osteogenic protein. This is supported by the results of in vitro and in vivo studies performed to determine the structural integrity of the recovered γ-irradiated hOP-1 before application in the baboon. Recoveries by high-performance liquid chromatography (HPLC) and sodium dodecyl sulfate/polyacrylamide gel electrophoresis (SDS/PAGE)/immunoblot analyses indicated that doses of 2.5–3 Mrads of γ-irradiation did not significantly affect the structural integrity of the recovered hOP-1. Biological activity of the recovered hOP-1 was confirmed in vitro by showing induction of alkaline phosphatase activity in rat osteosarcoma cells (ROS) and in vivo by de novo endochondral bone formation in the subcutaneous space of the rat. These findings in the adult primate indicate that a single application of γ-irradiated hOP-1 combined

[1]Bone Research Laboratory, Medical Research Council/University of the Witwatersrand, Johannesburg, South Africa.
[2]Creative BioMolecules, Hopkinton, Massachusetts, U.S.A.
[3]Stryker Biotech., Hopkinton, Massachusetts, U.S.A.
[4]Center for Tissue Regeneration and Repair, University of California Davis, School of Medicine, Sacramento, California, U.S.A.

with the irradiated xenogeneic bovine collagenous matrix carrier is effective in regenerating and maintaining the architecture of the induced bone at doses of 0.5 mg/g and 2.5 mg/g of carrier matrix. (J Bone Miner Res 2000;15:1798–1809)

Key words: bone morphogenetic proteins, osteogenic protein-1, bone induction, collagenous matrices, γ-irradiation, primates

INTRODUCTION

BONE REGENERATION in clinical contexts requires three key components: an osteoinductive signal; an insoluble substratum, which delivers the signal and acts as a scaffold for new bone formation; and host cells capable of differentiation into bone cells in response to the osteoinductive signal. The signals responsible for osteoinduction are conferred by the family of the bone morphogenetic proteins (BMPs). BMPs are members of a superfamily of morphogens that include the transforming growth factor βs (TGF-βs), the growth/differentiating factors (GDFs), and cartilage-derived morphogenetic proteins (CDMPs).[1–6] In addition, the BMPs show significant amino acid identities with developmentally critical regulatory genes such as decapentaplegic (DPP) and 60A in Drosophila, Vegetal (Vg-1) in Xenopus and activins and inhibins.[1–4] A striking and discriminating feature of BMPs is their ability to induce de novo cartilage and bone formation in extraskeletal (heterotopic) sites, recapitulating embryonic bone development.[1–4] Originally, the osteogenic potential of BMPs was shown by reconstituting dissociatively extracted demineralized bone matrix with purified solubilized proteins.[7] This was followed by molecular cloning and expression of several recombinant human BMPs (BMP-2 to BMP-6, osteogenic protein 1 [OP-1] and OP-2.[8–11] Recombinant human BMP-2, BMP-4, and OP-1 (BMP-7) singly initiate endochondral bone formation in the subcutaneous space of the rat when combined with insoluble collagenous bone matrix, the inactive residue obtained after dissociative extraction of bone matrix with 4 M guanidinium-HCl.[12–14] In addition to BMPs/OPs, other related signaling proteins display heterotopic bone inductive activities in the rodent subcutaneous assay, including recombinantly produced DPP and 60A,[15] gene products expressed early in Drosophila development, and GDF-5 (CDMP-1),[16] a BMP/OP-related protein that may be critical during skeletogenesis, as suggested by mutations of the GDF-5 gene in brachypodism affected mice[17] and humans.[18]

The presence of several related but different BMPs with osteogenic activity points to multiple interactions during both embryonic development and bone regeneration in postnatal life. The fact that a single BMP/OP initiates bone formation does not preclude the requirement and interactions of other morphogens deployed synchronously and sequentially during the cascade of bone formation by induction.[1–4] The apparent redundancy of BMP/OP family members may have biological and therapeutic relevance in bone induction, which may proceed via the combined action of several BMPs/OPs, resident within the natural milieu of the extracellular matrix of bone.

The necessity of the insoluble substratum (collagenous matrix) in the induction of tissue morphogenesis and regeneration by an osteogenic signal (BMPs/OPs) illustrates the critical importance of the extracellular matrix for cell recruitment, attachment, proliferation, and differentiation.[1,3,7] Although the therapeutic use of recombinant BMPs/OPs requires sterilization of both soluble signal and insoluble substratum combined to produce an osteogenic device, comprehensive studies on the therapeutic efficacy of bone formation by irradiated osteogenic proteins and irradiated matrices are lacking. Here we report on the characterization and biological activity of hOP-1 after irradiation and on the long-term evaluation of bone regeneration by the irradiated hOP-1 device in calvarial defects of adult baboons. Moreover, we compared the relative inductive efficacy of partially purified baboon BMPs, known to contain several BMPs/OPs in addition to as yet poorly characterized mitogens, with the regenerates induced by the single and recombinant hOP-1 device in the same primate model.

MATERIALS AND METHODS

Preparation of the osteogenic devices

Mature recombinant human OP-1 is a glycosylated 36-kDa homodimer of 139 amino acid residue chains. Stock solutions of hOP-1 were prepared in 50% ethanol, 0.01% trifluoroacetic acid, and protein concentration determined by absorbance readings at 280 nm using an extinction coefficient of 2.0 for a 1.0-mg/ml solution. Demineralized bone matrix, prepared from diaphyseal segments of bovine cortical bones, was dissociatively extracted in 4 M guanidinium-HCl[7] and the resulting inactive insoluble collagenous matrix was treated with 0.1 M acetic acid at 55°C for 1 h, washed with distilled water, and dried. Aliquots of carrier matrix (1 g) were combined with 0.1, 0.5, and 2.5 mg of hOP-1 and lyophilized to produce the hOP-1 device. Bovine collagenous matrix was prepared with liquid vehicle without hOP-1, lyophilized, and used as control. The hOP-1 devices were packaged in borosilicate glass vials and sealed under vacuum. The devices were then sterilized at ambient temperature with γ-radiation (Cobalt-60 source) using an irradiation dose of approximately 0.3 Mrads/h for a total of 2.5–3.0 Mrads. The irradiation was performed at a contract facility (Isomedix, Northborough, MA, U.S.A., or Radiation Technologies, Inc., NJ, U.S.A.). This dose of irradiation was selected because 2.5 Mrads is accepted by the medical device industry and the Food and Drug Administration (Rockville, MD, U.S.A.) as the minimum required dose to sterilize med-

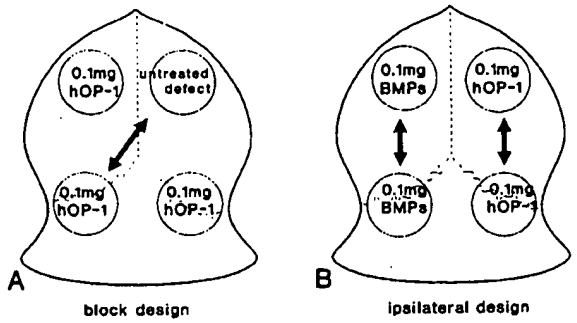

FIG. 1. Calvarial model and implantation design in 24 adult male baboons. In 20 animals (12 and 8 for tissue harvest on day 90 and day 365, respectively), (A) a block design was used to allocate three identical doses of the irradiated device (either 0, 0.1, 0.5, or 2.5 mg/g of bovine collagenous matrix in triplicate). Remaining defects (n = 20) were left untreated and sequentially alternated in each animal (arrow). (B) An ipsilateral design was used in the remaining four animals to investigate the relative efficiency of bone-derived BMPs (0.1, 0.5, and 2.5 mg) delivered by irradiated bovine collagenous matrix (n = 10). Remaining contralateral defects (n = 6) were implanted with 0.1 mg and 0.5 mg of hOP-1 irradiated device.

ical supplies.[19-21] For this collagen-based device, 1.5 Mrads was determined to be the minimum dose required to achieve a 10^{-6} sterility assurance level.[22] In addition to inactivating bacteria, 2.5 Mrads γ-irradiation has been shown to reduce viral titers by 3–5 logs using model virus systems.[23]

Baboon acid–demineralized bone matrix was extracted in 4 M guanidinium-HCl,[7] and partial purification was achieved by sequential chromatography of the protein extract on heparin-Sepharose, hydroxyapatite, and Sephacryl S-200 columns, washed and eluted as described.[19,20] To increase specific osteogenic activity of the preparation, Sephacryl S-200 fractions were chromatographed on a second heparin-Sepharose affinity column (20-ml bed volume). The recovered 500-mM NaCl step-eluted fraction was concentrated, exchanged with 5 mM HCl to a final concentration of 1 mg/ml protein (7.5 mg total amount), and sterilized by filtration (0.22 μm; Millex; Millipore Corp., Bedford, MA, U.S.A.). Aliquots were combined with 25 mg of rat insoluble collagenous matrix and assayed for osteogenic activity in the subcutaneous space of the rat as described.[24-26] Implants were harvested on day 12 and osteogenic activity in the rat was assessed by measuring alkaline phosphatase activity, calcium content, and histology. For preparation of devices, bone-derived BMPs in 500 μl of 5 mM HCl were added to 1 g of irradiated bovine collagenous matrix per sample at doses of 0.1 (n = 4), 0.5 (n = 4), and 2.5 mg (n = 2) and lyophilized.

Characterization and biological activity of hOP-1 device after γ-irradiation

To determine the recovery of the recombinant morphogen from the collagenous matrix, hOP-1 was eluted from the matrix with 8 M urea buffer, and the integrity and yield of the recovered protein was assessed by reversed-phase high-performance liquid chromatography (rpHPLC) in acetonitrile gradient. The recovered hOP-1 also was analyzed by sodium dodecyl sulfate–polyacrylamide gel electrophoresis (SDS-PAGE) followed by immunoblot analysis using antibodies specific for hOP-1.[27] The biological activity of the proteins recovered from γ-irradiated and nonirradiated collagenous matrices was assayed using rat osteosarcoma (ROS) 17/2.8 cells cultured as described.[28] The alkaline phosphatase activity induced by hOP-1 recovered from irradiated and nonirradiated devices was compared with the activity induced by an hOP-1 standard.[14,28] To assess the in vivo osteogenic activity of the hOP-1 device after γ-irradiation, 3 doses of OP-1 (0.5, 1, and 2.5 μg) were combined with 25 mg of bovine collagenous matrix as carrier and sterilized with 2.5 Mrads of γ-irradiation. The pellets were implanted in the subcutaneous space of Long-Evans rats at bilateral sites over the pectoralis fascia.[14,26] Nonirradiated hOP-1 devices were used as positive controls. Implants were harvested on day 12 and assayed for tissue alkaline phosphatase activity, calcium content, and histology.[14,26]

TABLE 1. EFFECT OF γ-IRRADIATION OF THE RECOVERY OF hOP-1 FROM COLLAGENOUS MATRIX[a]

Irradiation	*hOP-1 recovery (mg/g collagenous matrix)*	*hOP-1 recovery (%)*
None (control)	2.13 ± 0.18	85%
2.5 Mrads	1.69 ± 0.24	67%

[a] The 2.5 mg of recombinant hOP-1 was combined with 1 g of bovine collagenous matrix and sterilized with 2.5 Mrads of γ-irradiation. The recombinant protein was eluted from irradiated and nonirradiated hOP-1 devices with 8 M urea buffer and analyzed by rpHPLC as described in the Materials and Methods section. Determinations were done in triplicate and are expressed as mean and SD.

Primate model for tissue induction

Twenty-four clinically healthy adult Chacma baboons (*Papio ursinus*), with a mean weight of 34.8 ± 3.1 kg, were selected from the primate colony of the University of the Witwatersrand, Johannesburg. Comparative histomorphometric studies between iliac crest biopsy specimens of humans and *Papio ursinus* showed a remarkable degree of similarity.[29] This makes the adult male baboon ideally suited for the study of comparative bone physiology and repair with relevance to man.[29] Criteria for selection, housing conditions and diet were as described.[30] Research protocols were approved by the Animal Ethics Screening Committee of the university, and conducted according to the *Guidelines for the Care and Use of Experimental Animals* prepared by the university, and in compliance with the *National Code for Animal Use in Research, Education and Diagnosis in South Africa*.[31] The orthotopic calvarial model in the baboon has been described in detail.[32-34] On

FIG. 2. Immunoblot analysis of recovered hOP-1 eluted from hOP-1 devices: effect of irradiation. Aliquots of collagenous matrix combined with hOP-1 were sterilized with 0.5–0.6, 1.5–1.8, and 2.5–3.0 Mrads of γ-irradiation. Proteins were eluted with 8 M urea buffer and analyzed for structural integrity by SDS/PAGE followed by immunoblot analysis and compared with doses of hOP-1 standard. Lane 1: hOP-1 standard, 0.5 ng; lane 2: nonirradiated collagenous matrix; lane 3: collagenous matrix, 0.5–0.6 Mrads; lane 4: collagenous matrix, 1.5–1.8 Mrads; lane 5: collagenous matrix, 2.5–3.0 Mrads; lane 6: nonirradiated hOP-1device, 1 ng; lane 7: hOP-1 device, 0.5–0.6 Mrads, 1 ng; lane 8: hOP-1 device, 1.5–1.8 Mrads, 1 ng; lane 9: hOP-1 device, 2.5–3.0 Mrads, 1 ng; lane 10: hOP-1 standard, 0.9 ng; lanes 11 and 12: molecular weight standard.

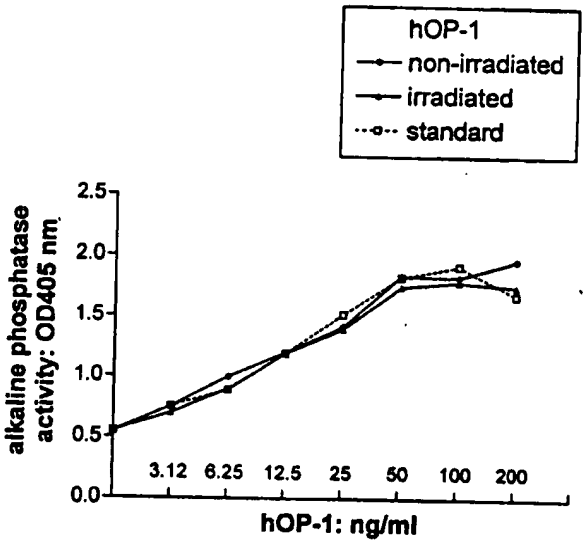

FIG. 3. Stimulation of alkaline phosphatase activity in ROS 17/2.8 cells by hOP-1. Confluent cells, cultured as described,[28] were treated with doses of hOP-1 eluted from irradiated and nonirradiated hOP-1 devices or with an hOP-1 standard. After removal of culture medium, washed cell layers were sonicated in 500 μl of extraction buffer (0.15 M NaCl and 3 mM $NaHCO_3$) containing 1% Triton X-100. Samples were assayed for alkaline phosphatase activity with *p*-nitrophenyl phosphate as substrate in 0.05 M glycine-NaOH buffer, pH 9.3, and absorbance was measured at 405 nm after stopping the reaction with 100 μl of 0.1 M NaOH.[21,23] The hOP-1 concentrations were based on rpHPLC recoveries, as described in the Materials and Methods section and the Results section.

each side of the calvaria, two full thickness defects, 25 mm in diameter, were created with a craniotome under saline irrigation.[32–34] After determination of the structural integrity and biological activity of the γ-irradiated hOP-1, a block design was used to allocate the position of the irradiated hOP-1 device in 80 calvarial defects in 20 adult male baboons (Fig. 1A). In each animal, three defects were implanted with an identical dose of hOP-1 in conjunction with the collagenous matrix as carrier. The remaining defect was left untreated, to determine whether hOP-1 had the ability to influence the untreated calvarial site at a distance from implantation. Thus, 15 defects in 5 baboons were implanted with 0.1 mg hOP-1, 15 defects with 0.5 mg hOP-1 and 15 defects with 2.5 mg hOP-1/g of collagenous matrix as carrier. In addition, 15 defects in 5 baboons were implanted with irradiated collagenous matrix without hOP-1 as control. To determine the relative efficacy of bone-derived partially purified baboon BMPs delivered by irradiated bovine collagenous matrix, experiments were performed in the remaining 4 baboons with a modified implantation design (Fig. 1B) in that in each animal, the two ipsilateral defects were implanted with doses of bone-derived BMPs (0.1, 0.5, and 2.5 mg/g of irradiated bovine collagenous matrix). Remaining defects ($n = 6$) were implanted with 0.1 mg and 0.5 mg of irradiated hOP-1 per device.

Tissue harvest, histology, and histomorphometry

Anesthetized animals were killed with an intravenous overdose of sodium pentobarbitone, 16 animals on day 90 and 8 animals on day 365 after surgery. Bilateral carotid perfusion and harvest of specimens with surrounding calvaria were as described.[32–34] Specimen blocks were cut along the sagittal one-fourth of the implanted defects, dehydrated in ascending grades of ethanol, and embedded, undecalcified, in a polymethyl methacrylate resin (K-Plast; Medim, Buseck, Germany). Undecalcified serial sections, cut at 7 μm (Polycut-S; Reichert, Heidelberg, Germany), were stained, free-floating, with Goldner's trichrome or with 0.1% toluidine blue in 30% ethanol. Goldner's trichrome–stained sections were examined with a Provis AX70 research microscope (Olympus Optical Co., Japan) equipped with a calibrated Zeiss Integration Platte II (Oberkochem, Germany) with 100 lattice points for determination by the point-counting technique,[35] of mineralized bone, osteoid, and residual collagenous matrix volumes (in %). Sections were analyzed at 40×, superimposing the Zeiss graticule over five sources[36] selected for histomorphometry and defined as follows: two anterior and posterior interfacial regions (AIF and PIF), two anterior and posterior internal regions (AIN and PIN), and a central region (CEN).[32–34] This technique allows the histomorphometric evaluation of the distribution of bone regeneration across

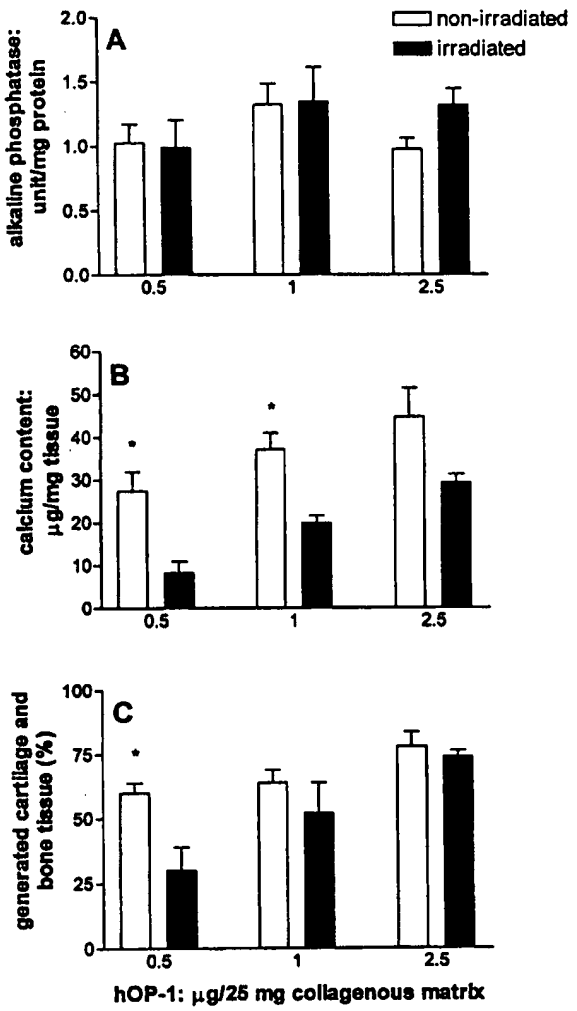

FIG. 4. In vivo biological activity of nonirradiated and irradiated hOP-1 devices. Doses of hOP-1, combined with 25 mg of bovine collagenous matrix as carrier were sterilized with 2.5 Mrads of γ-irradiation. Nonirradiated (control) and irradiated hOP-1 devices were implanted in the subcutaneous space of Long-Evans rats at bilateral sites over the pectoralis fascia. Generated tissues were removed on day 12 and subjected to (A) alkaline phosphatase activity and (B) calcium content determination. The alkaline phosphatase activity of the supernatant after homogenization of implants was determined with 0.1 M *p*-nitrophenyl phosphate as substrate (pH 9.3) at 37°C for 30 minutes.[26] Alkaline phosphatase is expressed as units of activity per milligram protein. Protein concentration in the supernatant was measured by the method of Lowry et al.[49] The calcium content of the acid-soluble fractions of the pellets was determined by colorimetric assay.[14] (C) Newly formed cartilage and bone (%) were examined on 1-µm sections stained with toluidine blue after fixation in Bouin's fluid and embedding in Historesin plastic medium (Reichert-Jung). Histomorphometric analysis was as described in the Materials and Methods section for baboon calvarial specimens. Values represent the mean ± SEM of four to five specimens per group; $^*p < 0.05$ versus nonirradiated specimens.

the defects.[32–34] Each source represented a field of 7.84 mm^2. The cross-sectional area (in mm^2) of newly generated bone tissue (mineralized bone, osteoid, and marrow)[36] in each calvarial defect was measured using a computerized image analysis system (Flexible Image Processing System; Council for Scientific and Industrial Research, Pretoria, South Africa) connected to a capturing video-camera (WV-CP410/G Panasonic; Panasonic, Osaka, Japan).[33] Morphometry (volumes and areas) was performed on four sections per implant, representing four parasagittal levels, approximately 2 mm apart from each other.[33]

Statistical analysis

The data were analyzed with the Statistical Analysis System.[37] An F test was performed using the General Linear Models procedure for an analysis of variance with multiple interactions.[32] Comparison of mean values was obtained using a Duncan's multiple-range test on the dependent variables included in the analysis. The significance probability value associated with the F value for each class variable was accepted as significant at $p < 0.05$.

RESULTS

Characterization of the hOP-1 device

The amount of hOP-1 recovered to assess the effect of irradiation of hOP-1 after elution from the 2.5-mg hOP-1 device is shown in Table 1. Chromatographic profiles obtained from rpHPLC of eluted hOP-1 from nonirradiated and irradiated collagenous matrices indicated that structurally intact hOP-1 could be recovered from hOP-1 devices sterilized by 2.5 Mrads of γ-irradiation (not shown). The structural integrity of the irradiated and recovered protein was confirmed by SDS/PAGE followed by immunoblot analysis, indicating that gamma irradiation does not significantly alter the immunoreactivity and the electrophoretic mobility of hOP-1 (Fig. 2). The biological activity of hOP-1 recovered from irradiated and nonirradiated devices was assessed using ROS 17/2.8 cells and induced levels of alkaline phosphatase activity comparable with that of the hOP-1 standard (Fig. 3). The effect of 2.5 Mrads of γ-irradiation on the in vivo biological activity of hOP-1 was assessed in the rat subcutaneous assay and the data are summarized in Fig. 4. Implantation of γ-irradiated hOP-1 devices resulted in a histologically reproducible pattern of endochondral bone differentiation comparable with that of tissues generated by nonirradiated hOP-1 devices and with comparable tissue alkaline phosphatase activity (Fig. 4A). γ-Irradiated specimens yielded less calcium when compared with nonirradiated samples (Fig. 4B) and contained lower amounts of newly generated cartilage and bone at the lowest dose of irradiated hOP-1 used (Fig. 4C).

Morphology of calvarial regeneration

Ninety days and 365 days after surgery, untreated defects showed minimal osteogenesis whether adjacent to defects treated with hOP-1 devices or to defects treated with col-

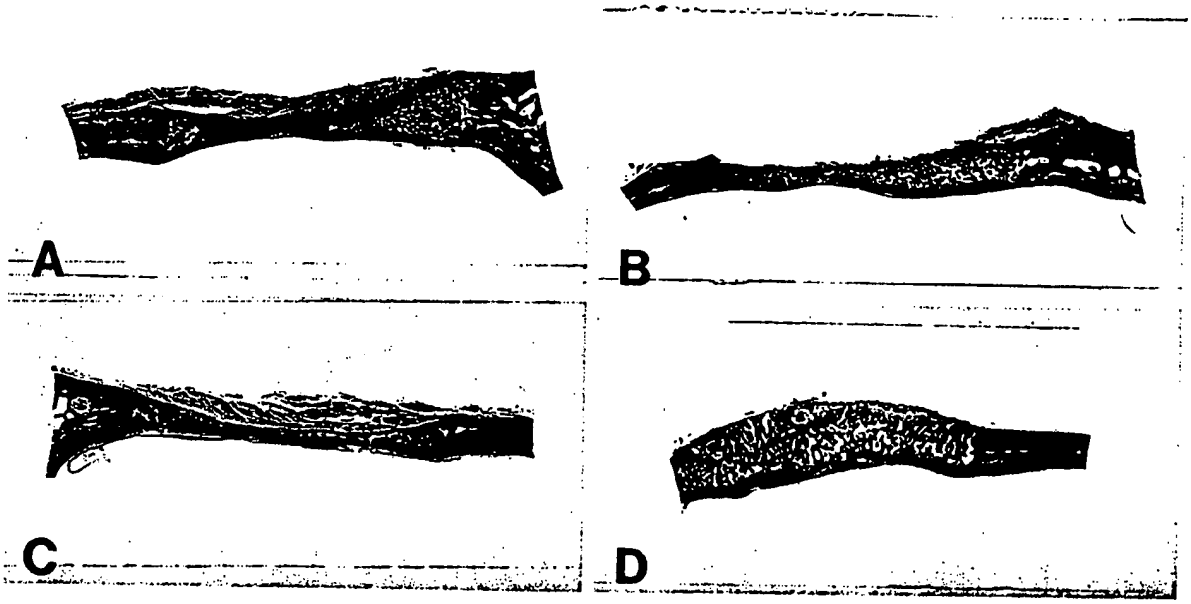

FIG. 5. Low power photomicrographs of calvarial specimens harvested on day 90. Undecalcified sections at 7 μm stained with Goldner's trichrome (original magnification ×2.5). (A) Irradiated bovine collagenous matrix without hOP-1 (control). (B and C) Regeneration of bone across the defects with doses of (B) 0.1 mg and (C) 0.5 mg of irradiated hOP-1 device. Newly formed trabeculae with thick osteoid seams (B), bone remodeling and the beginning of the formation of both pericranial and endocranial cortices (B and C). (D) Extensive induction of bone in a defect treated with 2.5 mg hOP-1; thick trabeculae of newly formed and mineralized bone connected to solid blocks of corticalized bone above the dura.

lagenous matrix alone (data not shown). On day 90, defects treated with bovine collagenous matrix without OP-1 (control) showed limited bone formation in continuity with the severed calvaria and complete dissolution of the implanted matrix (Fig. 5A). Defects treated with devices containing 0.1 mg and 0.5 mg hOP-1 resulted in bone regeneration across the defects (Fig. 5B), although the regenerated bone tissue appeared thinner than the original calvaria (Fig. 5C). Doses of 2.5 mg hOP-1/g of collagenous matrix induced a more pronounced osteogenic response, with numerous trabeculae covered by continuous osteoid seams facing newly generated marrow (Fig. 5D). On day 365, devices with 0.1, 0.5, and 2.5 mg hOP-1 induced complete bone regeneration, with reconstruction of the internal and external cortices of the calvaria (Fig. 6).

Macroscopic examination on day 90 showed areas of ossification beneath the fascia of the temporalis muscle, bilaterally, in animals that were treated in triplicate with the 2.5-mg hOP-1 device. In two animals, discrete flat ossicles, loose beneath the fascia, and ossification along the previously sutured fasciae and underlying muscle were observed. A third animal showed extensive ossification in the form of thick plates of newly formed bone covering almost the entirety of the temporalis muscle, bilaterally (Fig. 7A). Histological analysis showed formation of cortical and trabecular bone covered by thick osteoid seams (Figs. 7B and 7C). The finding of heterotopic osteogenesis above the temporalis muscle when the higher dose of the hOP-1 device was used in triplicate in the same animal may be the result of desorption of the recombinant protein from the surface of the carrier matrix, followed by diffusion of hOP-1 along the length of the surgical wound of the temporalis muscle during healing. However, only minor heterotopic flat ossicles were found macroscopically in the fasciae of animals from which tissues were harvested 1 year after the application of the higher dose of hOP-1.

On day 90, 0.1, 0.5, and 2.5 mg of bone-derived baboon BMPs delivered by irradiated bovine collagenous matrix induced new bone formation across the defects (Fig. 8), with newly formed and mineralized trabeculae being covered by continuous osteoid seams. Defects treated with 0.1 mg and 0.5 mg hOP-1 devices, which were harvested ipsilaterally to the defects treated with bone-derived BMPs, showed bone regeneration comparable with that of the previous series harvested on day 90 (Fig. 8D).

Morphometry: Effect of hOP-1 and bone-derived BMP doses on bone induction

Volume fractions (with levels of significance) of bone and osteoid in defects treated with the irradiated hOP-1 device are presented in Table 2. On day 90, 0.1, 0.5, and 2.5 mg hOP-1 devices induced greater amounts of bone and osteoid when compared with irradiated bovine matrix without hOP-1 (control; $p < 0.05$, Table 2), with the 2.5 mg dose showing the greater amount of bone when compared with 0.1 mg and 0.5 mg hOP-1 specimens ($p < 0.05$, Table 2). On day 365, the 0.1-, 0.5-, and 2.5-mg hOP-1 devices

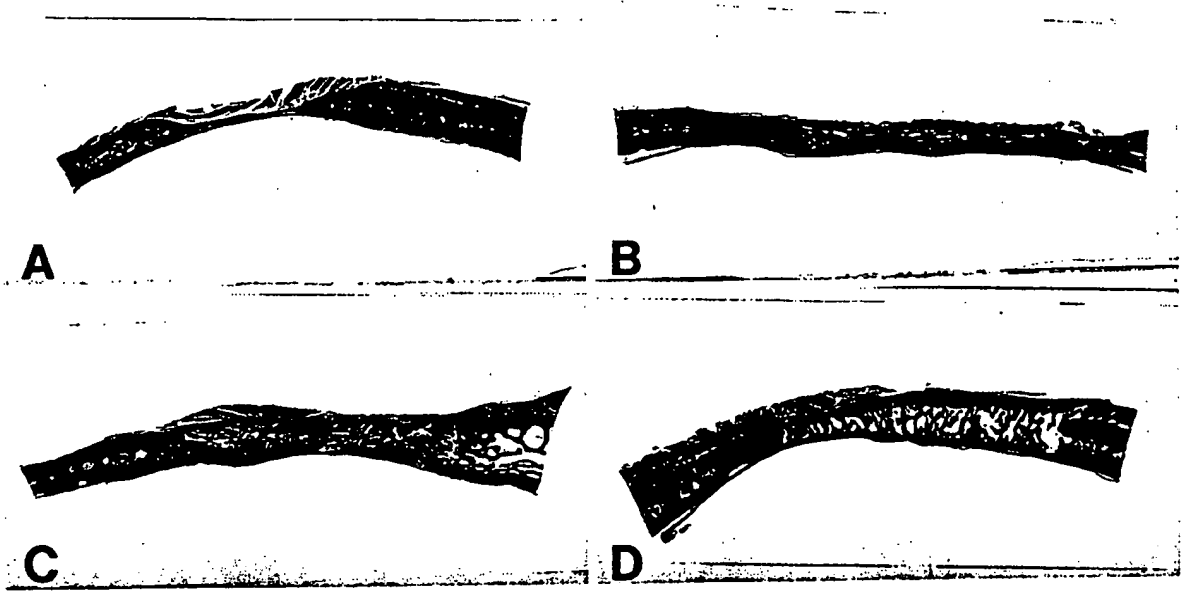

FIG. 6. Low-power photomicrographs of specimens of irradiated hOP-1 device harvested on day 365. Undecalcified sections at 7 μm stained with Goldner's trichrome (original magnification ×2.5). (A) Collagenous matrix without hOP-1 (control). (B–D) Complete reconstruction of defects with doses of (B) 0.1 mg, (C) 0.5 mg, and (D) 2.5 mg of the irradiated hOP-1 device. Maintenance of the generated bone tissue 1 year after a single application of hOP-1 and remodeling of the regenerates with doses of 0.1 mg and 0.5 mg hOP-1. (D) Reconstruction of both pericranial and endocranial cortices, with intervening trabeculae facing large areas of newly generated marrow in a defect treated with 2.5 mg of hOP-1.

showed greater amounts of bone when compared with control ($p < 0.05$, Table 2). Although doses of 0.1 mg and 0.5 mg hOP-1 generated comparable amounts of bone on day 90, on day 365 greater amounts of bone were found in specimens treated with 0.5 mg hOP-1 ($p < 0.05$ vs. 0.1 mg hOP-1, Table 2). Histomorphometric data of the present series of 80 calvarial defects were compared with previously published results using identical doses of nonirradiated hOP-1 devices[33] (Table 2). On day 90, on average, less bone formed in calvarial defects implanted with the irradiated hOP-1 device, including controls (Table 2). However, osteoid volumes generated by irradiated hOP-1 devices were found to be significantly greater ($p < 0.05$ vs. nonirradiated hOP-1, Table 2), with the exclusion of the 2.5-mg dose of hOP-1 (6.0 vs. 6.1%, respectively). On day 365, doses of 0.5 mg and 2.5 mg of irradiated hOP-1 showed greater amounts of bone when compared with equivalent doses of hOP-1 delivered by nonirradiated bovine matrix, and with a significant increase in bone volume between day 90 and day 365 ($p < 0.05$, Table 2).

Volume fractions of tissue components in calvarial defects treated with bone-derived baboon BMPs are shown in Table 3. Specimens generated by combining doses of baboon BMPs with irradiated bovine collagenous matrix showed substantial osteoid, comparable with osteoid volumes generated by irradiated hOP-1 devices (Table 3). Doses of 0.1 mg and 0.5 mg of baboon BMPs showed significantly less bone on day 90 when compared with doses of 0.1 mg and 0.5 mg of irradiated hOP-1 devices ($p < 0.05$, Table 3). The 2.5-mg baboon BMPs, in conjunction with irradiated bovine bone matrix, generated a comparable bone volume with the 2.5-mg hOP-1 device (Tables 2 and 3). Separate analysis of the irradiated 0.1-mg and 0.5-mg hOP-1 devices implanted in the two series of animals showed equal or comparable amounts of bone and osteoid volumes (Table 3). Greater amounts of residual collagenous matrix were found in specimens treated with 0.1 mg and 0.5 mg of baboon BMPs when compared with specimens of hOP-1 devices (Table 3).

Computer-generated data of cross-sectional areas (in mm^2) of specimens treated with the irradiated hOP-1 device on day 90 and day 365 are shown in Fig. 9. On day 90, irradiated hOP-1 devices generated less bone tissue area when compared with nonirradiated hOP-1 devices (Fig. 9A). On average on day 90, irradiation of both OP-1 and collagenous matrix resulted in regenerates with reduced tissue area when compared with normal calvaria (mean cross-sectional area, 60.8 ± 3.1 mm^2),[33] with the exception of the 2.5-mg dose of irradiated hOP-1 device (Fig. 9A). On day 365, defects treated with 0.5 mg and 2.5 mg of irradiated hOP-1 devices showed a significant increase compared with day 90 ($p < 0.05$), with remodeling that resulted in levels of bone tissue area comparable with normal calvaria (Fig. 9B). The 0.5-mg dose of hOP-1 showed the highest increase in bone tissue area from day 90 to 365, approaching levels of bone tissue area comparable with the 2.5-mg dose of hOP-1 (Fig. 9B).

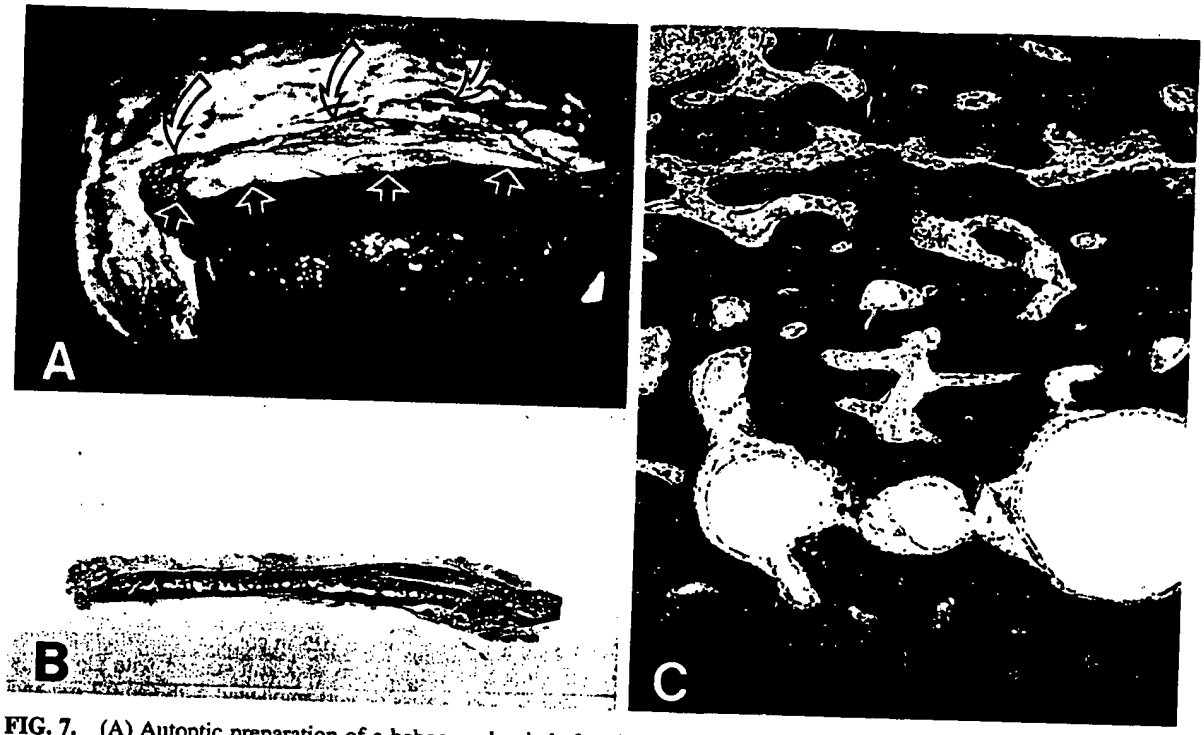

FIG. 7. (A) Autoptic preparation of a baboon calvaria before harvest of three defects that were treated with the 2.5-mg hOP-1 device. Thick plates of bone (white arrows) had formed between the temporalis fascia and the muscle, covering anterior-posteriorly and laterally, most of the underlying temporalis muscle (closed black arrows). The bone plates were united via the fascia to the temporalis crest bilaterally (open black arrows). (B) Low-power photomicrograph of the newly formed bone (frontal section) showing corticalization with formation of a pseudodiploic space. (C) Higher magnification of previous section; layers of mineralized bone covered by osteoid seams surrounding large central vascular spaces. Undecalcified section at 7 μm stained with Goldner's trichrome (B and C, original magnification, ×2.5 and ×30, respectively).

DISCUSSION

Information concerning the efficacy of irradiated osteogenic devices in nonhuman primates is an important prerequisite for clinical applications. A series of in vitro and in vivo studies were performed to determine the structural integrity and biological activity of the recoverable hOP-1 after γ-irradiation before preclinical application in calvarial defects of the adult baboon. Recoveries from rpHPLC and SDS/PAGE and immunoblot analysis indicated that doses of 2.5–3 Mrads of γ-irradiation did not significantly affect the structural integrity of hOP-1, although less hOP-1 could be recovered from the irradiated collagenous matrix. This possibly reflects some hOP-1 inactivation caused by cross-linking to the collagenous matrix. Biological activity of γ-irradiated hOP-1 was confirmed in vitro by assessing its induction of alkaline phosphatase activity in ROS cells, and in vivo by evaluating its induction of de novo endochondral bone formation in the subcutaneous space in the rat. Lower doses of γ-irradiated hOP-1, that is, 0.5 μg and 1 μg, generated less cartilage and less bone tissue of lower calcium content than nonirradiated controls. A single application of γ-irradiated recombinant morphogen in conjunction with the xenogeneic bovine collagenous matrix induced regeneration of large calvarial defects of the adult baboon. Comparison of the data with a previous series of calvarial defects treated with nonirradiated hOP-1 devices prepared with an identical collagenous matrix as carrier[33] showed that γ-irradiation resulted in reduced bone volume and reduced generated bone tissue area on day 90, as evaluated by histomorphometry. Control specimens of γ-irradiated collagenous matrix without hOP-1 showed a near 2-fold reduction in osteoconductive bone repair when compared with nonirradiated controls. These data suggest that less bone volume and bone tissue area on day 90 obtained with irradiated hOP-1 devices compared with nonirradiated devices is caused by, at least in part, a reduced performance of the irradiated substratum of the collagenous matrix, although optimal experiments to show this potentially reduced performance would have to be designed to compare the activity of γ-irradiated hOP-1 delivered by both irradiated and nonirradiated collagenous matrix. The operational reconstitution of a soluble signal (hOP-1) with an insoluble substratum (the collagenous matrix) underscores the critical role of the collagenous matrix for the induction of tissue morphogenesis and regeneration.[1,7,25] The importance of

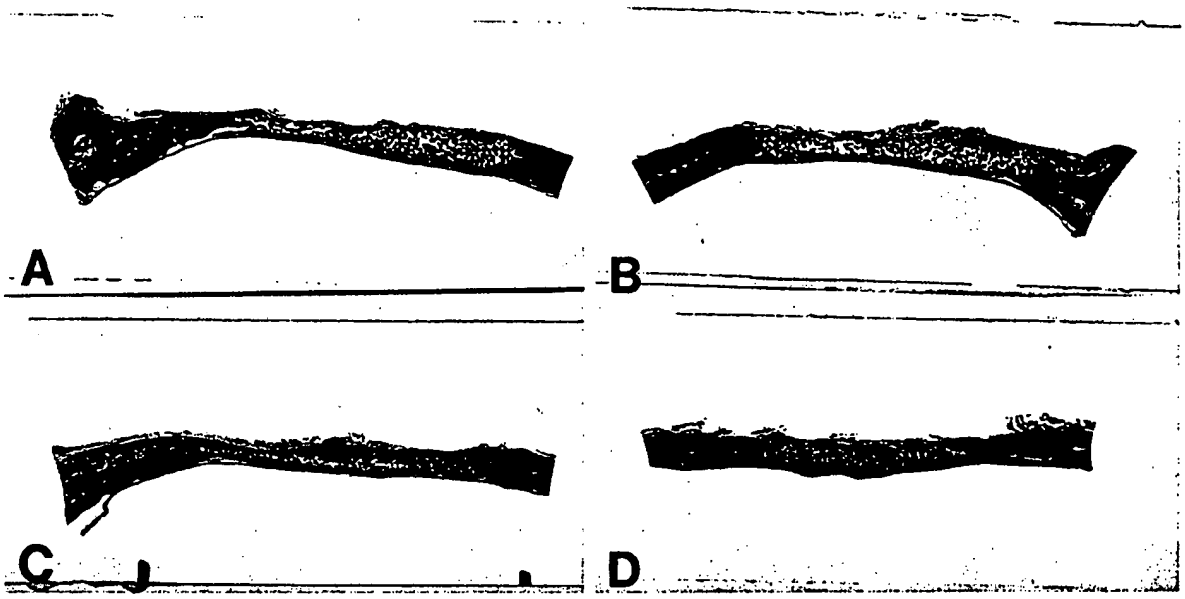

FIG. 8. Low-power photomicrographs of defects treated with bone-derived baboon BMPs in conjunction with irradiated bovine collagenous matrix as carrier and harvested on day 90. Undecalcified sections at 7 μm stained with Goldner's trichrome (original magnification, ×2.5). (A and B) Regeneration of bone across defects implanted with (A) 0.1 mg and (B) 0.5 mg of baboon BMPs, with trabeculae of newly formed bone facing newly generated marrow. (C and D) Induction of bone and remodeling with more compact structure in defects treated with (C) 2.5 mg of baboon BMPs and (D) 0.5 mg of irradiated hOP-1 device.

TABLE 2. EFFECT OF GAMMA IRRADIATION AND hOP-1 DOSES ON BONE INDUCTION BY hOP-1 DEVICES IMPLANTED IN 80 CALVARIAL DEFECTS PREPARED IN 20 ADULT BABOONS[a]

Days	*hOP-1 (mg)*	*Bone (%)*	*Osteoid (%)*	*Matrix (%)*
90	0.0	25.7 ± 2.9 (30.6 ± 2.6)	3.8 ± 0.5 (2.5 ± 0.2)	0.0 (4.2 ± 0.9)
	0.1	52.9 ± 1.6* (60.1 ± 1.1)	5.9 ± 0.2*,‡ (3.1 ± 0.2)	1.5 ± 0.4 (0.1 ± 0.05)
	0.5	48.4 ± 1.4* (60.8 ± 2.8)	4.9 ± 0.2*,‡ (2.9 ± 0.3)	0.3 ± 0.1 (0.3 ± 0.1)
	2.5	58.1 ± 1.7† (70.0 ± 0.9)	6.0 ± 0.3* (6.1 ± 0.3)	0.0 (0.0)
365	0.0	32.5 ± 2.8 (36.0 ± 6.1)	1.3 ± 0.1 (0.4 ± 0.1)	0.0 (0.0)
	0.1	51.6 ± 2.1*((64.9 ± 3.9)	1.3 ± 0.1 (0.8 ± 0.2)	0.0 (0.0)
	0.5	68.7 ± 1.9†,‡ (57.3 ± 5.5)	1.8 ± 0.1‡ (0.3 ± 0.1)	0.0 (0.0)
	2.5	73.7 ± 0.8†,‡ (64 ± 4.2)	1.7 ± 0.1‡ (0.3 ± 0.1)	0.0 (0.0)

[a] Doses of hOP-1, combined with 1 g of bovine collagenous matrix as carrier per sample, were subjected to irradiation (2.5 Mrads) and applied once at time of surgery in calvarial defects prepared in 20 adult baboons. Operated sites were harvested on day 90 and day 365 after bilateral carotid perfusion,[27–29] and serial undecalcified sections, cut at 7 μm, were analyzed by histomorphometry. Volume fractions of tissue components (in %) were calculated using a Zeiss Integration Platte II with 100 lattice points superimposed over 5 sources[31] in each of the four saggital sections used for analysis as described in the Materials and Methods section. Corresponding values of bone, osteoid, and matrix volumes (in %) obtained using nonirradiated hOP-1 devices[28] are shown in parenthesis. Bone refers to mineralized bone plus osteoid. Matrix refers to the residual collagenous carrier used for local delivery of hOP-1. Values are mean ± SEM.

* $p < 0.05$ versus 0.0 mg hOP-1 (control); † $p < 0.05$ versus 0.1 mg and 0.5 mg hOP-1 on day 90 and $p < 0.05$ versus 0.1 mg hOP-1 on day 365; ‡ $p < 0.05$ versus nonirradiated hOP-1.

the collagenous matrix for cell recruitment, attachment, proliferation, and differentiation has been previously reported.[38,39] Experiments using γ-irradiated bone matrices in rodents have indicated that irradiation damages collagen cross-linking, possibly by formation of free radicals, leading to peptide bond cleavage.[40,41] These changes may affect the instructive role of the substratum in defining the local microenvironment for osteoprogenitor cells proliferation and differentiation.[40] However, it was noteworthy that 1 year after the single application of the γ-irradiated hOP-1 device, bone and osteoid volumes and generated bone tissue areas were comparable with those of nonirradiated hOP-1 specimens. In particular by 1 year, regenerates induced by 0.5 mg and 2.5 mg of γ-irradiated hOP-1 induced greater amounts of bone and osteoid volumes when compared with nonirradiated hOP-1. This may be the result of sustained

TABLE 3. RELATIVE INDUCTIVE EFFICIENCY OF BONE-DERIVED BABOON BMPs COMBINED WITH BOVINE IRRADIATED COLLAGENOUS MATRIX AND HARVESTED ON DAY 90[a]

Treatment	*Bone (%)*	*Osteoid (%)*	*Matrix (%)*
0.1 mg BMPs	41.6 ± 2.4	5.4 ± 0.3	8.0 ± 1.1†
0.5 mg BMPs	40.7 ± 2.4	5.6 ± 0.5	13.1 ± 2.4†
2.5 mg BMPs	57.3 ± 0.3*	5.3 ± 0.3	0.0
0.1 mg hOP-1	53.5 ± 2.6* (52.9 ± 1.6)	5.7 ± 0.5 (5.9 ± 0.2)	1.1 ± 0.7 (1.5 ± 0.4)
0.5 mg hOP-1	52.5 ± 4.5* (48.4 ± 1.4)	4.8 ± 0.6 (4.9 ± 0.2)	0.0 (0.3 ± 0.1)

[a] BMP fractions, purified sequentially by liquid chromatography of guanidinium-extracted proteins from acid-demineralized baboon bone matrix, were combined at doses of 0.1, 0.5, and 2.5 mg with 1 g of γ-irradiated bovine collagenous matrix as carrier per sample, and after lyophilization, applied to 10 calvarial defects prepared in four adult male baboons. Remaining defects ($n = 6$) were implanted with 0.1 mg and 0.5 mg of irradiated hOP-1 device. Specimens were harvested on day 90 and serial undecalcified sections were analyzed by histomorphometry as described in the Materials and Methods section. Corresponding morphometric data on day 90 obtained using the 0.1-mg and 0.5-mg hOP-1 doses of the previous experiment (Table 2) are shown in parenthesis. Bone refers to mineralized bone plus osteoid. Matrix refers to the residual collagenous carrier used for local delivery of BMPs on hOP-1. Values are mean ± SEM.

* $p < 0.05$ versus 0.1 mg and 0.5 mg bone-derived BMPs; † $p < 0.05$ versus 2.5 mg BMPs and hOP-1 devices.

osteogenesis over time in γ-irradiated specimens as shown by the presence of substantial osteoid volumes on day 90.

Doses of 0.1 mg and 0.5 mg of bone-derived baboon BMPs combined with γ-irradiated bovine collagenous matrix yielded significantly less bone but substantial osteoid volumes when compared with 0.1-mg and 0.5-mg doses of γ-irradiated hOP-1. Although the partially purified BMP preparation was not subjected to γ-irradiation, thus precluding a direct comparison with irradiated hOP-1 specimens, it is noteworthy that 2.5 mg of partially purified BMPs and 2.5 mg of hOP-1 delivered by bovine collagenous matrix induced almost identical bone and osteoid volumes by day 90. The hOP-1 specimens (2.5 mg) yielded greater bone tissue area when measured by histomorphometry (data not shown). Partially purified preparations from bone matrix are known to contain, in addition to specific BMPs/OPs, several other proteins and some as yet poorly characterized mitogens.[42] The partially purified preparation from bone matrix obtained using the chromatographic procedures described is known to contain BMP-2, BMP-3, and OP-1 but not detectable TGF-βs (N.S. Cunningham and A.H. Reddi, unpublished data, 1989). To date, more than 15 related proteins with BMP-like sequences and activity have been cloned, but little is known about their interaction during the cascade of bone formation by induction, or about the biological and therapeutic significance of this apparent redundancy. Recombinantly produced hBMP-2, hBMP-4, and OP-1 are capable of singly initiating bone formation in vivo.[12-14] It is likely that the endogenous mechanisms of bone repair and regeneration in postnatal life necessitate the deployment and concerted actions of several of the BMPs/OPs resident within the natural milieu of the extracellular matrix of bone. Whether the biological activity of partially purified BMPs is the result of the sum of a plurality of BMP activities or of a truly synergistic interaction among BMP family members deserves appropriate investigation. In addition to bone induction in postfetal life, BMPs/OPs are involved in inductive events that control pattern formation during embryonic morphogenesis and organogenesis in such disparate tissue as the kidney, eye, nervous system, lung, teeth, skin, and heart.[43] These strikingly pleiotropic effects of BMPs/OPs

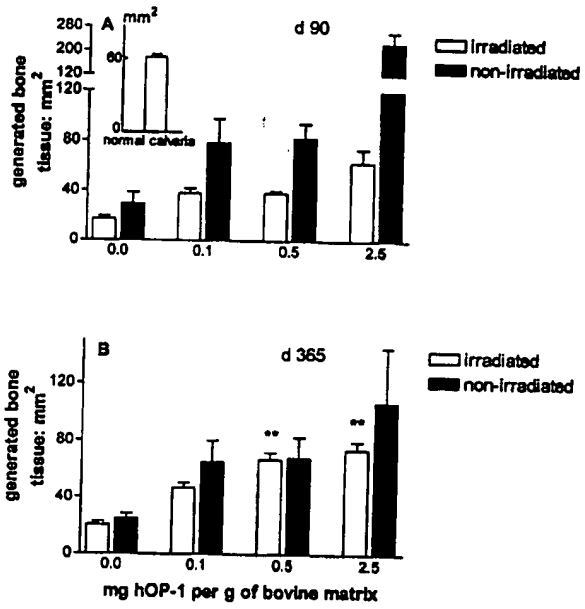

FIG. 9. Computerized analysis of new bone tissue area (mineralized bone, osteoid, and marrow) generated by doses of hOP-1 in conjunction with bovine collagenous matrix on (A) day 90 and (B) day 365. Specimens of irradiated hOP-1 device were compared with specimens of nonirradiated hOP-1 device prepared with an identical bovine collagenous matrix.[28] On day 90, doses of 0.1 mg and 0.5 mg of nonirradiated hOP-1 device showed a 2-fold increase in generated bone tissue ($p < 0.05$ vs. irradiated hOP-1 device), including collagenous matrix implanted without hOP-1 (A). On day 365, irradiated specimens showed a significant increase over 90 days ($p < 0.05$; B), approaching levels of bone tissue area induced by nonirradiated hOP-1 and comparable with the profile of normal unoperated calvaria (inset in A). *$p < 0.05$ versus nonirradiated hOP-1 specimens; **$p < 0.05$ versus irradiated specimens on day 90.

may spring from minor amino acid sequence variations in the carboxy-terminal region of the proteins,[44] as well as in the transduction of distinct signaling pathways by individual Smad proteins after transmembrane serine/threonine kinase receptor activation.[45]

In conclusion, the present findings illustrate the long-term efficacy of a single application of γ-irradiated hOP-1 delivered by a xenogeneic collagenous matrix in regenerating large defects of membranous bone of the adult primate. Ultimately, it will be necessary to gain insight into the potentially distinct spatial and temporal patterns of expression of other BMPs/OPs during morphogenesis and regeneration elicited by a single application of hOP-1. In vitro studies indicate that both hOP-1 and hBMP-2 modulate messenger RNA (mRNA) expression of related BMP family members.[46–48] In vivo studies may be useful in designing therapeutic approaches based on information of gene regulation by hOP-1.

ACKNOWLEDGMENTS

This work is supported by grants of the South African MRC, the University of the Witwatersrand, Johannesburg, and in part by a grant from the National Institutes of Health (DE 10712–01). We thank N. Ramoshebi for critical help during experiments and J. Tasker for critical reading of the manuscript.

REFERENCES

1. Reddi AH 1992 Regulation of cartilage and bone differentiation by bone morphogenetic proteins. Curr Opin Cell Biol 4:850–855.
2. Wozney JM 1992 The bone morphogenetic protein family and osteogenesis. Mol Reprod Dev 32:160–167.
3. Reddi AH 1994 Bone and cartilage differentiation. Curr Opin Genet Dev 4:737–744.
4. Centrella M, Horowitz M, Wozney JM, McCarthy TL 1994 Transforming growth factor β (TGF-β) family members and bone. Endocr Rev 15:27–39.
5. Lee S-J 1990 Identification of a novel member (GDF-1) of the transforming growth factor-β superfamily. Mol Endocrinol 4:1034–1040.
6. Chang SC, Hoang B, Thomas JT, Vukicevic S, Luyten FP, Ryba NJ, Kozak CA, Reddi AH, Moss M 1994 Cartilage-derived morphogenetic proteins. New members of the transforming growth factor-β superfamily predominantly expressed in long bones during human embryonic development. J Biol Chem 269:28227–28234.
7. Sampath TK, Reddi AH 1981 Dissociative extraction and reconstitution of extracellular matrix components involved in local bone differentiation. Proc Natl Acad Sci U S A 78:7599–7603.
8. Wozney JM, Rosen V, Celeste AJ, Mitsock LM, Whitters MJ, Kriz RW, Hewick RM, Wang EA 1988 Novel regulators of bone formation: Molecular clones and activities. Science 242: 1528–1534.
9. Celeste AJ, Iannazzi JM, Taylor JA, Hewick RC, Rosen V, Wang EA, Wozney JM 1990 Identification of transforming growth factor ί family members present in bone-inductive protein purified from bovine bone. Proc Natl Acad Sci USA 87:9843–9847.
10. Özkaynak E, Rueger DC, Drier EA, Corbett C, Ridge RJ, Sampath TK, Oppermann H 1990 OP-1 cDNA encodes an osteogenic protein in the TGF-ί family. EMBO J 9:2085–2093.
11. Özkaynak E, Schnegelsberg PNJ, Jin DF, Clifford GM, Warren FD, Drier EA, Oppermann H 1992 Osteogenic protein-2. A new member of the transforming growth factor-ί superfamily expressed early in embryogenesis. J Biol Chem 267:25220–25227.
12. Wang EA, Rosen V, D'Alessandro JS, Bauduy M, Cordes P, Harada T, Israel DI, Hewick RM, Kerns KM, LaPan P, Luxenberg DP, McQuaid D, Moutsatsos IK, Nove J, Wozney JM 1990 Recombinant human bone morphogenetic protein induces bone formation. Proc Natl Acad Sci USA 87:2220–2224.
13. Hammmonds RG, Schwall R, Dudley A, Berkemeier L, Lai C, Lee J, Cunningham N, Reddi AH, Wood WI, Mason AJ 1991 Bone inducing activity of mature BMP-2b produced from a hybrid BMP-2a/2b precursor. Mol Endocrinol 5:149–155.
14. Sampath TK, Maliakal JC, Hauschka PV, Jones WK, Sasak H, Tucker RF, White KH, Coughlin JE, Tucker MM, Pang RHL, Corbett C, Ozkaynak E, Oppermann H, Rueger DC 1992 Recombinant human osteogenic protein-1 (hOP-1) induces new bone formation in vivo with a specific activity comparable with natural bovine osteogenic protein and stimulates osteoblast proliferation and differentiation in vitro. J Biol Chem 267:20352–20362.
15. Sampath TK, Rashka KE, Doctor JS, Tucker RF, Hoffmann FM 1993 Drosophila TGF-β superfamily proteins induce endochondral bone formation in mammals. Proc Natl Acad Sci USA 90:6004–6008.
16. Hotten GC, Matsumoto T, Kimura M, Bechtold RF, Kron R, Ohara T, Tanaka H, Satoh Y, Okazaki M, Shirai T, Pan H, Kawai S, Pohl JS, Kudu A 1996 Recombinant human growth/differentiation factor 5 stimulates mesenchyme aggregation and chondrogenesis responsible for the skeletal development of limbs. Growth Factors 13:65–74.
17. Storm EE, Huynch TV, Copeland NG, Jenkins NA, Kingsley DM, Lee S-L 1994 Limb alterations in brachypodism mice due to mutations in a new member of the TGF-β superfamily. Nature 368:639–643.
18. Thomas JT, Lin K, Nandedkar M, Camargo M, Cervenka J, Luyten FP 1996 A human chondrodysplasia due to a mutation in a TGF-β superfamily member. Nat Genet 12:315–317.
19. Reddi AH 1998 Role of morphogenetic proteins in skeletal tissue engineering and regeneration. Nat Biotechnol 16:247–252.
20. Sterilization by Ionizing Radiation 1999 US Pharmacopeia 24: 2145.
21. Process Control Guidelines for Gamma Radiation Sterilization of Medical Devices 1984 Association for the Advancement of Medical Instrumentation, Arlington, VA, U.S.A.
22. Sterilization of Health Care Products—Requirements for Validation and Routine Control—Radiation Sterilization 1994 ANSI/AAMI/ISO 11137, Association for the Advancement of Medical Instrumentation, Arlington VA, U.S.A.
23. Wyatt DE, Keeathley JD, Williams CM, Broce R 1993 Is there life after irradiation? Part 1: Inactivation of Biological Contaminants. BioPharm.
24. Luyten FP, Cunningham NS, Ma S, Muthukumaran N, Hammonds RG, Nevins WB, Wood WI, Reddi AH 1989 Purification and partial amino acid sequence of osteogenin, a protein initiating bone differentiation. J Biol Chem 264:13377–13380.
25. Ripamonti U, Ma S, Cunningham N, Yeates L, Reddi AH 1992 Initiation of bone regeneration in adult baboons by osteogenin, a bone morphogenetic protein. Matrix 12:369–380.

26. Reddi AH, Huggins CB 1972 Biochemical sequences in the transformation of normal fibroblasts in adolescent rat. Proc Natl Acad Sci U S A 69:1601–1605.
27. Thomadakis G, Ramoshebi LN, Crooks J, Rueger DC, Ripamonti U 1999 Immunolocalization of bone morphogenetic protein-2 and -3 and osteogenic protein-1 during murine tooth root morphogenesis and in other craniofacial structures. Eur J Oral Sci 107:368–377.
28. Maliakal JC, Asahina I, Hauschka PV, Sampath TK 1994 Osteogenic protein-1 (BMP-7) inhibits cell proliferation and stimulates the expression of markers characteristics of osteoblastic phenotype in rat osteosarcoma (17/2.8) cells. Growth Factors 11:227–234.
29. Schnitzler CM, Ripamonti U, Mesquita JM 1993 Histomorphometry of iliac crest trabecular bone in adult male baboons in captivity. Calcif Tissue Int 52:447–454.
30. Ripamonti U 1991 Bone induction in nonhuman primates. An experimental study on the baboon (*Papio ursinus*). Clin Orthop 269:284–294.
31. Public Service Department 1990 National Code for Animal Use in Research, Education, Diagnosis and Testing of Drugs and Related Substances in South Africa. Public Service Department, Pretoria, South Africa.
32. Ripamonti U, Ma S, Cunningham N, Yeates L, Reddi AH 1993 Reconstruction of the bone-bone marrow organ by osteogenin, a bone morphogenetic protein, and demineralized bone matrix in calvarial defects of adult primates. Plast Reconstr Surg 91:27–36.
33. Ripamonti U, van den Heever B, Sampath TK, Tucker MM, Rueger DC, Reddi AH 1996 Complete regeneration of bone in the baboon by recombinant human osteogenic protein-1 (hOP-1, bone morphogenetic protein-7). Growth Factors 13: 273–289.
34. Ripamonti U, Bosch C, van den Heever B, Duneas N, Melsen B, Ebner R 1996 Limited chondro-osteogenesis by recombinant human transforming growth factor-β1 in calvarial defects of adult baboons (*Papio ursinus*). J Bone Miner Res 11:938–945.
35. Parfitt AM 1983 Stereologic basis of bone histomorphometry; theory of quantitative microscopy and reconstruction of the third dimension. In: Recker RR (ed.). Bone Histomorphometry: Techniques and Interpretation. CRC Press, Boca Raton, FL, U.S.A., pp. 53–87.
36. Parfitt AM, Drezner MK, Glorieux FH, Kanis JA, Malluche H, Meunier PJ, Ott SM, Recker RR 1987 Bone histomorphometry: Standardization of nomenclature, symbols, and units. J Bone Miner Res 2:595–610.
37. Statistical Analysis System 1989 SAS/STATS User's Guide, version 6, 4th ed, vol 1. SAS Institute, Inc., Cary, NC, U.S.A., pp. 209–244.
38. Reddi AH 1974 Importance of geometry of the extracellular matrix in endochondral bone differentiation. Adv Biol Med Phys 15:1–18.
39. Reddi AH 1984 Extracellular matrix and development. In: Piez KA, Reddi AH (eds.) Biochemistry of Extracellular Matrix. Elsevier, New York, NY, U.S.A., pp. 375–412.
40. Wientroub S, Reddi AH 1988 Influence of irradiation on the osteoinductive potential of demineralized bone matrix. Calcif Tissue Int 42:255–260.
41. Katz RW, Felthousen GC, Reddi AH 1990 Radiation-sterilized insoluble collagenous bone matrix is a functional carrier of osteogenin for bone induction. Calcif Tissue Int 47:183–185.
42. Hauschka PV, Mavrakos AE, Iafrati MD, Doleman SE, Klagsbrun M 1986 Growth factors in bone. J Biol Chem 261:12665–12674.
43. Reddi AH 1997 Bone morphogenetic proteins: An unconventional approach to isolation of first mammalian morphogens. Cytokine Growth Factor Rev 8:11–20.
44. Staehling-Hampton K, Jackson PD, Clark MJ, Brand AH, Hoffmann MF 1994 Specificity of bone morphogenetic protein-related factors: Cell fate and gene expression changes in *Drosophila* embryos induced by *decapentaplegic* bu t not *60A*. Cell Growth Differ 5:585–593.
45. Graff JM, Bansal A, Melton DA 1996 Xenopus mad proteins transduce distinct subsets of signals for the TGFβ superfamily. Cell 85:479–487.
46. Harris SE, Sabatini M, Harris MA, Feng JQ, Wozney JM, Mundy GR 1994 Expression of bone morphogenetic protein messenger RNA in prolonged cultures of fetal rat calvarial cells. J Bone Miner Res 9:389–394.
47. Chen D, Harris MA, Rossini G, Dunstan CR, Dallas SL, Feng JQ, Mundy GR, Harris SE 1997 Bone morphogenetic protein 2 (BMP-2) enhances BMP-3, BMP-4, and bone cell differentiation marker gene expression during the induction of mineralized bone matrix formation in cultures of fetal rat calvarial osteoblasts. Calcif Tissue Int 60:238–290.
48. Honda Y, Kniutsen R, Strong DD, Sampath TK, Baylink DJ, Mohan S 1997 Osteogenic protein-1 stimulates mRNA levels of BMP-6 and decreases mRNA levels of BMP-2 and -4 in human osteosarcoma cells. Calcif Tissue Int 60:297–301.
49. Lowry OH, Rosebrough NJ, Farr AL, Randall RJ 1951 Protein measurement with the folin phenol reagent. J Biol Chem 193:265–275.

Address reprint requests to:
Ugo Ripamonti, M.D., Ph.D.
Bone Research Laboratory
MRC/University of the Witwatersrand
Medical School, 7 York Road
Parktown 2193, Johannesburg, South Africa

Received in original form August 13, 1999; in revised form February 4, 2000; accepted March 2, 2000.

Exhibit F

THE JOURNAL OF BONE & JOINT SURGERY

GUST
003
VOL. 85-A No. 8
ISSN: 0021-9355
WWW.JBJS.ORG

JBJS

EXCELLENCE
THROUGH PEER
REVIEW

AUGUST 2003

THE JOURNAL OF BONE & JOINT SURGERY · AMERICAN VOLUME

SCIENTIFIC ARTICLES

1417
SHOULDER ARTHROPLASTY IN PATIENTS WITH A PRIOR ANTERIOR SHOULDER DISLOCATION. RESULTS OF A MULTICENTER STUDY
A translation of the abstract is available with the electronic versions of this article
J. Matsoukis, MD, W. Tabib, MD, P. Guiffault, MD, A. Mandelbaum, MD, Gilles Walch, MD, Chantal Némoz, PhD, and T. Bradley Edwards, MD

1425
A SINGLE PERCUTANEOUS INJECTION OF RECOMBINANT HUMAN BONE MORPHOGENETIC PROTEIN-2 ACCELERATES FRACTURE REPAIR
Thomas A. Einhorn, MD, Robert J. Majeska, PhD, Ahamed Mohaideen, MD, Eric M. Kagel, MD, Mary L. Bouxsein, PhD, Thomas J. Turek, and John M. Wozney, PhD

1436
EFFECT OF ACHILLES TENDON LENGTHENING ON NEUROPATHIC PLANTAR ULCERS. A RANDOMIZED CLINICAL TRIAL
Michael J. Mueller, PT, PhD, David R. Sinacore, PT, PhD, Mary Kent Hastings, MS/PT, ATC, Michael J Strube, PhD, and Jeffrey E. Johnson, MD

1446
EFFECT OF INTERMITTENT PNEUMATIC SOFT-TISSUE COMPRESSION ON FRACTURE-HEALING IN AN ANIMAL MODEL
Sang-Hyun Park, PhD, and Mauricio Silva, MD

1454
NECROTIZING FASCIITIS: CLINICAL PRESENTATION, MICROBIOLOGY, AND DETERMINANTS OF MORTALITY
Chin-Ho Wong, MBBS (Singapore), Haw-Chong Chang, MBBS (Singapore), FRCSEd (Ortho), MMed (Surgery), FRCS (Edin, Glas), Shanker Pasupathy, MBBS (Singapore), FRCS (Edin, Glas), Lay-Wai Khin, MBBS (Yangon), MSC (Singapore), Jee-Lim Tan, MBBS (Singapore), FRCS (Edin, Glas), FAMS, CASM (Sport Med), and Cheng-Ooi Low, MBBS (Singapore), FRCS (Glas), FAMS

1461
THE POSITION OF THE AORTA RELATIVE TO THE SPINE: A COMPARISON OF PATIENTS WITH AND WITHOUT IDIOPATHIC SCOLIOSIS
Daniel J. Sucato, MD, MS, and Clark Duchene, MD

1470
COMPARISON OF ROBOTIC-ASSISTED AND MANUAL IMPLANTATION OF A PRIMARY TOTAL HIP REPLACEMENT. A PROSPECTIVE STUDY
Matthias Honl, MD, Oliver Dierk, MD, Christian Gauck, MD, Volker Carrero, MD, Frank Lampe, MD, Sebastian Dries, MD, Markus Quante, MD, Karsten Schwieger, PhD, Ekkehard Hille, MD, and Michael M. Morlock, PhD

A COMPLETE VIDEO SUPPLEMENT TO THIS ARTICLE IS AVAILABLE FROM THE *VIDEO JOURNAL OF ORTHOPAEDICS*

How to Reach Us
Editorial and business offices: 20 Pickering Street, Needham, MA 02492-3157. Telephone: (781) 449-9780
www.jbjs.org · e-mail: mail@jbjs.org · Editorial Fax: (781) 449-9787 · Advertising Fax: (781) 449-3485 · Subscription Fax: (781) 449-9742
The Journal of Bone & Joint Surgery (ISSN: 0021-9355) (American Volume) is issued monthly.
The 2003 U.S. subscription price, payable in advance, is $135.00. Single copies, $25.00.
The Journal of Bone & Joint Surgery, periodicals postage paid at Boston, Massachusetts, and at additional mailing offices.
Postmaster: Send address changes to *The Journal of Bone & Joint Surgery*, 20 Pickering Street, Needham, MA 02492-3157.
The Journal of Bone and Joint Surgery®, JB&JS®, and JBJS® are registered in the U.S. Patent and Trademark Office.

AUGUST 2003

THE JOURNAL OF BONE & JOINT SURGERY · AMERICAN VOLUME

SCIENTIFIC ARTICLES

1479
ARTHROSCOPIC POSTERIOR LABRAL REPAIR AND CAPSULAR SHIFT FOR TRAUMATIC UNIDIRECTIONAL RECURRENT POSTERIOR SUBLUXATION OF THE SHOULDER
A translation of the abstract is available with the electronic versions of this article
Seung-Ho Kim, MD, Kwon-Ick Ha, MD, Jong-Hyuk Park, MD, Young-Min Kim, MD, Yong-Seuk Lee, MD, Jong-Youl Lee, MD, and Jae-Chul Yoo, MD

1488
ENDOSCOPIC DECOMPRESSION OF THE RETROCALCANEAL SPACE
Zachary Leitze, MD, Enzo J. Sella, MD, and John M. Aversa, MD

1497
THE POSTERIOR BRANCH OF THE AXILLARY NERVE: AN ANATOMIC STUDY
Craig M. Ball, MD, Thomas Steger, MD, Leesa M. Galatz, MD, and Ken Yamaguchi, MD

1502
NERVE LESIONS ASSOCIATED WITH LIMB-LENGTHENING
Monica Paschoal Nogueira, MD, Dror Paley, MD, FRCSC, Anil Bhave, PT, Andrew Herbert, MD, Catherine Nocente, PhD, and John E. Herzenberg, MD, FRCSC

1511
ARTHROSCOPIC ANTERIOR STABILIZATION OF THE SHOULDER. TWO TO SIX-YEAR FOLLOW-UP
A translation of the abstract is available with the electronic versions of this article
Seung-Ho Kim, MD, Kwon-Ick Ha, MD, Yang-Bum Cho, MD, Byung-Dam Ryu, MD, and Irvin Oh, MD

1519
RADIOGRAPHIC DEFINITION OF PELVIC OSTEOLYSIS FOLLOWING TOTAL HIP ARTHROPLASTY
Alexandra M. Claus, MD, PhD, C. Anderson Engh Jr., MD, Christi J. Sychterz, MS, John S. Xenos, MD, Karl F. Orishimo, MS, and Charles A. Engh Sr., MD

1527
HYDROXYAPATITE COATING OF EXTERNAL FIXATION PINS TO DECREASE AXIAL DEFORMITY DURING TIBIAL LENGTHENING FOR SHORT STATURE
A translation of the abstract is available with the electronic versions of this article
Victor L. Caja, MD, PhD, Gabriel Pizà, MD, PhD, and Antonio Navarro, MD, PhD

1532
SIMULTANEOUS BILATERAL, STAGED BILATERAL, AND UNILATERAL TOTAL KNEE ARTHROPLASTY. A SURVIVAL ANALYSIS
Merrill A. Ritter, MD, Leesa D. Harty, BA, Kenneth E. Davis, MS, John B. Meding, MD, and Michael Berend, MD

AUGUST 2003

THE JOURNAL OF BONE & JOINT SURGERY · AMERICAN VOLUME

SCIENTIFIC ARTICLES

1538
HETEROTOPIC OSSIFICATION AROUND THE ELBOW FOLLOWING BURNS IN CHILDREN: RESULTS AFTER EXCISION
Alok Gaur, MD, Marc Sinclair, MD, Enzo Caruso, MD, Giuseppe Peretti, MD, and David Zaleske, MD

1544
OSTEOGENIC ACTIVITY OF THE FOURTEEN TYPES OF HUMAN BONE MORPHOGENETIC PROTEINS (BMPs)
Hongwei Cheng, MD, PhD, Wei Jiang, BA, Frank M. Phillips, MD, Rex C. Haydon, MD, PhD, Ying Peng, MD, Lan Zhou, MD, PhD, Hue H. Luu, MD, Naili An, MD, Benjamin Breyer, MD, Pantila Vanichakarn, BS, Jan Paul Szatkowski, BS, Jae Yoon Park, BS, and Tong-Chuan He, MD, PhD

CASE REPORTS

1553
PERMANENT PARTIAL CERVICAL SPINAL CORD INJURY IN A PROFESSIONAL FOOTBALL PLAYER WHO HAD ONLY CONGENITAL STENOSIS. A CASE REPORT
Craig D. Brigham, MD, and Tim E. Adamson, MD

1557
BILATERAL CHRONIC EXERTIONAL COMPARTMENT SYNDROME OF THE DORSAL PART OF THE FOREARM: THE ROLE OF MAGNETIC RESONANCE IMAGING IN DIAGNOSIS. A CASE REPORT
P. Raj Kumar, MS, FRCS(Orth), J.P.R. Jenkins, FRCP, FRCR, and S.P. Hodgson, FRCS, FRCS(Orth)

1560
GANGLION OF THE TRIANGULAR FIBROCARTILAGE COMPLEX. A REPORT OF THREE CASES
Shinji Nishikawa, MD, and Satoshi Toh, MD

CURRENT CONCEPTS REVIEW

1564
UPPER-EXTREMITY CONGENITAL ANOMALIES
Scott H. Kozin, MD

SELECTED INSTRUCTIONAL COURSE LECTURE

1578
NONPROSTHETIC MANAGEMENT OF PROXIMAL HUMERAL FRACTURES
Joseph P. Iannotti, MD, PhD, Matthew L. Ramsey, MD, Gerald R. Williams, MD, and Jon J.P. Warner, MD

AUGUST 2003

THE JOURNAL OF BONE & JOINT SURGERY · AMERICAN VOLUME

THE ORTHOPAEDIC FORUM

1594
FINANCING GRADUATE MEDICAL EDUCATION: SORTING OUT THE CONFUSION
Aaron S. Covey, MD, MBA, and Gary E. Friedlaender, MD

1605
WHO DID WHAT? (MIS)PERCEPTIONS ABOUT AUTHORS' CONTRIBUTIONS TO SCIENTIFIC ARTICLES BASED ON ORDER OF AUTHORSHIP
Mohit Bhandari, MD, MSc, Thomas A. Einhorn, MD, Marc F. Swiontkowski, MD, and James D. Heckman, MD

1610
LETTERS TO THE EDITOR

EVIDENCE-BASED ORTHOPAEDICS

1622
GLOSSARY

1623
ULTRASONOGRAPHY IN NEONATAL HIP INSTABILITY REDUCED THE NEED FOR SPLINTS

1624
TWO WEEKS OF PREDNISOLONE WAS AS EFFECTIVE AS FOUR WEEKS IN IMPROVING CARPAL TUNNEL SYNDROME SYMPTOMS

1625
PHYSICAL THERAPY WAS EFFECTIVE FOR PATELLOFEMORAL PAIN

SPECIALTY UPDATE

1626
WHAT'S NEW IN SPINE SURGERY
Jack E. Zigler, MD, Paul A. Anderson, MD, Scott D. Boden, MD, Keith H. Bridwell, MD, and Alexander R. Vaccaro, MD

DEPARTMENTS

Follows Table of Contents
INSTRUCTIONS TO AUTHORS

1641
THE ORTHOPAEDIC CALENDAR

Adv 28, 42, 56, 68, 76, 84
ABSTRACTS FROM *THE JOURNAL OF BONE AND JOINT SURGERY [BR]*

1637
OBITUARY: THOMAS ST. GERMAIN WHITECLOUD III, MD, 1940-2003

1639
OBITUARY: LEONARD F. PELTIER, MD, PHD, 1920-2003

1644
BOOK REVIEWS

OSTEOGENIC ACTIVITY OF THE FOURTEEN TYPES OF HUMAN BONE MORPHOGENETIC PROTEINS (BMPs)

BY HONGWEI CHENG, MD, PHD, WEI JIANG, BA, FRANK M. PHILLIPS, MD, REX C. HAYDON, MD, PHD, YING PENG, MD, LAN ZHOU, MD, PHD, HUE H. LUU, MD, NAILI AN, MD, BENJAMIN BREYER, MD, PANTILA VANICHAKARN, BS, JAN PAUL SZATKOWSKI, BS, JAE YOON PARK, BS, AND TONG-CHUAN HE, MD, PHD

Investigation performed at The University of Chicago Medical Center, Chicago, Illinois

Background: Bone morphogenic proteins (BMPs) are known to promote osteogenesis, and clinical trials are currently underway to evaluate the ability of certain BMPs to promote fracture-healing and spinal fusion. The optimal BMPs to be used in different clinical applications have not been elucidated, and a comprehensive evaluation of the relative osteogenic activity of different BMPs is lacking.

Methods: To identify the BMPs that may possess the most osteoinductive activity, we analyzed the osteogenic activity of BMPs in mesenchymal progenitor and osteoblastic cells. Recombinant adenoviruses expressing fourteen human BMPs (BMP-2 to BMP-15) were constructed to infect pluripotent mesenchymal progenitor C3H10T1/2 cells, preosteoblastic C2C12 cells, and osteoblastic TE-85 cells. Osteogenic activity was determined by measuring the induction of alkaline phosphatase, osteocalcin, and matrix mineralization upon BMP stimulation.

Results: BMP-2, 6, and 9 significantly induced alkaline phosphatase activity in pluripotential C3H10T1/2 cells, while BMP-2, 4, 6, 7, and 9 significantly induced alkaline phosphatase activity in preosteoblastic C2C12 cells. In TE-85 osteoblastic cells, most BMPs (except BMP-3 and 12) were able to induce alkaline phosphatase activity. The results of alkaline phosphatase histochemical staining assays were consistent with those of alkaline phosphatase colorimetric assays. Furthermore, BMP-2, 6, and 9 (as well as BMP-4 and, to a lesser extent, BMP-7) significantly induced osteocalcin expression in C3H10T1/2 cells. In C2C12 cells, osteocalcin expression was strongly induced by BMP-2, 4, 6, 7, and 9. Mineralized nodules were readily detected in C3H10T1/2 cells infected with BMP-2, 6, and 9 (and, to a lesser extent, those infected with BMP-4 and 7).

Conclusions: A comprehensive analysis of the osteogenic activity of fourteen types of BMPs in osteoblastic progenitor cells was conducted. Our results suggest an osteogenic hierarchical model in which BMP-2, 6, and 9 may play an important role in inducing osteoblast differentiation of mesenchymal stem cells. In contrast, most BMPs are able to stimulate osteogenesis in mature osteoblasts.

Clinical Relevance: These findings have implications for the development of effective formulas for bone-healing and spinal fusion. The efficacy of osteogenesis may depend not only on the type of BMP or the combination of BMPs that is used but also on the cell types that are present.

Bone is the only tissue that undergoes continuous remodeling throughout life and is one of the few organs that retains the potential for regeneration in adult life[1,2]. Bone regeneration is required to achieve fracture-healing and spinal fusion, and various surgical and biological strategies have been used to promote osteogenesis in these situations. It has been known for almost half a century that demineralized bone can induce de novo bone formation[3]. Subsequent studies have identified the molecular identity of the bone-forming factors in demineralized bone that have been termed bone morphogenetic proteins (BMPs)[4-6]. As members of the transforming growth factor-beta (TGF-β) superfamily, BMPs play important roles in skeletal development and bone formation[7-10]. BMPs initiate their signaling transduction by binding to a heterodimeric complex of two transmembrane serine-threonine kinase receptors, BMP receptor (BMPR) type I and BMPR type II[11-13]. The activated receptor kinases, in turn, phosphorylate the transcription factors Smad 1, 5, and 8. The phosphorylated Smads then form a heterodimeric complex with Smad 4 in the nucleus and activate the expression of target genes in

A commentary is available with the electronic versions of this article, on our web site (www.jbjs.org) and on our quarterly CD-ROM (call our subscription department, at 781-449-9780, to order the CD-ROM).

concert with other coactivators[14-22].

Several recombinant forms of BMP, most notably rhBMP-2 and rhBMP-7, have been shown to induce bone formation in vivo[23-34], and both of these forms have been tested in clinical trials[35-37]. Initial data from these trials have suggested that BMP-induced bone formation is at least equivalent to autogenous bone-grafting when used to treat tibial nonunions and to promote spinal fusions[35,36]. In addition to direct application, BMPs may be delivered by adenoviral vectors, retroviral vectors, or ex vivo transduced cells. Several investigators have confirmed the ability of virally mediated gene transfer of BMPs to induce bone formation in various animal models[28,30,31,33,38-54].

Although a number of studies have confirmed the effectiveness of BMPs in promoting osteogenesis, no comprehensive evaluation of the relative osteoinductive activity of each BMP either alone or in combination has been performed, to our knowledge. Therefore, it remains unclear whether BMPs other than those currently being tested in clinical trials are more potent stimulators of new-bone formation. The purpose of the present study was to determine the distinct osteogenic activities of the fourteen types of human BMPs and their potential synergistic effects on osteogenesis. The effects of all BMPs were tested in osteoblast progenitor cells (C3H10T1/2 and C2C12 lines) as well as in committed osteoblastic cells (TE-85 line).

Materials and Methods

Cell Culture and Chemicals

Human embryonic kidney cell line HEK 293, mouse pluripotential mesenchymal precursor lines C2C12 and C3H10T1/2, and human osteosarcoma line TE-85 were obtained from the American Type Culture Collection (ATCC, Manassas, Virginia). The C3H10T1/2 line used in this study was derived from mouse embryonic fibroblasts and generally is considered to be a pluripotential stem-cell line that can differentiate into various lineages, including osteoblasts. The C2C12 line was derived from mouse myoblasts that retain the potential to differentiate into osteoblasts and therefore is considered to be composed of committed osteoblastic precursor cells. Human TE-85 cells are committed osteoblasts. HEK 293 and C2C12 cells were maintained in complete Dulbecco modified Eagle medium (DMEM) supplemented with 10% fetal calf serum (FBS; Mediatech, Herndon, Virginia), 100 U of penicillin, and 100 μg of streptomycin at 37°C in 5% CO_2. C3H10T1/2 cells were maintained in Basal Medium Eagle in Earle's BSS, supplemented with 10% FBS, 100 U of penicillin, and 100 μg of streptomycin at 37°C in 5% CO_2. TE-85 cells were maintained in complete Eagle minimum essential medium (EMEM), supplemented with 10% FBS, 100 U of penicillin, and 100 μg of streptomycin at 37°C in 5% CO_2. Unless indicated otherwise, all chemicals were purchased from Sigma-Aldrich (St. Louis, Missouri) or Fisher Scientific (Pittsburgh, Pennsylvania).

Construction of Recombinant Adenoviruses Expressing BMPs

The cDNA clones for human BMP-2, 3 (also known as osteogenin), 4, 5, 6, 8 (also known as OP-2), 9 (also known as GDF-2), 10, 12 (also known as GDF-7 or CDMP-3), and 13 (also known as GDF-6 or CDMP-2) were kindly provided by the Genetics Institute (Cambridge, Massachusetts). The coding sequences for BMP-7 (also known as OP-1), 11 (also known as GDF-11), 14 (also known as GDF-5 or CDMP-1), and 15 (also known as GDF-9) were amplified from a human osteosarcoma cDNA library with use of the polymerase chain reaction technique. The coding regions of the above fourteen BMPs were subcloned into pAdTrack-CMV, resulting in pAdTrack-BMPs, and recombinant adenoviruses expressing BMPs (AdBMPs) were subsequently generated as previously described[55]. For a control, we used an analogous adenovirus expressing only green fluorescent protein (GFP) (i.e., AdGFP) as previously described[56]. Details on vector constructions are available upon request. Each cell line was exposed to the viral vectors for sixteen hours at a multiplicity of infection (MOI) that was optimal for each construct.

Colorimetric Determination of Alkaline Phosphatase Activity

Exponentially growing C2C12, C3H10T1/2, and TE-85 cells were seeded in forty-eight-well cell-culture plates and were infected with AdBMPs or AdGFP (MOI = 50~200). The induction of alkaline phosphatase activity was assessed at three, five, seven, and nine days after infection. Alkaline phosphatase activity was determined with use of p-nitrophenyl phosphate (Sigma-Aldrich) as a substrate. Absorbance at 405 nm was recorded at one, two, and three minutes after the cell lysate was mixed with the substrate. Each assay condition was done in triplicate and normalized with the concentrations of total cellular proteins. Enzyme activity was expressed as nanomoles of p-nitrophenol produced per minute per milligram of total cellular proteins.

Histochemical Staining of Alkaline Phosphatase Activity

Exponentially growing C2C12, C3H10T1/2, and TE-85 cells were seeded in forty-eight-well cell-culture plates and were infected with AdBMPs and AdGFP. The induction of alkaline phosphatase expression was detected at five days after infection with use of histochemical staining assays. Briefly, infected cells were fixed with 0.05% (v/v) glutaraldehyde (Sigma-Aldrich) at room temperature for ten minutes. After being washed with phosphate-buffered saline (PBS) solution, cells were stained with use of a mixture of 0.1 mg/mL naphthol AS-MX phosphate and 0.6 mg/mL fast blue BB salt (Sigma-Aldrich). Histochemical staining was recorded with use of bright-field microscopy.

Induction of Mineralized Matrix Formation (Alizarin Red S Staining)

Exponentially growing C2C12 and C3H10T1/2 cells were seeded in forty-eight-well cell-culture plates and were infected with AdBMPs and AdGFP. Infected cells were cultured in the presence of ascorbic acid (50 μg/mL) and β-glycerophosphate (10 mM). At twenty-one days after infection, mineralized matrix nodules were stained for calcium precipitation by means of alizarin red S staining as follows. Cells were washed with PBS and fixed with 0.05% (v/v) glutaraldehyde at room tem-

perature for ten minutes. After being washed with distilled water, fixed cells were incubated with 0.4% alizarin red S (Sigma-Aldrich) for five minutes, followed by extensive washing with distilled water and by further incubation with PBS for ten minutes. The staining of calcium mineral deposits was recorded with use of bright-field microscopy.

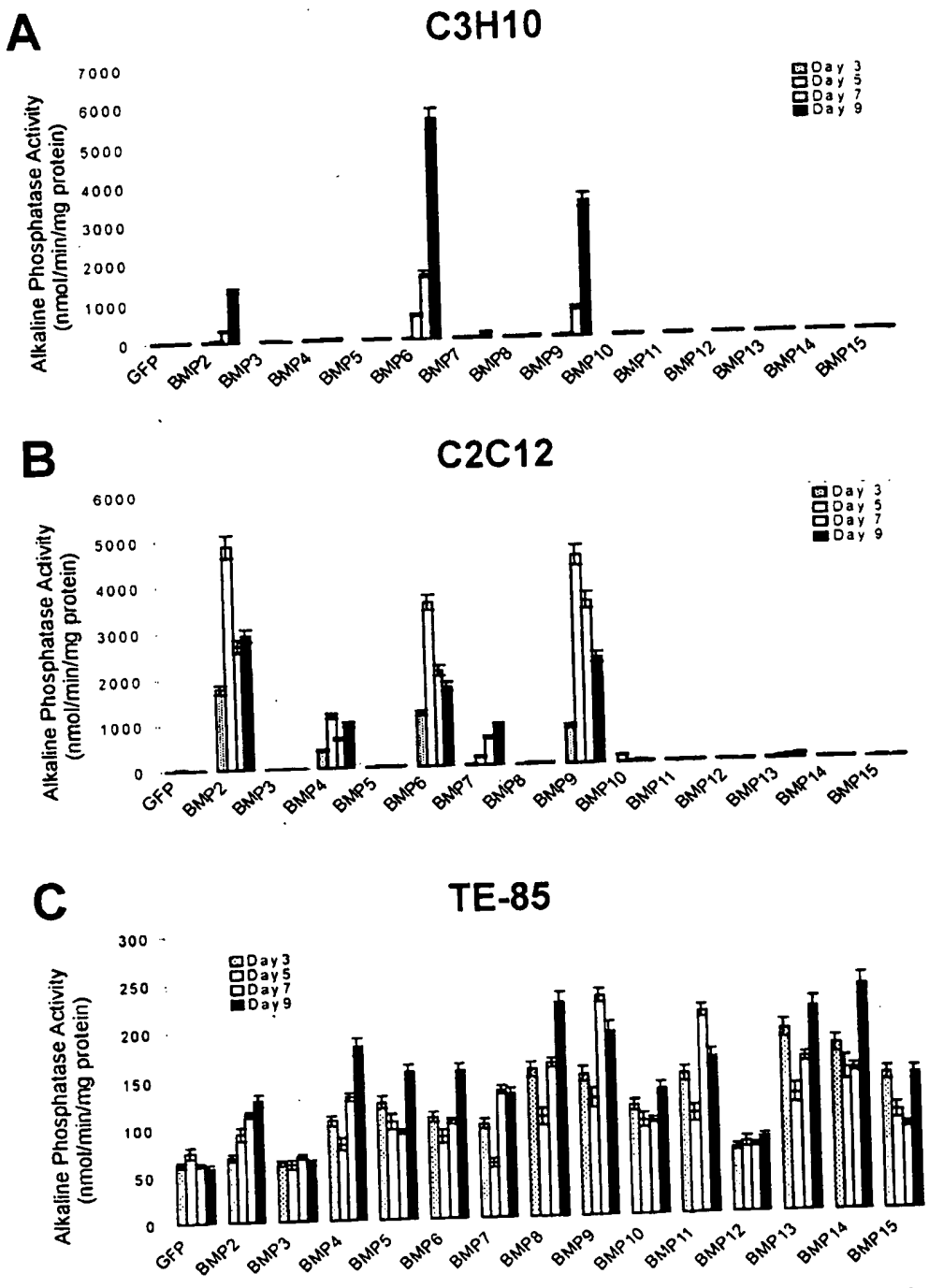

Fig. 1

Effects of individual BMPs on the induction of alkaline phosphatase activity in osteogenic progenitor and osteoblastic cells. Subconfluent pluripotential C3H10T1/2 cells *(A)*, osteoblastic precursor C2C12 cells *(B)*, and osteoblastic TE-85 *(C)* cells were infected with AdBMPs and the control AdGFP. Cells were lysed at the indicated times for colorimetric assays of alkaline phosphatase activity with use of p-nitrophenyl phosphate as a substrate. Representative results from at least three independent experiments are shown.

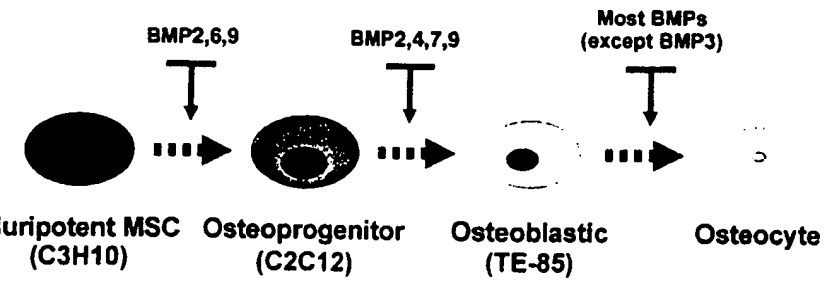

Fig. 2

Distinct osteogenic activity of human BMPs. Our findings suggest that, among all of the BMPs that were examined, BMP-2, 6, and 9 may be the most potent agents to induce osteoblast lineage-specific differentiation of mesenchymal progenitor cells while most BMPs can effectively promote the terminal differentiation of committed osteoblastic precursors and osteoblasts. It is conceivable that combinations of BMPs also may be able to induce osteogenesis in early mesenchymal stem cells. Understanding the potentially overlapping and/or converging signaling pathways of different BMPs could help us to develop efficacious osteogenic formulas of BMPs for various clinical applications.

Total RNA Isolation and Northern Blot Analysis

Exponentially growing C2C12 and C3H10T1/2 cells were seeded in 25-cm^2 cell-culture flasks and were infected with AdBMPs and AdGFP. At seven days (for C2C12) or ten days (for C3H10T1/2) after infection, total RNA was isolated with use of the RNAgents Total RNA Isolation kit (Promega, Madison, Wisconsin) according to the manufacturer's instructions. Five micrograms of total RNA was subjected to Northern blot analysis with use of a ^{32}P-labeled DNA probe specific for mouse osteocalcin. The same blots were reprobed with a control probe derived from mouse GAPDH (glyceraldehyde-6-phosphate dehydrogenase).

Results

Expression of the Fourteen Types of Human BMPs with Use of Recombinant Adenoviral Vectors

To elucidate the osteogenic activity of individual BMPs, we constructed a series of recombinant adenoviruses that express human BMP-2, 3, 4, 5, 6, 7, 8, 9, 10, 11, 12, 13, 14 and 15. We did not include BMP-1 in the present study because of its established inability to induce bone formation[37]. All AdBMPs also included a GFP-expression cassette, allowing us to track transduction efficiency. To avoid a potential cytopathic effect of adenoviral infection, we used MOIs that resulted in approximately 50% transduction efficiency at twenty-four hours after infection. An analogous GFP-expressing virus, AdGFP, was used as a control. Adenoviral vector-mediated expression of individual BMPs was confirmed with either Western blot or quantitative reverse transcriptase-polymerase chain reaction analyses (data not shown).

Distinct Effect of BMPs on Induction of the Early Osteogenic Marker Alkaline Phosphatase

In order to identify the most potent osteogenic BMPs, we evaluated the effect of individual BMPs on osteoblastic lineage-specific differentiation in two commonly used osteoblastic progenitor cell lines as well as in osteoblastic TE-85 cells. Osteoblastic lineage-specific differentiation of these cells was monitored by measuring alkaline phosphatase activity at various time-points after infection. Alkaline phosphatase activity was determined with two types of assays, a quantitative colorimetric assay and a qualitative histochemical staining assay. When alkaline phosphatase activity was measured with use of a colorimetric enzymatic assay, only BMP-2, 6, and 9 induced a notable increase in alkaline phosphatase in mesenchymal progenitor C3H10T1/2 cells (Fig. 1, *A*). As early as five days after infection, BMP-6 induced a more than thirteenfold increase in alkaline phosphatase activity, escalating to a 293-fold increase at nine days after infection. Similarly, at nine days after infection, BMP-2 and BMP-9 were shown to induce a sixty-eight-fold and 181-fold increase in alkaline phosphatase activity, respectively (Table I). BMP-4, 7, and 8 induced a detectable, but only marginal, increase in alkaline phosphatase activity in C3H10T1/2 cells (Fig. 1, *A* and Table I).

In the preosteoblastic C2C12 cells, at least four BMPs (BMP-2, 4, 6, and 9) induced a marked increase in alkaline phosphatase activity at three days after infection, peaking at around five days and declining at nine days after infection (Fig. 1, *B* and Table I). BMP-7 was shown to induce alkaline phosphatase activity at later time-points (e.g., Day 7 and Day 9). Interestingly, BMP-10 and BMP-13 induced a more than tenfold increase in alkaline phosphatase activity at Day 3 and Day 9, respectively. A longer latency in alkaline phosphatase induction was observed in C3H10T1/2 compared with C2C12 cells. For instance, in C3H10T1/2 cells, there was no detectable alkaline phosphatase induction by any BMPs at three days after infection, and induced alkaline phosphatase activity was shown to increase at seven to nine days after infection (Fig. 1 and Table I). The time-course difference in BMP-induced alkaline phosphatase activity in C3H10T1/2 and C2C12 cells

TABLE I Fold Changes in BMP-Induced Alkaline Phosphatase Activity

	C3H10T1/2				C2C12			
	Day 3	Day 5	Day 7	Day 9	Day 3	Day 5	Day 7	Day 9
GFP*	1.00	1.00	1.00	1.00	1.00	1.00	1.00	1.00
BMP-2	1.00	1.26	8.20	67.63	213.75	294.13	260.40	470.33
BMP-3	0.33	0.53	0.93	0.75	0.75	0.75	0.60	1.67
BMP-4	1.00	0.89	1.47	2.63	47.25	69.00	62.20	152.00
BMP-5	0.22	0.79	0.87	1.13	1.25	1.13	1.80	5.00
BMP-6	0.89	13.47	45.60	292.63	140.25	215.13	201.40	280.00
BMP-7	1.33	0.79	1.07	7.88	3.75	10.50	58.20	140.67
BMP-8	1.11	0.74	1.13	3.00	1.50	0.88	2.20	4.00
BMP-9	1.33	1.58	19.93	180.50	99.75	273.50	342.60	371.00
BMP-10	0.44	0.58	0.73	1.50	18.00	2.25	5.40	5.33
BMP-11	0.67	0.89	0.67	1.88	2.25	1.63	2.40	4.00
BMP-12	0.56	0.68	0.73	1.13	2.50	1.88	1.20	6.00
BMP-13	1.20	0.58	0.93	1.88	2.25	2.75	7.20	15.67
BMP-14	1.00	0.53	0.87	1.50	2.00	1.38	1.80	3.67
BMP-15	1.00	0.84	0.60	0.88	1.50	1.13	1.00	3.33

*GFP = green fluorescent protein.

may reflect their different pluripotency.

In TE-85 osteoblastic cells, most of the BMPs examined (except BMP-3 and 12) exhibited the ability to induce alkaline phosphatase activity, although there was marked basal alkaline phosphatase activity in this line (Fig. 1, *C*). The maximum level of alkaline phosphatase activity induced by BMPs in TE-85 cells was notably lower than that in C3H10T1/2 and C2C12 cells, suggesting that, as an osteoblastic cell line, TE-85 may only have a limited potential for alkaline phosphatase induction.

The results of histochemical assays of alkaline phosphatase activity were largely consistent with those obtained from the colorimetric measurement described above. In C3H10T1/2 cells, only BMP-2, 6, and 9 were shown to induce an increase in alkaline phosphatase activity, while no such induction was observed in the cells infected with other BMPs (Appendix). In C2C12 cells, BMP-2, 6, and 9 were shown to induce the greatest increase in alkaline phosphatase activity, while BMP-4 and 7 induced a modest increase in alkaline phosphatase activity. No other BMPs were shown to induce an appreciable increase in alkaline phosphatase activity. However, all BMPs except BMP-3 and 10 were shown to induce alkaline phosphatase activity in TE-85 cells. The histochemical staining assays were also performed at different time-points after infection, and the results were consistent with those shown in Figure 1 (data not shown). The staining results were reproducible in at least three batches of experiments. Taken together, these results support an osteogenic hierarchy model, in which BMP-2, 6, and 9 may exhibit the greatest ability to induce osteoblast lineage-specific differentiation.

Distinct Effects of BMPs on Induction of the Late Osteogenic Marker Osteocalcin in Mesenchymal Progenitor Cells

We next measured the expression of osteocalcin, a marker of late osteoblastic differentiation, in response to the exogenous expression of AdBMPs. Total RNA was isolated from the infected cells at seven days (for C2C12) or ten days (for C3H10T1/2) after infection and were subjected to Northern blot analysis with a radiolabeled probe derived from the 3'-untranslated region of mouse osteocalcin. As demonstrated in the Appendix, the ability of different BMPs to induce the expression of osteocalcin was largely consistent with the findings on alkaline phosphatase induction, except that the induction of osteocalcin expression displayed an even longer latency period. Specifically, in C3H10T1/2 cells, BMP-2, 6, and 9 substantially induced osteocalcin expression at ten days after infection, while BMP-4 and 7 also induced osteocalcin expression. Similarly, in C2C12 cells, only those five BMPs were shown to induce osteocalcin expression at seven days after infection. Interestingly, we also found that BMP-6-induced osteocalcin expression in C2C12 cells peaked at three days after infection (data not shown) and started to decline at seven days. We also analyzed BMP-induced osteocalcin expression in both cell lines at earlier time-points (e.g., three and five

days after infection) and found that osteocalcin was either not detectable or marginally detectable (with the exception of BMP-6 in C2C12 cells; data not shown). The relative delay in osteocalcin expression suggests that the decline observed in alkaline phosphatase activity after Day 5 in C2C12 cells may correspond to a shift from an early to a late osteoblastic phenotype in the precursor cells. Overall, BMP-2, 6, and 9 exhibited the greatest ability to induce both early and late bone formation markers in C3H10T1/2 and C2C12 cells.

BMP-Induced Matrix Mineralization

Next, we sought to evaluate the ability of BMPs to induce matrix mineralization with use of a functional assay of terminally differentiated osteoblasts. C3H10T1/2 cells were infected with AdBMPs and AdGFP. At twenty-one days after infection, cells were fixed and were stained with alizarin red S. As shown in the Appendix, mineralized nodules were readily detected in the cells infected with AdBMP-2, AdBMP-6, and AdBMP-9. In AdBMP-4 and AdBMP-7-infected cells, mineralized nodules were detectable but sparse. These results were reproducible in at least three independent experiments. Similar results were obtained in experiments involving C2C12 cells (data not shown).

Discussion

Successful bone regeneration mediated by biofactors could revolutionize the clinical management of musculoskeletal disorders as well as fracture-healing and spinal fusion[58]. Several biological factors, such as transforming growth factor-Beta (TGFβ), bone morphogenetic proteins (BMPs), fibroblast growth factors (FGFs), platelet-derived growth factor (PDGF), insulin-like growth factors (IGFs), and LIM mineralization protein-1 (LMP-1), have been investigated for their potential use in bone regeneration and skeletal repair[59-73]. BMPs have been shown to be most promising, and clinical trials of BMP-2 and 7 are ongoing[74-80]. These BMPs have shown varying degrees of success in the clinical setting, and further studies on their mechanisms of action and optimal formulations are required to optimize effectiveness of this strategy for promoting osteogenesis.

In the present study, we carried out a comparative analysis of the distinct osteogenic activity of fourteen human BMPs. We chose to use adenovirus-mediated gene transfer of BMPs rather than using recombinant proteins because a number of recombinant BMPs are not commercially available. Gene therapy may circumvent some of the difficulties associated with direct BMP delivery. It also enables prolonged, high-level protein expression as opposed to the relatively short half-life of locally applied BMPs, and it obviates the need for carrier molecules with their associated difficulties. Recombinant adenoviral vectors expressing several BMP genes have been shown to promote osteogenesis in animal studies[28,30,31,33,39,41-43,46,49,51]. Using osteoblastic progenitor cell lines, we demonstrated that BMP-2, 6, and 9 exhibited the greatest ability to induce both early and late osteogenic markers as well as matrix mineralization. When committed osteoblastic cells were studied, a wider range of BMPs was found to stimulate alkaline phosphatase activity. Consistent with a recent gene disruption study[81], BMP-3 exhibited no osteogenic activity and effectively antagonized the osteogenic activity of BMP-2, 4, 6, 7, and 9.

To the best of our knowledge, this line of investigation is the first of its kind to evaluate the osteogenic activity of most, if not all, human BMPs in a comprehensive fashion. Our results suggest an osteogenic hierarchical model in which BMP-2, 6, and 9 play an important role in inducing osteoblast differentiation of mesenchymal stem cells (Fig. 2). Bone formation is a complex process that can occur through either endochondral or intramembranous ossification. It is, therefore, unclear whether these data help to predict the best BMPs for clinical applications, although comprehensive testing in an animal model will help to assess the correlation between osteogenic activity in stem cells and bone formation.

It is intriguing, however, that BMP-9 emerged as one of the most potent inducers of osteogenic differentiation. Originally identified from fetal mouse liver cDNA libraries, BMP-9 (also known as GDF-2) is a relatively uncharacterized member of the BMP family[82]. Human BMP-9 has been mapped to 10q21.1, and its precursor protein contains 428 amino acid residues. Human BMP-9 shares approximately 80% homology with its mouse counterpart (www.ncbi.nlm.nih.gov/UniGene). BMP-9 is highly expressed in the developing mouse liver, and recombinant human BMP-9 (rhBMP-9) stimulates hepatocyte proliferation[82]. BMP-9 also has been shown to be a potent synergistic factor for hematopoietic progenitor-cell generation and colony formation[83] and also may play a role in the induction and maintenance of the neuronal cholinergic phenotype in the central nervous system[84]. In a parallel study with BMP-2, BMP-9 was shown to promote chondrogenic differentiation of human pluripotent mesenchymal cells[85]. When applied with a biological carrier in an earlier study, recombinant human BMP-9 protein was shown to exert only mild osteoinductive activity in vivo[82]. Using a recombinant adenoviral vector expressing a chimeric BMP-9 gene (i.e., mouse BMP-9 precursor protein region fused with human BMP-9 mature protein region), Helm et al. recently demonstrated that BMP-9 exhibits an apparent osteoinductive effect[31,33]. More recently, Dumont et al. demonstrated that human mesenchymal stem cells transduced ex vivo with BMP-9 effectively induced spinal fusion in rodents[86]. Thus, although the mechanisms behind BMP-9-mediated osteogenic signaling remain to be defined, BMP-9 could represent an extremely effective bone-forming agent.

Our data also suggest that BMP-6 is one of the most promising osteogenic BMPs. Although considerable basic science and in vitro data have been collected on BMP-6, its osteogenic activity has not been investigated to any substantial degree in animal studies or clinical trials. BMP-6-deficient mice are largely unremarkable, with the exception of a defect in the sternum[87]. The expression of BMP-6 during embryogenesis is closely coupled with that of BMP-2, and the lack of noticeable defects in BMP-6-deficient mice is thought to be due to functional compensation by BMP-2[87]. Nevertheless, our results corroborate the findings of a recent study in which BMP-6 was shown to effectively induce bone formation by

both intramembranous and endochondral ossification pathways[34]. When the calf muscles of athymic nude rats were injected with AdBMP-4, AdBMP-6, or AdBMP-2, AdBMP-6 was shown to induce the most rapid tissue calcification[48]. These findings are consistent with our observation that BMP-6 induces the earliest increase of alkaline phosphatase activity in both C2C12 and C3H10T1/2 cells.

The observation that BMP-2 exhibited potent osteogenic activity in our study is consistent with early data from human clinical trials[35,37]. Its relative success in enhancing bone formation in these trials serves to corroborate our in vitro findings. BMP-7 exhibited little osteogenic activity in osteoblastic progenitor cell lines but did stimulate alkaline phosphatase in relatively mature osteoblasts, which is important given the considerable attention that BMP-7 has received during translational research. These findings are consistent with the relatively moderate success of rhBMP-7 (i.e., OP-1) in a recent clinical trial[36]. It is conceivable that synergism between BMPs can be exploited to increase their osteogenic activity above that of a single BMP alone, potentially presenting an additional strategy to optimize bone regeneration.

Our data confirm that the response to BMPs is dependent on the cell types that are present at the site of BMP delivery. In a clinical situation in which the predominant cell type present is likely to be osteoblasts, our data would support the majority of BMPs as being capable of promoting osteogenesis and therefore healing. Alternatively, in a situation in which pluripotential cells are abundant, BMP-2, 6, and 9 may be most effective. Currently, there is considerable interest in attempting to place progenitor cells derived from various sources (e.g., peripheral blood cells and bone marrow) at the site of desired osteogenesis. The results of the present study suggest that BMP-2, 6, and 9 might be optimal in this application.

In conclusion, we have demonstrated the relative effectiveness of all fourteen BMPs individually and in various combinations to stimulate markers of osteogenesis in osteoblastic progenitor cells and in committed osteoblasts. Future studies will attempt to elucidate the major signaling differences among BMPs so that maximal synergy can be achieved by combining BMPs that act through overlapping or converging signaling pathways. Ultimately, these studies may help to elucidate the molecular mechanisms underlying bone formation and lead to the development of more efficacious approaches to bone regeneration.

Appendix

eA Representative results of the alkaline phosphatase activity and the expression of osteocalcin and matrix mineralization induced by the various BMPs can be found in the electronic version of this article, on our web site at www.jbjs.org (go to the article citation and click on "Supplementary Material") and on our quarterly CD-ROM (call our subscription department, at 781-449-9780, to order the CD-ROM). ■

NOTE: The authors thank the Genetics Institute for providing human BMP cDNAs.

Hongwei Cheng, MD, PhD
Wei Jiang, BA
Rex C. Haydon, MD, PhD
Ying Peng, MD
Lan Zhou, MD, PhD
Hue H. Luu, MD
Naili An, MD
Benjamin Breyer, MD
Pantila Vanichakarn, BS
Jan Paul Szatkowski, BS
Jae Yoon Park, BS
Tong-Chuan He, MD, PhD
Department of Surgery, Section of Orthopaedic Surgery, Molecular Oncology Laboratory (H.C., W.J., F.M.P., R.C.H., Y.P., L.Z., H.H.L., N.A., B.B., P.V., J.P.S., J.Y.P. and T.-C.H), Committee on Genetics (Y.P. and T.-C.H.), Committee on Cancer Biology (N.A. and T.-C.H.), The University of Chicago Medical Center, 5841 South Maryland Avenue, MC3079, Chicago, IL 60637. E-mail address for T.-C. He: tche@surgery.bsd.uchicago.edu

Frank M. Phillips, MD
The Rush Arthritis and Orthopaedics Institute, 1725 West Harrison Street, Suite 1063, Chicago, IL 60612. E-mail address: frank.phillips@midwestortho.com

In support of their research or preparation of this manuscript, one or more of the authors received grants or outside funding from Schweppe Foundation (T.-C.H.), the Orthopaedic Research and Education Foundation (T.-C.H. and R.C.H.), the North American Spine Society (F.M.P. and T.-C.H.), and the Aircast Foundation (T.-C.H.). None of the authors received payments or other benefits or a commitment or agreement to provide such benefits from a commercial entity. No commercial entity paid or directed, or agreed to pay or direct, any benefits to any research fund, foundation, educational institution, or other charitable or nonprofit organization with which the authors are affiliated or associated. Human BMP cDNAs were provided by Genetics Institute (Cambridge, Massachusetts).

References

1. **Olsen BR, Reginato AM, Wang W.** Bone development. *Annu Rev Cell Dev Biol.* 2000;16:191-220.
2. **Reddi AH.** Role of morphogenetic proteins in skeletal tissue engineering and regeneration. *Nat Biotechnol.* 1998;16:247-52.
3. **Urist MR.** Bone: formation by autoinduction. *Science.* 1965;150:893-9.
4. **Urist MR, Nilsson O, Rasmussen J, Hirota W, Lovell T, Schmalzreid T, Finerman GA.** Bone regeneration under the influence of a bone morphogenetic protein (BMP) beta tricalcium phosphate (TCP) composite in skull trephine defects in dogs. *Clin Orthop.* 1987;214:295-304.
5. **Wozney JM, Rosen V, Celeste AJ, Mitsock LM, Whitters MJ, Kriz RW, Hewick RM, Wang EA.** Novel regulators of bone formation: molecular clones and activities. *Science.* 1988;242:1528-34.
6. **Ozkaynak E, Schnegelsberg PN, Jin DF, Clifford GM, Warren FD, Drier EA, Oppermann H.** Osteogenic protein-2. A new member of the transforming growth factor-beta superfamily expressed early in embryogenesis. *J Biol Chem.* 1992;267:25220-7.
7. **Hogan BL.** Bone morphogenetic proteins: multifunctional regulators of vertebrate development. *Genes Dev.* 1996;10:1580-94.
8. **Urist MR.** Bone morphogenetic protein: the molecularization of skeletal system development. *J Bone Miner Res.* 1997;12:343-6.
9. **Zou H, Choe KM, Lu Y, Massague J, Niswander L.** BMP signaling and vertebrate limb development. *Cold Spring Harb Symp Quant Biol.* 1997;62:269-72.

10. **Kingsley DM.** Genetic control of bone and joint formation. *Novartis Found Symp.* 2001;232:213-22.

11. **Kingsley DM.** The TGF-beta superfamily: new members, new receptors, and new genetic tests of function in different organisms. *Genes Dev.* 1994; 8:133-46.

12. **Massague J, Wels-Garcia F.** Serine/threonine kinase receptors: mediators of transforming growth factor beta family signals. *Cancer Surv.* 1996;27:41-64.

13. **Yamashita H, Ten Dijke P, Heldin CH, Miyazono K.** Bone morphogenetic protein receptors. *Bone.* 1996;19:569-74.

14. **Massague J.** TGF-beta signal transduction. *Annu Rev Biochem.* 1998;67: 753-91.

15. **Lyons KM, Pelton RW, Hogan BL.** Patterns of expression of murine Vgr-1 and BMP-2a RNA suggest that transforming growth factor-beta-like genes coordinately regulate aspects of embryonic development. *Genes Dev.* 1989;3:1657-68.

16. **Heldin CH, Miyazono K, ten Dijke P.** TGF-beta signalling from cell membrane to nucleus through SMAD proteins. *Nature.* 1997;390:465-71.

17. **Kawabata M, Imamura T, Miyazono K.** Signal transduction by bone morphogenetic proteins. *Cytokine Growth Factor Rev.* 1998;9:49-61.

18. **Itoh S, Itoh F, Goumans MJ, Ten Dijke P.** Signaling of transforming growth factor-beta family members through Smad proteins. *Eur J Biochem.* 2000; 267:6954-67.

19. **Yamaguchi A, Komori T, Suda T.** Regulation of osteoblast differentiation mediated by bone morphogenetic proteins, hedgehogs, and Cbfa1. *Endocr Rev.* 2000;21:393-411.

20. **Wrana JL.** Regulation of Smad activity. *Cell.* 2000;100:189-92.

21. **Hoffmann A, Gross G.** BMP signaling pathways in cartilage and bone formation. *Crit Rev Eukaryot Gene Expr.* 2001;11:23-45.

22. **von Bubnoff A, Cho KW.** Intracellular BMP signaling regulation in vertebrates: pathway or network? *Dev Biol.* 2001;239:1-14.

23. **Heckman JD, Boyan BD, Aufdemorte TB, Abbott JT.** The use of bone morphogenetic protein in the treatment of non-union in a canine model. *J Bone Joint Surg Am.* 1991;73:750-64.

24. **Gerhart TN, Kirker-Head CA, Kriz MJ, Holtrop ME, Hennig GE, Hipp J, Schelling SH, Wang E.** Healing segmental femoral defects in sheep using recombinant human bone morphogenetic protein. *Clin Orthop.* 1993;293:317-26.

25. **Lee SC, Shea M, Battle MA, Kozitza K, Ron E, Turek T, Schaub RG, Hayes WC.** Healing of large segmental defects in rat femurs is aided by RhBMP-2 in PLGA matrix. *J Biomed Mater Res.* 1994;28:1149-56.

26. **Bostrom MP, Camacho NP.** Potential role of bone morphogenetic proteins in fracture healing. *Clin Orthop.* 1998;355 Suppl:S274-82.

27. **Cheng SL, Lou J, Wright NM, Lai CF, Avioli LV, Riew KD.** In vitro and in vivo induction of bone formation using a recombinant adenoviral vector carrying the human BMP-2 gene. *Calcif Tissue Int.* 2001;68:87-94.

28. **Krebsbach PH, Gu K, Franceschi RT, Rutherford RB.** Gene therapy-directed osteogenesis: BMP-7-transduced human fibroblasts form bone in vivo. *Hum Gene Ther.* 2000;11:1201-10.

29. **Partridge K, Yang X, Clarke NM, Okubo Y, Bessho K, Sebald W, Howdle SM, Shakesheff KM, Oreffo RO.** Adenoviral BMP-2 gene transfer in mesenchymal stem cells: in vitro and in vivo bone formation on biodegradable polymer scaffolds. *Biochem Biophys Res Commun.* 2002;292:144-52.

30. **Riew KD, Wright NM, Cheng S, Avioli LV, Lou J.** Induction of bone formation using a recombinant adenoviral vector carrying the human BMP-2 gene in a rabbit spinal fusion model. *Calcif Tissue Int.* 1998;63:357-60.

31. **Varady P, Li JZ, Cunningham M, Beres EJ, Das S, Engh J, Alden TD, Pittmann DD, Kerns KM, Kallmes DF, Helm GA.** Morphologic analysis of BMP-9 gene therapy-induced osteogenesis. *Hum Gene Ther.* 2001;12:697-710.

32. **Varady P, Li JZ, Alden TD, Kallmes DF, Williams MB, Helm GA.** CT and radionuclide study of BMP-2 gene therapy-induced bone formation. *Acad Radiol.* 2002;9:632-7.

33. **Helm GA, Alden TD, Beres EJ, Hudson SB, Das S, Engh JA, Pittman DD, Kerns KM, Kallmes DF.** Use of bone morphogenetic protein-9 gene therapy to induce spinal arthrodesis in the rodent. *J Neurosurg.* 2000;92 (2 Suppl): 191-6.

34. **Sandhu HS, Khan SN, Suh DY, Boden SD.** Demineralized bone matrix, bone morphogenetic proteins, and animal models of spine fusion: an overview. *Eur Spine J.* 2001;10 Suppl 2:S122-31.

35. **Boden SD, Zdeblick TA, Sandhu HS, Heim SE.** The use of rhBMP-2 in interbody fusion cages. Definitive evidence of osteoinduction in humans: a preliminary report. *Spine.* 2000;25:376-81.

36. **Friedlaender GE.** OP-1 clinical studies. *J Bone Joint Surg Am.* 2001;83 Suppl 1 (Pt 2):S160-1.

37. **Valentin-Opran A, Wozney J, Csimma C, Lilly L, Riedel GE.** Clinical evaluation of recombinant human bone morphogenetic protein-2. *Clin Orthop.* 2002;395:110-20.

38. **Whang K, Tsai DC, Nam EK, Aitken M, Sprague SM, Patel PK, Healy KE.** Ectopic bone formation via rhBMP-2 delivery from porous bioabsorbable polymer scaffolds. *J Biomed Mater Res.* 1998;42:491-9.

39. **Alden TD, Pittman DD, Beres EJ, Hankins GR, Kallmes DF, Wisotsky BM, Kerns KM, Helm GA.** Percutaneous spinal fusion using bone morphogenetic protein-2 gene therapy. *J Neurosurg.* 1999;90 (1 Suppl):109-14.

40. **Oyama M, Tatlock A, Fukuta S, Kavalkovich K, Nishimura K, Johnstone B, Robbins PD, Evans CH, Niyibizi C.** Retrovirally transduced bone marrow stromal cells isolated from a mouse model of human osteogenesis imperfecta (OIM) persist in bone and retain the ability to form cartilage and bone after extended passaging. *Gene Ther.* 1999;6:321-9.

41. **Alden TD, Pittman DD, Hankins GR, Beres EJ, Engh JA, Das S, Hudson SB, Kerns KM, Kallmes DF, Helm GA.** In vivo endochondral bone formation using a bone morphogenetic protein 2 adenoviral vector. *Hum Gene Ther.* 1999; 10:2245-53.

42. **Baltzer AW, Lattermann C, Whalen JD, Wooley P, Weiss K, Grimm M, Ghivizzani SC, Robbins PD, Evans CH.** Genetic enhancement of fracture repair: healing of an experimental segmental defect by adenoviral transfer of the BMP-2 gene. *Gene Ther.* 2000;7:734-9.

43. **Baltzer AW, Lattermann C, Whalen JD, Ghivizzani S, Wooley P, Krauspe R, Robbins PD, Evans CH.** Potential role of direct adenoviral gene transfer in enhancing fracture repair. *Clin Orthop.* 2000;379 Suppl:S120-5.

44. **Bosch P, Musgrave D, Ghivizzani S, Latterman C, Day CS, Huard J.** The efficiency of muscle-derived cell-mediated bone formation. *Cell Transplant.* 2000;9:463-70.

45. **Breitbart AS, Grande DA, Mason JM, Barcia M, James T, Grant RT.** Gene-enhanced tissue engineering: applications for bone healing using cultured periosteal cells transduced retrovirally with the BMP-7 gene. *Ann Plast Surg.* 1999;42:488-95.

46. **Franceschi RT, Wang D, Krebsbach PH, Rutherford RB.** Gene therapy for bone formation: in vitro and in vivo osteogenic activity of an adenovirus expressing BMP7. *J Cell Biochem.* 2000;78:476-86.

47. **Gazit D, Turgeman G, Kelley P, Wang E, Jalenak M, Zilberman Y, Moutsatsos I.** Engineered pluripotent mesenchymal cells integrate and differentiate in regenerating bone: a novel cell-mediated gene therapy. *J Gene Med.* 1999;1:121-33.

48. **Lieberman JR, Le LQ, Wu L, Finerman GA, Berk A, Witte ON, Stevenson S.** Regional gene therapy with a BMP-2-producing murine stromal cell line induces heterotopic and orthotopic bone formation in rodents. *J Orthop Res.* 1998;16:330-9.

49. **Lou J, Xu F, Merkel K, Manske P.** Gene therapy: adenovirus-mediated human bone morphogenetic protein-2 gene transfer induces mesenchymal progenitor cell proliferation and differentiation in vitro and bone formation in vivo. *J Orthop Res.* 1999;17:43-50.

50. **Mason JM, Grande DA, Barcia M, Grant R, Pergolizzi RG, Breitbart AS.** Expression of human bone morphogenic protein 7 in primary rabbit periosteal cells: potential utility in gene therapy for osteochondral repair. *Gene Ther.* 1998;5:1098-104.

51. **Musgrave DS, Bosch P, Ghivizzani S, Robbins PD, Evans CH, Huard J.** Adenovirus-mediated direct gene therapy with bone morphogenetic protein-2 produces bone. *Bone.* 1999;24:541-7.

52. **Okubo Y, Bessho K, Fujimura K, Iizuka T, Miyatake SI.** Osteoinduction by bone morphogenetic protein-2 via adenoviral vector under transient immunosuppression. *Biochem Biophys Res Commun.* 2000;267:382-7.

53. **Ripamonti U, Ramoshebi LN, Matsaba T, Tasker J, Crooks J, Teare J.** Bone induction by BMPs/OPs and related family members in primates. *J Bone Joint Surg Am.* 2001;83 Suppl 1(Pt 2):S116-27.

54. **Lee JY, Musgrave D, Pelinkovic D, Fukushima K, Cummins J, Usas A, Robbins P, Fu FH, Huard J.** Effect of bone morphogenetic protein-2-expressing muscle-derived cells on healing of critical-sized bone defects in mice. *J Bone Joint Surg Am.* 2001;83:1032-9.

55. **He TC, Zhou S, da Costa LT, Yu J, Kinzler KW, Vogelstein B.** A simplified system for generating recombinant adenoviruses. *Proc Natl Acad Sci USA.* 1998;95:2509-14.

56. **He TC, Sparks AB, Rago C, Hermeking H, Zawel L, da Costa LT, Morin PJ, Vogelstein B, Kinzler KW.** Identification of c-MYC as a target of the

APC pathway. *Science.* 1998;281:1509-12.

57. **Sarras MP Jr.** BMP-1 and the astacin family of metalloproteinases: a potential link between the extracellular matrix, growth factors and pattern formation. *Bioessays.* 1996;18:439-42.

58. **Einhorn TA, Lee CA.** Bone regeneration: new findings and potential clinical applications. *J Am Acad Orthop Surg.* 2001;9:157-65.

59. **Noda M, Camilliere JJ.** In vivo stimulation of bone formation by transforming growth factor-beta. *Endocrinology.* 1989;124:2991-4.

60. **Joyce ME, Terek RM, Jingushi S, Bolander ME.** Role of transforming growth factor-beta in fracture repair. *Ann NY Acad Sci.* 1990;593:107-23.

61. **Lind M, Schumacker B, Soballe K, Keller J, Melsen F, Bunger C.** Transforming growth factor-beta enhances fracture healing in rabbit tibiae. *Acta Orthop Scand.* 1993;64:553-6.

62. **Nielsen HM, Andreassen TT, Ledet T, Oxlund H.** Local injection of TGF-beta increases the strength of tibial fractures in the rat. *Acta Orthop Scand.* 1994;65:37-41.

63. **Critchlow MA, Bland YS, Ashhurst DE.** The effect of exogenous transforming growth factor-beta 2 on healing fractures in the rabbit. *Bone.* 1995;16:521-7.

64. **Sumner DR, Turner TM, Purchio AF, Gombotz WR, Urban RM, Galante JO.** Enhancement of bone ingrowth by transforming growth factor-beta. *J Bone Joint Surg Am.* 1995;77:1135-47.

65. **Canalis E, Centrella M, McCarthy T.** Effects of basic fibroblast growth factor on bone formation in vitro. *J Clin Invest.* 1988;81:1572-7.

66. **Kato T, Kawaguchi H, Hanada K, Aoyama I, Hiyama Y, Nakamura T, Kuzutani K, Tamura M, Kurokawa T, Nakamura K.** Single local injection of recombinant fibroblast growth factor-2 stimulates healing of segmental bone defects in rabbits. *J Orthop Res.* 1998;16:654-9.

67. **Nakamura T, Hara Y, Tagawa M, Tamura M, Yuge T, Fukuda H, Nigi H.** Recombinant human basic fibroblast growth factor accelerates fracture healing by enhancing callus remodeling in experimental dog tibial fracture. *J Bone Miner Res.* 1998;13:942-9.

68. **Radomsky ML, Thompson AY, Spiro RC, Poser JW.** Potential role of fibroblast growth factor in enhancement of fracture healing. *Clin Orthop.* 1998;355 Suppl:S283-93.

69. **Radomsky ML, Aufdemorte TB, Swain LD, Fox WC, Spiro RC, Poser JW.** Novel formulation of fibroblast growth factor-2 in a hyaluronan gel accelerates fracture healing in nonhuman primates. *J Orthop Res.* 1999;17:607-14.

70. **Nash TJ, Howlett CR, Martin C, Steele J, Johnson KA, Hicklin DJ.** Effect of platelet-derived growth factor on tibial osteotomies in rabbits. *Bone.* 1994; 15:203-8.

71. **Thaller SR, Dart A, Tesluk H.** The effects of insulin-like growth factor-1 on critical-size calvarial defects in Sprague-Dawley rats. *Ann Plast Surg.* 1993; 31:429-33.

72. **Trippel SB.** Potential role of insulinlike growth factors in fracture healing. *Clin Orthop.* 1998;355 Suppl:S301-13.

73. **Boden SD, Titus L, Hair G, Liu Y, Viggeswarapu M, Nanes MS, Baranowski C.** Lumbar spine fusion by local gene therapy with a cDNA encoding a novel osteoinductive protein (LMP-1). *Spine.* 1998;23:2486-92.

74. **Linkhart TA, Mohan S, Baylink DJ.** Growth factors for bone growth and repair: IGF, TGF beta and BMP. *Bone.* 1996;19(1 Suppl):1S-12S.

75. **Wozney JM, Rosen V.** Bone morphogenetic protein and bone morphogenetic protein gene family in bone formation and repair. *Clin Orthop.* 1998;346: 26-37.

76. **Groeneveld EH, Burger EH.** Bone morphogenetic proteins in human bone regeneration. *Eur J Endocrinol.* 2000;142:9-21.

77. **Azari K, Doll BA, Sfeir C, Mu Y, Hollinger JO.** Therapeutic potential of bone morphogenetic proteins. *Expert Opin Investig Drugs.* 2001;10:1677-86.

78. **Lieberman JR, Daluiski A, Einhorn TA.** The role of growth factors in the repair of bone. Biology and clinical applications. *J Bone Joint Surg Am.* 2002; 84:1032-44.

79. **Alden TD, Varady P, Kallmes DF, Jane JA Jr, Helm GA.** Bone morphogenetic protein gene therapy. *Spine.* 2002;27(16 Suppl 1):S87-93.

80. **Yoon ST, Boden SD.** Osteoinductive molecules in orthopaedics: basic science and preclinical studies. *Clin Orthop.* 2002;395:33-43.

81. **Bahamonde ME, Lyons KM.** BMP3: to be or not to be a BMP. *J Bone Joint Surg Am.* 2001;83 Suppl 1(Pt 1):S56-62.

82. **Song JJ, Celeste AJ, Kong FM, Jirtle RL, Rosen V, Thies RS.** Bone morphogenetic protein-9 binds to liver cells and stimulates proliferation. *Endocrinology.* 1995;136:4293-7.

83. **Ploemacher RE, Engels LJ, Mayer AE, Thies S, Neben S.** Bone morphogenetic protein 9 is a potent synergistic factor for murine hemopoletic progenitor cell generation and colony formation in serum-free cultures. *Leukemia.* 1999;13:428-37.

84. **Lopez-Coviella I, Berse B, Krauss R, Thies RS, Blusztajn JK.** Induction and maintenance of the neuronal cholinergic phenotype in the central nervous system by BMP-9. *Science.* 2000;289:313-6.

85. **Majumdar MK, Wang E, Morris EA.** BMP-2 and BMP-9 promotes chondrogenic differentiation of human multipotential mesenchymal cells and overcomes the inhibitory effect of IL-1. *J Cell Physiol.* 2001;189: 275-84.

86. **Dumont RJ, Dayoub H, Li JZ, Dumont AS, Kallmes DF, Hankins GR, Helm GA.** Ex vivo bone morphogenetic protein-9 gene therapy using human mesenchymal stem cells induces spinal fusion in rodents. *Neurosurgery.* 2002; 51:1239-45.

87. **Solloway MJ, Dudley AT, Bikoff EK, Lyons KM, Hogan BL, Robertson EJ.** Mice lacking Bmp6 function. *Dev Genet.* 1998;22:321-39.

88. **Jane J, Dunford B, Kron A, Pittman DD, Sasaki T, Li JZ, Li H, Alden TD, Dayoub H, Hankins GR, Kallmes DF, Helm GA.** Ectopic osteogenesis using adenoviral bone morphogenetic protein (BMP)-4 and BMP-6 gene transfer. *Mol Ther.* 2002;6:464-70.

Exhibit G

Gene Therapy

www.nature.com/gt

- *Knocking out the bad allele*
- *Muscle stem cells aiding gene therapy*
- *Mouse model for* in vivo *somatic gene repair detection*
- *Characterising relative bone-forming activities of 14 BMPs*
- *Ca^{2+}-phosphate transfection-enabled gene analysis*

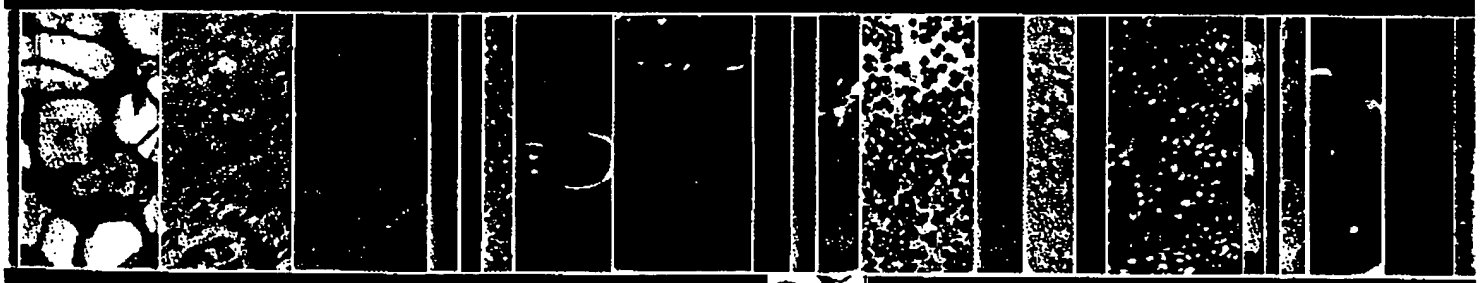

Volume 11 Number 17

nature publishing group

September 2004

Gene Therapy

Volume 11 • Number 17 • September 2004

Contents

News and Commentary

1301 *Knocking out the bad allele*
S Garofalo & R Quarto

Research Articles

1303 *High Ca^{2+}-phosphate transfection efficiency enables single neuron gene analysis*
M Jiang, L Deng & G Chen

1312 *Characterization of the distinct orthotopic bone-forming activity of 14 BMPs using recombinant adenovirus-mediated gene delivery*
Q Kang, MH Sun, H Cheng, Y Peng, AG Montag, AT Deyrup, W Jiang, HH Luu, J Luo, JP Szatkowski, P Vanichakarn, JY Park, Y Li, RC Haydon & T-C He

1321 *Muscle stem cells can act as antigen-presenting cells: implication for gene therapy*
B Cao, J Bruder, I Kovesdi & J Huard

1331 *Inhibition of papilloma progression by antisense oligonucleotides targeted to HPV11 E6/E7 RNA*
GA Clawson, GQ Miranda, A Sivarajah, P Xin, W Pan, D Thiboutot & ND Christensen

1342 *Recombinant adeno-associated virus-mediated kallikrein gene therapy reduces hypertension and attenuates its cardiovascular injuries*
T Wang, H Li, C Zhao, C Chen, J Li, J Chao, L Chao, X Xiao & DW Wang

1351 *A LacZ-based transgenic mouse for detection of somatic gene repair events in vivo*
HD Nickerson & WH Colledge

Brief Communication

1358 *New strategy for transfection: mixtures of medium-chain and long-chain cationic lipids synergistically enhance transfection*
L Wang & RC MacDonald

nature publishing group

Gene Therapy (2004) 11, 1312–1320

www.nature.com/gt

RESEARCH ARTICLE

Characterization of the distinct orthotopic bone-forming activity of 14 BMPs using recombinant adenovirus-mediated gene delivery

Q Kang[1,2,5], MH Sun[1,5], H Cheng[1,5], Y Peng[1,3], AG Montag[1,4], AT Deyrup[1,4,6], W Jiang[1], HH Luu[1], J Luo[1], JP Szatkowski[1], P Vanichakarn[1], JY Park[1], Y Li[1], RC Haydon[1] and T-C He[1,3]

[1]*Molecular Oncology Laboratory, Department of Surgery, The University of Chicago Medical Center, Chicago, IL, USA;* [2]*The Children's Hospital of Chongqing University of Medical Sciences, Chongqing, China;* [3]*Committee on Genetics, The University of Chicago, Chicago, IL, USA; and* [4]*Department of Pathology, The University of Chicago, Chicago, IL, USA*

Efficacious bone regeneration could revolutionize the clinical management of bone and musculoskeletal disorders. Although several bone morphogenetic proteins (BMPs) (mostly BMP-2 and BMP-7) have been shown to induce bone formation, it is unclear whether the currently used BMPs represent the most osteogenic ones. Until recently, comprehensive analysis of osteogenic activity of all BMPs has been hampered by the fact that recombinant proteins are either not biologically active or not available for all BMPs. In this study, we used recombinant adenoviruses expressing the 14 types of BMPs (AdBMPs), and demonstrated that, in addition to currently used BMP-2 and BMP-7, BMP-6 and BMP-9 effectively induced orthotopic ossification when either AdBMP-transduced osteoblast progenitors or the viral vectors were injected into the quadriceps of athymic mice. Radiographic and histological evaluation demonstrated that BMP-6 and BMP-9 induced the most robust and mature ossification at multiple time points. BMP-3, a negative regulator of bone formation, was shown to effectively inhibit orthotopic ossification induced by BMP-2, BMP-6, and BMP-7. However, BMP-3 exerted no inhibitory effect on BMP-9-induced bone formation, suggesting that BMP-9 may transduce osteogenic signaling differently. Our findings suggest that BMP-6 and BMP-9 may represent more effective osteogenic factors for bone regeneration.
Gene Therapy (2004) 11, 1312–1320. doi:10.1038/sj.gt.3302298; Published online 22 July 2004

Keywords: *bone formation; bone morphogenetic protein; bone regeneration; osteogenesis; osteoblast differentiation; recombinant adenovirus*

Introduction

Bone regeneration is critical to the effective management of many bone and musculoskeletal disorders, such as fracture healing, spinal fusion, and osteoporosis, which are responsible for a large portion of healthcare expenditure in the developed countries—approximately $14 billion is spent annually on treating osteoporotic fractures in the US alone.[1] Bone is a highly mineralized tissue and is one of the few organs that retains the potential for regeneration in adult life. Bone also undergoes continuous remodeling throughout life.[2,3] Three major types of cells are present in bone tissues: bone-forming osteoblasts, bone-resorbing osteoclasts, and chondrocytes. Osteoblasts are derived from the mesenchymal stem cells, which also serve as precursor cells for myocytes, adipocytes, and chondrocytes. It has been known for almost half a century that demineralized bone can induce *de novo* bone formation.[4] The molecular identity of the bone-forming factors in demineralized bone was subsequently revealed to be bone morphogenetic proteins (BMPs).[5] BMPs belong to the TGFβ superfamily, and play an important role in embryonic development and bone formation.[6,7] At least 15 types of BMPs have been identified in humans. BMP signal transduction begins via interaction with the heterodimeric complex of two transmembrane serine/threonine kinase receptors, BMPR type I and BMPR type II.[8,9] The activated receptor kinases phosphorylate the transcription factors Smads 1, 5, and/or 8. The phosphorylated Smads then form a heterodimeric complex with Smad 4 in the nucleus and activate the expression of target genes in concert with other coactivators.[10–12]

Although the molecular mechanisms underlying osteoblast differentiation remain to be defined, BMPs play an important role in regulating osteoblast differentiation and subsequent bone formation. Traditionally, various bone grafts have been used to promote osteogenesis in bone and musculoskeletal disorders. The identification of BMPs has generated great interest due to their potential use in bone regeneration.[3] Several recombinant forms of BMPs, mostly rhBMP-2 and rhBMP-7 (a.k.a., OP-1), have been shown to induce bone formation *in vivo*,[13–24] and both rhBMP-2 and rhBMP-7 have been

Correspondence: Dr T-C He, Molecular Oncology Laboratory, Department of Surgery, The University of Chicago Medical Center, 5841 South Maryland Avenue, MC3079, Chicago, IL 60637, USA
[5]*QK, MHS, and HC Contributed equally to this work*
[6]*Current address: Department of Pathology, Emory University, Atlanta, GA, USA.*
Received 18 August 2003; accepted 7 February 2004; published online 22 July 2004

tested in clinical trials.[25–27] In addition to the direct application of recombinant BMP proteins, numerous reports have confirmed the ability of adenoviral or retroviral vector-mediated gene transfer of several BMPs to induce bone formation in animal models.[18,20,21,23,28–44]

Although a plethora of studies have demonstrated the ability of several BMPs, mostly BMP-2 and BMP-7, to promote osteogenesis, it is unclear whether or not BMPs other than those currently being tested in clinical trials are more potent stimulators of new bone formation. Thus, it is important to conduct a comprehensive comparative analysis of the *in vivo* osteogenic activity of all BMPs. This line of investigation has been hampered by the fact that recombinant proteins are either not biologically active or not available for all BMPs. We have recently constructed a panel of recombinant adenoviral vectors that express the 14 types of human BMPs (BMP-2–BMP-15).[45] Recombinant adenoviral vectors are ideal for this line of investigation for following reasons.[46–51] First, adenoviral vectors can transduce osteoblast progenitor cells with high efficiency. Second, the biologically active BMPs are continuously produced inside mammalian cells. Third, BMP-mediated bone osteoblast differentiation does not require long-term expression. Fourth, adenoviral vectors can be used in both *in vitro* and *in vivo* studies. In this study, we sought to carry out a comprehensive analysis of the distinct *in vivo* bone-forming activity of the 14 types of human BMPs. Using an orthotopic ossification animal model, we demonstrate that BMP-2, BMP-6, and BMP-9 (BMP-7 to a lesser extent) are the most potent osteoinductive BMPs. Our findings strongly suggest that, in addition to BMP-2 and BMP-7 that are currently used in clinical trails, BMP-6 and BMP-9 could represent equally, if not more effective osteogenic factors for bone regeneration in a clinical setting.

Results

Distinct ability to induce an osteogenic marker, alkaline phosphatase (ALP), by 14 BMPs in the osteoblast progenitor C2C12 cells in vitro

In order to comprehensively analyze the distinct osteogenic activity of BMPs, we have recently constructed a panel of recombinant adenoviral vectors that express the 14 types of human BMPs, designated as AdBMPs.[45] As shown in Figure 1a, the level of transgene expression of the AdBMPs were in general comparable (ie, <2-fold difference among different BMPs), as demonstrated by RT-PCR analysis. These PCR products should be specifically derived from the adenoviral vector-mediated expression (rather than from the endogenous genes), as the 3′-end primer was derived from the SV40 poly-A cassette. Using these adenoviral vectors, we have recently demonstrated that BMPs displayed a distinct ability to induce osteoblast differentiation of mesenchymal progenitor cells *in vitro*.[45] In this study, we sought to determine the relative *in vivo* osteogenic activity of the 14 types of BMPs. We first tested the ability of individual AdBMPs to induce the earlier osteogenic marker alkaline phosphatase in the C2C12 line, which is myoblastic and can be trans-differentiated into osteoblast progenitors upon BMP stimulation. As shown in Figure 1b, ALP activity was remarkably induced by five of the 14 BMPs at four days after AdBMP infections. Among the five osteogenic BMPs, BMP-2, BMP-6, and BMP-9 induced the ALP activity to a much greater extent

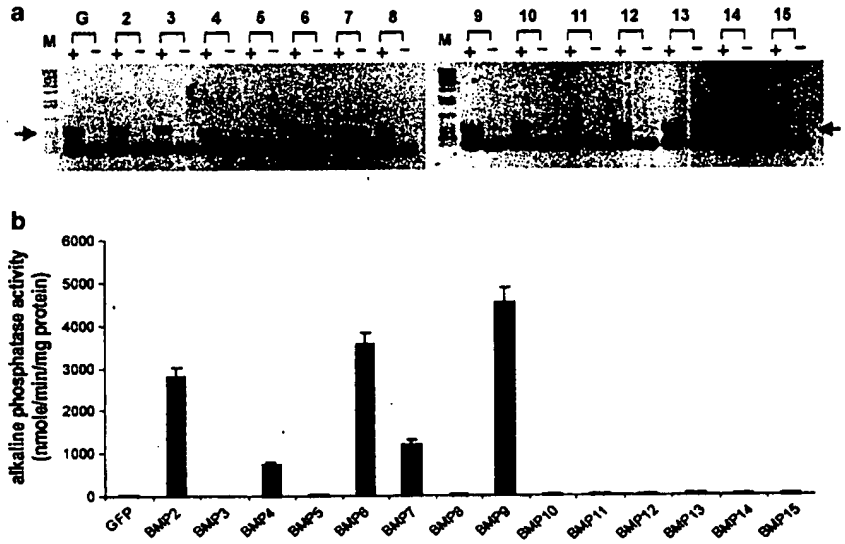

Figure 1 Induction of alkaline phosphatase activity by the 14 types of human BMPs in C2C12 cells. (a) Relative level of AdBMP-mediated transgene expression. C2C12 cells were infected with AdBMPs or AdGFP for 40 h. Total RNA was isolated and converted into cDNA products by reverse transcription, which were used for RT-PCR reactions using BMP-specific primers (5′-end) and a 3′-end primer derived from SV40 polyA. Resultant products ranged from 500 to 600 bps (indicated by arrows). '+', PCR products from +RT reactions of the original cDNA synthesis; '−', PCR products from −RT reactions of the original cDNA synthesis; 'M', 1-Kb Plus ladder from Invitrogen; 'G', AdGFP; '2–15', AdBMP-2 to AdBMP-15. (b) Subconfluent C2C12 cells were infected with AdBMPs and the control AdGFP. At 4 days after infection, cells were lysed for colorimetric assays of alkaline phosphatase activity using p-nitrophenyl phosphate as a substrate. Representative results from at least three independent experiments are shown. See Materials and methods for details.

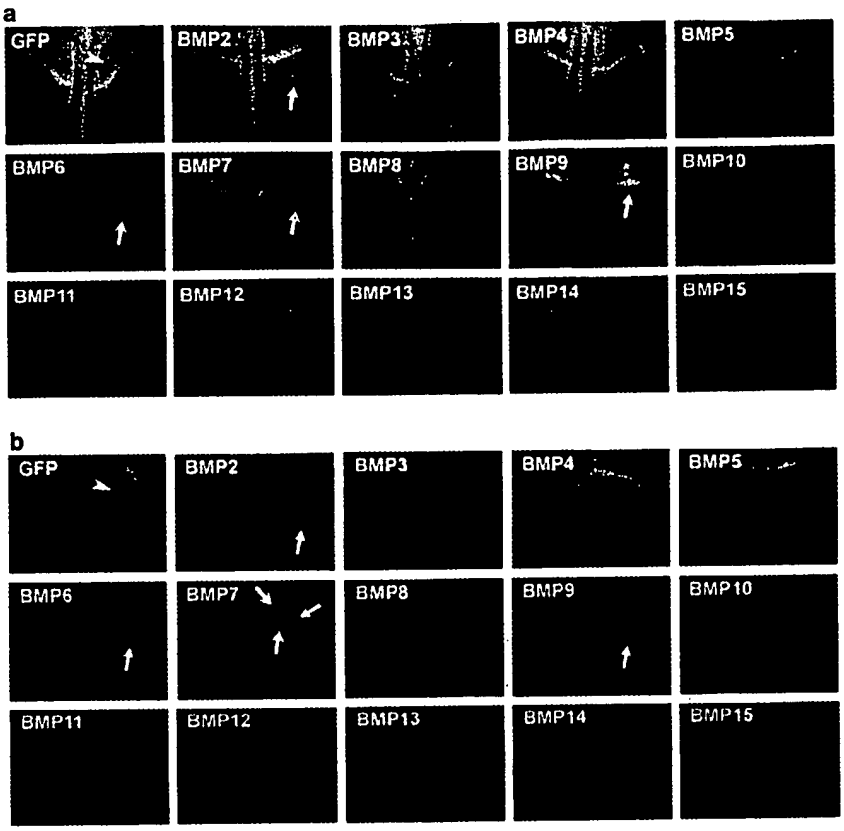

Figure 2 Orthotopic bone formation induced by AdBMP-transduced C2C12 in athymic nude mice. Exponentially growing C2C12 cells were infected with AdBMPs or the control AdGFP for 15 h. Approximately 5 × 10⁶ of the infected cells were injected into the right quadriceps of athymic nude mice (a triangle indicated in the GFP group as an example). At 3 weeks (a) and 5 weeks (b) after injections, mice were killed and subjected to X-ray radiography. Each experimental group contained four mice, and representative radiographies from three batches of experiments were shown.

(approx. 169-, 215-, and 273-fold over the GFP control, respectively), while BMP-4 and BMP-7 increased ALP activity by 44- and 73-fold, respectively. These findings are consistent with our previous studies.[45] It should be pointed out that several BMPs (eg, BMP-10, and BMP-13) also induced a 2–3-fold increase of ALP activity over the basal level under the same assay conditions.

Orthotopic bone formation effectively induced by several but not all BMPs in athymic mice

We next sought to test the *in vivo* osteogenic effect of the 14 BMPs. In order to effectively assess the osteogenic ability of the BMPs, we used an orthotopic ossification animal model, in which C2C12 cells were first transduced with AdBMPs and subsequently implanted into the quadriceps muscles of athymic nude mice by intramuscular injection. Orthotopic ossification was assessed by X-ray radiography and histological evaluation at 3 and 5 weeks after injections. As illustrated in Figure 2, ossification was readily detected on X-ray radiographies from the animals injected with AdBMP-2, 6, 7, and 9-transduced C2C12 cells at 3 weeks (Figure 2a) and 5 weeks (Figure 2b). For BMP-6 and BMP-9, histologic examination at both time points (Figure 3a and b) revealed robust and highly mineralized woven bone with scattered osteoblast-rimming and occasional osteoclasts. Osteoid was also present. In addition, BMP-6 showed bone marrow elements with a range of hematopoietic cells. At the 3-week time point, BMP-2 was characterized by well-calcified foci without bone formation; however, at the 5-week time point, these foci had developed into mature bone. BMP-7, on the other hand, was shown to induce much weaker ossification. Interestingly, we failed to detect any signs of ossification in the animals injected with AdBMP-4-transduced C2C12 cells, which is surprising because we have demonstrated that BMP-4 is capable of inducing ALP activity *in vitro* (Figure 1b).[45] These results were reproducible in two additional rounds of animal studies using different batches of AdBMP-4 preparations, which were consistently shown to induce ALP activity in C2C12 cells *in vitro* (data not shown). Further, our RT-PCR analysis demonstrated that the expression level of BMP-4 was comparable with that of other BMPs, especially BMP-2, BMP-6, and BMP-9 under the same assay condition (Figure 1a). Currently, we are still searching for any satisfactory explanations for this discrepancy between BMP-4's *in vitro versus in vivo* osteogenic activity. Nevertheless, all of the above findings were reproducible in three batches of independent experiments. The remaining samples had no evidence of ossification at 5 weeks. The injection site in these sections demonstrated exuberant granulation tissue and reparative changes.

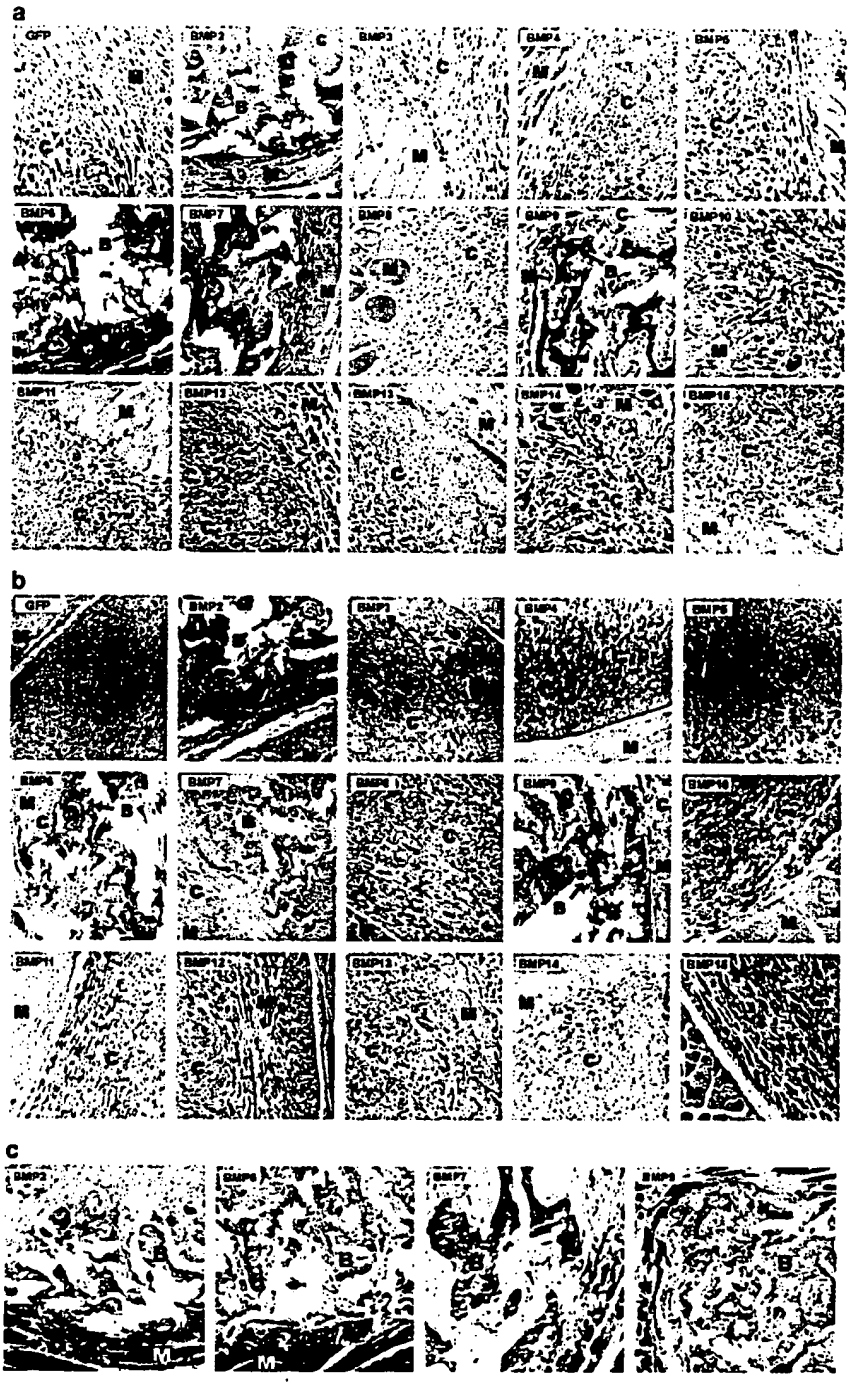

Figure 3 Histological evaluation of AdBMP-induced orthotopic ossification. (a) H & E staining of the AdBMP-transduced C2C12 injection sites at 3 weeks. (b) H & E staining of the AdBMP-transduced C2C12 injection sites at 5 weeks. (c). Masson's Trichrome staining of the AdBMP-transduced C2C12 injection sites at 3 weeks. Muscle fibers and cytoplasm were stained red and collage of osteoid matrix were stained blue. B, osteoid matrix (indicated by arrows); C, injected C2C12 cells; and M, muscle cells. Magnification, × 200.

Histology of BMP-induced bone formation

We next examined the histology of the recovered injection sites. Overall, the histology correlated well with the findings from X-ray radiography. At the 3-week time point, BMP-2, BMP-6, BMP-7, and BMP-9 demonstrated varying degrees of ossification. BMP-2 and BMP-7 were the least developed with small foci of woven bone (Figure 3a). Both BMP-6 and BMP-9, however, had multiple foci of immature woven trabecular bone. In addition, BMP-9 demonstrated focal cartilaginous differentiation. The bone in BMP-6 and BMP-9-treated animals formed a shell-like rim around a proliferating mass of

spindle-shaped C2C12 cells. The 5-week samples demonstrated increased maturation with more mature osteoid matrix and trabecular bone-like structures with accentuation of the shell-like rim, especially in BMP-6 and BMP-9-treated animals. There was less extensive ossification in the BMP-2 sections. Bone marrow elements were present in the BMP-6 sections and chondrocytes and cartilaginous matrix were increased in the BMP-9 sections (Figure 3b). Interestingly, the injected C2C12 cells formed a desmoid-like cell mass in nonosteogenic BMP injections and the GFP control. Even in the animals injected with BMP-2, BMP-6, BMP-7, and BMP-9-transduced C2C12 cells, such cell mass was still visible, and multiple ossification centers were observed at the periphery of the cell mass. BMP-2-, BMP-6-, BMP-7-, and BMP-9-induced osteogenesis was further confirmed by Masson's Trichrome staining (Figure 3c).

Antagonistic effect of BMP-3 on BMP-induced bone formation

We sought to investigate how the osteogenic BMPs were affected by BMP-3, a known negative regulator of bone formation, as BMP-3 knockout animals exhibited an increase in bone density.[52] When C2C12 cells transduced by AdBMP-3 and one of the four osteogenic AdBMPs were coinjected intramuscularly for 3 weeks, BMP-2 and BMP-6-induced ossification was completely blocked by BMP-3, and most of the BMP-7-induced ossification was inhibited by BMP-3 (Figure 4a). However, BMP-3 coinjection did not exert any effect on BMP-9-induced calcification (Figure 4a), strongly suggesting that BMP-9 may exert its osteogenic activity via a distinct signaling mechanism. Similar results were obtained for the 5-week groups (data not shown). The histological findings were consistent with those from X-ray radiographic results (Figure 4b). The three samples without ossification demonstrated C2C12 cell proliferation with entrapped skeletal muscle while the BMP-3+BMP-9 sections had multiple foci of woven trabecular bone similar to BMP-9 injection alone.

Bone formation induced by direct intramuscular injection of AdBMPs

Recent studies suggest that skeletal muscles may harbor pluripotent mesenchymal stem cells, including osteoblast progenitors.[34,44,53] We next tested the osteoinductive activity of the 14 BMPs via direct intramuscular injection of AdBMPs. At the 3 and 5-week time points, we did not observe apparent ossification on X-ray radiography (data not shown). However, when the 5-week injection sites

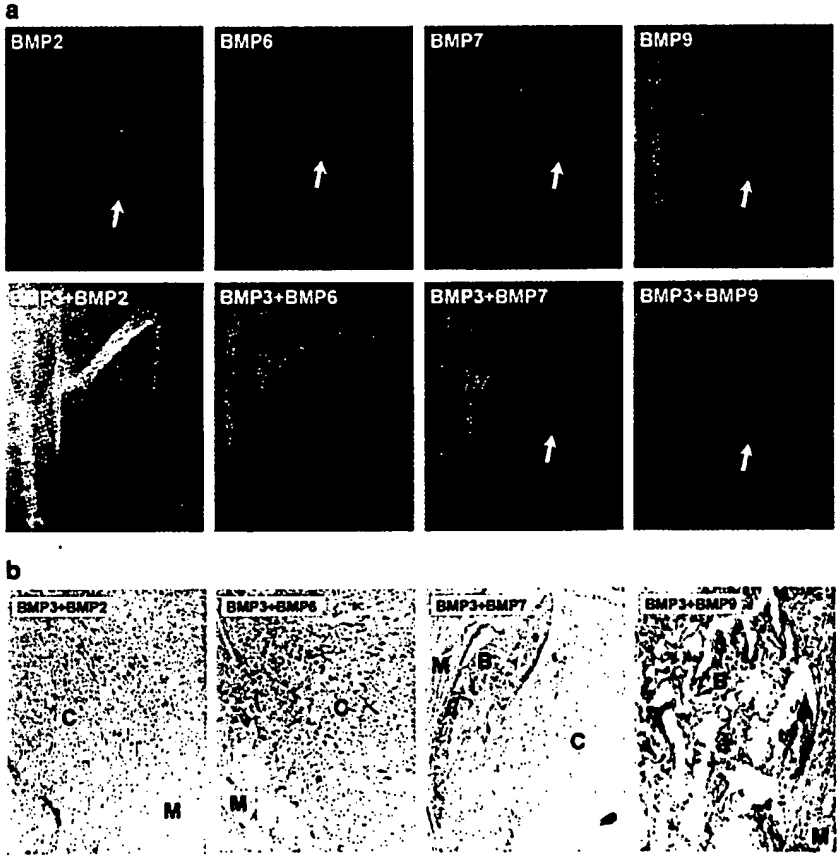

Figure 4 BMP-3-mediated inhibition of bone formation induced by BMP-2, BMP-6, and BMP-7, but not by BMP-9. (a) Osteogenic AdBMPs (ie, BMP-2, -6, -7, and -9)-transduced C2C12 cells were either injected alone (top row) or coinjected with AdBMP-3 (bottom row) into the right quadriceps of athymic mice. Animals were killed at 3 weeks and subjected to X-ray radiography. Ossification sites were indicated by arrows. Each experimental group contained four mice, and representative radiographies from three batches of experiments are shown. (b) Histological evaluation of the BMP-3 coinjection sites. B, osteoid matrix; C, injected C2C12 cells; and M, muscle cells. Magnification, × 150.

were examined histologically, various degrees of cartilaginous and/or osteoid matrix formation were observed in BMP-2, BMP-6, BMP-7, and BMP-9-injected animals (Figure 5). Samples derived from BMP-2 and, to a lesser extent, BMP-7 injection sites contained more cartilage-like chondrocyte-containing structure, while osteoid matrix and mature lamellar bone were present with evidence of bone marrow colonization and remodeling in BMP-6 and BMP-9-injected animals. Unlike in the experiments with C2C12 injections, direct intramuscular injections with AdBMPs (ie, the above-mentioned four osteogenic BMPs) induced more diffuse ossification. This may also explain why the calcification (ie, by BMP-9) was not readily detected by X-ray radiography. These findings also suggest that orthotopic osteogenesis induced by direct intramuscular injection with osteogenic AdBMPs may be less efficient than that induced by introduction of AdBMP-transduced osteoblast progenitor cells, implying that osteoblast progenitor cell-based gene therapy may be a more efficacious approach to bone regeneration, although it is possible that the reduced bone formation was resulted from the potentially less-efficient gene transfer associated with direct intramuscular injections than that with AdBMP-transduced C2C12 cells.

Discussion

Successful bone regeneration mediated by biofactors could revolutionize the clinical management of musculoskeletal disorders, including fracture healing and spinal fusion.[54] Several biological factors, such as TGFβ, BMP, FGF, PDGF, IGF, and LMP-1, have been investigated for their potential use in bone regeneration and skeletal repair.[55–69] BMPs have been shown to be the most promising, and clinical trials with recombinant BMP-2 and -7 are ongoing.[54,70–73] These BMPs have shown varying degrees of success in the clinical setting and further study on their mechanisms of action and optimal formulations is required to optimize effectiveness of this strategy for promoting osteogenesis.

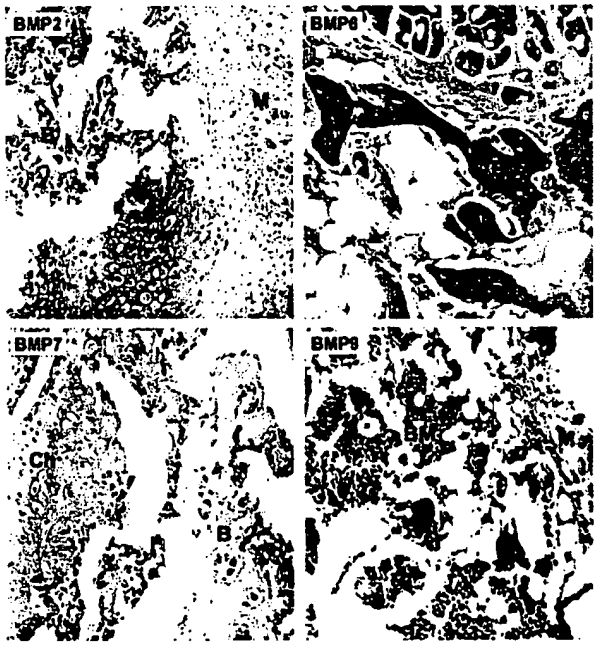

Figure 5 Orthotopic bone formation induced by direct intramuscular injection of AdBMPs. Approximately 10^9 PFU of AdBMPs or AdGFP were directly injected into the quadriceps of athymic mice. Animals were killed at 5 weeks after injection and subjected to X-ray radiography (not shown). Each experimental group had four mice. Representative results from two independent experiments are shown. BMP-6-treated sample was decalcified. B, osteoid matrix; BM, bone marrow cells; Ch, chondrocytes; and M, muscle cells. Magnification, × 200.

To the best of our knowledge, this reported study represents the first of its kind to evaluate the *in vivo* osteogenic activity of BMPs in a comprehensive fashion. The observation that BMP-2 exhibited osteogenic activity in our study is consistent with early data from human clinical trials.[25,27] While BMP-7 exhibited apparent osteogenic activity, its ability to induce ossification was significantly less robust than that of BMP-2, BMP-6, and BMP-9. These findings mirror the moderate success of the rhBMP-7 (ie, OP-1) in a recent clinical trial.[26]

It is intriguing, however, that BMP-6 and BMP-9 emerged as the most potent inducers of orthotopic ossification *in vivo*. Although considerable genetic and developmental studies have been conducted to elucidate the biological functions of BMP-6, its osteogenic activity has not been investigated to any significant degree in animal studies or clinical trials. BMP-6-deficient mice are largely unremarkable, with the exception of a defect in the sternum.[74] Its expression during embryogenesis is closely coupled with BMP-2, and the lack of noticeable defects in BMP-6-deficient mice may be due to functional compensation by BMP-2.[74] Nevertheless, our findings corroborate well with a recent study in which BMP-6 was shown to induce the most rapid tissue calcification when compared with BMP-2 or BMP-4 in an athymic nude rat model,[75] although for reasons to be determined AdBMP-4 reproducibly failed to induce orthotopic bone formation in this study.

BMP-9 is one of the least studied members of the BMP family. Originally identified from fetal mouse liver cDNA libraries, BMP-9 (a.k.a., GDF-2) is highly expressed in the developing mouse liver, and recombinant human BMP-9 (rhBMP-9) stimulates hepatocyte proliferation.[76] BMP-9 has also been shown to be a potent synergistic factor for hematopoietic progenitor cell generation and colony formation,[77] and may also play a role in the induction and maintenance of the neuronal cholinergic phenotype in the central nervous system.[78] In addition, it has recently been shown that BMP-9 exhibits an apparent osteoinductive effect in rat models.[21,23,79] However, the mechanisms underlying BMP-9-mediated osteogenic signaling remain to be defined. It is a very intriguing finding that BMP-9-mediated bone formation was not inhibited by BMP-3 in our studies. This result strongly suggests that BMP-9 may transduce a distinct osteogenic signaling pathway that is significantly different from that of BMP-2, BMP-6, and BMP-7. Through an expression profiling analysis, we have recently identified a group of downstream targets that may play an important role in the osteogenic BMP signaling pathway mediated by BMP-2, BMP-6, and BMP-9.[80] Interestingly, while BMP-2, BMP-6, and BMP-9 induced a very similar overall gene expression pattern, the clustering analysis revealed that BMP-2 and BMP-9 exhibited a more similarly related expression pattern.[80]

In conclusion, we have demonstrated the relative osteogenic ability of 14 BMPs and identified BMP-6 and BMP-9 (in addition to the currently used BMP-2 and BMP-7) as the most potent BMPs to induce orthotopic bone formation *in vivo*. Our results also suggest that the stem/progenitor cell-based *ex vivo* gene therapy may represent a more effective approach to bone regeneration. Future studies will focus on elucidating the major signaling differences among BMPs so that maximal synergy in bone formation can be achieved by combining BMPs that act through overlapping or converging signaling pathways. This line of investigation would help to elucidate the molecular mechanisms underlying bone formation and lead to the development of more efficacious approaches towards bone regeneration.

Materials and methods

Cell culture and chemicals

HEK 293 and C2C12 cell lines were obtained from the ATCC (Manassas, VA, USA), and were maintained in complete DMEM supplemented with 10% fetal calf serum (FCS, Mediatech, Herndon, VA, USA), 100 U of penicillin, and 100 μg of streptomycin at 37°C in 5% CO_2. Unless indicated otherwise, all chemicals were purchased from Sigma-Aldrich (St Louis, MO, USA).

Recombinant adenoviral vectors expressing BMPs

The cDNA clones for human BMP-2, -3 (a.k.a., osteogenin), -4, -5, -6, -8 (a.k.a., OP-2), -9 (a.k.a., GDF-2), -10, -12 (a.k.a., GDF-7 or CDMP-3), and -13 (a.k.a., GDF6 or CDMP2) were kindly provided by the Genetics Institute (Cambridge, MA, USA). The coding sequences for BMP-7 (a.k.a., OP-1), -11 (a.k.a., GDF-11), -14 (a.k.a., GDF-5 or CDMP-1), and -15 (a.k.a., GDF-9) were PCR amplified from a human osteosarcoma cDNA library. The coding regions of the above BMPs were subcloned into pAdTrack-CMV, resulting in pAdTrack-BMPs; recombinant adenoviruses expressing BMPs (ie, AdBMPs) were subsequently generated as previously described.[45,81] For a control, we used an analogous adenovirus expressing only GFP (ie, AdGFP), as previously described.[81] Details on vector constructions are available upon request.

RNA purification and reverse transcriptase-PCR analysis

The RT-PCR analysis was carried out as previously described.[80] Specifically, C2C12 cells were seeded in 25 cm^2 cell culture flasks, and infected with an optimal and compatible titer of AdBMPs or AdGFP. At 40 h after infection, total RNA was isolated using RNAgent Total RNA Isolation kit (Promega, Madison, WI, USA) according to the manufacturer's instructions. Total RNA (10 μg) was used to generate cDNA templates for reverse transcriptase-PCR. The first-strand cDNA synthesis was performed using a hexamer (Promega, Madison, WI, USA) and Superscript II reverse transcriptase (Invitrogen). The first-strand cDNA products were further diluted 50-fold and used as PCR templates. Expression level was determined by touchdown PCR analysis using respective pairs of oligonucleotides to amplify the 3′-end of each BMP gene and the 5′-end of SV40 poly A region. Touchdown PCR was performed by using the following program: 94°C × 2 min for one cycle, 12 cycles at 92°C × 20 s, 68°C × 30 s, and 70°C × 45 s with a decrease of one degree per cycle, and 35 cycles at 92°C × 20 s, 55°C × 30 s, and 70°C × 45 s. The amplified products (ranging from 500–600 bps) were resolved on 1% agarose gels, and visualized under UV light after ethidium bromide staining.

Determination of alkaline phosphatase activity

Exponentially growing C2C12 cells were seeded in 48-well cell culture plates, and infected with AdBMPs or AdGFP (multiplicities of infection, or MOIs = 50–200). The induction of alkaline phosphatase activity was assessed at 4 days after infection. Alkaline phosphatase activity was determined by using *p*-nitrophenyl phosphate (Sigma-Aldrich) as a substrate. Absorbance at 405 nm was recorded at 1, 2, and 3 min after the cell lysate was mixed with the substrate. Each assay condition was carried out in triplicate and normalized with the concentrations of total cellular proteins. Enzyme activity was expressed as nanomoles of *p*-nitrophenol produced per minute per mg of total cellular proteins.

Orthotopic bone formation in athymic nude mice

The use of animals was approved by the Institutional Animal Care and Use Committee. Young athymic nude mice (male, 5–6 months, Frederick Cancer Research Center) were used in this study. Each experimental group had four animals. For the injection with adenovirus-transduced C2C12 cells, subconfluent C2C12 cells were infected with AdBMPs or AdGFP at preoptimized titers (MOIs ~ 50–100). At 15 h after infection, cells were collected and resuspended in PBS at an approximate density of 1×10^8 cells/ml. In total, 50 μl of the cell suspension (approx. 5×10^6 cells) was used for the intramuscular injection of right quadriceps. For cell mixing experiments, approximately 2.5×10^6 cells of AdBMP-3- and AdBMP-infected cells were combined prior to intramuscular injections. For direct intramuscular injections, approximately 10^9 PFU of AdBMPs or AdGFP were briefly dialyzed against PBS to remove CsCl, and suspended in a final volume of 50 μl for direct injections into the right quadriceps. Injected animals resumed activities immediately without any restraints on food and drink. At 3 and 5 weeks after injections, animals were killed and subjected to X-ray radiography. The injected sites were harvested for histological evaluation. Representative results from three independent batches of experiments are shown.

H & E staining and Masson's Trichrome staining

After X-ray radiography, the injected thighs were recovered, fixed in 10% formalin overnight, and embedded in paraffin. Serial sections at 12 μm of the embedded specimens were carried out, and mounted onto treated slides. The sections were stained with hematoxylin and eosin (H & E) and Masson's Trichrome. Some samples were subjected to calcification prior to H & E staining.

Note added in proof

While this report was under review, Li LZ *et al* coincidently analyzed the osteogenic activity of BMP-2, BMP-4, BMP-6, BMP-7, and BMP-9 (*Gene Therapy 2003;*

10:1735–1743). Their findings also suggest that BMP-9 is one of the most osteogenic BMPs in rat models of bone formation.

Acknowledgements

We thank Dr Mark Bolander of Mayo Clinic for valuable discussion and critical review of the manuscript. We thank the Genetics Institute of Cambridge, MA, for providing human BMP cDNAs. We apologize to the researchers whose original work was not cited due to space constraints. The work was supported in part by research grants from the Aircast Foundation, the Brinson Foundation, North American Spine Society, and the Orthopaedic Research and Education Foundation. Q Kang was a recipient of an International Postdoctoral Fellowship from the National Institutes of Health (F05 AT002014-01).

References

1 DeWitt N. Bone and cartilage. *Nature* 2003; 423: 315.
2 Olsen BR, Reginato AM, Wang W. Bone development. *Annu Rev Cell Dev Biol* 2000; 16: 191–220.
3 Reddi AH. Role of morphogenetic proteins in skeletal tissue engineering and regeneration. *Nat Biotechnol* 1998; 16: 247–252.
4 Urist MR. Bone: formation by autoinduction. *Science* 1965; 150: 893–899.
5 Wozney JM *et al*. Novel regulators of bone formation: molecular clones and activities. *Science* 1988; 242: 1528–1534.
6 Hogan BL. Bone morphogenetic proteins: multifunctional regulators of vertebrate development. *Genes Dev* 1996; 10: 1580–1594.
7 Zou H *et al*. BMP signaling and vertebrate limb development. *Cold Spring Harb Symp Quant Biol* 1997; 62: 269–272.
8 Massague J, Weis-Garcia F. Serine/threonine kinase receptors: mediators of transforming growth factor beta family signals. *Cancer Surv* 1996; 27: 41–64.
9 Yamashita H, Ten Dijke P, Heldin CH, Miyazono K. Bone morphogenetic protein receptors. *Bone* 1996; 19: 569–574.
10 Heldin CH, Miyazono K, ten Dijke P. TGF-beta signalling from cell membrane to nucleus through SMAD proteins. *Nature* 1997; 390: 465–471.
11 Massague J. TGF-beta signal transduction. *Annu Rev Biochem* 1998; 67: 753–791.
12 Wrana JL. Regulation of Smad activity. *Cell* 2000; 100: 189–192.
13 Heckman JD, Boyan BD, Aufdemorte TB, Abbott JT. The use of bone morphogenetic protein in the treatment of non-union in a canine model. *J Bone Joint Surg Am* 1991; 73: 750–764.
14 Gerhart TN *et al*. Healing segmental femoral defects in sheep using recombinant human bone morphogenetic protein. *Clin Orthop* 1993; 349: 317–326.
15 Lee SC *et al*. Healing of large segmental defects in rat femurs is aided by RhBMP-2 in PLGA matrix. *J Biomed Mater Res* 1994; 28: 1149–1156.
16 Bostrom MP, Camacho NP. Potential role of bone morphogenetic proteins in fracture healing. *Clin Orthop* 1998; 355 (Suppl): S274–S282.
17 Cheng SL *et al*. *In vitro* and *in vivo* induction of bone formation using a recombinant adenoviral vector carrying the human BMP-2 gene. *Calcif Tissue Int* 2001; 68: 87–94.
18 Krebsbach PH, Gu K, Franceschi RT, Rutherford RB. Gene therapy-directed osteogenesis: BMP-7-transduced human fibroblasts form bone *in vivo* (in process citation). *Hum Gene Ther* 2000; 11: 1201–1210.
19 Partridge K *et al*. Adenoviral BMP-2 gene transfer in mesenchymal stem cells: *in vitro* and *in vivo* bone formation on biodegradable polymer scaffolds. *Biochem Biophys Res Commun* 2002; 292: 144–152.
20 Riew KD *et al*. Induction of bone formation using a recombinant adenoviral vector carrying the human BMP-2 gene in a rabbit spinal fusion model. *Calcif Tissue Int* 1998; 63: 357–360.
21 Varady P *et al*. Morphologic analysis of BMP-9 gene therapy-induced osteogenesis. *Hum Gene Ther* 2001; 12: 697–710.
22 Varady P *et al*. CT and radionuclide study of BMP-2 gene therapy-induced bone formation. *Acad Radiol* 2002; 9: 632–637.
23 Helm GA *et al*. Use of bone morphogenetic protein-9 gene therapy to induce spinal arthrodesis in the rodent. *J Neurosurg* 2000; 92: 191–196.
24 Sandhu HS, Khan SN, Suh DY, Boden SD. Demineralized bone matrix, bone morphogenetic proteins, and animal models of spine fusion: an overview. *Eur Spine J* 2001; 10 (Suppl. 2): S122–S131.
25 Boden SD, Zdeblick TA, Sandhu HS, Heim SE. The use of rhBMP-2 in interbody fusion cages. Definitive evidence of osteoinduction in humans: a preliminary report. *Spine* 2000; 25: 376–381.
26 Friedlaender GE. OP-1 clinical studies. *J Bone Joint Surg Am* 2001; 83-A: S160–S161.
27 Valentin-Opran A *et al*. Clinical evaluation of recombinant human bone morphogenetic protein-2. *Clin Orthop* 2002; 395: 110–120.
28 Whang K *et al*. Ectopic bone formation via rhBMP-2 delivery from porous bioabsorbable polymer scaffolds. *J Biomed Mater Res* 1998; 42: 491–499.
29 Alden TD *et al*. Percutaneous spinal fusion using bone morphogenetic protein-2 gene therapy. *J Neurosurg* 1999; 90: 109–114.
30 Oyama M *et al*. Retrovirally transduced bone marrow stromal cells isolated from a mouse model of human osteogenesis imperfecta (oim) persist in bone and retain the ability to form cartilage and bone after extended passaging. *Gene Therapy* 1999; 6: 321–329.
31 Alden TD *et al*. *In vivo* endochondral bone formation using a bone morphogenetic protein 2 adenoviral vector. *Hum Gene Ther* 1999; 10: 2245–2253.
32 Baltzer AW *et al*. Genetic enhancement of fracture repair: healing of an experimental segmental defect by adenoviral transfer of the BMP-2 gene. *Gene Therapy* 2000; 7: 734–739.
33 Baltzer AW *et al*. Potential role of direct adenoviral gene transfer in enhancing fracture repair. *Clin Orthop* 2000; 379 (Suppl): S120–S125.
34 Bosch P *et al*. The efficiency of muscle-derived cell-mediated bone formation. *Cell Transplant* 2000; 9: 463–470.
35 Breitbart AS *et al*. Gene-enhanced tissue engineering: applications for bone healing using cultured periosteal cells transduced retrovirally with the BMP-7 gene. *Ann Plast Surg* 1999; 42: 488–495.
36 Franceschi RT, Wang D, Krebsbach PH, Rutherford RB. Gene therapy for bone formation: *in vitro* and *in vivo* osteogenic activity of an adenovirus expressing BMP7. *J Cell Biochem* 2000; 78: 476–486.
37 Gazit D *et al*. Engineered pluripotent mesenchymal cells integrate and differentiate in regenerating bone: a novel cell-mediated gene therapy. *J Gene Med* 1999; 1: 121–133.
38 Lieberman JR *et al*. Regional gene therapy with a BMP-2-producing murine stromal cell line induces heterotopic and orthotopic bone formation in rodents. *J Orthop Res* 1998; 16: 330–339.
39 Lou J, Xu F, Merkel K, Manske P. Gene therapy: adenovirus-mediated human bone morphogenetic protein-2 gene transfer induces mesenchymal progenitor cell proliferation and differentiation *in vitro* and bone formation *in vivo*. *J Orthop Res* 1999; 17: 43–50.

40 Mason JM *et al*. Expression of human bone morphogenic protein 7 in primary rabbit periosteal cells: potential utility in gene therapy for osteochondral repair. *Gene Therapy* 1998; 5: 1098–1104.
41 Musgrave DS *et al*. Adenovirus-mediated direct gene therapy with bone morphogenetic protein-2 produces bone. *Bone* 1999; 24: 541–547.
42 Okubo Y *et al*. Osteoinduction by bone morphogenetic protein-2 via adenoviral vector under transient immunosuppression. *Biochem Biophys Res Commun* 2000; 267: 382–387.
43 Ripamonti U *et al*. Bone induction by BMPs/OPs and related family members in primates. *J Bone Joint Surg Am* 2001; 83-A: S116–S127.
44 Lee JY *et al*. Effect of bone morphogenetic protein-2-expressing muscle-derived cells on healing of critical-sized bone defects in mice. *J Bone Joint Surg Am* 2001; 83-A: 1032–1039.
45 Cheng H *et al*. Osteogenic activity of the 14 types of human bone morphogenetic proteins (BMPs). *J Bone Joint Surgery Am* 2003; 85-A: 1544–1552.
46 Robbins PD, Tahara H, Ghivizzani SC. Viral vectors for gene therapy. *Trends Biotechnol* 1998; 16: 35–40.
47 Kay MA, Glorioso JC, Naldini L. Viral vectors for gene therapy: the art of turning infectious agents into vehicles of therapeutics. *Nat Med* 2001; 7: 33–40.
48 Alemany R, Balague C, Curiel DT. Replicative adenoviruses for cancer therapy. *Nat Biotechnol* 2000; 18: 723–727.
49 Breyer B *et al*. Adenoviral vector-mediated gene transfer for human gene therapy. *Curr Gene Ther* 2001; 1: 149–162.
50 Thomas CE, Ehrhardt A, Kay MA. Progress and problems with the use of viral vectors for gene therapy. *Nat Rev Genet* 2003; 4: 346–358.
51 Sun MH *et al*. Bone morphogenetic proteins and bone regeneration: from biology to clinical applications. *Adv Osteoporotic Fract Manag* 2003; 2: 70–78.
52 Bahamonde ME, Lyons KM. BMP3: to be or not to be a BMP. *J Bone Joint Surg Am* 2001; 83-A; S56–S62.
53 Lee JY *et al*. Enhancement of bone healing based on *ex vivo* gene therapy using human muscle-derived cells expressing bone morphogenetic protein 2. *Hum Gene Ther* 2002; 13: 1201–1211.
54 Lieberman JR, Daluiski A, Einhorn TA. The role of growth factors in the repair of bone. Biology and clinical applications. *J Bone Joint Surg Am* 2002; 84-A: 1032–1044.
55 Noda M, Camilliere JJ. *In vivo* stimulation of bone formation by transforming growth factor-beta. *Endocrinology* 1989; 124: 2991–2994.
56 Joyce ME, Terek RM, Jingushi S, Bolander ME. Role of transforming growth factor-beta in fracture repair. *Ann N Y Acad Sci* 1990; 593: 107–123.
57 Lind M *et al*. Transforming growth factor-beta enhances fracture healing in rabbit tibiae. *Acta Orthop Scand* 1993; 64: 553–556.
58 Nielsen HM, Andreassen TT, Ledet T, Oxlund H. Local injection of TGF-beta increases the strength of tibial fractures in the rat. *Acta Orthop Scand* 1994; 65: 37–41.
59 Critchlow MA, Bland YS, Ashhurst DE. The effect of exogenous transforming growth factor-beta 2 on healing fractures in the rabbit. *Bone* 1995; 16: 521–527.
60 Sumner DR *et al*. Enhancement of bone ingrowth by transforming growth factor-beta. *J Bone Joint Surg Am* 1995; 77: 1135–1147.
61 Canalis E, Centrella M, McCarthy T. Effects of basic fibroblast growth factor on bone formation *in vitro*. *J Clin Invest* 1988; 81: 1572–1577.
62 Kato T *et al*. Single local injection of recombinant fibroblast growth factor-2 stimulates healing of segmental bone defects in rabbits. *J Orthop Res* 1998; 16: 654–659.
63 Nakamura T *et al*. Recombinant human basic fibroblast growth factor accelerates fracture healing by enhancing callus remodeling in experimental dog tibial fracture. *J Bone Miner Res* 1998; 13: 942–949.
64 Radomsky ML, Thompson AY, Spiro RC, Poser JW. Potential role of fibroblast growth factor in enhancement of fracture healing. *Clin Orthop* 1998; 355 (Suppl): S283–S293.
65 Radomsky ML *et al*. Novel formulation of fibroblast growth factor-2 in a hyaluronan gel accelerates fracture healing in nonhuman primates. *J Orthop Res* 1999; 17: 607–614.
66 Nash TJ *et al*. Effect of platelet-derived growth factor on tibial osteotomies in rabbits. *Bone* 1994; 15: 203–208.
67 Thaller SR, Dart A, Tesluk H. The effects of insulin-like growth factor-1 on critical-size calvarial defects in Sprague–Dawley rats. *Ann Plast Surg* 1993; 31: 429–433.
68 Trippel SB. Potential role of insulinlike growth factors in fracture healing. *Clin Orthop* 1998; 355 (Suppl): S301–S313.
69 Boden SD *et al*. Lumbar spine fusion by local gene therapy with a cDNA encoding a novel osteoinductive protein (LMP-1). *Spine* 1998; 23: 2486–2492.
70 Linkhart TA, Mohan S, Baylink DJ. Growth factors for bone growth and repair: IGF, TGF beta and BMP. *Bone* 1996; 19: 1S–12S.
71 Azari K *et al*. Therapeutic potential of bone morphogenetic proteins. *Expert Opin Investig Drugs* 2001; 10: 1677–1686.
72 Alden TD *et al*. Bone morphogenetic protein gene therapy. *Spine* 2002; 27: S87–S93.
73 Yoon ST, Boden SD. Osteoinductive molecules in orthopaedics: basic science and preclinical studies. *Clin Orthop* 2002; 395: 33–43.
74 Solloway MJ *et al*. Mice lacking Bmp6 function. *Dev Genet* 1998; 22: 321–339.
75 Jane J *et al*. Ectopic osteogenesis using adenoviral bone morphogenetic protein (BMP)-4 and BMP-6 gene transfer. *Mol Ther* 2002; 6: 464.
76 Song JJ *et al*. Bone morphogenetic protein-9 binds to liver cells and stimulates proliferation. *Endocrinology* 1995; 136: 4293–4297.
77 Ploemacher RE *et al*. Bone morphogenetic protein 9 is a potent synergistic factor for murine hemopoietic progenitor cell generation and colony formation in serum-free cultures. *Leukemia* 1999; 13: 428–437.
78 Lopez-Coviella I *et al*. Induction and maintenance of the neuronal cholinergic phenotype in the central nervous system by BMP-9. *Science* 2000; 289: 313–316.
79 Dumont RJ *et al*. *Ex vivo* bone morphogenetic protein-9 gene therapy using human mesenchymal stem cells induces spinal fusion in rodents. *Neurosurgery* 2002; 51: 1239–1245.
80 Peng Y *et al*. Transcriptional characterization of bone morphogenetic proteins (BMPs)-mediated osteogenic signaling. *J Cell Biochem* 2003; 90: 1149–1165.
81 He TC *et al*. A simplified system for generating recombinant adenoviruses. *Proc Natl Acad Sci USA* 1998; 95: 2509–2514.

Exhibit H

February 1, 1999

Journal of Cellular Biochemistry

Apoptosis/IGF Receptor Signaling

Visit Wiley Journals Online
www.interscience.wiley.com

WILEY-LISS

Journal of Cellular Biochemistry

Volume 72 • Number 2 • February 1, 1999

ARTICLES

Identification of DERMO-1 as a Member of Helix-Loop-Helix Type Transcription Factors Expressed in Osteoblastic Cells
Masato Tamura and Masaki Noda 167

Effects of GDF7/BMP12 on Proliferation and Alkaline Phosphatase Expression in Rat Osteoblastic Osteosarcoma ROS 17/2.8 Cells
Koichi Furuya, Akina Nifuji, Vicki Rosen, and Masaki Noda 177

Coexpression of the Lysyl Oxidase-Like Gene (LOXL) and the Gene Encoding Type III Procollagen in Induced Liver Fibrosis
Youngho Kim, Simone Peyrol, Chi-Kwong So, Charles D. Boyd, and Katalin Csiszar 181

Integrin α3β1 Expressed by Human Colon Cancer Cells Is a Major Carrier of Oncodevelopmental Carbohydrate Epitopes
Nicole L. Prokopishyn, Wilma Puzon-McLaughlin, Yoshikazu Takada, and Suzanne Laferté 189

Cell Adhesion and Proliferation Mediated Through the G1 Domain of Versican
Bing L. Yang, Yaou Zhang, Liu Cao, and Burton B. Yang 210

Somatostatin-Dependent Adenylyl Cyclase Activity in Nonactivated and Mitogen-Activated Human T Cells: Evidence for Uncoupling of sst3 Receptor From Adenylyl Cyclase
Nathalie Giannetti, Branka Horvat, Nicole Gautier, Christelle El Ghamrawy, Chantal Rabourdin-Combe, Alain Enjalbert, and Slavica Krantic 221

Gamma Interferon Induces Expression of Mad1 Gene in Macrophage, Which Inhibits Colony-Stimulating Factor-1–Dependent Mitogenesis
Arunangsu Dey, Leopold Kim, and Wei Li 232

Modulation of Nuclear Matrix Protein Phosphorylation by Histones: Possible Involvement of NM-Associated Protein Kinase CK2 Activity
Sherif Tawfic, Alan T. Davis, Russell A. Faust, Markus Gapany, and Khalil Ahmed 242

Osteoprotegerin and Osteoprotegerin Ligand Effects on Osteoclast Formation From Human Peripheral Blood Mononuclear Cell Precursors
Victoria Shalhoub, Judy Faust, William J. Boyle, Colin R. Dunstan, Mike Kelley, Steve Kaufman, Sheila Scully, Gwyneth Van, and David L. Lacey 251

Extracellular Sphingomyelinase Induces Interleukin-6 Synthesis in Osteoblasts
Haruhiko Tokuda, Osamu Kozawa, Atsushi Harada, and Toshihiko Uematsu 262

(continued on next page)

Cover shows colon cancer stained with an antibody to the IGF-I receptor. The positive cells are stained brown. The IGF-I receptor is expressed in many human tumors, often over-expressed, and its down-regulation results in apoptosis of tumor cells. See article by Romano et al. in this issue, pp. 294.

WILEY-LISS

A JOHN WILEY & SONS, INC., PUBLICATION
New York • Chichester • Brisbane • Toronto • Singapore

WILEY InterScience
www.interscience.wiley.com

(continued from previous page)

Unspecific Activation of Caspases During the Induction of Apoptosis by Didemnin B in Human Cell Lines
Karina L. Johnson, David R. Grubb, and Alfons Lawen 269

Characterization of the Human 36-kDa Carboxyl Terminal LIM Domain Protein (hCLIM1)
Masayo Kotaka, Sai-Ming Ngai, Merce Garcia-Barcelo, Stephen K.W. Tsui, Kwok-Pui Fung, Cheuk-Yu Lee, and Mary M.Y. Waye 279

Effects of Prolactin on Aldosterone Secretion in Rat Zona Glomerulosa Cells
Mei-Mei Kau, Ming-Jae Lo, Shiow-Chwen Tsai, Jiann-Jong Chen, Hsiao-Fung Pu, Eileen Jea Chien, Ling-Ling Chang, and Paulus S. Wang 286

Dissociation Between Resistance to Apoptosis and the Transformed Phenotype in IGF-I Receptor Signaling
Gaetano Romano, Marco Prisco, Tommaso Zanocco-Marani, Francesca Peruzzi, Barbara Valentinis, and Renato Baserga 294

Volume 72, Number 2, was mailed the week of December 21, 1998.

Journal of Cellular Biochemistry 72:177–180 (1999)

Effects of GDF7/BMP12 on Proliferation and Alkaline Phosphatase Expression in Rat Osteoblastic Osteosarcoma ROS 17/2.8 Cells

Koichi Furuya,[1] Akina Nifuji,[1] Vicki Rosen,[2] and Masaki Noda[1]*

[1]Department of Molecular Pharmacology, Medical Research Institute, Tokyo Medical and Dental University, Tokyo 101, Japan
[2]Genetics Institute, Cambridge, Massachusetts 02140

Abstract Growth and differentiation factor 7(GDF7), also later called as bone morphogenetic protein (BMP)12, is a new member of the BMP superfamily, which induces formation of tendon-like tissue formation in the ectopic implantation experiments. We examined the effect of BMP12 on proliferation and expression of phenotype-related genes in rat osteoblastic osteosarcoma ROS17/2.8 cells. BMP12 treatment enhanced proliferation of ROS17/2.8 cells within 3 days and this effect was observed at least up to day 6 of the treatment. The cell number was increased by about 50% on day 3 and about two-fold by day 6. These effects were observed at the dose range between 40 and 1,000 ng/ml. Treatment with BMP12 also enhanced alkaline phosphatase activity by about 50% in ROS17/2.8 cells within 24 h of the treatment. The effect peaked at 48 h and was still observed at 72 h. The enhancing effect of BMP12 on alkaline phosphatase was observed similarly at the doses ranging from 40 to 1,000 ng/ml. These data indicate that BMP12 has positive effects on proliferation and phenotypic expression of ROS 17/2.8 cells. J. Cell. Biochem. 72:177–180, 1999.

Key words: GDF7; osteoblast; growth factor; proliferation; differentiation

Bone morphogenetic proteins (BMPs) are the members of TGFβ superfamily and are playing crucial roles not only in osteogenesis but also in formation or induction of various tissues and organs during development. BMPs form a distinct group consisting of four subfamilies which are classified according to the homology in their mature regions [Hogan, 1996]. One of these subfamilies consists of growth/differentiation factor (GDF) 5 (cartilage derived bone morphogenetic protein [CDMP]-1) [Storm et al., 1994; Chang et al., 1994], GDF7 (BMP12) [Storm et al., 1994; Celeste et al., 1995], and BMP13 (GDF6) [Storm et al., 1994; Dube and Celeste, 1995]. These three GDFs were identified recently by degenerative PCR and their mature regions are close to one another except the glycine-rich insert in GDF7 [Storm et al., 1994].

Mutations in Gdf5 gene cause brachypodism (bp) in mice [Storm et al., 1994]. Bp mice are featured by their short limbs with joint anomalies, while the mice do not show major changes in axial skeletal structures [King et al., 1996]. Furthermore, cartilage- and bone-inducing activity of GDF5/CDMP-1 was demonstrated [Chang et al., 1994; Hötten et al., 1996]. Together with these observations, the expression pattern of their transcripts during development suggests that GDF5 regulates formation of bones and joints in limbs [Storm et al., 1994; Chang et al., 1994; Hötten et al., 1996; Storm and Kingsley, 1996]. More recently, BMP12 was identified to be the human homologue of murine GDF7, which was found prior to BMP12, based on the comparison of their predicted amino acid sequences [Celeste et al., 1995].

Ectopic implantation studies of BMP12 demonstrated that it induced formation of tendon/ligament-like tissues in subcutaneous tissues

Contract grant sponsor: Ministry of Education; Contract grant numbers: 09307034, 10877223, 10044246; Contract grant sponsor: "Research for Future" Program of Japan Society for Promotion of Sciences; Contract grant number: 96I 00205.

*Correspondence to: Masaki Noda, Professor, Department of Molecular Pharmacology, Medical Research Institute, Tokyo Medical and Dental University, 3–10, Kanda Surugadai, 2-chome, Chiyoda-ku, Tokyo,101, Japan. E-mail: noda.mph@mri.tmd.ac.jp

Received 17 February 1998; Accepted 6 July 1998

[Wolfman et al., 1995] or in muscle [Cox and Rosen, 1996]. Ultrastructural analysis and Northern analysis of the ectopically induced tendon/ligament-like tissues indicated that the tissue revealed several features characteristic to tendon and ligament tissues [Wolfman et al., 1995; Cox and Rosen, 1996]. Furthermore, it was reported that BMP12/GDF7 was expressed at the site of developing joints in mouse embryos [Wolfman et al., 1995]. Because tendons and ligaments attach to bones, formation of tendon and ligament is coordinated with that of bone. It was also indicated that BMP12 inhibited muscle differentiation and did not direct myoblast to become osteoblastic cells in vitro [Inada et al., 1996]. However, BMP12 effects on osteoblastic cells per se was not studied in detail. We report here that BMP12 stimulates both proliferation and expression of alkaline phosphatase in osteoblastic osteosarcoma ROS17/2.8 cells.

MATERIALS AND METHODS

Cell Culture

ROS17/2.8 or ROS25/1 cells were grown in modified Ham's F-12 nutrient mixture [Majeska et al., 1980] (Gibco BRL, Grand Island, NY) supplemented with 5% fetal bovine serum (FBS) on 10 cm diameter dish (Coster Corp. Cambridge, MA). For experiments, confluent cells were fed with fresh media 1 day before harvesting with 0.125% trypsin. The cells were plated into 2 cm^2 well (Nunc A/S Roskilde, Denmark) at 20,000 cells/cm^2 and cultured overnight. On the next day, the cells were rinsed twice with serum-free F-12 and were cultured in the presence or absence of BMP12 in serum-free medium. The day when BMP12 treatments started was defined as the day 0.

Cell Count

At several time points, the cells were harvested with 0.125% trypsin and were resuspended in 9 ml Isoton III(Coulter Electronics Ltd. Beds, England) in counting vials, and counted by Coulter Counter Model ZM (Coulter Electronics Ltd. Beds, England).

Alkaline Phosphatase Assay

The cells were lysed and scraped into 0.25 ml of a buffer containing 10 mM Tris HCl pH 7.5, 0.5 mM $MgCl_2$, 0.1% Triton X-100. These cell lysates were homogenized by freeze-and-thaw followed by sonication. The AP activity in the samples were assayed using Na^2 p-nitrophenyl phosphate(PNPP) as substrate. Protein contents in each sample were determined according to Coomassie blue G method [Noda et al., 1990].

Statistical Analysis

Statistical evaluation was conducted by employing Student's *t*-test.

RESULT

To investigate whether BMP12 affects proliferation of the cells in osteoblastic lineage, we first examined its effect on ROS 17/2.8 cells. Treatment with 400 ng/ml BMP12 increased the number of ROS17/2.8 cells within 3 days under serum-free condition while no increase was observed in the control group. The increase by the BMP12 treatment was observed up to day 6 in culture (Fig. 1). We then examined several doses of BMP12 with regard to the effect on cell growth. ROS17/2.8 cell were treated with BMP12 at 40, 400, and 1,000 ng/ml. After the treatment for 4 days, cell numbers in the groups treated with BMP12 at the above-mentioned dose range increased by 60–90% compared with that of control group (Fig. 2). These results indicate that BMP12 stimulates proliferation of osteoblastic ROS17/2.8 cells.

We next examined the effect of BMP12 on the expression of osteoblastic phenotype in ROS17/2.8 cells. We examined alkaline phosphatase (AP) activity as a phenotypic marker which is

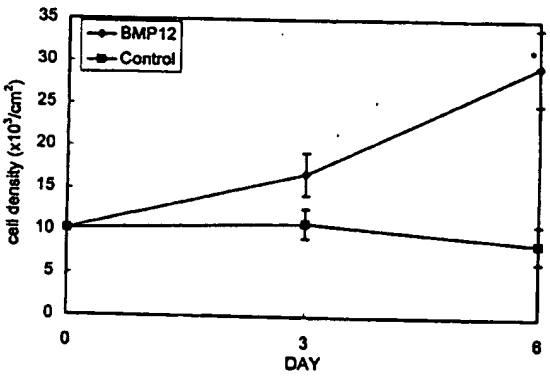

Fig. 1. Time-course of the BMP12 effect on cell growth of ROS 17/2.8 cells. The cells were treated with 400 ng/ml BMP12 (circle) or vehicle (square) as a control. After treatment for 3 and 6 days, these cells were harvested and counted. The media were replaced on day 3. The data represent mean ± S.E.M. of the cells in four wells obtained from one of two independent experiments with similar results. Asterisks indicate statistically significant difference against control. $^*P < 0.05$.

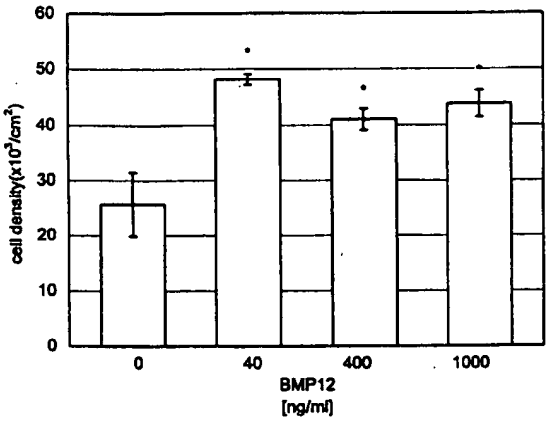

Fig. 2. BMP12 effects on the growth of ROS 17/2.8 cells. The cells were treated with 0, 40, 400, or 1,000 ng/ml BMP12 for 4 days. The cells were harvested and counted. The media were changed on day 3. The data represent mean ± S.E.M. of four samples for each treatment. Asterisks indicate statistically significant difference against control. $^*P < 0.05$.

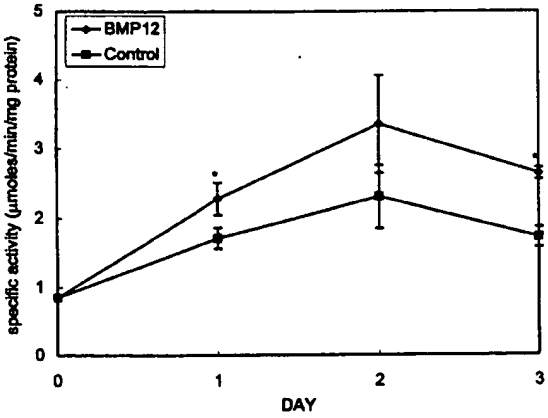

Fig. 3. Time-course of BMP12 effect on alkaline phosphatase activity in ROS 17/2.8 cells. The cells were treated with 400 ng/ml BMP12 (circle) or vehicle (square). After treatment for 1, 2, and 3 days, the cells were harvested and were assayed as described in Materials and Methods section. The data represent mean ± S.E.M. of eight (day 0), four (days 2 and 3) samples. Asterisks indicate statistically significant difference against control. $^*P < 0.05$.

expressed during differentiation of osteoblastic cells although it is not absolutely specific to the cells in osteoblastic lineage. We treated ROS17/2.8 cells with 400 ng/ml of BMP12 for 1, 2, and 3 days. For each time point, the AP specific activity of the groups treated with BMP12 was higher than that of the control group (Fig. 3). AP activity was similarly enhanced by BMP12 treatment within a range of doses at 40 and 400 ng/ml in these cells (Fig. 4). The BMP12 effect

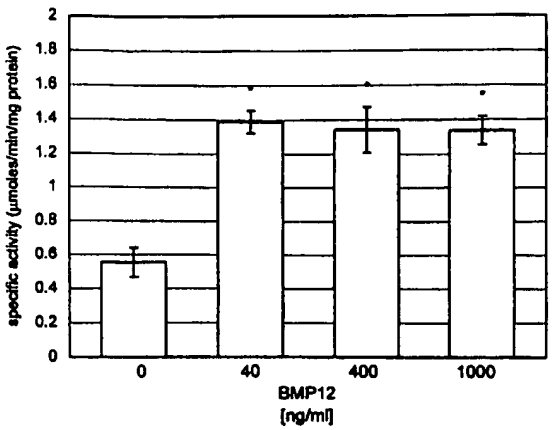

Fig. 4. BMP12 effect on alkaline phosphatase activity in ROS 17/2.8 cells. The cells were treated with 0, 4, 40, 400, and 1,000 ng/ml BMP12 for 3 days. The cells were harvested and assayed as described in Materials and Methods. The data represent mean ± S.E.M. of four samples for each treatment. Asterisks indicate statistically significant difference against the control. $^*P < 0.05$.

on ROS17/2.8 cells was specific since BMP12 did not increase alkaline phosphatase activity and only slightly increased cell number in the less mature type cells, ROS25/1 [data not shown].

DISCUSSION

In this study, we report that BMP12 enhances proliferation and expression of alkaline phosphatase (AP) in ROS 17/2.8 cells. It was reported that BMP12 induced formation of tendon/ligament-like tissues when implanted ectopically [Wolfman et al., 1995; Cox and Rosen, 1996] and that BMP12 transcripts are expressed in joints of mouse embryos [Wolfman et al., 1995]. Our observation on BMP12 regulation of osteoblasts may suggest its possible roles in the sites common for both osteoblasts or tendon cells such as those in the insertions of the tendon-ligaments to bones. Alternatively, during the differentiation pathways starting from mesenchymal cells to osteoblasts and tendon/ligament cells, BMP12 sensitive fractions of the cells may represent a certain group of pluri-potential progenitors. In this regard, some fraction in the ROS-17/2.8 cells could be those which are relatively immature and could be corresponding to such pluri-potential cells, since we observed previously that these cells are heterogeneous with regard to the levels of alkaline phosphatase even though they are clonal cells [Noda M, unpublished data]. The relatively low levels of the BMP12 effects could be also due to

the relatively small size of the fraction of responding cells. To investigate the effect on phenotypic expression, we measured AP activity of these cells. Although it was reported that BMP12 did not increase AP activity in these cells in the presence of 5% serum [Inada et al., 1996], AP activity in BMP12 treated cells was enhanced compared to that in the control cells in serum-free condition in our experiments. This difference in the responses of the cells is possibly due to the treatment condition and may imply that the effect of BMP12 might be masked by the presence of serum which contains a number of factors. We compared the cell number as well as AP activities in ROS17/2.8 cells treated with three different doses of BMP12. BMP12 enhanced cell growth and AP activity similarly irrespective of the doses tested suggesting that the saturation dose for enhancement is also less than 40 ng/ml.

It is still not known which receptors expressed on ROS 17/2.8 cells could mediate the signal of BMP12. Recently, it was reported that GDF5, which is highly related to BMP12, preferentially bound to BMP receptor type I B(BMPRIB) [Nishitoh et al., 1996]. Since not many types of BMP receptors have been reported [Yamashita et al., 1996], it is likely that BMP12 may share one or several of the already identified BMP receptors, however we cannot exclude the possibility of the presence of unknown specific receptors which could mediate BMP12 signal. Presence or absence of serum may change the activity of BMP receptors via certain kinases, though this point also needs further investigation.

In conclusion, we showed that a new BMP family member, BMP12, which induces tendon/ligament like tissue enhanced proliferation and AP expression in ROS 17/2.8. The stimulatory effects of this protein on both growth of and phenotypic expression in ROS17/2.8 cells suggest that BMP12 could be involved in the regulation of the functions as one of the positive regulatory factors for osteoblasts.

ACKNOWLEDGMENTS

This research was partially supported by grants in aid from the Core Research for Evolutional Science and Technology of Japan Science and Technology Corporation (JST). This work was also in part supported by a program of Cell Fate Modulation Research Unit, Medical Research Institute, Tokyo Medical and Dental University.

REFERENCES

Celeste AJ, Ross JL, Yamaji N, Wozney JM. 1995. The molecular cloning of human bone morphogenetic proteins-10, -11 and -12, three new members of the transforming growth factor-β superfamily. J Bone Miner Res 10:S336.

Chang CS, Hoang B, Thomas JT, Vukicevie S, Luyten FP, Ryba NJP, Kozak CA, Reddi AH, Moos M. 1994. Cartilage-derived morphogenetic proteins. J Biol Chem 269:28227–28234.

Cox K, Rosen V. 1996. Ultrastructural analysis of cells and extracellular matrix at the site of recombinant human BMP-12 induced tendon/ligament-like tissue in the rat quadriceps muscle. J Bone Miner Res 11:S401.

Dube JL, Celeste AJ. 1995. Human bone morphogenetic protein-13, a molecule which is highly related to human bone morphogenetic protein-12. J Bone Miner Res 10:S336.

Hogan BLM. 1996. Bone morphogenetic proteins: Multifunctional regulators of vertebrate development. Genes Dev 10:1580–1594.

Hötten GC, Matsumoto T, Kimura M, Bechtold RF, Kron R, Ohara T, Tanaka H, Satoh Y, Okazaki M, Shirai T, Pan H, Kawai S, Pohl JS, Kudo A. 1996. Recombinant human growth/differentiation factor 5 stimulates mesenchyme aggregation and chondrogenesis responsible for the skeletal development of limbs. Growth Factor 13:65–74.

Inada M, Katagiri T, Akiyama S, Namiki M, Komaki M, Yamaguchi A, Kamoi K, Rosen V, Suda T. 1996. Bone morphogenetic protein-12 and -13 inhibit terminal differentiation of myoblasts, but do not induce their differentiation into osteoblasts. Biochem Biophys Res Commun 222:317–322.

King JA, Storm EE, Marker PC, Dileone RJ, Kingsley DM. 1996. The role of BMPs and GDFs in development of region-specific skeletal structures. Ann NY Acad Sci USA 785:70–79.

Majeska RJ, Rodan SB, Rodan GA. 1980. Parathyroid hormone-responsive clonal cell lines from rat osteosarcoma. Endocrinology 107:1494–1503.

Nishitoh H, Ichijo H, Kimura M, Matsumoto T, Maskishima F, Ymaguchi A, Yamashita H, Enomoto S, Miyazono K. 1996. Identification of type I and type II serine/threonine kinase receptors for growth/differentiation factor-5. J Biol Chem 271:21345–21352.

Noda M, Vogel RL, Hasson DM, Rodan GA. 1990. Leukemia inhibitory factor suppresses proliferation, alkaline phosphatase activity, and type I collagen messenger ribonucleic acid level and enhances osteopontin mRNA level in murine ostioblast-like (MC3T3E1) cells. Endocrinology 127:185–190.

Storm EE, Huynh TV, Copeland NG, Jenkins NA, Kingsley DM, Lee S-J. 1994. Limb alterations in brachypodism mice due to mutations in a new member of the TGFβ-superfamily. Nature 368:639–642.

Storm EE, Kingsley DM. 1996. Joint patterning defects caused by single and double mutations in members of the bone morpho-genetic protein (BMP) family. Development 122:3969–3979.

Wolfman NM, Celeste AJ, Cox K, Hattersley G, Nelson R, Yamaji N, DiBlasino-Smith E, Nove J, Song JJ, Wozney JM, Rosen V. 1995. Preliminary characterization of the biological activities of rhBMP-12. J Bone Miner Res 10:S148.

Yamashita H, ten Dijke P, Heldin C-H, Miyazono K. 1996. Bone morphogenetic protein receptors. Bone 19:569–574.

Exhibit I

Journal of Clinical Periodontology

Official Journal of The European Federation of Periodontology

Founded by the British, Dutch, French, German, Scandinavian, and Swiss Societies of Periodontology

Journal of Clinical Periodontology · Vol. 31 No. 8 August 2004

Contents

Locally delivered doxycycline improves the healing following non-surgical periodontal therapy in smokers	589	*C. Tomasi & J. L. Wennström*
A model of periodontitis in the rat: effect of lipopolysaccharide on bone resorption, osteoclast activity, and local peptidergic innervation	596	*A. L. Dumitrescu, S. A. El-Aleem, B. Morales-Aza & L. F. Donaldson*
Healing of intrabony defects following surgical treatment with or without an Er:YAG laser A pilot study	604	*A. Sculean, F. Schwarz, M. Berakdar, P. Windisch, N. B. Arweiler & G. E. Romanos*
The effect of a chlorhexidine regimen on de novo plaque formation	609	*S. Sekino, P. Ramberg, N. G. Uzel, S. Socransky & J. Lindhe*
The short-term effectiveness of non-surgical treatment in reducing protease activity in gingival crevicular fluid from chronic periodontitis patients	615	*C. M. S. Figueredo, A. Areas, L. A. Miranda, R. G. Fischer & A. Gustafsson*
High and low brushing force in relation to efficacy and gingival abrasion	620	*G. A. Van der Weijden, M. F. Timmerman, P. A. Versteeg, M. Piscaer & U. Van der Velden*
The association of periodontal disease parameters with systemic medical conditions and tobacco use	625	*J. Molloy, L. F. Wolff, A. Lopez-Guzman & J. S. Hodges*
Association of periodontal disease to anxiety and depression symptoms, and psychosocial stress factors	633	*A. C. O. Solis, R. F. M. Lotufo, C. M. Pannuti, E. C. Brunheiro, A. H. Marques & F. Lotufo-Neto*
The electric toothbrush: analysis of filaments under stereomicroscope	639	*L. Checchi, E. Farina, P. Felice & M. Montevecchi*
Baseline radiographic defect angle of the intrabony defect as a prognostic indicator in regenerative periodontal surgery with enamel matrix derivative	643	*E. Tsitoura, R. Tucker, J. Suvan, L. Laurell, P. Cortellini & M. Tonetti*
Therapy with adjunctive doxycycline local delivery in patients with type 1 diabetes mellitus and periodontitis	648	*A. F. Martorelli de Lima, C. C. Cury, D. B. Palioto, A. M. Duro, R. C. da Silva & L. F. Wolff*
Effect of recombinant human bone morphogenetic protein-12 (rhBMP-12) on regeneration of periodontal attachment following tooth replantation in dogs A pilot study	654	*R. G. Sorensen, G. Polimeni, A. Kinoshita, J. M. Wozney & U. M. E. Wikesjö*
Periodontal repair in dogs: effect of recombinant human bone morphogenetic protein-12 (rhBMP-12) on regeneration of alveolar bone and periodontal attachment A pilot study	662	*U. M. E. Wikesjö, R. G. Sorensen, A. Kinoshita, X. J. Li & J. M. Wozney*
Matrix metalloproteinases, their physiological inhibitors and osteoclast factors are differentially regulated by the cytokine profile in human periodontal disease	671	*G. P. Garlet, W. Martins Jr, B. A. L. Fonseca, B. R. Ferreira & J. S. Silva*
A longitudinal study of the relationship between periodontal disease and bone mineral density in community-dwelling older adults	680	*A. Yoshihara, Y. Seida, N. Hanada & H. Miyazaki*
Genetic variations in the matrix metalloproteinase-1 promoter and risk of susceptibility and/or severity of chronic periodontitis in the Czech population	685	*L. I. Holla, M. Jurajda, A. Fassmann, N. Dvorakova, V. Znojil & J. Vacha*
The anti-plaque efficacy of a chlorhexidine mouthrinse used in combination with toothbrushing with dentifrice	691	*D. A. C. Van Strydonck, Ph. Demoor, M. F. Timmerman, U. van der Velden & G. A. van der Weijden*
British Society of Periodontology	696	

This journal is abstracted or indexed in: Chemical Abstracts, Science Citation Index/SCISEARCH, Research Alert, Medical Documentation Service, Current Contents: Life Sciences; Clinical Medicine, Excerpta Medica/EMBASE.

Printed in Denmark by P. J. Schmidt A/S, Vojens

0303-6979(200408)31:08;1-J

J Clin Periodontol 2004; 31: 662–670 doi: 10.1111/j.1600-051X.2004.00541.x
Printed in Denmark. All rights reserved

Journal of Clinical Periodontology

Periodontal repair in dogs: effect of recombinant human bone morphogenetic protein-12 (rhBMP-12) on regeneration of alveolar bone and periodontal attachment

A pilot study

Ulf M. E. Wikesjö[1], Rachel G. Sorensen[2], Atsuhiro Kinoshita[3], X. Jian Li[4] and John M. Wozney[4]

[1]Laboratory for Applied Periodontal and Craniofacial Regeneration, Department of Periodontology, Temple University School of Dentistry, Philadelphia, PA, USA; [2]Clinical Research & Development, Wyeth Research, Cambridge, MA, USA; [3]Section of Preventative Oral Health Care Science, Department of Oral Health Care Promotion, School of Oral Health Care Science, Faculty of Dentistry, Tokyo Medical and Dental University, Japan; [4]Musculoskeletal Sciences, Wyeth Research, Cambridge, MA, USA

Wikesjö UME, Sorensen RG, Kinoshita A, Li XJ, Wozney JM: Periodontal repair in dogs: effect of recombinant human bone morphogenetic protein-12 (rhBMP-12) on regeneration of alveolar bone and periodontal attachment. A pilot study. J Clin Periodontol 2004; 31: 662–670. doi: 10.1111/j.1600-051X.2004.00541.x.

Abstract

Objectives: Recombinant human bone morphogenetic protein-2 (rhBMP-2) has been shown to stimulate alveolar bone and cementum formation in periodontal defects but not a functionally oriented periodontal ligament (PDL). Subcutaneous and intramuscular implants of BMP-12 have been shown to induce tendon formation and ligament-like tissue. The objective of this study was to evaluate rhBMP-12 for periodontal regeneration, in particular PDL formation.

Methods: Six young adult Hound Labrador mongrel dogs were used. Routine supraalveolar periodontal defects were created around the mandibular premolar teeth. Three animals received rhBMP-12(0.04 mg/ml) in an absorbable collagen sponge (ACS) carrier vs. rhBMP-12(0.2 mg/mL)/ACS in contralateral defects. Three animals received rhBMP-12(1.0 mg/ml)/ACS vs. rhBMP-2(0.2 mg/ml)/ACS (total implant volume/defect ~1 ml). The animals were euthanized 8 weeks postsurgery and block biopsies were processed for histometric analysis.

Results: Bone regeneration appeared increased in sites receiving rhBMP-2/ACS compared to sites receiving rhBMP-12/ACS. Cementum regeneration was similar comparing sites implanted with rhBMP-2/ACS to sites implanted with rhBMP-12/ACS. In contrast, sites receiving rhBMP-12/ACS exhibited a functionally oriented PDL bridging the gap between newly formed bone and cementum whereas this was a rare observation in sites receiving rhBMP-2/ACS. Ankylosis appeared increased in sites receiving rhBMP-2/ACS compared to those receiving rhBMP-12/ACS.

Conclusions: The outcomes of this study suggest that rhBMP-12 may have significant effects on regeneration of the PDL. Additional preclinical evaluation is needed to confirm these initial observations prior to clinical application.

Key words: cementum; dogs; periodontal ligament; periodontal regeneration; tissue engineering

Accepted for publication 29 October 2003

Recombinant human bone morphogenetic protein-2 (rhBMP-2) has been shown to stimulate clinically significant regeneration of alveolar bone and cementum in experimental periodontal defects (Ishikawa et al. 1994, Sigurdsson et al. 1995a, b, 1996, Kinoshita et al. 1997, Wikesjö et al. 1999, 2003a–c, Choi et al. 2002, Selvig et al. 2002). Induced bone appears to integrate with the resident bone. Radiographic and histologic evaluations suggest that the newly formed bone exhibits characteristics of the contiguous resident bone. However, rhBMP-2 treatment does not appear to induce a functionally oriented periodontal ligament (PDL) and frequently results in ankylosis (Sigurdsson et al. 1995a, b, 1996, King et al. 1997, 1998a, b, King & Hughes 1999, 2001, Wikesjö et al. 1999, 2003a–c, Talwar et al. 2001, Selvig et al. 2002). Wikesjö et al. (1999) reported ankylosis in animals receiving rhBMP-2 in an absorbable collagen sponge (ACS) carrier without correlation to rhBMP-2 dose. The ankylotic union between the teeth and the newly formed bone was commonly observed in the coronal aspect of the supraalveolar defects evaluated. Cellular cementum, extending from the apical extension of the defect, often merged with the ankylotic bone. Similar observations have been made for rhBMP-2 in other candidate carriers (Sigurdsson et al. 1995a, b, 1996, Wikesjö et al. 2003a) and for osteogenic protein-1 (OP-1/BMP-7) (Ripamonti et al. 1996, Giannobile et al. 1998). In the absence of extensive bone regeneration, commonly in more limited periodontal defects, ankylosis has not been a dominant observation (Ishikawa et al. 1994, Kinoshita et al. 1997, Blumenthal et al. 2002, Choi et al. 2002). In these cases, cementum regeneration with a fibrous attachment may be observed.

BMP-12, a member of the transforming growth factor-β/BMP gene family (Chang et al. 1994, Wolfman et al. 1997), is currently being evaluated for tendon and ligament repair. BMP-12 is the human homologue of mouse growth/differentiation factor-7 (GDF-7) (Hattersley et al. 1998). GDF-5, -6, or -7 have been found to induce connective tissue formation rich in type I collagen fibers resembling neonatal tendon and ligament when implanted in vivo. Analysis of the expression pattern of GDF-5, -6, or -7 suggests that they act as signaling molecules during embryonic tendon, ligament, and joint formation (Wolfman et al. 1997). In the tissue induced by this BMP subgroup, proteins specific to bone (osteocalcin, alkaline phosphatase) are absent but those specific to tendon and ligament are present (Inada et al. 1996, Wolfman et al. 1997, Hattersley et al. 1998). It is believed that the intracellular signaling pathway of BMP-12 is different from that of BMP-2. However, Furuya et al. (1999) reported increased alkaline phosphatase activity in rat osteoblastic osteosarcoma ROS 17/2.8 cells in the presence of BMP-12. Valcourt et al. (1999) reported differences in the expression of BMP-2 or -4 and BMP-12 or -13 in the MC615 chondrocyte cell line. The level of type II collagen mRNA was increased in the presence of BMP-2 or -4 but no effect was seen in the presence of BMP-12 or -13. Expression of the matrix Gla protein gene, a cartilage marker, was decreased in the presence of BMP-2 or -4 but stable in the presence of BMP-12 or -13. Bone Gla protein, a bone phenotype marker, was induced in the BMP-2 or -4 treated cells but not detected in the BMP-12 or -13 treated cells. MC615 chondrocytes also express chondrocytic and osteoblastic markers in the presence of BMP-2 or -4 but not to BMP-12 or -13. This is consistent with previous in vivo studies showing the osteoinductive properties of BMP-2 and -4 (Wozney 1998) and neotendon/ligament induction without bone formation with BMP-12 and -13 (Wolfman et al. 1997).

Subcutaneous and intramuscular implants of BMP-12 (1–100 μg) have been found to induce formation of tendon and ligament tissue in the adult rat (Wolfman et al. 1995, 1997). BMP-12 and rhBMP-2 have been evaluated in the rat tendon-bone attachment model. BMP-12-treated sites induced a new attachment with a distinct fibrocartilaginous zone at the bone–tendon interface. The untreated tendons showed poor healing response and failure to reform a morphologically normal attachment site. In that study, rhBMP-2 led to tendon ossification and narrow fibrocartilaginous interface with a lower failure load (Hattersley et al. 1998). Formation of neotendon/ligament and bone resulted when BMP-12 and rhBMP-2 were implanted together. High doses of BMP-12 and -13 (>100 μg) induced ectopic bone formation in vivo and direct injection into adult rat tendons/ligaments resulted in new connective tissue and endochondreal ossification.

The objective of this study was to evaluate the effect of rhBMP-12 on regeneration of alveolar bone and cementum, and in particular PDL formation.

Material and Methods

Animals

Six male Hound Labrador mongrel dogs, age 18–24 months, weight approximately 20 kg, exhibiting intact mandibular premolar dentition without crowding or evidence of periodontal disease, obtained from an USDA-approved dealer, were used. Animal selection and management, surgery protocol, and periodontal defect preparation followed routines approved by the Animal Care and Use Committee, Wyeth Research, Cambridge, MA, USA. The animals had access to standard laboratory diet and water until the beginning of the study. Oral prophylaxis was performed within 2 weeks prior to the experimental surgeries.

BMP constructs

Using aseptic routines rhBMP-12 (Wyeth Research), supplied at a concentration of 1.5 mg/ml, was diluted with MFR 00906 buffer (0.5% sucrose, 2.5% glycine, 30 mM L-glutamatic acid, 0.01% polysorbate 80, pH 4.5; Wyeth Research) to produce rhBMP-12 stock dilutions at 0.04, 0.2, and 1.0 mg/ml. Lyophilized rhBMP-2 (Wyeth Research) reconstituted to 4.45 mg/ml liquid concentration was diluted with MFR 00906 buffer to produce a rhBMP-2 stock dilution at 0.2 mg/ml.

For the manufacture of the BMP constructs a 1 × 2″ absorbable collagen sponge (Helistat® ACS, Integra Life Sciences, Plainsboro, NJ, USA) was placed onto a sterile field. The sponge was cut into equal halves and one half was discarded. A 0.65-ml aliquot of the rhBMP-12 or rhBMP-2 stock solutions was uniformly dispensed over the entire surface of the 1 × 1″ sponge. The rhBMP-12/ACS or rhBMP-2/ACS constructs remained covered for 30 min to allow for incorporation of rhBMP-12 or rhBMP-2. Tissue binding studies have indicated similar binding times for rhBMP-2 and rhBMP-12. The prepared rhBMP-2/ACS or rhBMP-12/ACS constructs were cut into pieces to fit the supraalveolar periodontal defect.

Surgical procedure

Food was withheld the night preceding surgery. Animals were pre-anesthetized with buprenorphine HCl (0.01–0.03 mg/kg)/acepromazine (0.1 mg/kg)/atropine (0.02–0.04 mg/kg) SQ, sedated with methohexital (4–8 mg/kg to effect), and maintained on gas anesthesia (1–3% isoflurane/O_2 to effect). To maintain hydration, a sterile I.V. catheter was placed and animals received a constant rate infusion of lactated Ringer's solution (10–20 ml/kg/h I.V.) while anesthetized. Prophylactic antibiotics (cefazolin; 22 mg/kg SQ) were administered within 1 h of surgery and redosed postsurgery.

In the maxilla, buccal sulcular incisions were made from the canine to the fourth premolar to reflect buccal mucoperiosteal flaps. The first, second and third premolar teeth were extracted bilaterally, and the fourth premolars were reduced in height and exposed pulpal tissues sealed (Cavit®, ESPE, Seefeld/Oberbayern, Germany) to alleviate potential trauma from the maxillary teeth to the experimental mandibular sites postsurgery. After extractions, the flaps were re-apposed and sutured (GORE-TEX™ Suture CV5, W.L. Gore & Associates Inc., Flagstaff, AZ, USA) ensuring primary wound closure.

Supraalveolar, critical size, periodontal defects were created around the third and fourth mandibular premolar teeth in the right and left jaw quadrants following buccal and lingual mucoperiosteal flap elevation (Wikesjö et al. 1994). Briefly, alveolar bone was removed around the circumference of the teeth with chisels and water-cooled rotating burs. The first and second premolars were extracted bilaterally, and the first molars were amputated at the level of the reduced alveolar crest. The root surfaces of the third and fourth premolar teeth were instrumented with curettes, chisels, and water-cooled rotating diamonds to remove the cementum. The crowns of the teeth were reduced to approximately 2 mm coronal to the cemento-enamel junction (CEJ) and the cut surfaces smoothed. Exposed pulpal tissues were sealed (Cavit®). Clinical defect height from the CEJ to the reduced alveolar crest was set to 6 mm as measured with a periodontal probe (Fig. 1).

Wound management

Three animals received rhBMP-12(0.04 mg/ml)/ACS versus rhBMP-12 (0.2 mg/ml)/ACS in contralateral supraalveolar periodontal defects and three animals received rhBMP-12(1.0 mg/ml)/ACS versus rhBMP-2(0.2 mg/ml)/ACS (total implant volume/defect ~ 1 ml). The rhBMP-12/ACS or rhBMP-2/ACS construct was fitted into the furcation and interproximal areas and layered to cover the buccal and lingual aspects of the premolar teeth (Fig. 1). Following placement of rhBMP-12/ACS or rhBMP-2/ACS, the periostea were fenestrated at the base of the flaps to allow tension-free flap apposition. The flaps were advanced and the flap margins adapted 3–4 mm coronal to the teeth and sutured (GORE-TEX™).

Postsurgery care

The animals were fed a canned soft dog food diet. Buprenorphine HCl (0.015 mg/kg I.M. bid for 48 h) was administered for pain control. A broad-spectrum antibiotic (enrofloxacin, 2.5 mg/kg, I.M., twice daily for 14 days) was used for infection control. Plaque control was maintained by once daily topical application of chlorhexidine (Chlorhexidine Gluconate 20%, Xttrium Laboratories, Inc., Chicago, IL, USA; 40 ml of a 2% solution) until gingival suture removal, thereafter, once daily (Monday through Friday) until the completion of study. Gingival sutures were removed at approximately 8 days postsurgery.

Clinical recordings

Observations of experimental sites with regards to gingival health, maintenance of suture line closure, edema, and evidence of tissue necrosis or infection were made daily until suture removal, and at least twice weekly thereafter. Radiographs were obtained immediately postsurgery, and at 4 and 8 weeks postsurgery.

Histological processing

At 8 weeks postsurgery, the animals were pre-anesthetized with buprenorphine HCl (0.01–0.03 mg/kg)/acepromazine (0.1 mg/kg)/atropine (0.02–0.04 mg/kg), anesthetized with pentobarbital (30 mg/kg IV bolus), and euthanized with Euthanasia-5 solution I.V. (1 ml/10 kg; Henry Schein, Port Washington, NY, USA). Following euthanasia, block sections including teeth, bone and soft tissues were collected and radiographed to estimate bone regeneration. The specimens were rinsed in sterile saline, sectioned, and fixed in 10% neutral buffered formalin for 8–10 weeks.

The tissue blocks were trimmed, washed, and subsequently decalcified with EDTA (Luna 1992). The specimens were then washed, dehydrated with gradients of alcohol, and cleared in xylene using an automatic tissue processor (Tissue-Tek; Sakura, Torrance, CA, USA). Specimens were infiltrated and embedded in methylmethacrylate allowed to polymerize for 3–5 days at room temperature. Using a Reichert Jung Polycut (Leica, Deerfield, IL, USA), 5-μm sections were taken 100 μm apart through the root canal area and stained with a modified Goldner's trichrome stain.

Analysis

The most central stained section of each root for the third and fourth premolar teeth were identified by the size of the root canal. This section and the immediate stained step serial section on either side were subjected to histometric analysis. Thus, three subsequent step serial sections, representing 0.2 mm of the mid-portion of the mesial and the distal root for each premolar tooth, were used for analysis. One masked experi-

Fig. 1. Critical size, supraalveolar periodontal defect before and after application of rhBMP-12/ACS. The surgical reduction of the native periodontal attachment and alveolar bone approximates 6 mm.

enced examiner using an image analysis software (Image-Pro Plus™, Media Cybernetic, Silver Springs, MD, USA) with a custom program for the supra-alveolar periodontal defect model performed the histometric analysis. The following measurements were recorded for the buccal and lingual tooth surfaces of each section:

- Defect height: distance between apical extension of root planing and CEJ.
- Cementum regeneration (continuous): distance between apical extension of root planing and coronal extension of a continuous layer of new cementum or cementum-like deposit on the planed root.
- Cementum regeneration (total): distance between apical extension of root planing and coronal extension of new cementum or cementum-like deposit on the planed root.
- Bone regeneration (height): distance between apical extension of root planing and coronal extension of new alveolar bone along the planed root.
- Bone regeneration (area): area represented by new alveolar bone along the planed root.
- Bone regeneration (density): ratio of regenerated bone/marrow spaces.
- Root resorption: combined linear heights of distinct resorption lacunae on the planed root.
- Ankylosis: combined linear heights of ankylotic union between new alveolar bone and the planed root.

Summary statistics (means ± SD) based on animal means for the experimental conditions were calculated using the selected step serial sections.

Presence of a periodontal attachment with functionally oriented fibers inserting into the newly formed cementum was examined twice, independently, by two masked experienced examiners. Briefly, the specimens were viewed under polarized light at × 10 and × 20. The region of interest was the space between the newly formed bone and dentin or new cementum. Each specimen was scored as outlined in Table 1. The final score for each root was the average of the scores from the buccal and lingual aspect of the root. Summary statistics (means ± SD) based on animal means for the experimental conditions were calculated using the duplicate registrations for each root.

Table 1. Outline of periodontal ligament scores

Score	Fiber density	Fiber attachment
0	none	none
1	very low	attached to bone only
2	low	attached to bone only
3	low	attached to dentin or new cementum
4	mid	attached to dentin or new cementum
5	high/same as native PDL	attached to dentin or new cementum

Statistical testing of differences between treatment conditions was not performed due to the small sample size.

Results

Clinical and radiographic observations

All animals, irrespective of treatment or dose, exhibited defect exposure generally limited to the cut top surface of the teeth, accompanied by some redness and swelling. Gingival exposures were observed as early as day 4 and as late as day 28 postsurgery. One site healed without exposure. This site, implanted with rhBMP-2/ACS, showed decreasing swelling and was hard on palpation by day 10 postsurgery. To reduce chances of infection, systemic antibiot chlorhexidine regimens were ex until the end of study.

Radiographic evidence of bon mation in sites implanted with rh 12/ACS is shown in Fig. 2. formation ranged from 0–20% c defect height at sites receiving rhBMP-12 at 0.04 mg/ml, 0–40% of the defect height at sites receiving rhBMP-12 at 0.2 mg/ml, and approximated 10–30% of the defect height at sites implanted with rhBMP-12 at 1.0 mg/ml. One defect showed evidence of root resorption in the furcation area. Two sites exhibited evidence of root resorption at the cervical aspect of the teeth. Sites receiving rhBMP-2/ACS exhibited comparatively enhanced bone formation (Fig. 2). Two sites showed bone formation extending above the CEJ. One of these sites exhibited bone voids indicative of seroma formation over the cut coronal surface of the teeth (Fig. 2). The third site receiving rhBMP-2/ACS showed evidence of bone fill approximating 50% of the defect height and evidence of significant root resorption at the cervical aspect of the teeth.

Histological evaluation

Representative photomicrographs for defect sites receiving rhBMP12/ACS and rhBMP-2/ACS are shown in Figs. 3 and 4. Sites implanted with rhBMP-12/ACS or rhBMP-2/ACS exhibited new bone formation of varying extents assuming characteristics, trabeculation and cortex formation of the contiguous resident bone. In general, bone formation at sites receiving rhBMP-2/ACS was more extensive than that at sites receiving rhBMP-12/ACS. There were no remarkable differences in bone formation between sites receiving rhBMP-12/ACS at the various rhBMP-12 concentrations. The newly formed bone usually adapted a "physiologic form" along the root surface except for one site implanted with rhBMP-2/ACS where bone formation was considerably more ensive.

A PDL space was observed between newly formed bone and the pre- sly denuded root surface for all erimental conditions. Commonly the space was terminated by ankylosis he presence of extensive bone ation. This observation was shared for sites implanted with rhBMP-2/ACS and rhBMP-12/ACS. A new cellular cementum extending from the apical aspect of the defect was observed for all defect sites without remarkable differences between treatments. In contrast, the fibrovascular tissue within the PDL space in sites receiving rhBMP-12/ACS included functionally oriented collagen fibers apparently extending from the newly formed cementum to the newly formed bone. Sites receiving rhBMP-2/ACS exhibited collagen fibers of varying orientation, commonly aligned along the long-axis of the teeth.

Several defect sites, irrespective of treatment protocol, exhibited exposures of the surgically submerged teeth. Nevertheless, in 8 of the 11 exposed sites the junctional epithelium arrested at the CEJ. In three sites, the junctional epithelium arrested within the coronal aspect of the defect. Most of the defects (11/12) exhibited cervical root resorption. Root resorption of surface erosion character, commonly observed following any regenerative protocol in this

Fig. 2. Healing in contralateral supraalveolar periodontal defects receiving rhBMP-12 (1.0 mg/mL)/ACS (left) or rhBMP-2 (0.2 mg/mL)/ACS (right) at week 8 postsurgery. Note the comparatively robust bone formation in sites receiving rhBMP-2 (0.2 mg/mL)/ACS. The green line indicates the level of the surgical reduction of the native periodontal attachment and alveolar bone.

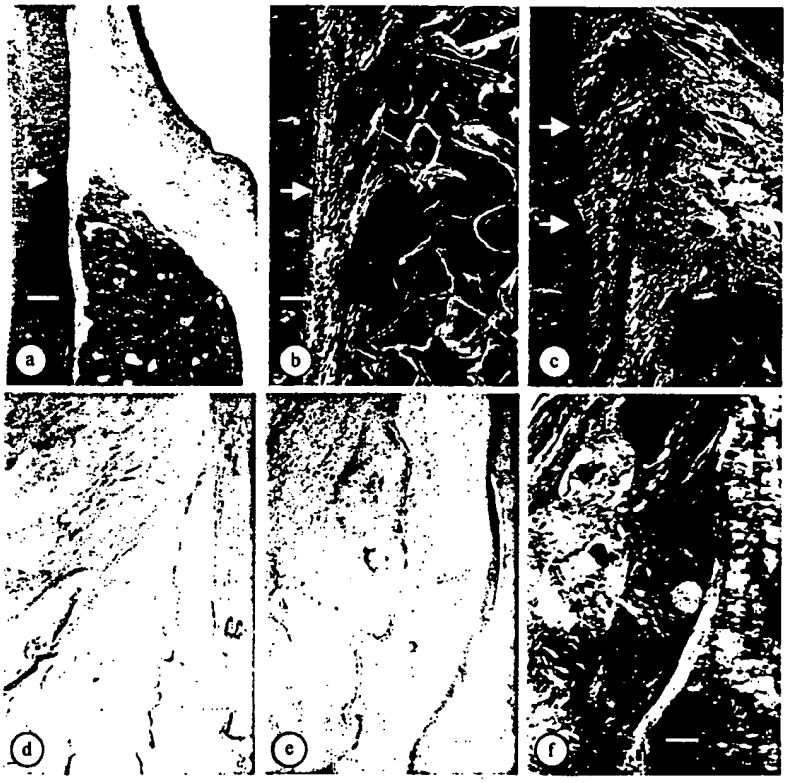

Fig. 3. Photomicrographs of contralateral defect sites receiving rhBMP-12(0.04 mg/ml)/ACS (a–c) and rhBMP-12(0.2 mg/ml)/ACS (d–f). Note new cementum formation including a functionally oriented periodontal ligament. The green line indicates the level of the surgical reduction of the native periodontal attachment and alveolar bone. The green arrow indicates the coronal extension of the newly formed bone in (a) and (c). Blue arrows exemplify areas with a functionally oriented PDL. Original magnifications: × 2.5: a, × 4: d, × 8: b/c, and × 10: e/f; modified Goldner's trichrome stain and polarized light.

animal model, was observed in all defect sites.

Histometric evaluation

The results of the histometric evaluation are shown in Table 2. Bone regeneration averaged 52%, 56%, and 58% of the defect height for sites receiving rhBMP-12/ACS (rhBMP-12 at 0.04, 0.2, and 1.0 mg/ml, respectively). The corresponding value for sites receiving rhBMP-2/ACS approximated 71%. Bone regeneration area was similar among sites receiving rhBMP-12/ACS ranging form 2.1 ± 1.1 to 3.2 ± 2.1 mm^2. Bone regeneration area was numerically higher (5.0 ± 5.0 mm^2), however considerably variable, among sites receiving rhBMP-2/ACS. There were minimal differences in bone density among sites receiving rhBMP-12/ACS or rhBMP-2/ACS; mineralized bone matrix approximated 50% of the new bone area irrespective of treatment. There were also limited differences between treatments relative to cementum formation. Continuous cementum regeneration averaged 1.4 ± 0.8 mm (24% of the defect height) for sites receiving rhBMP-12 (1.0 mg/ml)/ACS. The corresponding values for sites receiving rhBMP-12 (0.04 mg/ml)/ACS, rhBMP-12 (0.2 mg/ml)/ACS or rhBMP-2/ACS were 2.2 ± 1.0 (37%), 2.4 ± 1.3 (41%), and 2.5 ± 1.4 mm (43%), respectively. There were limited differences between treatments relative to total new cementum formation. Similarly, root resorption appeared limited and similar among the treatments. However, ankylosis appeared comparatively increased in sites receiving rhBMP-12 (1.0 mg/ml)/ACS and rhBMP-2/ACS.

The results of the evaluation of the PDL fibers are shown in Table 3. Sites receiving rhBMP-12/ACS exhibited a functionally oriented PDL of relatively high density inserting into newly formed cementum. In contrast, sites receiving rhBMP-2/ACS exhibited collagen fibers of relatively low density oriented in a parallel fashion along the newly formed cementum, inserting into newly formed bone only. There were no remarkable differences between the rhBMP-12 concentrations with the exception that sites receiving rhBMP-12 (0.04 mg/ml)/ACS showed a more consistent reaction than sites receiving rhBMP-12 at higher concentrations.

Discussion

The objective of this study was to evaluate the effect of rhBMP-12 on regeneration of alveolar bone and cementum, and in particular PDL formation. Routine supraalveolar periodontal defects were created around the mandibular premolar teeth in 6 Hound Labrador mongrels. Three animals received rhBMP-12 (0.04 mg/ml)/ACS versus rhBMP-12 (0.2 mg/ml)/ACS, and three animals received rhBMP-12 (1.0 mg/ml)/ACS versus rhBMP-2 (0.2 mg/ml)/ACS in contralateral defects. The animals were euthanized following an 8-week healing interval and block biopsies of the defect sites were processed for histologic and histo-

metric analysis. Bone regeneration appeared increased in sites receiving rhBMP-2/ACS compared to sites implanted with rhBMP-12/ACS. Cementum regeneration was generally similar amongst sites implanted with rhBMP-12/ACS and rhBMP-2/ACS. However, defect sites receiving rhBMP-12/ACS exhibited a functionally oriented PDL bridging the gap between newly formed cementum and alveolar bone whereas this was a rare observation in sites receiving rhBMP-2/ACS.

This study utilized a canine model system including 6-mm, critical size, supraalveolar periodontal defects. The supraalveolar periodontal defect model can be considered a "litmus test" for candidate protocols in the evaluation of their potential for regeneration of alveolar bone, cementum, and periodontal attachment (Wikesjö & Selvig 1999). The defect dimensions provide for clinically relevant regeneration of alveolar bone and cementum. The defect morphology allows for an unbiased strategy of analysis as detailed herein and elsewhere (Wikesjö et al. 1994). Alveolar bone and cementum regeneration has been shown not to exceed 15% of the defect height over an 8-week healing interval in sham-surgery controls. Another characteristic of healing in sham-surgery controls is the lack of regeneration of a periodontal attachment with functionally oriented fibers inserting into the new cementum, as seen in the native periodontal attachment. In contrast, the new attachment is predominately characterized by fibrovascular tissue including fibers oriented along the long-axis of the root surface with or without apparent new cementum formation. Substantial regeneration in this model system warrants clinical pursuit of the protocol evaluated, while limited regeneration would be less deserving. Our extensive experience with this model system prompted us to not include a sham-surgery or buffer/ACS control in this initial study.

Previous studies have used the supraalveolar periodontal defect model to assess the effect of various root conditioning protocols, bone derivatives and bone substitutes, growth, differentiation and extracellular matrix factors, devices for guided tissue regeneration (GTR), as stand-alone protocols or in combinations (Wikesjö et al. 1988, 1990, 1991a, b, 1992, 1998, 1999, 2003a–e, Wikesjö & Nilvéus 1990, Haney et al. 1993, Sigurdsson et al. 1994, 1995a, b, 1996, Kim et al. 1998, Trombelli et al. 1999, Tatakis et al. 2000, Selvig et al. 2002). Only the application of GTR as a stand-alone protocol (Haney et al. 1993, Sigurdsson et al. 1994, 1995b, Wikesjö et al. 2003a, b, d) and rhBMP-2 employing various carrier systems (Sigurdsson et al. 1995a, b, 1996, Wikesjö et al. 1999, 2003a–c,

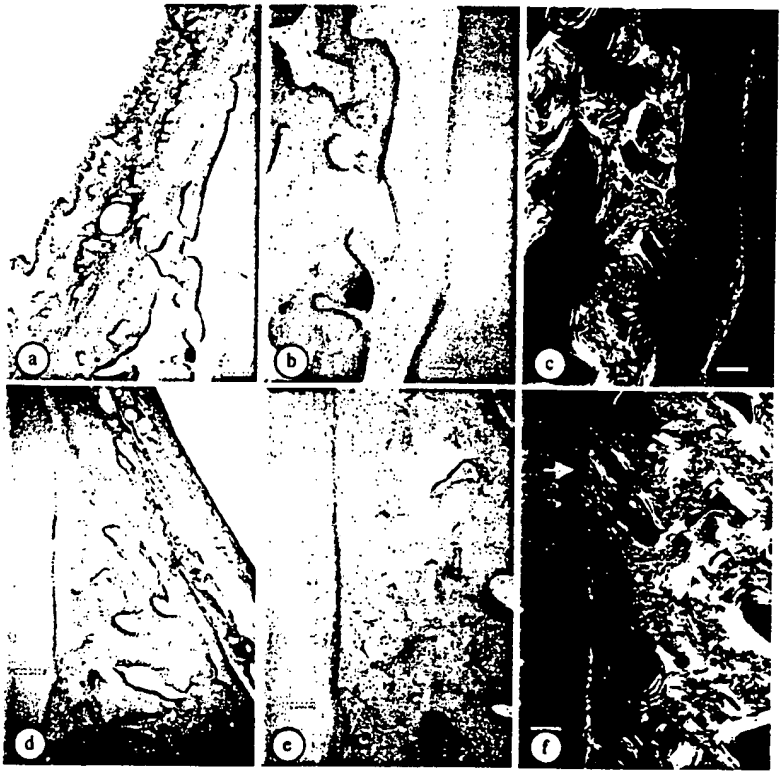

Fig. 4. Photomicrographs of contralateral defect sites receiving rhBMP-2 (0.2 mg/ml)/ACS (a–c) and rhBMP-12 (1.0 mg/ml)/ACS (d–f). Note new cementum formation with an indistinct, limitly appreciable periodontal ligament (PDL) in the site receiving rhBMP-2 (0.2 mg/mL)/ACS. The site receiving rhBMP-12 (1.0 mg/ml)/ACS exhibits new cementum formation with a functionally oriented PDL. The green line indicates the level of the surgical reduction of the native periodontal attachment and alveolar bone. The blue arrow exemplifies areas with a functionally oriented PDL. Original magnifications: × 4: a/d; × 10: b/c/e/f; modified Goldner's trichrome stain and polarized light.

Table 2. Histometric observations for sites receiving rhBMP-12/ACS (rhBMP-12 at 0.04, 0.2, and 1.0 mg/ml) or rhBMP-2/ACS (rhBMP-2 at 0.2 mg/ml)

	Defect height	Bone height	Bone area	Bone density	Cementum continuous	Cementum total	Root resorption	Ankylosis
rhBMP-12(0.04)/ACS	6.0 ± 0.7	3.1 ± 1.9	3.2 ± 2.1	56.7 ± 14.3	2.2 ± 1.0	2.6 ± 1.3	1.0 ± 0.8	0.04 ± 0.2
rhBMP-12(0.2)/ACS	5.9 ± 0.8	3.3 ± 2.2	2.9 ± 2.1	49.6 ± 22.8	2.4 ± 1.3	2.7 ± 1.4	0.9 ± 0.9	0.2 ± 0.4
rhBMP-12(1.0)/ACS	5.9 ± 0.5	3.4 ± 1.3	2.1 ± 1.1	50.9 ± 14.2	1.4 ± 0.8	2.3 ± 0.9	1.2 ± 0.7	0.4 ± 0.6
rhBMP-2(0.2)/ACS	5.8 ± 0.4	4.1 ± 1.6	5.0 ± 5.0	43.5 ± 10.1	2.5 ± 1.4	3.0 ± 1.2	1.4 ± 1.3	0.6 ± 0.7

Group means ± SD (mm); bone area (mm^2), bone density (%).
rhBMP, recombinant human bone morphogenetic protein.

Table 3. Periodontal ligament scores for sites receiving rhBMP-12/ACS (rhBMP-12 at 0.04, 0.2, and 1.0 mg/ml) or rhBMP-2/ACS (rhBMP-2 at 0.2 mg/ml)

Animal	rhBMP-12(0.04)	rhBMP-12(0.2)	rhBMP-12(1.0)	rhBMP-2(0.2)
1	4.8 ± 0.2	4.5 ± 0.2	–	–
2	4.2 ± 0.6	2.9 ± 0.3	–	–
3	4.7 ± 0.4	4.2 ± 0.6	–	–
4	–	–	1.9 ± 0.5	1.4 ± 0.3
5	–	–	3.3 ± 0.8	2.4 ± 0.3
6	–	–	4.0 ± 0.5	1.6 ± 0.3
Group	4.6 ± 0.3	3.9 ± 0.9	3.1 ± 1.1	1.8 ± 0.5

Animal and group means (± SD) from duplicate examinations by two independent examiners. rhBMP, recombinant human bone morphogenetic protein.

Selvig et al. 2002) have been shown to support clinically meaningful regeneration of alveolar bone and cementum. The application of occlusive or novel macro-porous membranes for GTR resulted in clinically relevant regeneration of alveolar bone adopting a "physiologic form" along the root surface, formation of a cellular cementum and a functionally oriented PDL with cementum inserting collagen fibers (Sigurdsson et al. 1994, 1995b, Wikesjö et al. 2003a, b, d). Surgical implantation of rhBMP-2 resulted in substantial regeneration of alveolar bone, usually encompassing the entire 5–6-mm supraalveolar defect, and regeneration of cellular cementum although without a functionally oriented PDL (Sigurdsson et al. 1995a, b, 1996, Wikesjö et al. 1999, 2003a–c, Selvig et al. 2002). Following an 8-week healing interval, fibrovascular tissue was observed including collagen fibers that were essentially oriented parallel to the newly formed cementum. With observations extending up to 24 weeks postsurgery, the regenerated cementum was observed interfacing fatty marrow (Wikesjö et al. 2003a). Ankylosis was regularly observed located in the coronal third of the supraalveolar defect. In the present study, the observations at sites implanted with rhBMP-2/ACS are consistent with these observations from previous studies evaluating rhBMP-2 using a variety of carrier technologies.

Surgical implantation of rhBMP-12/ACS followed the pattern of bone and cementum formation observed following implantation of rhBMP-2/ACS; however, bone formation appeared less extensive. Quantitative comparisons to previous studies utilizing the supraalveolar periodontal defect model system with an 8-week interval may not necessarily be meaningful since this study included exposed teeth, whereas previous studies have not included exposed teeth in the analysis. However, the exposures were commonly limited to the most cervical aspect of the defects; the gingival epithelium arrested at or within a short distance from the CEJ. Thus, the healing events produced were sufficient to satisfy the specific objective of this study that is to evaluate the formation of a new PDL. Sites receiving rhBMP-2/ACS exhibited connective tissue fibers of low density mainly attached to the newly formed bone. Sites receiving rhBMP-12/ACS exhibited a new fibrous attachment of comparatively high density attached to newly formed bone, dentin, or new cementum. The observations at sites receiving rhBMP-2/ACS are consistent with that of previous studies evaluating rhBMP-2 technologies in this model system (Sigurdsson et al. 1995a, b, 1996, Wikesjö et al. 1999, 2003a–c, Selvig et al. 2002). The observations of a fibrous attachment inserting into newly formed cementum on the previously denuded root surface are novel and consistent with tissue reactions to this BMP technology in other model systems (Wolfman et al. 1995, 1997). It must be noted however that previous studies have reported formation of a functional periodontal attachment following application of rhBMP-2 or other BMP technologies for periodontal regeneration (Ishikawa et al. 1994, Ripamonti et al. 1994, Kinoshita et al. 1997, Giannobile et al. 1998, Kuboki et al. 1998, Blumenthal et al. 2002, Choi et al. 2002). Such observations may likely be explained by the use of indiscriminant model systems, however, it cannot be ruled out that genuine differences in biologic potential may exist among technologies.

Ankylosis appeared less appreciable particularly in defects receiving rhBMP-12/ACS at 0.04 and 0.2 mg/ml compared to defects receiving rhBMP-12 (1.0 mg/ml)/ACS or rhBMP-2/ACS in this study. However, the study protocol only allowed direct comparisons between rhBMP-12(1.0 mg/ml)/ACS and rhBMP-2/ACS in the same animals, hence this perceived difference may be explained by differences between animals rather than experimental protocol. Nevertheless, root resorption and ankylosis in the cervical third of the defects, a frequent observation in this demanding defect model following surgical implantation of rhBMP-2 (Sigurdsson et al. 1995a, b, 1996 Wikesjö et al. 1999, 2003a–c, Selvig et al. 2002), were commonly observed. Root resorption and ankylosis are rarely encountered in the apical aspect of the supraalveolar periodontal defect and thus do not appear to be a healing aberration in more limited periodontal defects (Kinoshita et al. 1997, Choi et al. 2002). Ankylosis has also not been found to be a healing aberration following surgical implantation of BMPs in the absence of extensive bone regeneration (Ripamonti et al. 1994, Kinoshita et al. 1997, Choi et al. 2002).

Conclusions

The outcomes of this pilot study suggests that rhBMP-12 may have significant effects on the regeneration of the PDL. Additional preclinical evaluation is needed to confirm these initial observations prior to clinical testing.

Acknowledgments

Mary Stevens and Janet Golden, Wyeth Research, are acknowledged for excellent histotechnical support.

References

Blumenthal, N. M., Koh-Kunts, G., Alves, M. E. A. F., Miranda, D., Sorensen, R. G., Wozney, J. M. & Wikesjö, U. M. E. (2002) Effect of surgical implantation of recombinant human bone morphogenetic protein-2 in a bioabsorbable collagen sponge or a calcium phosphate putty carrier in intrabony periodontal defects in the baboon. *Journal of Periodontology* **73**, 1494–1506.

Chang, S. C., Hoang, B., Thomas, J. T., Vukicevic, S., Luyten, F. P., Ryba, N. J., Kozak, C. A., Reddi, A. H. & Moos, M. (1994) Cartilage-derived morphogenetic proteins. New members of the transforming growth factor-beta superfamily predominantly expressed in long bones during human

embryonic development. *The Journal of Biological Chemistry* **269**, 28227–28234.

Choi, S-H., Kim, C-K., Cho, K-S., Huh, J-S., Sorensen, R. G., Wozney, J. M. & Wikesjö, U. M. E. (2002) Effect of recombinant human bone morphogenetic protein-2/absorbable collagen sponge (rhBMP-2/ACS) on healing in 3-wall intrabony defects in dogs. *Journal of Periodontology* **73**, 63–72.

Furuya, K., Nifuji, A., Rosen, V. & Noda, M. (1999) Effects of GDF7/BMP 12 on proliferation and alkaline phosphatase expression in rat osteoblastic osteosarcoma ROS 17/2.8 cells. *Journal of Cellular Biochemistry* **72**, 177–180.

Giannobile, W. V., Ryan, S., Shih, M-S., Su, D. L., Kaplan, P. L. & Chan, T. C. K. (1998) Recombinant human osteogenic protein-1 (OP-1) stimulates periodontal wound healing in Class III furcation defects. *Journal of Periodontology* **69**, 129–137.

Haney, J. M., Nilvéus, R. E., McMillan, P. J. & Wikesjö, U. M. E. (1993) Periodontal repair in dogs: expanded polytetrafluoroethylene barrier membranes support wound stabilization and enhance bone regeneration. *Journal of Periodontology* **64**, 883–890.

Hattersley, G., Cox, K., Soslowsky, L. J., Thomopoulos, S., Hewick, R., Joyce, M. E. & Rosen, V. (1998) Bone morphogenetic proteins 2 and 12 alter the attachment of tendon to bone in a rat model: a histological and biomechanical investigation. Transactions of the 44th Annual Meeting Orthopaedic Research Society.

Inada, M., Katagiri, T., Akiyama, S., Namiki, M., Komaki, M., Yamaguchi, A., Kamoi, K., Rosen, V. & Suda, T. (1996) Bone morphogenetic protein-12 and -13 inhibit terminal differentiation of myoblasts, but do not induce their differentiation into osteoblasts. *Biochemical and Biophysical Research Communications* **222**, 317–322.

Ishikawa, I., Kinoshita, A., Oda, S. & Roongruangphol, T. (1994) Regenerative therapy in periodontal diseases. Histological observations after implantation of rhBMP-2 in the surgically created periodontal defects in adults dogs. *Dentistry in Japan* **31**, 141–146.

Kim, C-K., Cho, K-S., Choi, S-H., Prewett, A. & Wikesjö, U. M. E. (1998) Periodontal repair in dogs: effect of allogeneic freeze-dried demineralized bone matrix implants on alveolar bone and cementum regeneration. *Journal of Periodontology* **69**, 26–33.

King, G. N., King, N., Cruchley, A. T., Wozney, J. M. & Hughes, F. J. (1997) Recombinant human bone morphogenetic protein-2 promotes wound healing in rat periodontal fenestration defects. *Journal of Dental Research* **76**, 1460–1470.

King, G. N. & Hughes, F. J. (1999) Effects of occlusal loading on ankylosis, bone, and cementum formation during bone morphogenetic protein-2-stimulated periodontal regeneration in vivo. *Journal of Periodontology* **70**, 1125–1135.

King, G. N. & Hughes, F. J. (2001) Bone morphogenetic protein-2 stimulates cell recruitment and cementogenesis during early wound healing. *Journal of Clinical Periodontology* **28**, 465–475.

King, G. N., King, N. & Hughes, F. J. (1998a) The effect of root surface demineralization on bone morphogenetic protein-2-induced healing of rat periodontal fenestration defects. *Journal of Periodontology* **69**, 561–570.

King, G. N., King, N. & Hughes, F. J. (1998b) Effect of two delivery systems for recombinant human bone morphogenetic protein-2 on periodontal regeneration in vivo. *Journal of Periodontal Research* **33**, 226–236.

Kinoshita, A., Oda, S., Takahashi, K., Yokota, S. & Ishikawa, I. (1997) Periodontal regeneration by application of recombinant human bone morphogenetic protein-2 to horizontal circumferential defects created by experimental periodontitis in beagle dogs. *Journal of Periodontology* **68**, 103–109.

Kuboki, Y., Sasaki, M., Saito, A., Takita, H. & Kato, H. (1998) Regeneration of periodontal ligament and cementum by BMP-applied tissue engineering. *European Journal of Oral Sciences* **106** (Suppl. 1), 197–203.

Luna, L. G. (1992) *Histopathologic Methods and Color Atlas of Special Stains and Tissue Artifacts*. 1st edition p. 113. Gaithersburg, MD: American Histolab, Inc., Publications Division.

Ripamonti, U., Heliotis, M., Rueger, D. C. & Sampath, T. K. (1996) Induction of cementogenesis by recombinant human osteogenic protein-1 (hop-1/bmp-7) in the baboon (*Papio ursinus*). Short communication. *Archives of Oral Biology* **41**, 121–126.

Ripamonti, U., Heliotis, M., van den Heever, B. & Reddi, A. H. (1994) Bone morphogenetic proteins induce periodontal regeneration in the baboon (*Papio ursinus*). Brief communication. *Journal of Periodontal Research* **29**, 439–445.

Selvig, K. A., Sorensen, R. G., Wozney, J. M. & Wikesjö, U. M. E. (2002) Bone repair following recombinant human bone morphogenetic protein-2 stimulated periodontal regeneration. *Journal of Periodontology* **73**, 1020–1029.

Sigurdsson, T. J., Hardwick, R., Bogle, G. C. & Wikesjö, U. M. E. (1994) Periodontal repair in dogs: space provision by reinforced ePTFE membranes enhances bone and cementum regeneration in large supraalveolar defects. *Journal of Periodontology* **65**, 350–356.

Sigurdsson, T. J., Lee, M. B., Kubota, K., Turek, T. J., Wozney, J. M. & Wikesjö, U. M. E. (1995a) Periodontal repair in dogs: Recombinant human bone morphogenetic protein-2 significantly enhances periodontal regeneration. *Journal of Periodontology* **66**, 131–138.

Sigurdsson, T. J., Nygaard, L., Tatakis, D. N., Fu, E., Turek, T. J., Jin, L., Wozney, J. M. & Wikesjö, U. M. E. (1996) Periodontal repair in dogs: evaluation of rhBMP-2 carriers. *The International Journal of Periodontics & Restorative Dentistry* **16**, 525–537.

Sigurdsson, T. J., Tatakis, D. N., Lee, M. B. & Wikesjö, U. M. E. (1995b) Periodontal regenerative potential of space providing expanded polytetrafluoroethylene membranes and recombinant human bone morphogenetic proteins. *Journal of Periodontology* **66**, 511–521.

Talwar, R., Di Silvio, L., Hughes, F. J. & King, G. N. (2001) Effects of carrier release kinetics on bone morphogenetic protein-2-induced periodontal regeneration in vivo. *Journal of Clinical Periodontology* **28**, 340–347.

Tatakis, D. N., Wikesjö, U. M. E., Razi, S. S., Sigurdsson, T. J., Lee, M. B., Nguyen, T., Ongpipattanakul, B. & Hardwick, R. (2000) Periodontal repair in dogs: effect of transforming growth factor-β_1 on alveolar bone and cementum regeneration. *Journal of Clinical Periodontology* **27**, 698–704.

Trombelli, L., Lee, M. B., Promsudthi, A., Guglielmoni, P. G. & Wikesjö, U. M. E. (1999) Periodontal repair in dogs: histologic observations of guided tissue regeneration with a prostaglandin E_1 analog/methacrylate composite. *Journal of Clinical Periodontology* **26**, 381–387.

Valcourt, U., Ronziere, M. C., Winkler, P., Rosen, V., Herbage, D. & Mallein-Gerin, F. (1999) Different effects of bone morphogenetic proteins 2, 4, 12, and 13 on the expression of cartilage and bone markers in the MC615 chondrocyte cell line. *Experimental Cell Research* **251**, 264–274.

Wikesjö, U. M. E., Bogle, G. C. & Nilvéus R. E. (1992) Periodontal repair in dogs: effect of a composite graft protocol on healing in supraalveolar periodontal defects. *Journal of Periodontology* **63**, 107–113.

Wikesjö, U. M. E., Claffey, N., Christersson, L. A., Franzetti, L. C., Genco, R. J., Terranova, V. P. & Egelberg, J. (1988) Repair of periodontal furcation defects in beagle dogs following reconstructive surgery including root surface demineralization with tetracycline hydrochloride and topical fibronectin application. *Journal of Clinical Periodontology* **15**, 73–80.

Wikesjö, U. M. E., Claffey, N. & Egelberg, J. (1991a) Periodontal repair in dogs: effect of heparin treatment of the root surface. *Journal of Clinical Periodontology* **18**, 60–64.

Wikesjö, U. M. E., Claffey, N., Nilvéus, R. & Egelberg, J. (1991b) Periodontal repair in dogs: effect of root surface treatment with stannous fluoride or citric acid on root resorption. *Journal of Periodontology* **62**, 180–184.

Wikesjö, U. M. E., Guglielmoni, P. G., Promsudthi, A., Cho, K- S., Trombelli, L., Selvig, K. A., Jin, L. & Wozney, J. M. (1999) Periodontal repair in dogs: effect of rhBMP-2 concentration on regeneration of alveolar bone and periodontal attachment. *Journal of Clinical Periodontology* **26**, 392–400.

Wikesjö, U. M. E., Hagen, K. & Nielsen, D. D. (1990) Periodontal repair in dogs: effect of saliva contamination of the root surface. *Journal of Periodontology* **61**, 559–563.

Wikesjö, U. M. E., Kean, C. J. C. & Zimmerman, G. J. (1994) Periodontal repair in dogs: supraalveolar defect models for evaluation of safety and efficacy of periodontal reconstruc-

tive therapy. *Journal of Periodontology* **65**, 1151–1157.

Wikesjö, U. M. E., Lim, W. H., Razi, S. S., Sigurdsson, T. J., Lee, M. B., Tatakis, D. N. & Hardwick, W. R. (2003e) Periodontal repair in dogs: a bioresorbable calcium carbonate coral implant enhances space provision for alveolar bone regeneration in conjunction with guided tissue regeneration. *Journal of Periodontology* **74**, 955–962.

Wikesjö, U. M. E., Lim, W. H., Thomson, R. C., Cook, A. D., Wozney, J. M. & Hardwick, W. R. (2003a) Periodontal repair in dogs: evaluation of a bioresorbable space-pro viding macro-porous membrane with re combinant human bone morphogenetic protein-2. *Journal of Periodontology* **74**, 635–647.

Wikesjö, U. M. E., Lim, W. H., Thomson, R. C. & Hardwick, W. R. (2003d) Periodontal repair in dogs: Gingival tissue exclusion, a critical requirement for guided tissue regeneration? *Journal of Clinical Periodontology* **30**, 655–664.

Wikesjö, U. M. E. & Nilvéus, R. (1990) Periodontal repair in dogs: effect of wound stabilization on healing. *Journal of Periodontology* **61**, 719–724.

Wikesjö, U. M. E., Razi, S. S., Sigurdsson, T. J., Tatakis, D. N., Lee, M. B., Ongpipattanakul, B., Nguyen, T. & Hardwick, R. (1998) Periodontal repair in dogs: effect of recombinant human transforming growth factor-beta$_1$ on guided tissue regeneration. *Journal of Clinical Periodontology* **25**, 475–481.

Wikesjö, U. M. E. & Selvig, K. A. (1999) Periodontal wound healing and regeneration. *Periodontology 2000* **19**, 21–39.

Wikesjö, U. M. E., Xiropaidis, A. V., Thomson, R. C., Cook, A. D., Selvig, K. A. & Hardwick, W. R. (2003b) Periodontal repair in dogs: rhBMP-2 significantly enhances bone formation under provisions for guided tissue regeneration. *Journal of Clinical Periodontology* **30**, 705–714.

Wikesjö, U. M. E., Xiropaidis, A. V., Thomson, R. C., Cook, A. D., Selvig, K. A. & Hardwick, W. R. (2003c) Periodontal repair in dogs: space-providing ePTFE devices increase rhBMP-2/ACS induced bone formation. *Journal of Clinical Periodontology* **30**, 715–725.

Wolfman, N. M., Celeste, A. J., Cox, K., Hattersley, G., Nelson, R., Yamaji, N., DiBlasio-Smith, E., Nove, J., Song, J. J., Wozney, J. M. & Rosen, V. (1995) Preliminary characterization of the biological activities of rhBMP-12. *Journal of Bone and Mineral Research* **10** (Suppl. 1), 148.

Wolfman, N. M., Hattersley, G., Cox, K., Celeste, A. J., Nelson, R., Yamaji, N., Dube, J. L., DiBlasio-Smith, E., Nove, J., Song, J. J., Wozney, J. M. & Rosen, V. (1997) Ectopic induction of tendon and ligament in rats by growth and differentiation factors 5, 6, and 7, members of the TGF-beta gene family. *The Journal of Clinical Investigation* **100**, 321–330.

Wozney, J. M. (1998) The bone morphogenetic protein family: multifunctional regulators in the embryo and adult. *European Journal of Oral Sciences* **106** (Suppl. 1), 160–166.

Address:
Dr Ulf ME Wikesjö
Laboratory for Applied Periodontal and Craniofacial Regeneration
Temple University School of Dentistry
Department of Periodontology
3223 North Broad Street
Philadelphia, PA 19140
USA
E-mail: wikesjo@comcast.net

Exhibit J

JOURNAL OF BONE AND MINERAL RESEARCH

The Official Journal of the American Society for Bone and Mineral Research

JOURNAL OF BONE AND MINERAL RESEARCH

VOLUME 13 NUMBER 3 MARCH 1998

REVIEW

The Nuclear Vitamin D Receptor: Biological and Molecular Regulatory Properties Revealed — M.R. Haussler, G.K. Whitfield, C.A. Haussler, J.-C. Hsieh, P.D. Thompson, S.H. Selznik, C.E. Dominguez, and P.W. Jurutka — 325

CLINICAL REVIEW

Renal and Nonrenal 25-Hydroxyvitamin D-1α-Hydroxylases and Their Clinical Expression — N.H. Bell — 350

ORIGINAL ARTICLES

Persistence of Ca^{2+}-Sensing Receptor Expression in Functionally Active, Long-Term Human Parathyroid Cell Cultures — M.-C. Roussanne, J. Gogusev, B. Hory, P. Duchambon, J.C. Souberbielle, B. Nabarra, D. Pierrat, E. Sarfati, T. Drüeke, and A. Bourdeau — 354

Do Dietary Calcium and Age Explain the Controversy Surrounding the Relationship Between Bone Mineral Density and Vitamin D Receptor Gene Polymorphisms? — S.L. Ferrari, R. Rizzoli, D.O. Slosman, and J.-P. Bonjour — 363

Human Trabecular Bone Cells Are Able to Express Both Osteoblastic and Adipocytic Phenotype: Implications for Osteopenic Disorders — M.E. Nuttall, A.J. Patton, D.L. Olivera, D.P. Nadeau, and M. Gowen371 — 371

Cartilage-Derived Morphogenetic Proteins and Osteogenic Protein-1 Differentially Regulate Osteogenesis — L. Erlacher, J. McCartney, E. Piek, P. ten Dijke, M. Yanagishita, H. Oppermann, and F.P. Luyten — 383

IL-6 Mediates the Effects of IL-1 or TNF, but Not PTHrP or $1,25(OH)_2D_3$, on Osteoclast-like Cell Formation in Normal Human Bone Marrow Cultures — R.D. Devlin, S.V. Reddy, R. Savino, G. Ciliberto, and G.D. Roodman — 393

The Mouse Mammary Tumor Cell Line, MMT060562, Produces Prostaglandin E_2 and Leukemia Inhibitory Factor and Supports Osteoclast Formation In Vitro via a Stromal Cell–Dependent Pathway — T. Akatsu, K. Ono, Y. Katayama, T. Tamura, M. Nishikawa, N. Kugai, M. Yamamoto, and N. Nagata — 400

Contortrostatin, a Homodimeric Snake Venom Disintegrin, Is a Potent Inhibitor of Osteoclast Attachment — B. Mercer, F. Markland, and C. Minkin — 409

(Continued)

Bone Mineral, Histomorphometry, and Body Composition in Adults with Growth Hormone Receptor Deficiency	L.K. Bachrach, R. Marcus, S.M. Ott, A.L. Rosenbloom, O. Vasconez, V. Martinez, A.L. Martinez, R.G. Rosenfeld, and J. Guevara-Aguirre	415
Identification of a Novel Isoform of Mouse Dentin Matrix Protein 1: Spatial Expression in Mineralized Tissues	M. MacDougall, T.T. Gu, X. Luan, D. Simmons, and J. Chen	422
Expression of Type X Collagen and Matrix Calcification in Three-Dimensional Cultures of Immortalized Temperature-Sensitive Chondrocytes Derived from Adult Human Articular Cartilage	B.O. Oyajobi, A. Frazer, A.P. Hollander, R.M. Graveley, C. Xu, A. Houghton, P.V. Hatton, R.G.G. Russell, and B.M.J. Stringer	432
Mechanism of Mechanically Induced Intercellular Calcium Waves in Rabbit Articular Chondrocytes and in HIG-82 Synovial Cells	M. Grandolfo, A. Calabrese, and P. D'Andrea	443
Homologous Up-Regulation of Vitamin D Receptors Is Tissue Specific in the Rat	R.C. Gensure, S.D. Antrobus, J. Fox, M. Okwueze, S.Y. Talton, and M.R. Walters	454
Morphometric X-Ray Absorptiometry: Reference Data for Vertebral Dimensions	J.A. Rea, P. Steiger, G.M. Blake, E. Potts, I.G. Smith, and I. Fogelman	464
Calciotropic Hormones and Bone Markers in the Elderly	J.C. Gallagher, H.K. Kinyamu, S.E. Fowler, B. Dawson-Hughes, G.P. Dalsky, and S.S. Sherman	475
Effect of Two Training Regimens on Bone Mineral Density in Healthy Perimenopausal Women: A Randomized Controlled Trial	A. Heinonen, P. Oja, H. Sievänen, M. Pasanen, and I. Vuori	483
Bone Turnover Response to Changes in Calcium Intake Is Altered in Girls and Adult Women in Families with Histories of Osteoporosis	K.O. O'Brien, S.A. Abrams, L.K. Liang, K.J. Ellis, and R.F. Gagel	491
Exercise Before Puberty May Confer Residual Benefits in Bone Density in Adulthood: Studies in Active Prepubertal and Retired Female Gymnasts	S. Bass, G. Pearce, M. Bradney, E. Hendrich, P.D. Delmas, A. Harding, and E. Seeman	500
Effects of Zinc Supplementation on Vertebral and Femoral Bone Mass in Rats on Strenuous Treadmill Training Exercise	C. Seco, B. Biol, M. Revilla, E.R. Hernández, J. Gervás, J. González-Riola, L.F. Villa, and H. Rico	508

ABSTRACTS

Bone and Tooth Society Spring Meeting, 1998 513

ANNOUNCEMENTS 536

JOURNAL OF BONE AND MINERAL RESEARCH
Volume 13, Number 3, 1998
Blackwell Science, Inc.

Cartilage-Derived Morphogenetic Proteins and Osteogenic Protein-1 Differentially Regulate Osteogenesis

LUDWIG ERLACHER,[1,2] JOHN MCCARTNEY,[3] ESTER PIEK,[4] PETER TEN DIJKE,[4] MASAKI YANAGISHITA,[1] HERMANN OPPERMANN,[3] and FRANK P. LUYTEN[1]

ABSTRACT

Cartilage-derived morphogenetic proteins-1 and -2 (CDMP-1 and CDMP-2) are members of the bone morphogenetic protein (BMP) family, which play important roles in embryonic skeletal development. We studied the biological activities of recombinant CDMP-1 and CDMP-2 in chondrogenic and osteogenic differentiation and investigated their binding properties to type I and type II serine/threonine kinase receptors. In vivo, CDMP-1 and CDMP-2 were capable of inducing dose-dependently de novo cartilage and bone formation in an ectopic implantation assay. In vitro studies using primary chondrocyte cultures showed that both CDMP-1 and CDMP-2 stimulated equally de novo synthesis of proteoglycan aggrecan in a concentration-dependent manner. This activity was equipotent when compared with osteogenic protein-1 (OP-1). In contrast, CDMPs were less stimulatory than OP-1 in osteogenic differentiation as evaluated by alkaline phosphatase activity and expression levels of bone markers in ATDC5, ROB-C26, and MC3T3-E1 cells. CDMP-2 was the least osteogenic in these assays. Receptor binding studies of CDMP-1 and CDMP-2 revealed that both have affinity for the BMP receptor type IB (BMPR-IB) and BMPR-II, and weakly for BMPR-IA. Moreover, using a promoter/reporter construct, transcriptional activation signal was transduced by BMPR-IB in the presence of BMPR-II upon CDMP-1 and CDMP-2 binding. Our data show that distinct members of the BMP family differentially regulate the progression in the osteogenic lineage, and this may be due to their selective affinity for specific receptor complexes. (J Bone Miner Res 1998;13:383–392)

INTRODUCTION

Cartilage-derived morphogenetic proteins-1 and -2 (CDMP-1 and CDMP-2) are two members of the transforming growth factor-β (TGF-β) superfamily. During development they are expressed predominantly in and around skeletal elements and in the joint interzones.[1,2] CDMP-1 and CDMP-2 are 82% identical in their biologically active carboxy-terminal domains. They are most closely related to the bone morphogenetic protein (BMP) subgroups BMP-5/BMP-6/osteogenic protein-1 (OP-1) and BMP-2/BMP-4.[1]

The physiological role of CDMP-1, the human homolog of mouse growth differentiation factor-5 (Gdf-5), has been established by its linkage to mouse and human skeletal disorders, brachypodism, and Hunter-Thompson chondrodysplasia, respectively.[1–3] Both phenotypes are characterized by skeletal abnormalities restricted to the limbs and synovial joints and are associated with null mutations in the *cdmp1/gdf5* gene. These genetic studies provide direct evidence for the involvement of CDMP-1 in the patterning and tissue specification of the appendicular skeletal structures. The primary role of CDMP-2, the human homolog of mouse Gdf-6, is so far unknown. Besides its involvement in skeletal morphogenesis, its high levels of expression in

[1]Craniofacial and Skeletal Diseases Branch, National Institute of Dental Research, National Institutes of Health, Bethesda, Maryland, U.S.A.
[2]Present address: Clinic of Internal Medicine III, Department of Rheumatology, Vienna, Austria.
[3]Creative BioMolecules Inc., Hopkinton, Massachusetts, U.S.A.
[4]Ludwig Institute for Cancer Research, Uppsala, Sweden.

postnatal cartilaginous tissues suggest a possible role in the promotion and maintenance of the cartilaginous phenotype.[1,4]

TGF-β superfamily members elicit their biological response through binding to a heteromeric complex of two types of serine/threonine kinase receptors (i.e., type I and type II). Various type I and type II receptors for BMPs have been identified.[5] Receptor binding studies have revealed that BMPs have an affinity for several distinct receptor complexes.[6] Interestingly, as shown for OP-1, BMPs appear to utilize different heteromeric receptor complexes to elicit their diverse biological functions.[7]

The expression pattern of the CDMPs is restricted to skeletal structures during embryonic development and therefore suggests a more defined role in the regulation of chondrogenic and osteogenic differentiation. Therefore, we have investigated skeletal lineage progression using recombinant CDMP-1 and CDMP-2 and compared their activities with OP-1.[8] Our data show that both CDMPs and OP-1 promote chondrogenesis; however, CDMPs are significantly less osteogenic than OP-1. Furthermore, receptor binding studies indicate that the distinct biological profile of the CDMPs when compared with OP-1 may be explained by their selective affinity for specific heteromeric receptor complexes.

MATERIALS AND METHODS

Expression of CDMP-1 and CDMP-2 in Escherichia coli

A cDNA encoding the mature *cdmp-1* was tailored for insertion into an *E. coli* expression vector by site-directed mutagenesis using the Kunkel method.[9] Following the pro-domain and in close proximity to the RXXR processing site, a leucine residue was converted to a methionine translational initiation codon with a corresponding *Nco*I restriction site, while a 3× *Xho*I site was similarly introduced immediately after the translational stop codon. The *Nco*I-*Xho*I fragment containing the open reading frame for mature *cdmp-1* was ligated with a tetracycline-resistant pBR322-derived expression vector. Fermentation was done in shaker flasks using 2YT medium with the addition of indol acrylic acid at the appropriate time for the induction of the tryptophan promoter and led to accumulation of large inclusion bodies. A cDNA for *cdmp-2* was similarly tailored for expression. Since the yield of expression was quite low, we used part of the N-terminal region of the highly expressed *cdmp-1* and spliced it with the 7-cysteine domain of *cdmp-2* at the first cysteine, where both genes share a *Pst*I site. Induced cell cultures (250 ml) were centrifuged (11,000*g* for 10 minutes at 4°C), followed by resuspension of the cell pellets in 50 ml of 25 mM Tris, 10 mM EDTA, pH 8.0 (1× TE) plus 100 μg/ml lysozyme. The cell suspensions were incubated overnight at 37°C, then chilled on ice and disrupted by sonication. Inclusion bodies were isolated by centrifugation (11,000*g* for 20 minutes at 4°C) and resuspension in 1× TE. The final washed inclusion body pellets were resuspended in 40 ml of 1× TE, 15% glycerol, and stored at −20°C.

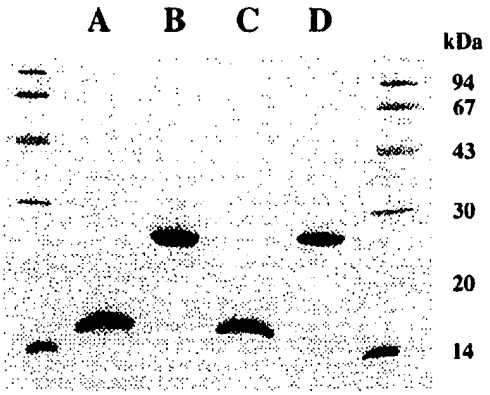

FIG. 1. SDS-PAGE analysis of recombinant CDMP-1 and CDMP-2. Lane A, 5 μg CDMP-1 after reduction and alkylation; lane B, 5 μg CDMP-1 nonreduced; lane C, 5 μg CDMP-2 after reduction and alkylation; lane D, 5 μg CDMP-2 nonreduced.

Protein folding and protein purification

Reduced and denatured inclusion body protein solutions were prepared by dissolving aliquots of pelleted inclusion bodies in 100 mM Tris, 10 mM EDTA, 6 M guanidine HCl, 10 mM dithiothreitol, pH 8.0 (final protein concentration 4-6 mg/ml). The inclusion body protein solutions were incubated at 37° C for 30 minutes then diluted 40-fold with refolding buffer (100 mM Tris, 10 mM EDTA, 1 M NaCl, 2% 3-[(3-cholamidopropyl) dimethylammonio]-2-hydroxy-1-propanesulfonic acid (CHAPS), 5 mM reduced glutathione, 2.5 mM oxidized glutathione, pH 8.7). The refolding reactions were incubated for 72 h at 4°C. The folding reactions were dialyzed extensively against 10 mM HCl, then clarified by centrifugation (11,000*g* for 20 minutes at 4°C). The solutions were concentrated using a stirred cell concentrator and YM10 MWCO membranes (Amicon, Beverly, MA, U.S.A.). The concentrated proteins were then lyophilized. The lyophilized proteins were resuspended in 0.8 ml 0.1% trifluoracetic acid (TFA), 70% acetonitrile, then diluted to 2 ml with 0.1% TFA (final acetonitrile concentration 30%). The protein solutions were fractionated by semipreparative C4 reverse phase-high pressure liquid chromatography (HPLC) using a linear acetonitrile gradient (30–100% in 0.1% TFA). Aliquots of each fraction were analyzed on SDS-PAGE (15%) gels in nonreduced conditions and after reduction and alkylation. Peak dimer fractions were pooled and ultraviolet absorbance spectra obtained. Concentrations were estimated from absorbance at 280 nm. Protein pools were stored at −20°C. The average yield of properly folded protein per liter of bacterial fermentation were ~50–60 mg for CDMP-1 and 40–50 mg for CDMP-2.

In vivo subcutaneous implantation assay

To evaluate the potential of CDMP-1 and CDMP-2 to induce cartilage and bone at nonskeletal sites in vivo, in-

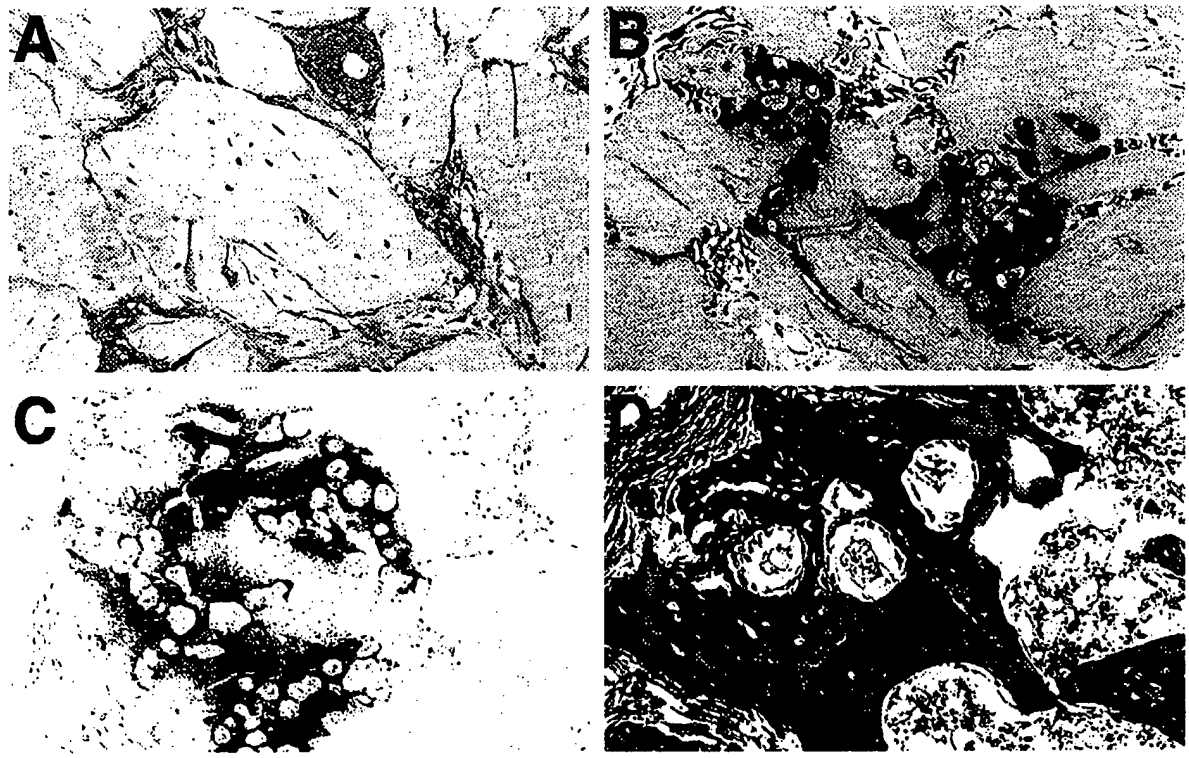

FIG. 2. In vivo ectopic induction of cartilage and bone by CDMPs. A) Negative control consisting of guanidine-extracted demineralized rat bone matrix (residue used as carrier; day 10; toluidine blue staining). (B) One microgram of CDMP-1-treated tissue showing newly formed cartilage islands between the rat carrier matrix particles (day 10; toluidine blue staining). (C) One microgram of CDMP-1-treated tissue showing Von Kossa staining of implants after 10 days. (D) One microgram of CDMP-1-treated tissue showing Masson's trichrome staining of newly formed woven bone and bone marrow in implants after 21 days. (A, B, and C) Magnification ×400; (D) ×200.

creasing doses of recombinant growth factors were reconstituted with 25 mg of rat collagen carrier, lyophilized, and implanted subcutaneously in the thoracic region of 28- to 35-day-old male Long-Evans rats as described.[10] Implants without the addition of CDMPs served as negative controls. The animals were sacrificed 10 and 21 days after implantation, and their implants were fixed, plastic embedded, and sectioned. Sections were subsequently stained with toluidine blue, von Kossa, or Masson's trichrome. Cartilage and bone-forming activity were further quantitated by determining the specific activity of alkaline phosphatase (ALP).[10]

Cell culture

The mouse embryonic teratocarcinoma cell line ATDC5, the mouse calvarial osteoblastic clonal cell line MC3T3-E1, the mouse myoblast cell line C2C12, and R mutant Mv1Lu cells were cultured in a 1:1 mixture of Dulbecco's modified Eagle's medium (DMEM) and Ham's F-12 containing 5% fetal bovine serum (FBS) and antibiotics (100 U/ml penicillin G, 100 mg/ml streptomycin, and 0.25 μg/ml amphotericin B; Life Technologies, Gaithersburg, MD, U.S.A.). The rat osteoprogenitor-like cell line ROB-C26 was grown in alpha-minimal essential medium (Life Technologies) containing 10% FBS and antibiotics. All experiments were performed under serum-free conditions using a chemically defined basal medium (BM). The serum-free BM consisted of Ham's F-12/DMEM (1/1) with ITS + culture supplement (Collaborative Biomedical Products, Bedford, MA), alpha-ketoglutarate (1×10^{-4} M), ceruloplasmin (0.25 U/ml), cholesterol (5 μg/ml), phosphatidylethanolamine (2 μg/ml), alpha-tocopherol acid succinate (9×10^{-7} M), reduced glutathione (10 μg/ml), taurine (1.25 μg/ml), triiodothyronine (1.6×10^{-9} M), hydrocortisone (1×10^{-9} M), and parathyroid hormone (5×10^{-10} M), β-glycerophosphate (10 mM final concentration), and L-ascorbic acid 2-sulfate (50 μg/ml) (Sigma Chemical Co., St. Louis, MO, U.S.A.).

For proteoglycan biosynthesis and ALP activity assays, cells were plated at a density of 4×10^4 cells in BM in 24-multiwell plates (Costar, Cambridge, MA, U.S.A.). Growth factors were added the next day, and the culture media were replaced every other day. Cultures were maintained at 37°C in humidified air and 5% CO_2. To determine DNA synthesis, 1×10^6 cells were plated out in BM in 100 mm tissue culture dishes (Falcon, Becton Dickinson Labware, Lincoln Park, NJ, U.S.A.) and cultured similarly.

Human fetal limbs from 52- to 79-day-old fetuses were kindly provided by the Central Laboratory for Human Embryology, University of Washington, Seattle, WA, U.S.A..

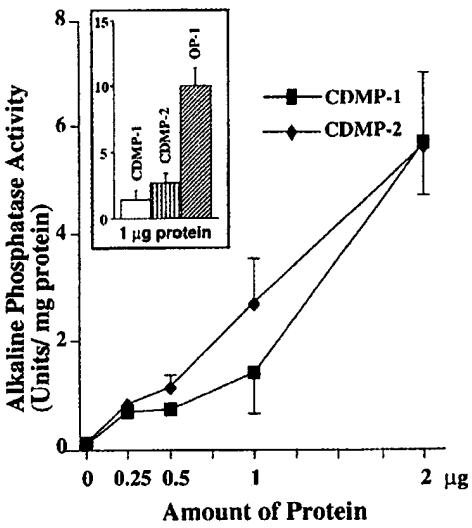

FIG. 3. ALP activity in CDMP-1 and CDMP-2 containing in vivo implants. ALP activity was measured to determine the extent of chondro/osteogenesis induced by increasing concentrations of purified refolded bacterially expressed CDMP-1 and CDMP-2. Values represent the means and standard deviations of the means of four to eight observations. Comparison of ALP activity between equal amounts (1 µg) of CDMP-1, CDMP-2, and OP-1 is depicted in the inset. Experiments were repeated three times.

This was approved by the Office of Human Subjects Research of the National Institutes of Health. The cartilaginous cores were carefully dissected from the surrounding fetal tissue, and the chondrocytes were released by a 6-h digestion in 0.2% collagenase B (Boehringer Mannheim, Indianapolis, IN, U.S.A.) in BM at 37°C. Postnatal bovine articular chondrocytes were prepared as described.[11] For the evaluation of newly synthesized proteoglycans and for DNA-content measurement, chondrocytes were plated out in BM in the same density as described above for the cell lines.

DNA determination

DNA content from chondrocytes and ATDC5 cells was determined after 1, 2, and 10 days of culture using bisbenzimide (Hoechst 33258, Sigma).[12]

ALP activity

ALP activity was determined in sonicated cell homogenates after 4, 6, and/or 10 days of treatment.[13] Briefly, after extensive washing with phosphate buffered saline (PBS), cell layers were sonicated in 500 µl of PBS containing Triton X-100 (0.05% final concentration). Aliquots of 50–100 µl were assayed for enzyme activity in assay buffer (0.1 M sodium barbital buffer, pH 9.3) and p-nitrophenyl phosphate (Sigma) as substrate. Absorbance was measured at 400 nm. Activity was normalized to protein content measured by the Bradford protein assay using bovine serum

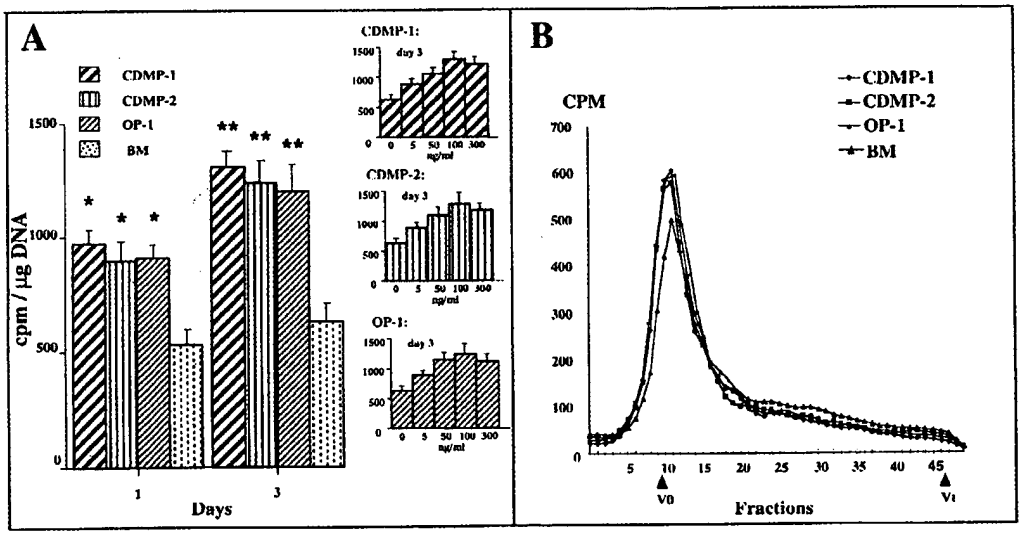

FIG. 4. [^{35}S]sulfate incorporation and analysis of the hydrodynamic size of newly synthesized macromolecules in primary fetal chondrocyte cultures. (A) Quadruplicate cultures of chondrocytes were treated for 24 and 72 h with CDMP-1 (100 ng/ml), CDMP-2 (100 ng/ml), or OP-1 (100 ng/ml). Cell cultures were labeled with [^{35}S]sulfate for 6 h, and the incorporated radiolabel was calculated per microgram of DNA content. Dose–response data were performed with four doses of CDMP-1, CDMP-2, and OP-1 and are shown in insets. The bars represent the means and standard deviations of the means. Experiments were repeated three times. (B) For the analysis of the hydrodynamic size of newly synthesized macromolecules, [^{35}S]-labeled materials were applied to a Sephacryl S-500 HR column. *$p < 0.03$ versus BM. **$p < 0.03$ versus BM and $p < 0.04$ versus day 1.

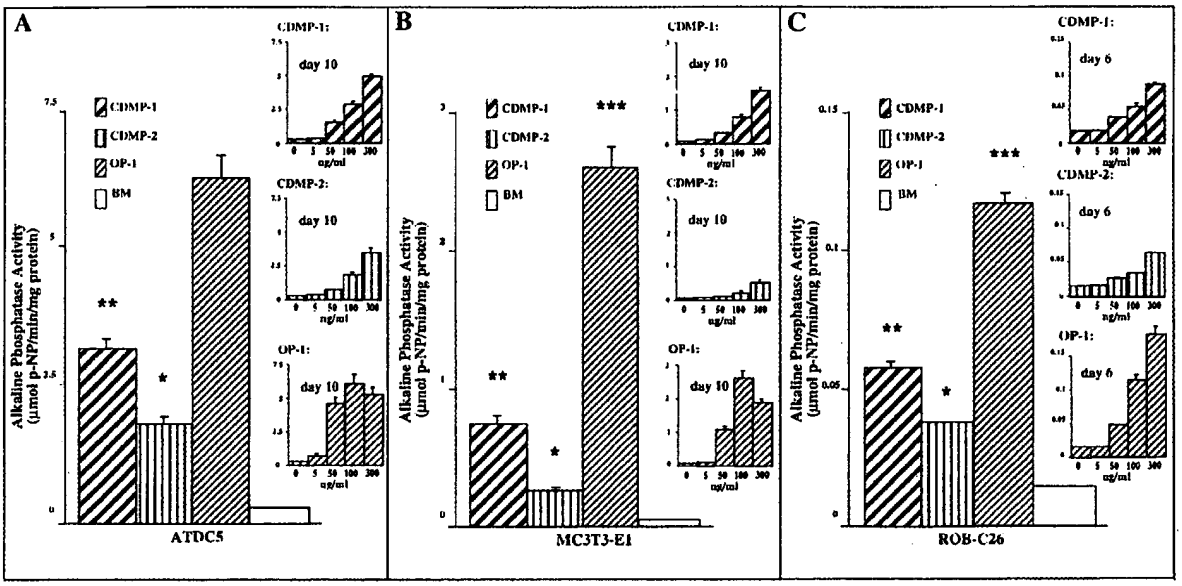

FIG. 5. Effect of CDMP-1, CDMP-2 and OP-1 on ALP activity of ATDC5, MC3T3-E1, and ROB-C26 cells. Quadruplicate cultures of (A) ATDC5, (B) MC3T3-E1, and (C) ROB-C26 cells were grown in the presence or absence of CDMP-1 (100 ng/ml), CDMP-2 (100 ng/ml), or OP-1 (100 ng/ml). Dose–response data with four doses of CDMP-1, CDMP-2, and OP-1 are shown in insets. The error bars indicate the standard deviations of the means of four observations: $***p < 0.03$ versus CDMP-1, CDMP-2, and BM; $**p < 0.03$ versus CDMP-2 and BM; and $*p < 0.03$ versus BM.

albumin (BSA) as standard (Bio-Rad, Richmond, CA, U.S.A.).

Proteoglycan biosynthesis

Rates of [^{35}S]sulfate incorporation into macromolecules were evaluated as described.[11] Briefly, cell cultures were labeled with 50 μCi/ml of [^{35}S]sulfate for 6 h at 37°C. Newly synthesized [^{35}S]sulfate-labeled macromolecules of both cell extracts (4 M guanidine-HCl in 50 mM Tris, pH 7.2), and media were determined after removal of unincorporated isotope using Sephadex G-25 (PD-10, Pharmacia Biotech, Piscataway, NJ, U.S.A.) gel chromatography. The values were normalized to DNA content. To determine the size of the newly synthesized material, 500 μl aliquots of the radiolabeled fraction were analyzed on a Sephacryl S-500 HR column (1 × 30 cm; Pharmacia Biotech), previously equilibrated with 4 M guanidine HCl, 0.5% Triton X-100 in 50 mM sodium acetate buffer, pH 6.0, at a flow rate of 0.4 ml/minute. Each fraction was measured for radioactivity. A small quantity of [^{3}H]glucosamine was added as an internal elution position marker.

RNA isolation and Northern blot analysis

Total RNA was extracted using the acidic guanidine-phenol-chloroform method.[14] For Northern blot analysis, equal amounts (5 μg) of total RNA were electrophoresed on 1.2% agarose-formaldehyde gels and transferred to Nytran membranes (Schleicher and Schuell, Keene, NH, U.S.A.). The blots were prehybridized for 30 minutes at 68°C in hybridization buffer (Express Hyb, Clontech, Palo Alto, CA, U.S.A.), and hybridization was performed for 1 h at 68°C in the same buffer with ^{32}P-labeled cDNA probes. Probes included mouse cDNAs encoding biglycan, decorin, bone sialoprotein (BSP), osteocalcin,[15] and human ALP. A probe for glyceraldehyde-3-phosphate dehydrogenase (GAPDH) was used as control cDNA probe. After hybridization, the filters were washed four times in 2× sodium chloride/sodium citrate (SSC), 0.5% SDS, and twice in 0.2× SSC, 1% SDS at room temperature for 10 minutes The blots were then exposed to Kodak XAR-5 films (Eastman Kodak, Rochester, NY, U.S.A.) at –70°C for up to 24 h and quantitated using a phosphorimager (Molecular Dynamics, Sunnyvale, CA, U.S.A.). The amounts of detected transcripts were normalized to GAPDH.

Radiolabeling of CDMP-1 and CDMP-2

CDMP-1 and CDMP- 2 were iodinated with chloramine-T.[16] Both ligands were radiolabeled to an equal specific activity.

Affinity cross-linking and immunoprecipitation

Cells were incubated 3 h on ice in binding buffer (PBS containing 0.9 mM $CaCl_2$, 0.49 mM $MgCl_2$, and 0.1% BSA) in the presence of 200–400 pM of iodinated ligand. After incubation, the cells were washed and cross-linking was performed using 1 mM bis(sulfosuccinimidyl)suberate (Pierce Chemical Co., Rockford, IL, U.S.A.) and 0.28 mM disuccinimidyl suberate for 15 minutes. The cells were

washed, scraped off the plates, centrifuged, resuspended in solubilization buffer, and incubated for 20 minutes on ice. Immunoprecipitation of the cross-linked materials was performed as described.[17] Two T 75 flasks of subconfluent cells were used for each immunoprecipitation.[18] The immune complexes were eluted by boiling for 3 minutes in SDS sample buffer containing 10 mM dithiotreitol and separated by SDS-PAGE. These gels were then dried and followed by Bio-Imaging analysis (Fuji, BAS2000; Fuji, Tokyo, Japan) or autoradiography.

Transcriptional activation response assay

Chemically mutagenized Mv1Lu cells were cotransfected with a p3TP-Lux promoter/reporter construct, BMPR-II, and plasmids containing various type I receptor cDNAs. One day after transfection, cells were treated for 20 h with CDMP-1 or CDMP-2 under serum-free conditions. Luciferase activity in the cell lysate was analyzed using the luciferase assay system (Promega Biotech, Madison, WI, U.S.A.) according to the manufacturer's protocol and a luminometer (MGM Instruments, Hamden, CT, U.S.A.).

Statistical analysis

Statistical significance was defined as a p-value < 0.05 with the Mann–Whitney U-test.

RESULTS

Production of recombinant CDMP-1 and CDMP-2

The mature domains of *cdmp-1* and *cdmp-2* were expressed in *E. coli,* refolded, and purified using reverse phase HPLC (data not shown). Aliquots (5 μg) of the purified protein preparations were analyzed by SDS-PAGE before and after reduction and alkylation (Fig. 1). The nonreduced proteins migrated as a major band around 28 kDa, while the reduced fractions showed a band at 16 kDa. These findings are consistent with appropriate homodimer formation.

CDMP-1 and CDMP-2 induce cartilage and bone formation in vivo

Histologic evaluation of the in vivo bioassay showed that implantation of the carrier without the addition of CDMPs did not initiate cartilage or bone formation (Fig. 2A). CDMP-1, CDMP-2, and OP-1 induced islands of chondrocytes 10 days after implantation (Fig. 2B). Furthermore, Von Kossa staining indicated ongoing de novo mineralization (Fig. 2C). At day 21, bone formation was apparent in the implants (Fig. 2D). A dose response experiment was performed for CDMP-1 and CDMP-2 and biochemical analysis of day 10 implants produced comparable, dose-dependent increases in ALP activity (Fig. 3). However, CDMPs were significantly less active in this in vivo assay than OP-1 ($p < 0.03$; Fig. 3, inset).

CDMP-1,CDMP-2, and OP-1 equally stimulate proteoglycan synthesis in primary chondrocytes

CDMP-1, CDMP-2, and OP-1 increased [^{35}S]sulfate incorporation into proteoglycans equally. This effect was apparent in both fetal chondocytes (Fig. 4A) and postnatal articular chondrocytes (data not shown) and was concentration- and time-dependent. Analysis of the hydrodynamic size of the newly synthesized macromolecules demonstrated the presence of the large proteoglycan species, which eluted in the void volume of a Sephacryl S-500 HR column, consistent with a cartilage phenotype (Fig. 4B). Cell proliferation, as measured by DNA content, was not affected by growth factor treatment (data not shown).

CDMPs are less osteogenic than OP-1 in osteoblast-like cell lines

We analyzed the expression of osteogenic markers in the mouse osteo/chondroprogenitor cell line ATDC5, the osteoblastic mouse clonal cell line MC3T3-E1, and the rat osteoprogenitor-like cell line ROB-C26 to determine whether CDMPs promote osteogenic differentiation. Treatment with both CDMP-1 and CDMP-2 resulted in an increase of ALP activity when compared with basal medium in all the cell lines ($p < 0.03$) (Fig. 5). This effect was significantly less with CDMP-2 than CDMP-1 ($p < 0.03$). In contrast, OP-1 was 2- to 3-fold more stimulatory than CDMP-1 ($p < 0.03$). Interestingly, in human fetal chondrocytes (52-79 days), OP-1 increased ALP values more than 10-fold, whereas CDMP-1 and CDMP-2 only slightly enhanced this activity (Fig. 6A). In the myoblast cell line C2C12, osteogenic differentiation was promoted by OP-1 but not by the CDMPs (Fig. 6B).

Further analysis of osteogenic differentiation was performed using Northern blot analysis of osteogenic markers. In ATDC5 cells, cultured in the presence of the indicated morphogens, OP-1 and CDMP-1 increased ALP mRNA levels (Fig. 7). In addition, transcripts for BSP were strongly up-regulated after OP-1 treatment, while CDMP-1 was less potent in this regard (Fig. 7). CDMP-2 only slightly enhanced BSP expression (Fig. 7). The expression of osteocalcin mRNA was not detected (data not shown). Northern blot analysis for the small proteoglycan species biglycan and decorin showed that OP-1 up-regulated decorin expression (Fig. 7). These data support differential regulation of osteogenic differentiation by OP-1, CDMP-1, and CDMP-2.

CDMP-1 and CDMP-2 bind to BMPR-IB and BMPR-II in nontransfected cells

To identify which type I and type II receptors have affinity for CDMP-1 and CDMP-2, binding studies were performed using ^{125}I-labeled CDMPs in various cell lines and in primary chondrocytes. ROB-C26 cells were affinity-labeled with iodinated CDMP-1 and CDMP-2, and the cross-linked complexes were immunoprecipitated using antisera to a panel of type I and type II receptors and analyzed by SDS-PAGE under reducing conditions. Cross-linked complexes of 80-90 kDa could be immunoprecipitated by

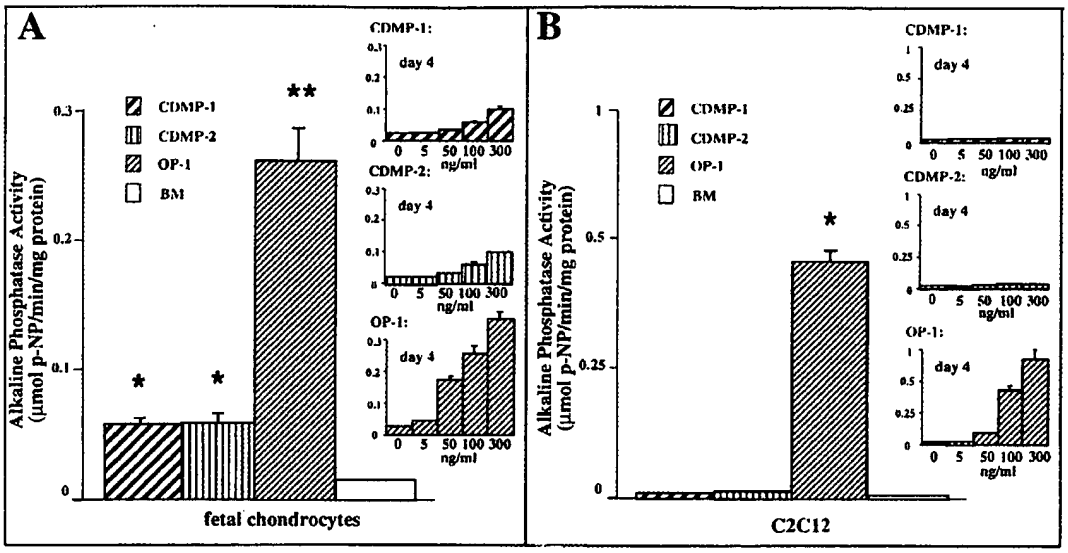

FIG. 6. ALP activity in primary fetal chondrocytes and C2C12 cells treated with CDMP-1, CDMP-2, and OP-1. Quadruplicate cultures of (A) primary fetal chondrocytes and (B) C2C12 cells were cultured in the presence or absence of CDMP-1 (100 ng/ml), CDMP-2 (100 ng/ml), or OP-1 (100 ng/ml) under serum-free conditions. The specific activity of ALP was quantitated after 4 days of treatment. Dose–response data with four doses of CDMP-1, CDMP-2, and OP-1 are depicted in insets. The bars represent the means and standard deviations of the means. Experiments were repeated three times. (A) $*p < 0.03$ versus BM and $**p < 0.03$ versus CDMP-1, CDMP-2, and BM. (B) $*p < 0.03$ versus CDMP-1, CDMP-2, and BM.

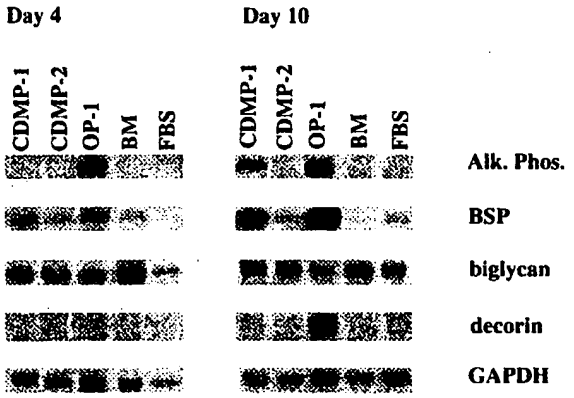

FIG. 7. Northern analysis of CDMP-1, CDMP-2, and OP-1-treated samples on the expression of osteogenic markers in ATDC5 cells. Cells were cultured with or without CDMP-1 (100 ng/ml), CDMP-2 (100 ng/ml), OP-1 (100 ng/ml), or 5% FBS for 4 and 10 days. Total RNA from each culture (5 µg) was separated on 1.2% agarose formaldehyde-agarose gels, blotted, and subsequently hybridized with the respective cDNA probes as described in Materials and Methods. GAPDH expression levels are shown to verify equal loading of mRNA (bottom).

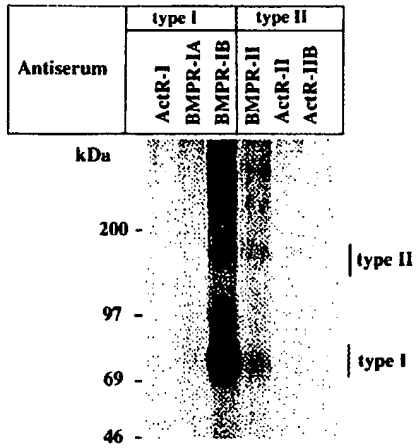

FIG. 8. Binding of CDMP-2 to type I and type II receptors in ROB-C26 cells. Binding and affinity cross-linking of ^{125}I-radiolabeled CDMP-2 were performed using ROB-C26 cells, followed by immunoprecipitation using antisera against type I and type II receptors. Samples were analyzed by SDS-PAGE and autoradiography using Bio-Imaging Analyzer.

antisera to BMPR-IB and BMPR-II for both CDMP-1 and CDMP-2. Their binding characteristics were similar, and one representative autoradiograph is shown in Fig. 8. A high molecular weight complex of 150–200 kDa, which may represent a type II receptor complex, was coimmunoprecipitated by the BMPR-IB (Fig. 8). Coimmunoprecipitation of the type I receptor complex was also detected by the BMPR-II antiserum (Fig. 8). A weak band could be seen after immunoprecipitation with the antiserum against

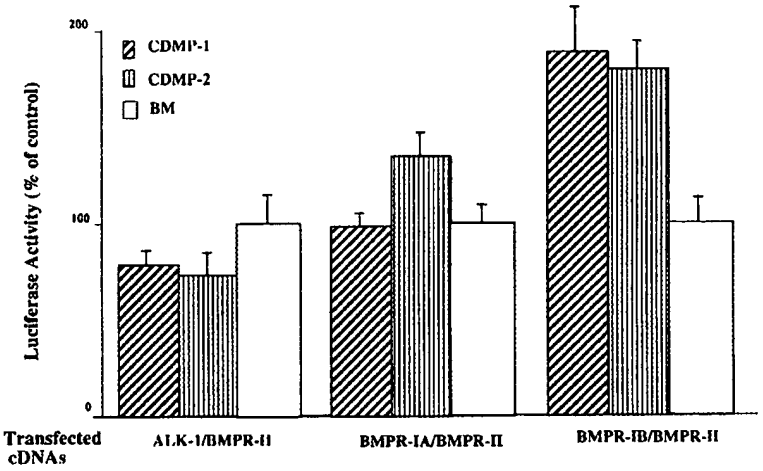

FIG. 9. Signal transduction by CDMP-1 and CDMP-2 in transfected R mutant Mv1Lu cells. (A) p3TP-Lux promoter/reporter construct was co-transfected with a cDNA for BMPR-II and plasmids containing activin receptor-like kinase (ALK)-I (negative control), BMPR-IA, or BMPR-IB into R mutant Mv1Lu cells. One day after transfection, cells were treated for 20 h with CDMP-1 (300 ng/ml) or CDMP-2 (300 ng/ml) followed by the measurement of the luciferase activity in the cell lysates. The bars represent the means and standard deviations of the means of three independent experiments.

BMPR-IA, whereas antisera against activin receptor (ActR)-I, ActR-II and ActR-IIB did not immunoprecipitate any appreciable amounts of CDMP cross-linked complexes (Fig. 8).

CDMPs transduce a transcriptional activation signal by BMPR-IB and BMPR-II in transfected cells

To investigate whether CDMP-1 and CDMP-2 are able to transduce a signal upon binding to their respective type I and type II receptor complexes, the signaling activity of CDMPs was analyzed in R mutant Mv1Lu cells using the p3TP-Lux promoter/reporter construct. The BMPR-IB/BMPR-II complex mediated an efficient signal for both CDMPs, which was in agreement with our binding data (Fig. 9). Furthermore, CDMP-2 but not CDMP-1 transduced a weak signal through the BMPR-IA/BMPR-II complex (Fig. 9). No activation was observed with other type I receptors in the complex. Cells transfected with either type I or type II receptors only did not respond to the CDMPs (data not shown).

DISCUSSION

Our study compared for the first time the activity of recombinant CDMP-1, CDMP-2, and OP-1 in the initiation and progression of chondrogenic and osteogenic differentiation both in vivo and in vitro. Our findings suggest that the CDMPs are equipotent in stimulating cartilage matrix synthesis when compared with OP-1, but have markedly reduced activity in the promotion of osteogenesis. Furthermore, CDMP-2 appeared to be less osteogenic than CDMP-1 in vitro. In addition, our data indicate that the underlying molecular basis for the differential biological responses between CDMP-1, CDMP-2, and OP-1 might be their relative affinities for specific receptor complexes.

The in vivo assay for ectopic induction of cartilage and bone formation, using rat bone residue as the delivery system, confirmed that CDMP-1 and -2 are not only structurally but also functionally related to BMPs 2, 4, 5, 6, 7.[19,20] Ectopic bone induction for Gdf-5/CDMP-1 has previously been reported.[20] Our data showed that CDMP-1 and CDMP-2 equally induce cartilage and bone formation. Interestingly, CDMPs appear to be significantly less active in this in vivo assay than OP-1. It is conceivable that the use of other carriers might affect the outcome of the cartilage and bone-inducing properties of the morphogens.

We studied the promotion of cartilage differentiation by CDMP-1 and -2 in vitro using primary cell cultures. The enhanced de novo proteoglycan aggrecan synthesis in primary chondroblasts originating from fetal limbs, as well as in postnatal articular chondrocyte cultures, supports the stimulatory role of the CDMPs in chondrogenic differentiation. It is of note that we were unable to detect differences in type II collagen expression levels by Northern analysis under the culture conditions described (data not shown). This may be due to already high expression levels at the start of the culture, because we are mainly enhancing an already existing cartilage phenotype. Only in low density monolayer cultures could we detect an up-regulation of this chondrogenic marker in the presence of CDMPs or OP-1 (data not shown). No differences in the stimulation of cartilage matrix synthesis were observed between CDMP-1, CDMP-2, and OP-1 treatments. Enhancement of matrix synthesis in chondrocyte cultures has been reported for other BMPs previously.[11,21,22] These and our data suggest that in these cell cultures BMPs/CDMPs may use the same signaling pathways regulating cartilage matrix synthesis. In contrast, using ALP activity as a marker for chondrocyte maturation/bone formation, the CDMPs are not, or only to a limited extent, affecting this marker when compared with OP-1. To explore further a difference in the promotion of the progression in the osteogenic lineage, we found that CDMPs were significantly less osteogenic than OP-1 in various osteoblast-like cell lines. It is noteworthy that the osteogenic differentiation induced by OP-1 as observed in ATDC5 cells, is associated with an increase of BSP and decorin, reflecting a full commitment in the osteogenic lineage with bone matrix deposition. The modest osteogenic activity of CDMP-1 is in contrast to previously published data, reporting no effect of Gdf-5, the mouse ho-

molog of CDMP-1, on osteoblastic cells cultured in serum-containing media.[17,20] This difference may be due to the fact that we used a chemically defined serum-free medium. Indeed, we have demonstrated that biological responses to BMPs in in vitro models are diminished in the presence of FBS.[23] In addition, this low osteogenic activity of the CDMPs was most pronounced in C2C12 cells, where no increase in ALP activity by CDMPs was observed, whereas OP-1 and as previously described BMP-2 convert these cells into the osteoblastic lineage in low serum conditions.[24] Therefore, the combined data suggest that the signaling cascade(s) with regard to osteogenesis may be distinct from these involved in cartilage differentiation, and that different members of the BMP family signal through specific pathways. In addition, our Northern analysis data in ATDC-5 cells provide further evidence that CDMP-1 and CDMP-2, although highly related (80% sequence identity in the mature biologically active region) may have distinct biological profiles depending on the cell populations.

In a first attempt to identify the molecular basis for specific biological activities elicited by various BMPs/CDMPs, in particular chondrogenesis and osteogenesis, we set out to characterize the receptor complexes for the CDMPs. We demonstrated in this manuscript that CDMP-1 and CDMP-2 bind predominantly to the BMPR-IB and BMPR-II receptors. In addition, our transcriptional response data showed that CDMPs signal through this BMPR-IB/BMPR-II complex. This is in agreement with the findings that Gdf-5 binds and signals through this complex.[17] Recently, using the in vivo developing chick limb model and in vitro micromass cultures, Kawakami et al. found that BMPR-IB and BMPR-II are the critical receptor complexes in chondrogenesis of limb mesenchymal cells.[25] These authors demonstrated intense expression of BMPR-IB in the developing limb, and showed that a dominant negative BMPR-IB receptor markedly inhibited chondrogenesis as measured by cartilage nodule formation and de novo proteoglycan synthesis. Taken together, the preferential binding of the CDMPs to the BMPR-IB/BMPR-II complex and the evidence of the direct association of this complex with chondrogenesis provides a molecular cascade for the stimulation of chondrogenic differentiation by the CDMPs. In contrast, OP-1 binds and signals through other receptor complexes besides BMPR-IB/BMPR-II.[6,7] Therefore, our data further support the possibility of the existence of distinct molecular pathways associated with osteogenesis and chondrogenesis.

A potential limitation in the interpretation of the data relates to the preparation method of the recombinant proteins because the CDMPs are bacterially refolded proteins while OP-1 was produced in mammalian cells.[19] Contaminants or the presence of inappropriately folded proteins in the CDMP preparations may affect their biological responses. However, we have consistently found the same results using at least three different batches of HPLC-purified proteins. In addition, our data show that the CDMPs and OP-1 have identical effects in dose response experiments on the proteoglycan synthesis in human fetal chondrocyte cultures, while only OP-1 stimulates ALP levels in the same cultures. Finally, the differential responses for CDMP-1 when compared with CDMP-2, most strikingly observed in ATDC-5 cells (Fig. 7), makes it unlikely that the distinct biological responses are due to different protein preparation methods.

In conclusion, we reported the expression of functional recombinant CDMP-1 and CDMP-2 and their biological activities in chondrogenic and osteogenic models in vivo and in vitro. The data show a weak osteogenic potential of the CDMPs when compared with OP-1. This differential response may be due to specific ligand–receptor interactions. Our studies suggest that the BMPs/CDMPs may provide powerful experimental tools to further unravel the mechanisms leading to cartilage or bone formation.

ACKNOWLEDGMENTs

We are grateful to Drs. Hynda K. Kleinmann, Terrig J. Thomas, Chee-Keng Ng, and Malcolm Moos for critical review of the manuscript. We thank Drs. Marian Young and Larry Fisher for providing cDNA probes, Dr. Peter Hauschka for providing ATDC5, and Drs. Hideki Nishitoh and Arnold Kahn for providing the ROB-C26 cells. Ludwig Erlacher is funded by an Erwin-Schrödinger Fellowship of the Austrian Society "Fonds zur Förderung der Wissenschaften."

REFERENCES

1. Chang SC, Hoang B, Thomas JT, Vukicevic S, Luyten FP, Ryba NJP, Kozak CA, Reddi AH, Moos M 1994 Cartilage-derived morphogenetic proteins: New members of the transforming growth factor-beta superfamily predominantly expressed in long bones during human embryonic development. J Biol Chem **269**:28227–28234.
2. Storm EE, Huynh TV, Copeland NG, Jenkins NA, Kingsley DM, Lee SJ 1994 Limb alterations in brachypodism mice due to mutations in a new member of the TGF beta-superfamily. Nature **368**:639–643.
3. Thomas JT, Lin K, Nandedkar M, Camargo M, Cervenka J, Luyten FP 1996 A human chondrodysplasia due to a mutation in a TGF-beta superfamily member. Nat Genet **12**:315–317.
4. Luyten FP 1995 Cartilage-derived morphogenetic proteins: Key regulators in chondrocyte differentiation? Acta Orthop Scand Suppl **266**:51–54.
5. ten Dijke P, Miyazono K, Heldin CH 1996 Signaling via hetero-oligomeric complexes of type I and type II serine/threonine kinase receptors. Curr Opin Cell Biol **8**:139–145.
6. ten Dijke P, Yamashita H, Sampath TK, Reddi AH, Estevez M, Riddle DL, Ichijo H, Heldin CH, Miyazono K 1994 Identification of type I receptors for osteogenic protein-1 and bone morphogenetic protein-4. J Biol Chem **269**:16985–16988.
7. Yamashita H, ten Dijke P, Huylebroeck D, Sampath TK, Andries M, Smith JC, Heldin CH, Miyazono K 1995 Osteogenic protein-1 binds to activin type II receptors and induces certain activin-like effects. J Cell Biol **130**:217–226.
8. Asahina I, Sampath TK, Hauschka PV 1996 Human osteogenic protein-1 induces chondroblastic, osteoblastic and/or adipocytic differentiation of clonal murine target cells. Exp Cell Res **222**:38–47.
9. Kunkel TA 1985 Rapid and effective site-specific mutagenesis without phenotypic selection. Proc Natl Acad Sci USA **82**:488–492.
10. Luyten FP, Cunningham NS, Ma S, Muthukumaran N, Hammonds RG, Nevins WB, Wood WI, Reddi AH 1989 Purifica-

tion and partial amino acid sequence of osteogenin, a protein initiating bone differentiation. J Biol Chem **264**:13377–13380.
11. Luyten FP, Chen P, Paralkar V, Reddi AH 1994 Recombinant bone morphogenetic protein-4, transforming growth factor-beta 1, and activin A enhance the cartilage phenotype of articular chondrocytes in vitro. Exp Cell Res **210**:224–229.
12. Labarca C, Paigen K 1980 A simple, rapid and sensitive DNA assay procedure. Anal Biochem **102**:344–352.
13. Reddi AH, Huggins CB 1972 Citrate and alkaline phosphatase during transformation of fibroblasts by the matrix and minerals of bone. Proc Soc Exp Biol Med **140**:807–810.
14. Chomczynski P, Sacchi N 1987 Single-step method of RNA isolation by acid guanidinium thiocyanate-phenol-chloroform extraction. Anal Biochem **162**:156–159.
15. Fisher LW, Stubbs JT 3rd, Young MF 1995 Antisera and cDNA probes to human and certain animal model bone matrix noncollagenous proteins. Acta Orthop Scand Suppl **266**:61–65.
16. Frolik CA, Wakefield LM, Smith DM, Sporn MB 1984 Characterization of a membrane receptor for transforming growth factor-beta in normal rat kidney fibroblasts. J Biol Chem **259**:10995–11000.
17. Nishitoh H, Ichijo H, Kimura M, Matsumoto T, Makishima F, Yamaguchi A, Yamashita H, Enomoto S, Miyazono K 1996 Identification of type I and type II serine/threonine kinase receptors for growth/differentiation factor-5. J Biol Chem **271**:21345–21352.
18. ten Dijke P, Yamashita H, Ichijo H, Franzen P, Laiho M, Miyazono K, Heldin CH 1994 Characterization of type I receptors for transforming growth factor-beta and activin. Science **264**:101–104.
19. Sampath TK, Maliakal JC, Hauschka PV, Jones WK, Sasak H, Tucker RF, White KH, Coughlin JE, Tucker MM, Pang RH, Corbett C, Özkaynak E, Oppermann H, Rueger DC 1992 Recombinant human osteogenic protein-1 (hOP-1) induces new bone formation in vivo with a specific activity comparable with natural bovine osteogenic protein and stimulates osteoblast proliferation and differentiation in vitro. J Biol Chem **267**:20352–20362.
20. Hötten GC, Matsumoto T, Kimura M, Bechtold RF, Kron R, Ohara T, Tanaka H, Satoh Y, Okazaki M, Shirai T, Pan H, Kawai S, Pohl JS, Kudo A 1996 Recombinant human growth/differentiation factor 5 stimulates mesenchyme aggregation and chondrogenesis responsible for skeletal development of limbs. Growth Factors **13**:65–74.
21. Vukicevic S, Luyten FP, Reddi AH 1989 Stimulation of the expression of osteogenic and chondrogenic phenotypes in vitro by osteogenin. Proc Natl Acad Sci USA **86**:8793–8797.
22. Carrington JL, Chen P, Yanagishita M, Reddi AH 1991 Osteogenin (bone morphogenetic protein-3) stimulates cartilage formation by chick limb bud cells in vitro. Dev Biol **146**:406–415.
23. Vukicevic S, Luyten FP, Reddi AH 1990 Osteogenin inhibits proliferation and stimulates differentiation in mouse osteoblast-like cells. Biochem Biophys Res Commun **166**:750–756.
24. Katagiri T, Yamaguchi A, Komaki M, Abe E, Takahashi N, Ikeda T, Rosen V, Wozney JM, Fujisawa-Sehara A, Suda A 1994 Bone morphogenetic protein-2 converts the differentiation pathway of C2C12 myoblasts into the osteoblast lineage. J Cell Biol **127**:1755–1766.
25. Kawakami Y, Ishikawa T, Shimabara M, Tanda N, Enomoto-Iwamoto M, Iwamoto M, Kuwana T, Ueki A, Noji S, Nohno T 1996 BMP signaling during bone pattern determination in the developing limb. Development **122**:3557–3566.

Address reprint requests to:
Dr. Frank P. Luyten
Division of Rheumatology
UZ Pellenberg
Weligerveld 1
3212 Pellenberg, Belgium

Received in original form May 30, 1997; in revised form September 30, 1997; accepted October 14, 1997.

Exhibit K

JOURNAL OF CELLULAR PHYSIOLOGY 187:265–276 (2001)

Divergence and Convergence of TGF-β/BMP Signaling

KOHEI MIYAZONO,[1,2]* KIYOSHI KUSANAGI,[2] AND HIROFUMI INOUE[2]

[1]*Department of Molecular Pathology, Graduate School of Medicine, University of Tokyo, Hongo, Bunkyo-ku, Tokyo Japan*

[2]*Department of Biochemistry, The JFCR Cancer Institute, Kami-ikebukuro, Toshima-ku, Tokyo, Japan*

The transforming growth factor-β (TGF-β) superfamily includes more than 30 members which have a broad array of biological activities. TGF-β superfamily ligands bind to type II and type I serine/threonine kinase receptors and transduce signals via Smad proteins. Receptor-regulated Smads (R-Smads) can be classified into two subclasses, i.e. those activated by activin and TGF-β signaling pathways (AR-Smads), and those activated by bone morphogenetic protein (BMP) pathways (BR-Smads). The numbers of type II and type I receptors and Smad proteins are limited. Thus, signaling of the TGF-β superfamily converges at the receptor and Smad levels. In the intracellular signaling pathways, Smads interact with various partner proteins and thereby exhibit a wide variety of biological activities. Moreover, signaling by Smads is modulated by various other signaling pathways allowing TGF-β superfamily ligands to elicit diverse effects on target cells. Perturbations of the TGF-β/BMP signaling pathways result in various clinical disorders including cancers, vascular diseases, and bone disorders. J. Cell. Physiol. 187: 265–276, 2001. © 2001 Wiley-Liss, Inc.

Transforming growth factor-β (TGF-β) is a potent growth inhibitor for a wide variety of cells including epithelial cells, vascular endothelial cells, hematopoietic cells, and immune lymphocytes (Roberts and Sporn, 1990; Miyazono et al., 1994; Blobe et al., 2000). Perturbations of the TGF-β signaling pathways result in loss of cell growth regulation which is one of the most crucial steps in oncogenesis. TGF-β is also a potent inducer of tissue fibrosis, which may provide a microenvironment suitable for growth of transformed cells.

Three isoforms of TGF-β, i.e. TGF-β1, TGF-β2, and TGF-β3, with similar structures and in vitro biological activities have been identified in mammals (Roberts and Sporn, 1990). Many other proteins also have structures essentially similar to TGF-β and are collectively referred to as the TGF-β superfamily. The TGF-β superfamily includes more than 30 proteins in mammals, e.g. activins, bone morphogenetic proteins (BMPs), and anti-Müllerian hormone (AMH, also termed Müllerian inhibiting substance or MIS) (Kawabata and Miyazono, 2000). Growth/differentiation factors (GDFs) also belong to the TGF-β superfamily. Some of them, including GDF-5, GDF-6, and GDF-7, are BMP-like proteins, but others have been only partially characterized.

In this review article, we discuss some recent progress in research on signal transduction by the TGF-β superfamily proteins, focusing on how a wide variety of ligands bind to limited number of receptors, and how the receptors and their signal transducer Smads transmit diverse signals in target cells. We also discuss how these molecules are linked to the pathogeneses of various clinical disorders.

LIMITED DIVERSITY OF SERINE/THREONINE KINASE RECEPTORS AND SMAD PROTEINS

As described above, the TGF-β superfamily includes more than 30 members in mammals. Two questions arise here; first is that why are there so many members of the TGF-β superfamily? and second that is it possible to classify these proteins into several groups?

Proteins of the TGF-β superfamily bind to two different types of signaling receptors termed as type II and type I receptors. Although some other cell surface proteins have been shown to bind TGF-β, type II and type I receptors are most important for TGF-β superfamily signaling (Massagué, 1998). Both type II and type I receptors contain serine/threonine kinase domains in their intracellular portions and exist on cell surface in various oligomeric forms, e.g. type II homomers, type I homomers, and type II-type I heteromers (Gilboa et al., 2000). The type II receptor kinases are constitutively active without ligand stimulation. Upon ligand binding

*Correspondence to: Kohei Miyazono, Department of Biochemistry, The JFCR Cancer Institute, 1-37-1 Kami-ikebukuro, Toshima-ku, Tokyo 170-8455, Japan.
E-mail: miyazono-ind@umin.ac.jp

Received 17 January 2001; Accepted 17 January 2001

Published online in Wiley InterScience, 4 April 2001.

and formation of type II and type I receptor complexes, followed by possible receptor conformational changes, type I receptors are phosphorylated and activated by type II receptor kinases. Type I receptor kinases then transmit intracellular signals by phosphorylating Smad proteins.

In mammals, only five type II receptors and seven type I receptors have been identified (Miyazono et al., 2000). The type II receptors include activin type II and type IIB receptors (ActR-II and ActR-IIB), TGF-β type II receptor (TβR-II), BMP type II receptor (BMPR-II), and AMH type II receptor (AMHR-II). Type I receptors are termed activin receptor-like kinases (ALKs) 1 through 7. It is theoretically possible to form more than 30 different combinations of type II and type I receptors. However, certain type II receptors tend to interact with certain type I receptors. Thus, the combinations of type II and type I receptors appear to be limited under physiological conditions and the variety of ligands converge at the receptor level.

The intracellular substrates, Smads, can be classified into three groups, i.e. receptor-regulated Smads (R-Smads), common-mediator Smads (Co-Smads), and inhibitory Smads (I-Smads) (Heldin et al., 1997). Specificity of the intracellular signals is determined by R-Smads, whereas Co-Smad serves as an adaptor molecule for R-Smads. In contrast, I-Smads antagonize signaling by R-Smads and Co-Smads. Five different R-Smads have been identified in mammals. Smad2 and Smad3 are activated by TGF-βs and activins (they are collectively referred to as type A R-Smads or AR-Smads in this review) whereas Smad1, Smad5 and Smad8 are activated by BMPs (referred to as type B R-Smads or BR-Smads). Thus, the variety of R-Smad signaling is also limited.

R-Smads are either AR-Smads or BR-Smads, but R-Smads in each subgroup are not equally activated by their cognate receptors. ALK-4 (also termed activin type IB receptor or ActR-IB), and ALK-5 (also known as TGF-β type I receptor or TβR-I) are the functional type I receptors for activins and TGF-βs, respectively. Although, Smad2 and Smad3 are structurally very similar to each other, they transmit distinct signals because of the differences in their ability to bind to specific DNA sequences, and possibly in other functions (Yagi et al., 1999). Smad2 is a signal transducer for activins during early embryogenesis (Nomura and Li, 1998; Waldrip et al., 1998), while Smad3 appears to be more important for TGF-β signaling in cell growth, movement and immune function in adult tissues (Ashcroft et al., 1999). In cultured keratinocytes, however, both Smad2 and Smad3 are activated by TGF-β, whereas only Smad3 is strongly phosphorylated by activin (Shimizu et al., 1998). Since Smad2 is more important than Smad3 in activin signaling during early embryogenesis, why Smad3 is preferentially activated by activin in keratinocytes remains to be elucidated.

Receptors and downstream signaling pathways for BMPs are also complex. ALK-3 and ALK-6, which are also termed BMP type IA and type IB receptors (BMPR-IA and BMPR-IB), respectively, are structurally similar to each other and function as BMP type I receptors by activating BR-Smads. In addition, ALK-2 binds certain BMPs, e.g. BMP-6 and BMP-7 (ten Dijke et al., 1994; Macías-Silva et al., 1998; Ebisawa et al., 1999). Specificity of the interaction of type I receptors with R-Smads is determined by a short region located between the kinase subdomains IV and V, the L45 loop, of type I receptor kinases (Feng and Derynck, 1997). The L45 loop of ALK-2 is less similar to those of ALK-3 and ALK-6 than those of ALK-4 and ALK-5 are. However, ALK-2 also activates BR-Smads, and transmits signals similar to those of ALK-3 and ALK-6 (Chen and Massagué, 1999). Interestingly, ALK-3 and ALK-6 activate all three BR-Smads, whereas ALK-2 can activate only Smad1 and Smad5, but not Smad8 (Ebisawa et al., 1999; Aoki et al., 2001). Functional differences between Smad8 and Smad1/5 have not been determined, but these BR-Smads have different motifs in their structures. For example, Smad1 and Smad5 have a PY motif in their linker regions, which is responsible for interaction with an E3 ubiquitin ligase, Smurf1 (Zhu et al., 1999), but Smad8 lacks this motif. Thus, Smad8 may be degraded by a mechanism distinct from that for Smad1 or Smad5. Differences in the activation patterns of BR-Smads by ALK-3/6 and ALK-2 may therefore generate different biological responses in target cells.

Non-Smad pathways may also be important in understanding the diversity of signals generated by the TGF-β superfamily proteins (Massagué 2000; Mulder, et al., 2000). MAP kinases, including ERK, JNK, and p38 MAP kinases, are activated by BMPs and TGF-βs in various cells, and might play important roles in TGF-β signaling in certain cell types. For example, the p38 MAP kinase plays crucial roles in the induction of chondrogenic phenotypes in chondroblastic cells and of apoptosis of lymphocytes (Nakamura et al., 1999; Kimura et al., 2000). However, activation of the MAP kinases by the TGF-β superfamily proteins depends on cell type and culture conditions, and these kinases are not always specifically activated by the TGF-β superfamily ligands (Massagué et al., 2000).

LIGANDS OF THE TGF-β SUPERFAMILY: ARE THERE ONLY TWO SUBFAMILIES?

Since R-Smads are classified into two groups and are specifically activated by cognate type I receptors, ligands of the TGF-β superfamily can also be classified into two subgroups depending on whether they activate AR-Smads or BR-Smads (Fig. 1).

All three TGF-β isoforms activate AR-Smads, since they bind TβR-II and TβR-I/ALK-5. Of four different isoforms of activins, biological activities of activin βC and activin βE have been poorly defined. They are specifically expressed in liver, but gene targeting of activin βC, activin βE or both did not result in any functional defects in liver development and function (Lau et al., 2000). Thus, the signaling activities of activins βC and βE remain to be determined, but they are thought to activate AR-Smads because of their structural similarity to activins βA and βB. Nodal plays important roles in mesoderm formation, anterior patterning, and left-right axis specification during early embryogenesis. Biochemical analyses and studies on crossing of different knock-out mice revealed that Nodal binds to ActR-IB and activates AR-Smads (Gu et al., 1999; Nomura and Li, 1998; Kumar et al., 2001). In addition to these ligands, certain GDFs may also

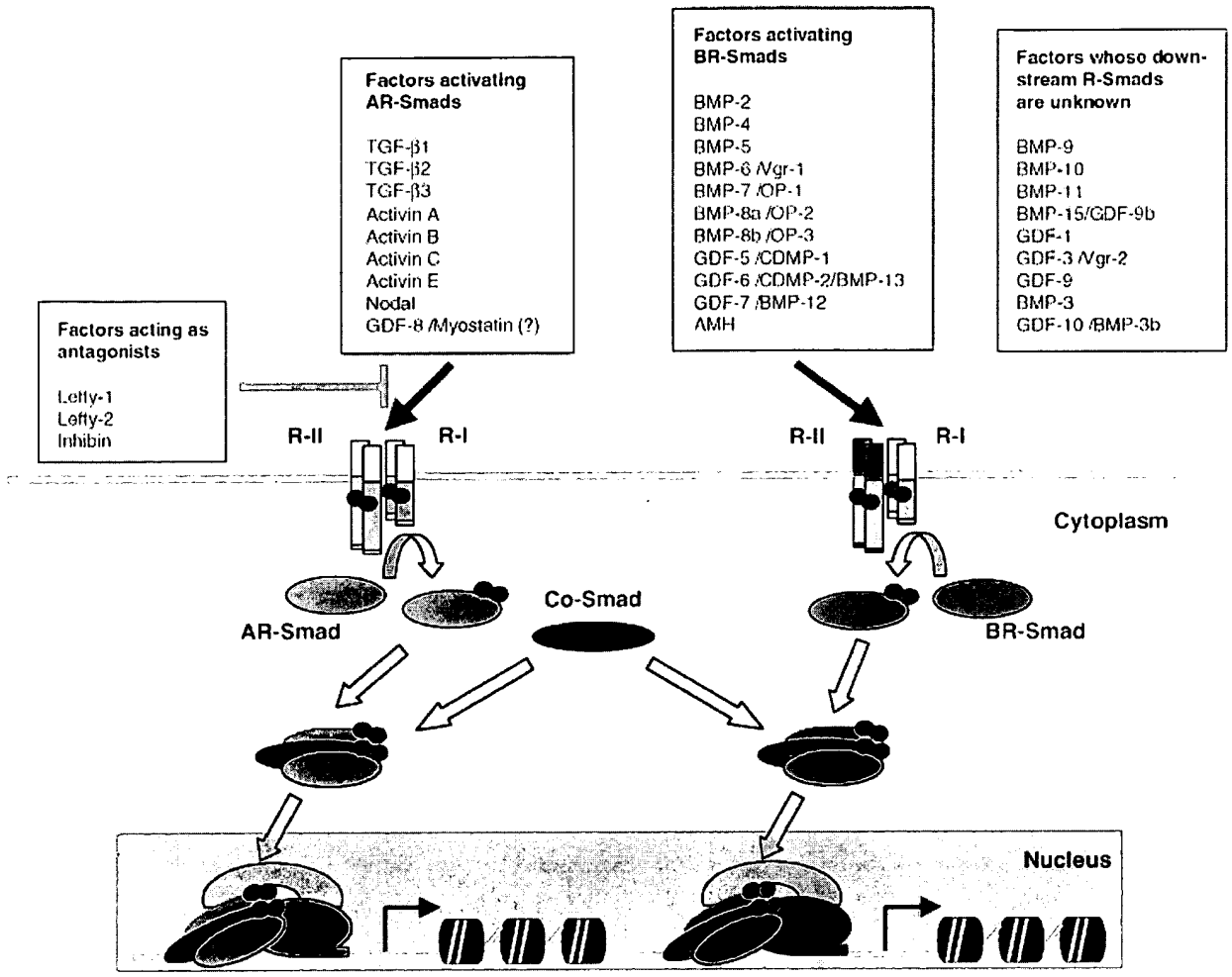

Fig. 1. Divergent members of the TGF -β superfamily, their receptors, and R-Smads. Factors activating AR-Smads bind to type II receptors including TβR-II, ActR-II, and ActR-IIB, and type I receptors, including ALK-4/ActR-IB, ALK-5/TβR-I, and possibly ALK-7. Factors activating BR-Smads bind to BMP-II, ActR-II, ActR-IIB, or AMHRII, and ALK2, ALK3/BMPR-IA or ALK-6/BMPR-IB. As an exception of this scheme, TGF-βs may bind to ALK-1 as well as ALK-5/TβR-I in endothelial cells, and ALK-1 activates BR-Smads.

activate AR-Smads. GDF-8, also termed myostatin, inhibits proliferation of skeletal muscle cells (Thomas et al., 2000). Null mutations of the *GDF-8 / myostatin* gene result in dramatic increase in skeletal muscle mass in mice and cattle (Grobet et al., 1997; McPherron et al., 1997; McPherron and Lee, 1997). GDF-8/myostatin activates p3TP-Lux promoter-reporter construct (Paralkar V., personal communication), which preferentially responds to AR-Smads, suggesting that GDF-8/myostatin transmits signals similar to those of TGF-βs and activins.

BMP-2 and BMP-4, the prototype of BMPs, induce bone and cartilage tissues in vivo (Reddi, 1998). They bind to ALK-3/BMPR-IA and activate BR-Smads. BMP-6 and BMP-7, which are structurally similar to each other, bind ALK-2 and also activate BR-Smads (Ebisawa et al., 1999; Miyazono, 2001). GDF-5, an inducer of cartilage-like structures in vivo, preferentially binds to ALK-6/BMPR-IB in the presence of different type II receptors, and also activates BR-Smads (Nishitoh et al., 1996). Thus, BMPs and their related molecules activate BR-Smads. In addition to those BMP-like molecules, AMH also activates BR-Smads through binding to ALK-6/BMPR-IB in the presence of AMHR-II (Gouédard et al., 2000).

After the cloning of ALK-7 (Kang and Reddi, 1996; Ryden et al., 1996; Tsuchida et al., 1996), efforts to isolate novel serine/threonine kinase receptors have not been successful. It is possible that there are yet unidentified serine/threonine kinase receptors which may be specifically expressed in certain tissues. However, it is more likely that there are only limited numbers of type II and type I receptors for the TGF-β superfamily. On the other hand, several molecules have been demonstrated to serve as co-receptors or co-factors for the TGF-β superfamily ligands. Betaglycan (also known as TGF-β type III receptor) has been shown to bind inhibin as well as TGF-β, but not activin (Lewis et al., 2000). Nodal requires *Xenopus* EGF-CFC protein or its mammalian homologues Cripto and Cryptic for

efficient receptor-binding and intracellular signaling (Shen and Schier, 2000). It is thus possible that these co-receptors and co-factors modulate the binding of ligands to signaling receptors and contribute to specific receptor binding of certain ligands.

Another important point is that certain members of the TGF-β superfamily compete with other members for receptor binding, and function as antagonists of these ligands. Lefty-1 and -2 and their *Xenopus* homologue Antivin play important roles in the determination of left-right asymmetry (Meno et al., 1999; Thisse and Thisse, 1999). Lefties have six conserved cysteine residues, and are structurally distantly related to members of the TGF-β superfamily. Although Lefty/Antivin may bind to activin receptor complexes, they do not transmit intracellular signals, and interfere with the signaling activity of Nodal.

The α-subunit of inhibin is also distantly related to other members of the TGF-β superfamily, and forms heterodimers with β-subunits which are components of activin dimers. Inhibins have been reported to function as antagonists of activins by binding to activin type II receptors through the β-subunits (Lebrun and Vale, 1997; Lewis et al., 2000). Certain BMPs have also been suggested to act as antagonists of other BMPs. However, further analyses are required to determine whether they actually function as BMP antagonists under physiological conditions.

Interaction of SMAD proteins with various partners

Since there are limited number of serine/threonine kinase receptors and Smads it is important to elucidate how the wide variety of biological activities of the TGF-β superfamily proteins is generated. Spatial and temporal expression patterns of ligands are important for exhibition of diverse biological activities. GDF-5 is expressed in appendicular skeleton and plays an important role in chondrogenesis (Francis-West et al., 1999). GDF-8/myostatin is preferentially expressed in skeletal muscles, and regulates the proliferation of myocytes (McPherron et al., 1997; Thomas et al., 2000). Certain GDFs/BMPs are specifically expressed in female and male reproduction systems, and play important roles in oogenesis and spermatogenesis (Elvin et al., 1999; Galloway et al., 2000). However, expression patterns of ligands do not fully explain why the TGF-β superfamily proteins have different biological effects in distinct cells.

TGF-β inhibits growth of most types of cells but induces growth of fibroblasts and osteoblasts in vitro (Urano et al., 1999). TGF-β inhibits the growth and most functions of lymphocytes but induces the synthesis of IgA in B lymphocytes (Cazac and Roes, 2000). BMPs induce differentiation of myoblasts into osteoblasts, while they induce differentiation of neuroepithelial cells into astrocytes in the presence of leukemia inhibitory factor (LIF) (Nakashima et al., 1999). BMP-like molecules are present in *Drosophila*, including Decapentaplegic (DPP), 60A-GBB, and Screw, but never induce bone formation in invertebrates. However, the DPP protein can induce formation of bone and cartilage tissues when subcutaneously injected into vertebrates. The question is that what could be the mechanisms for these diverse biological activities induced by the TGF-β superfamily proteins?

One possible mechanism is interaction of Smads with various proteins in the cytoplasm and in the nucleus in different fashions in various cells. Most importantly, Smads associate with various transcription factors in the nucleus and exhibit a wide array of biological activities in cooperation with these proteins in cells. Activity of Smads is also modified by signaling cross-talk with other signaling pathways (Miyazono et al., 2000), which may also lead to exhibition of diverse biological responses.

Proteins that interact with Smads are listed in Table 1. Smad-interacting proteins include those that regulate membrane anchoring of Smads, ubiquitin-dependent degradation, and transcription by Smads. In this section we focus on the function of Runx proteins. Runx is a transcription factor containing a Runt domain, which is important for DNA binding (Ito, 1999). Runx is also denoted polyomavirus enhancer binding protein-2 α subunit (PEBP2α), core binding factor-a (Cbfa), and acute myeloid leukemia (AML). Runx1, also known as PEBP2αB, Cbfa2, and AML1, plays an important role in definitive hematopoiesis. Abnormalities in the *Runx1 / AML1* gene induced by chromosomal translocation are found in approximately one-third of human acute leukemias. Germ-line mutations of the *Runx1 / AML1* gene are responsible for the human familial platelet disorder with predisposition to acute myelogenous leukemia (FPD/AML) (Song et al., 1999). Runx2 is also known as PEBP2αA and Cbfa1. Gene targeting of *Runx2 / Cbfa1* results in the loss of bone formation. Germ-line mutations of *Runx2 / Cbfa1* are responsible for the pathogenesis of human cleidocranial dysplasia syndrome (CCD). Runx3, also known as PEBP2αC and Cbfa3, induces IgA synthesis in B lymphocytes. These biological activities of Runx proteins are reminiscent of those induced by TGF-β and BMPs.

Physical interaction between Smads and Runx can be detected in mammalian cells (Hanai et al., 1999; Pardali et al., 2000; Zhang and Derynck, 2000; Zhang et al., 2000). In the immunoglobulin constant α region (Ig Cα) promoter region, Smad binding sites and Runx binding sites are located in close vicinity, therefore, the Smad-Runx complex binds to and enhances transcription from the IgCα promoter. Physical interaction and functional cooperation of Runx2 and BR-Smads have also been demonstrated (Zhang et al., 2000) indicating that these two proteins may cooperate in osteoblast differentiation. Importantly, expression of Runx1 is induced by BMPs and TGF-β in C2C12 cells. Runx1 prevents the differentiation of myoblasts into mature myocytes. However, Runx1 by itself is not sufficient for the induction of osteoblast differentiation; cooperation of BR-Smads with Runx1 is required for this process (Lee et al., 2000; Zhang et al., 2000).

TGF-β is a potent growth inhibitor of hematopoietic cells, but many leukemic cells are resistant to the growth inhibitory activity of TGF-β. Runx1/AML1 plays an important role in growth and differentiation of hematopoietic cells. A leukemia-associated fusion protein, AML1/ETO, has been shown to interact with AR-Smads, but fail to induce transcriptional responses induced by TGF-β (Jakubowiak et al., 2000). Abnormalities of the AML1 protein may thus play an important role in acquiring resistance to the effect of

TABLE 1. Smad interacting proteins

Smad-interacting protein	Smad	Interacting domain	Function
ATF-2	Smad3,4	MH1	ATF/CREB family member; functionally cooperates with Smad3
β-catenin	Smad4	MH1	Wnt signaling molecule; functionally cooperates with Smad4
β-tubulin	Smad2,3,4	Not determined	A component of microtubule; sequesters Smads in the cytoplasm
Calmodulin	Smad1,2	MH1	Multi-functional Ca^{2+}-binding protein; activates Smad1 activity and inhibits Smad2 activity
E1A	Smad3(1,2)	MH2	Adenoviral oncoprotein; inhibits TGF-β signaling by interfering Smad3-p300 interaction
Evi-1	Smad3	MH2	Zinc-finger transcriptional regulator; inhibits Smad3 activity
FAST1	Smad2,3	αHelix2 in MH2	Winged-helix transcriptional factor; functionality cooperates with Smad2/3
FAST2	Smad2,3	αhelix2 in mH2?	Winged-helix transcriptional factor; functionally cooperates with Smad2
Fos	Smad3	MH2	AP-1 transcription factor complex; functionally cooperates with Smads
C-terminally turncated Gli3	Smad1,2,3,4	Not determined	Zinc-finger transcriptional factor
GR	Smad3	MH2	Glucocorticoid receptor; Smad repressor
HEF1	Smad3	MH1, MH2	Negative regulator of TGF-β signaling; Smad3 mediates HEF1 degradation
Hgs/Hrs	Smad2,3	Not determined	FYVE domain protein; functionally cooperates with SARA and Smad2/3
HNF-4	Smad3,4	Not determined	Orphan nuclear receptor; functionally cooperates with Smad3/4
Hoxa-9	Smad4	Not determined	Homeodomain transcriptional repressor for TGF-β signaling
Hoxc-8	Smad1,4	MH1 and Linker	Homeodomain transcriptional repressor for BMP signaling
Hoxc-8	Smad6	MH2	Homeodomain transcriptional repressor for BMP signaling
Importin β	Smad3	NLS in MH1	A component of protein nuclear import
Jun	Smad3,4	MH1	AP-1 transcription factor complex; functionally cooperates with Smads
Lef1/Tcf	Smad2,3,4	MH1, MH2	Wnt signaling HMG box transcriptional factor; functionally cooperates with Smad2/3/4
Mixer/Milk	Smad2	MH2	Paired-like homeodomain transcriptional factors; functionally cooperate with Smad2
MSG1	Smad4	Linker and MH2	Nuclear transcriptional co-activator
NF-κB	Smad3	Not determined	Transcriptional factor; functionally cooperates with Smad3 in JunB promoter activation
OAZ	Smad1	MH2	Zinc-finger transcriptional factor; DNA-binding partner for BR-Smads
p300/CBP	Smad1,2,3,4	MH2	Transcriptional co-activator with intrinsic histone acetyltransferase activity
P/CAF	Smad3	MH2	Transcriptional co-activator with intrinsic histone acetyltransferase activity
Runx1/2/3	Smad1,2,3,5	MH2, MH1?	Runt-domain-containing transcriptional factors; functionally cooperates with Smads
SARA	Smad2,3	MH2	FYVE domain protein; Smad anchor to membrane, recruits Smad2 to receptor
SIP1	Smad1,2,3,5	MH2	Zinc-finger/homeodomain transcriptional repressor
Ski	Smad2,3,4	MH2	Transcriptional co-repressor; recruits histone deacetylase complex
SnoN	Smad2,3,4	MH2	Transcriptional co-repressor; recruits histone deacetylase complex
Smurf1	Smad1,5	PY motif in linker	Hect-class E3 ubiquitin ligase; ubiquitin-mediated degradation of Smad 1/5
Smurf2	Smad2(1,3)	PY motif in linker	Hect-class E3 ubiquitin ligase; ubiquitin-mediated degradation of Smad2
SNIP1	Smad1,2,4	MH2	TGF-β signaling suppressor; functionally cooperates with Smad4
Sp1	Smad2,3,4	MH1, MH2	Transcription factor; functionally cooperates with Smad2/3/4
STRAP	Smad7(2,3,6)	Not determined	WD40 repeat protein; inhibits TGF-β signaling with Smad7
TAK1	Smad6	Not determined	MAPKKK; mediates BMP-2 induced apoptosis
TFE3	Smad3,4	MH1	Transcription factor; functionally cooperates with Smad3/4
TGIF	Smad2,3	MH2	Transcriptional co-repressor; recruits histone deacetylases
Tob	Smad1,4,5,8	MH2	A member of Tob/BTG family proteins; negative regulator of BMP signaling
VDR	Smad3	MH1	Vitamin D receptor; functionally cooperates with Smad3

ATF-2, activating transcription factor-2; AP-1, activator protein-1; CBP, CREB-binding protein; CREB, cAMP-responsive-element binding protein; E1A, early region 1A; Evi-1, ectopic viral integration site-1; FAST, forkhead activin signal transducer; Gli3, glioblastoma gene product3; Gr, glucocorticoid receptor; HEF1, human enhancer of filamentation1; Hgs/Hrs, hepatocyte growth factor-regulated tyrosine kinase substrate; HNF-4, hepatocyte nuclear factor 4; Hoxa-9, homeobox gene a-9; Hoxc-8, homeobox gene c-8; Lef1/Tcf, lymphoid enhancer binding factor 1/T cell-specific facotr; MH, Mad homology domain; MSG1, melanocyte-specific gene1; NF-κB, nuclear factor κB; NLS, nuclear localization signal; OAZ, Olf-1/EBF associated zinc-finger; P/CAF, p300/CBP-associated factor; Runx, runt-related gene; SARA, Smad anchor for receptor activation; SIP1, Smad-interacting protein 1; Ski, Sloan-Kettering avain retrovirus; Sno, Ski-related novel gene; Smurf, Smad ubiquitination regulatory factor; SNIP-1, Smad nuclear interacting protein 1; Sp1, specificity protein 1; STRAP, serine-threonine kinase receptor-associated protein; TAK1, TGF-β-activated kinase 1; TFE3, transcription factor μE3; TGIF, 5TG3' interacting factor; Tob, transducer of ErbB-2, VDR, vitamin D receptor.

In this table, Smad-interacting proteins only in vertebrates are listed. References that described the Smad-interacting proteins listed in this table are as follows: ATF-2 (Sano et al., 1999); β-catenin (Nishita et al., 2000), β-tubulin (Dong et al., 2000); Jun/c-Fos (Zhang et al., 1998); calmodulin (Scherer and Graff, 2000); E1A (Nishihara et al., 1999); Evi-1 (Kurokawa et al., 1998); Xenopus FAST1 (Chen et al., 1997); FAST2 (Labbé et al., 1998); Gli3 (Liu et al., 1998); GR (Song et al., 1999); HEF1 (Liu et al., 2000); Hgs/Hrs (Miura et al., 2000); HNF-4 (Kardassis et al., 2000); Hoxa-9 (Shi et al., 2001); Hoxc-8 (Shi et al., 1999; Bai et al., 2000); importin β (Xiao et al., 2000); Lef1/Tcf (Labbé et al., 2000); Mixer/Milk (Germain et al., 2000); MSG1 (Yahata et al., 2000); NFκB (DiChiara et al., 2000; Lopez-Rovira et al., 2000); OAZ (Hata et al., 2000); P/CAF (Itoh et al., 2000); p300/CBP (Feng et al., 1998; Nishihara et al., 1998); Runx (Hanai et al., 1999; Pardali et al., 2000; Zhang et al., 2000; Lee et al., 2000); SARA (Tsukazaki et al., 1998); SIP1 (Verschueren et al., 1999); Ski (Luo et al., 1999; Akiyoshi et al., 1999; Sun et al., 1999a); SnoN (Stroschein et al., 1999; Sun et al., 1999b); Smurf1 (Zhu et al., 1999); Smurf2 (Lin et al., 2000); SNIP1 (Kim et al., 2000); Sp1 (Pardali et al., 2000; Feng et al., 2000); STRAP (Datta and Moses, 2000); TAK1 (Kimura et al., 2000); TFE3 (Hua et al., 1999); TGIF (Wotton et al., 1999; Melhuish and Wotton, 2000); Tob (Yoshida et al., 2000); VDR (Yanagisawa et al., 1999).

TGF-β on hematopoietic cells and development of leukemias.

Many other transcription factors interact with Smads. The forkhead transcription factor FAST1 specifically interacts with AR-Smads and plays an important role in formation of left-right asymmetry and mesoderm formation during early embryogenesis. Not much is known about transcription factors that interact with BR-Smads (Miyazono, 2001) but it has been shown that BR-Smads indirectly interact with STAT3 through a transcriptional coactivator, p300, leading to the differentiation of neuronal epithelial cells into astrocytes (Nakashima et al., 1999). Thus, by selecting various transcription factors as partners, Smads may be able to exhibit a wide range of biological activities in target cells.

An important unanswered question is that how growth inhibition is induced by TGF-β in target cells. BMPs and activins can inhibit the growth of certain cells but the potency and magnitude of growth inhibition they induce are less than those induced by TGF-β. TGF-β induces growth inhibition of various cells which is mediated by repression of c-*myc*, induction of *p21* and *p15* cyclin-dependent kinase (CDK) inhibitors, and suppression of tyrosine phosphatase *Cdc25A* (Massagué et al., 2000). However, it is still unclear why only TGF-β can induce potent growth inhibitory effects. Abnormalities of activins, activin receptors, BMPs, BMP receptors, or BR-Smads have not been identified in human cancer cells, except for a C-terminal truncation of Smad5 in certain leukemias (Jiang et al., 2000). Mutations in *Smad4* have been identified in various tumors but Smad4 is shared with TGF-β/activin and BMP signaling pathways. These findings suggest a specific role of TGF-β signaling pathway in oncogenesis.

Modulation of SMAD signaling

In the Smad signaling pathways, R-Smads are activated by serine/threonine kinase receptors, form complexes with Co-Smads, and translocate into the nucleus where they regulate transcription of target genes. Smads play major roles as receptor substrates and transcription factors but their activity is modulated by multiple regulatory mechanisms (Miyazono, 2000).

Various extracellular antagonists including Noggin, Chordin, Cerberus, and Gremlin, regulate BMP signaling (Massagué and Chen, 2000; Miyazono, 2000). Follistatin is an inhibitor for activins but is also known to antagonize the effects of certain BMPs. *Xenopus* BAMBI (its mammalian homologue is the *nma* gene product) is a pseudoreceptor for the TGF-β superfamily members (Onichtchouk et al., 1999). BAMBI is structurally similar to type I serine/threonine kinase receptors in the extracellular domain but lacks the intracellular kinase domain. By forming heteromeric complexes with serine/threonine kinase receptors BAMBI/Nma antagonizes the effects of TGF-β/BMPs.

I-Smads, i.e. Smad6 and Smad7, function as antagonists of TGF-β/BMP signaling inside cells. I-Smads stably interact with activated type I receptors and compete with R-Smads for receptor activation. In addition, Smad6 has been reported to form a complex with Smad1 and to compete with Smad4 in complex formation. Smad6 was also reported to interact with a homeobox protein, Hoxc8, and to act as a transcriptional repressor in the nucleus (Bai et al., 2000).

ERK MAP kinase interferes with Smad signaling under certain conditions. ERK1/2, activated by tyrosine kinase receptors or oncogenic Ras, phosphorylates linker regions of R-Smads, resulting in interference with nuclear translocation of R-Smads (Kretzschmar et al., 1999), although the molecular mechanisms of this have not been elucidated.

In addition to those molecules which primarily act in the cytoplasm certain molecules act as transcriptional co-repressors in the nucleus (Massagué and Chen, 2000 Miyazono, 2000). c-Ski and its related protein, SnoN, and TGIF interact with AR-Smads in the nucleus. They compete with transcriptional co-activators p300 and CBP, and recruit histone deacetylases to Smad complexes, resulting in transcriptional repression. TGF-β/Smad signaling is thus regulated by multiple mechanisms at extracellular, cytoplasmic and nuclear levels.

Importantly, expression of these regulatory molecules is regulated via negative feedback mechanisms (Miyazono, 2000). For example, expression of Noggin and BAMBI/Nma is regulated by TGF-β and BMPs. I-Smads are strongly induced by ligand stimulation. In addition, Smad7 is induced by various signals other than TGF-β/BMPs including NF-κB and interferon-γ signaling. Thus, cells treated with interleukin-1 or interferon-γ become resistant to the effects of TGF-β and possibly those of BMPs.

TGF-β/BMP signaling and diseases

Perturbations of TGF-β superfamily signaling result in various clinical disorders including some cancers, bone diseases, and vascular diseases. Involvement of TGF-β receptors and Smads in tumorigenesis has been discussed in several other review articles (Blobe et al., 2000; Massagué et al., 2000). The relationship of BMP signaling with bone diseases has also been discussed elsewhere (Reddi, 1998; Luyten et al., 2000). TGF-β has also been reported to be involved in some bone diseases. Recently, mutations in the N-terminal region of TGF-β1 precursor and hyperactivation of latent TGF-β have been found to result in Camurati-Engelmann disease (Janssens et al., 2000, Kinoshita et al., 2000). In this article, we show only a summary figure of the diseases induced by abnormalities of TGF-β/BMP signaling (Fig. 2) and focus on genetically-inherited vascular diseases induced by mutations of the TGF-β superfamily receptors.

BMPR-II is a type II receptor that specifically bind BMPs. BMPR-II is ubiquitously expressed in various tissues, and mice lacking the *BMPR-II* gene die during early embryogenic stages due to abnormal mesoderm formation (Beppu et al., 2000). Although the bioactivities of BMPs in vascular wall cells have not been fully determined, BMP-2 has been shown to inhibit the growth of smooth muscle cells and to prevent progression of vascular proliferative diseases (Nakaoka et al., 1997). Mutations in the human *BMPR-II* gene have been shown to be involved in the pathogenesis of primary pulmonary hypertension (PPH) (Deng et al., 2000; Lane et al., 2000). Familial PPH is inherited in autosomal dominant fashion with low penetrance. In PPH patients, obstruction of pre-capillary pulmonary arteries is

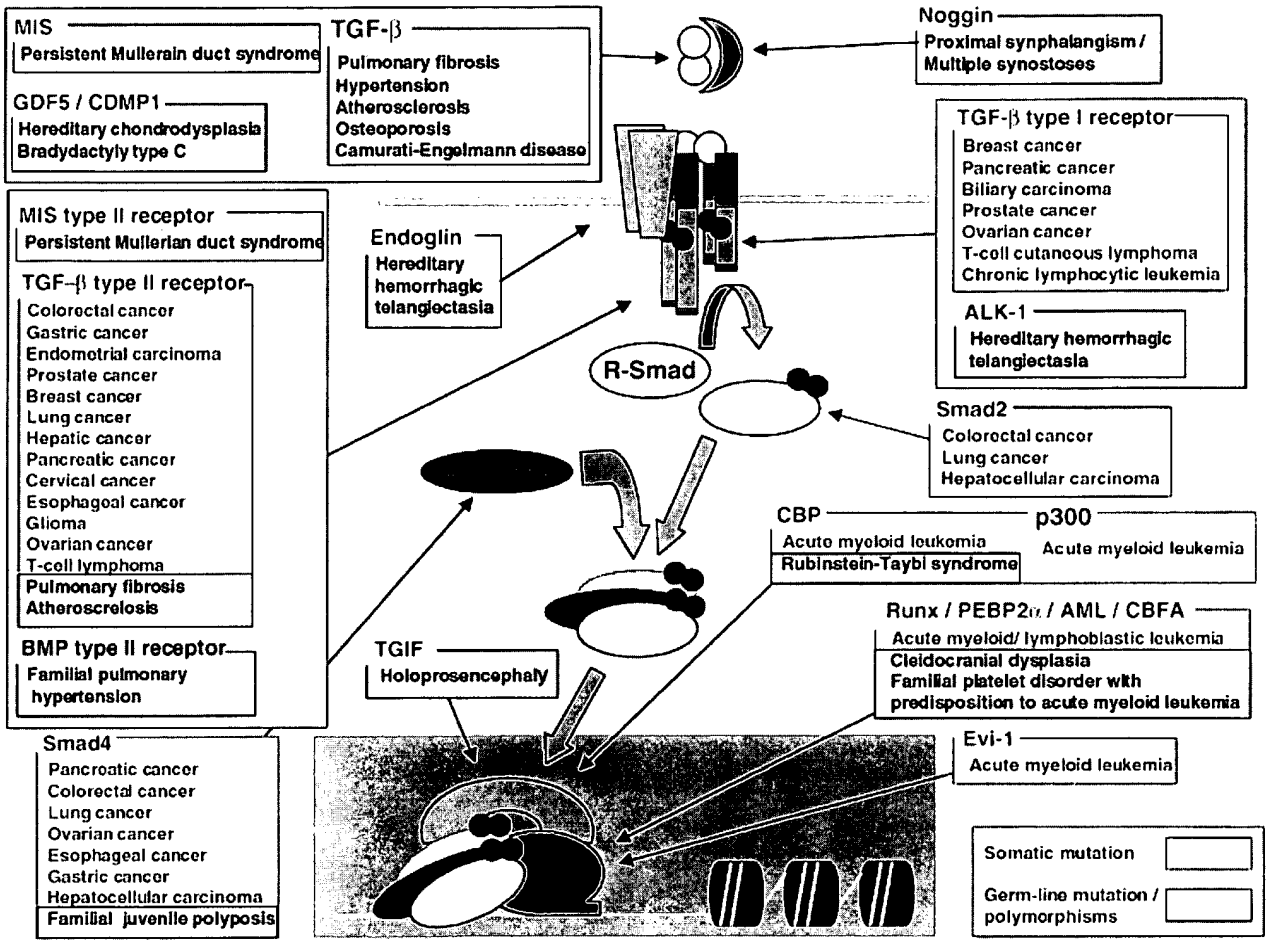

Fig. 2. Signaling by TGF-β superfamily ligands and diseases induced by mutations of the molecules involved in the signaling pathways. In addition to the diseases listed in this Figure, left-right laterality defects are induced by abnormalities of Lefty-2, Cryptic, or ActR-IIB (Kosaki K et al., 1999; Kosaki R et al., 1999; Bamford et al., 2000). References that described the diseases listed in this figure are as follows: TGF-β (Yamada et al., 1998; El-Gamel et al., 1999; Li et al., 1999; Bertoldo et al., 2000; Suthanthiran et al., 2000; Yokota et al., 2000); AMH /MIS and AMH/MIS type II receptor (Belville et al., 1999); GDF-5/CDMP-1 (Thomas et al., 1996; Polinkovsky et al., 1997; Thomas et al., 1997); Noggin (Gong et al., 1999); TβR-II (Markowitz et al., 1995; Myeroff et al., 1995; Kim et al., 1996a; Knaus et al., 1996; Togo et al., 1996; Vincent et al., 1996; de Jonge et al., 1997; Izumoto et al., 1997; McCaffrey et al., 1997; Goggins et al., 1998; Kang et al., 1998; Tanaka et al., 2000; Wang et al., 2000); TβR-I (Kim et al., 1996b; DeCoteau et al., 1997; Chen et al., 1998; Anbazhagan et al., 1999; Schiemann et al., 1999); Smad4/DPC4 (Hahn et al., 1996a; Hahn et al., 1996b; Nagatake et al., 1996; MacGrogan et al., 1997; Nishizuka et al., 1997; Howe et al., 1998; Bartsch et al., 1999; Schutte, 1999; Takakura et al., 1999; Woodford-Richens et al., 2000); Smad2 (Barrett et al., 1996; Eppert et al., 1996; Uchida et al., 1996; Yakicier et al., 1999); endoglin (McAllister et al., 1994; Pece-Barbara et al., 1999); ALK-1 (Johnson et al., 1996; Abdalla et al., 2000); BMPR-II (Deng et al., 2000; Lane et al., 2000; Thomson et al., 2000); TGIF (Gripp et al., 2000); CBP (Petrij et al., 1995; Borrow et al., 1996; Taki et al., 1997); p300 (Ida et al., 1997); Evi-1 (Pekarsky et al., 1997; Suzukawa et al., 1999); Runx (Erickson et al., 1992; Nucifora et al., 1994; Golub et al., 1995; Romana et al., 1995; Song et al., 1999; Zhou et al., 1999; Preudhomme et al., 2000).

observed due to proliferation of endothelial cells and smooth muscle cells. Lung-heart or lung transplantation is an effective treatment for the disease. Interestingly, mutations can be observed in various regions of the human *BMPR-II* gene including the extracellular domain and intracellular domain. BMPR-II has a unique, long C-terminal tail with approximately 530 amino acid residues which is not observed in other type II or type I receptors (Rosenzweig et al., 1995). The functional importance of the C-terminal tail of BMPR-II has not been reported (Ishikawa et al., 1995) but truncations of the C-terminal tail also lead to development of PPH. It will be interesting to examine whether certain BMP-like molecules specifically bind to BMPR-II in lung and regulate the function of pulmonary arteries.

Mutations of endoglin and ALK-1 are responsible for the pathogenesis of hereditary hemorrhagic telangiectasia (HHT) type I and type II, respectively (also known as Osler-Rendu-Weber syndrome) (McAllister et al., 1994; Johnson et al., 1996). HHT is characterized by arteriovenous malformations and recurrent bleeding due to vascular dysplasia. ALK-1 is a type I receptor specifically expressed in endothelial cells. ALK-1 is structurally similar to ALK-2 and has been shown to bind TGF-βs in the presence of TβR-II (Oh et al., 2000).

However, it is possible that other members of the TGF-β superfamily bind to ALK-1 under certain conditions. In endothelial cells, two different type I receptors, i.e., ALK-1 and ALK-5, may serve as receptors for TGF-βs. ALK-5/TβR-I activates AR-Smads, while ALK-1 phosphorylates BR-Smads. Thus, TGF-βs activate AR-Smads in most cell types, but phosphorylate both types of R-Smads in endothelial cells.

Structurally endoglin is weakly related to betaglycan. Betaglycan and possibly endoglin may function as co-receptors for the TGF-β superfamily proteins (Pece-Barbara et al., 1999). Endoglin may regulate ligand binding to signaling receptors and is specifically expressed in endothelial cells. In human umbilical endothelial cells, endoglin physically interacts with ALK-1 (Abdalla et al., 2000). How endoglin and ALK-1 cooperate in transduction of TGF-β/BMP signaling remains to be determined.

Analyses by gene targeting have revealed that both ALK-1 and endoglin null mice die during embryogenesis due to abnormalities in vascular development which are reminiscent of those in human HHT (Li et al., 1999; Oh et al., 2000; Urness et al., 2000). Both types of mice exhibit enlarged vasculatures lacking smooth muscle cells surrounding endothelial cells. Smad5$^{-/-}$ mice also exhibit defects in vascular tissues as well as other tissues (Chang et al., 1999; Yang et al., 1999). The vascular abnormalities in Smad5$^{-/-}$ mice are similar to those in ALK-1$^{-/-}$ mice, suggesting that Smad5 is a downstream signaling component of ALK-1. Mice lacking TGF-β1 or TβR-II also die of vascular abnormalities and anemia. However, the phenotypes of these mice are distinct from those of ALK-1 and endoglin null mice. Thus, TGF-β and TβR-II may act upstream of the endoglin/ALK-1/Smad5 signaling pathway but other pathways, i.e., the ALK-5/TβR-I and Smad2/3 pathway also play important roles in the vascular development induced by TGF-β and TβR-II.

CONCLUSION

The large number of TGF-β superfamily proteins is notable. Despite this, however, limited numbers of serine/threonine kinase receptors and Smad proteins are present in mammals and are sufficient for transmitting diverse intracellular signaling. Importantly, the TGF-β/BMP signaling is regulated by various mechanisms at extracellular, membrane, cytoplasmic, and nuclear levels. TGF-β ligands, receptors, and Smad proteins have been reported to be involved in the pathogeneses of various clinical diseases. In addition, molecules that regulate TGF-β/BMP signaling are also involved in the pathogeneses of various diseases. Thus, in order to elucidate the roles of TGF-β/BMPs in clinical disorders it is very important to understand the signaling mechanisms of those proteins in vivo. Some recently developed technologies, e.g. DNA microarray and proteome analyses may in the future be helpful in determining the signaling mechanisms of TGF-β/BMPs in vivo.

ACKNOWLEDGMENTS

We are grateful to Dr. V Paralkar for sharing unpublished observations. We also thank Ayako Sakai-Nishitoh for secretarial help.

LITERATURE CITED

Abdalla SA, Pece-Barbara N, Vera S, Tapia E, Paez E, Bernabeu C, Letarte M. 2000. Analysis of ALK-1 and endoglin in newborns from families with hereditary hemorrhagic telangiectasia type 2. Hum Mol Genet 9:1227–1237.

Akiyoshi S, Inoue H, Hanai J-i, Kusanagi K, Nemoto N, Miyazono K, Kawabata M. 1999. c-Ski acts as a transcriptional co-repressor in transforming growth factor-β signaling through interaction with Smads. J Biol Chem 274:35269–35277.

Anbazhagan R, Bornman DM, Johnston JC, Westra WH, Gabrielson E. 1999. The S387Y mutations of the transforming growth factor-β receptor type I gene is uncommon in metastases of breast cancer and other common types of adenocarcinoma. Cancer Res 59:3363–3364.

Aoki H, Fujii M, Imamura T, Takehara K, Kato M, Miyazono K. 2001. Synergistic effects of different bone morphogenetic protein type I receptors on osteoblast differentiation. J Cell Sci (in press).

Ashcroft GS, Yang X, Glick AB, Weinstein M, Letterio JL, Mizel DE, Anzano M, Greenwell-Wild T, Wahl SM, Deng C, Roberts AB. 1999. Mice lacking Smad3 show accelerated wound healing and an impaired local inflammatory response. Nat Cell Biol 1:260–266.

Bai S, Shi X, Yang X, Cao X. 2000. Smad6 as a transcriptional corepressor. J Biol Chem 275:8267–8270.

Bamford RN, Roessler E, Burdine RD, Saplakoglu U, dela Cruz J, Splitt M, Towbin J, Bowers P, Marino B, Schier AF, Shen MM, Muenke M, Casey B. 2000. Loss-of-function mutations in the *EGF-CFC* gene CFC1 are associated with human left-right laterality defects. Nat Genet 26:365–369.

Barrett MT, Schutte M, Kern SE, Reid BJ. 1996. Allelic loss and mutational analysis of the DPC4 gene in esophageal adenocarcinoma. Cancer Res 56:4351–4353.

Bartsch D, Hahn SA, Danichevski KD, Ramaswamy A, Bastian D, Galehdari H, Barth P, Schmiegel W, Simon B, Rothmund M. 1999. Mutations of the DPC4/Smad4 gene in neuroendocrine pancreatic tumors. Oncogene 18:2367–2371.

Belville C, Josso N, Picard JY. 1999. Persistence of Müllerian derivatives in males. Am J Med Genet 89:218–223.

Beppu H, Kawabata M, Hamamoto T, Chytil A, Minowa O, Noda T, Miyazono K. 2000. BMP type II receptor is required for gastrulation and early development of mouse embryos. Dev Biol 221:249–258.

Bertoldo F, D'Agruma L, Furlan F, Colapietro F, Lorenzi MT, Maiorano N, Iolascon A, Zelante L, Locascio V, Gasparini P. 2000. Transforming growth factor-β1 gene polymorphism, bone turnover, and bone mass in Italian postmenopausal women. J Bone Miner Res 15:634–639.

Blobe GC, Schiemann WP, Lodish HF. 2000. Role of transforming growth factor β in human disease. N Engl J Med 342:1350–1358.

Borrow J, Stanton VP Jr, Andresen JM, Becher R, Behm FG, Chaganti RS, Civin CI, Disteche C, Dube I, Frischauf AM, Horsman D, Mitelman F, Volinia S, Watmore AE, Housman DE. 1996. The translocation t(8;16)(p11;p13) of acute myeloid leukaemia fuses a putative acetyltransferase to the CREB-binding protein. Nat Genet 14:33–41.

Cazac BB, Roes J. 2000. TGF-β receptor controls B cell responsiveness and induction of IgA in vivo. Immunity 13:443–451.

Chang H, Huylebroeck D, Verschueren K, Guo Q, Matzuk MM, Zwijsen A. 1999. Smad5 knockout mice die at mid-gestation due to multiple embryonic and extraembryonic defects. Development 126:1631–1642.

Chen X, Weisberg E, Fridmacher V, Watanabe M, Naco G, Whitman M. 1997. Smad4 and FAST-1 in the assembly of activin-responsive factor. Nature 389:85–89.

Chen T, Carter D, Garrigue-Antar L, Reiss M. 1998. Transforming growth factor β type I receptor kinase mutant associated with metastatic breast cancer. Cancer Res 58:4805–4810.

Chen YG, Massagué J. 1999. Smad1 recognition and activation by the ALK1 group of transforming growth factor-β family receptors. J Biol Chem 274:3672–3677.

Datta PK, Moses HL. 2000. STRAP and Smad7 synergize in the inhibition of transforming growth factor-β signaling. Mol Cell Biol 20:3157–3167.

DeCoteau JF, Knaus PI, Yankelev H, Reis MD, Lowsky R, Lodish HF, Kadin ME. 1997. Loss of functional cell surface transforming growth factor β (TGF-β) type 1 receptor correlates with insensitivity to TGF-β in chronic lymphocytic leukemia. Proc Natl Acad Sci USA 94:5877–5881.

de Jonge RR, Garrigue-Antar L, Vellucci VF, Reiss M. 1997. Frequent inactivation of the transforming growth factor β type II receptor in small-cell lung carcinoma cells. Oncol Res 9:89–98.

Deng Z, Morse JH, Slager SL, Cuervo N, Moore KJ, Venetos G, Kalachikov S, Cayanis E, Fischer SG, Barst RJ, Hodge SE, Knowles JA. 2000. Familial primary pulmonary hypertension (gene *PPH1*) is caused by mutations in the bone morphogenetic protein receptor-II gene. Am J Hum Genet 67:737–744.

DiChiara MR, Kiely JM, Gimbrone MA Jr, Lee ME, Perrella MA, Topper JN. 2000. Inhibition of E-selectin gene expression by transforming growth factor β in endothelial cells involves coactivator integration of Smad and nuclear factor κ B-mediated signals. J Exp Med 192:695–704.

Dong C, Li Z, Alvarez R Jr, Feng XH, Goldschmidt-Clermont PJ. 2000. Microtubule binding to Smads may regulate TGFβ activity. Mol Cell 5:27–34.

Ebisawa T, Tada K, Kitajima I, Tojo A, Sampath TK, Kawabata M, Miyazono K, Imamura T. 1999. Characterization of bone morphogenetic protein-6 signaling pathways in osteoblast differentiation. J Cell Sci 112:3519–3527.

El-Gamel A, Awad MR, Hasleton PS, Yonan NA, Hutchinson JA, Campbell CS, Rahman AH, Deiraniya AK, Sinnott PJ, Hutchinson IV. 1999. Transforming growth factor-β (TGF-β1) genotype and lung allograft fibrosis. J Heart Lung Transplant 18:517–523.

Elvin JA, Yan C, Wang P, Nishimori K, Matzuk MM. 1999. Molecular characterization of the follicle defects in the growth differentiation factor 9-deficient ovary. Mol Endocrinol 13:1018–1034.

Eppert K, Scherer SW, Ozcelik H, Pirone R, Hoodless P, Kim H, Tsui LC, Bapat B, Gallinger S, Andrulis IL, Thomsen GH, Wrana JL, Attisano L. 1996. MADR2 maps to 18q21 and encodes a TGFβ-regulated MAD-related protein that is functionally mutated in colorectal carcinoma. Cell 86:543–552.

Erickson P, Gao J, Chang KS, Look T, Whisenant E, Raimondi S, Lasher R, Trujillo J, Rowley J, Drabkin H. 1992. Identification of breakpoints in t(8;21) acute myelogenous leukemia and isolation of a fusion transcript, AML1/ETO, with similarity to Drosophila segmentation gene, runt. Blood 80:1825–1831.

Feng X-H, Derynck R. 1997. A kinase subdomain of transforming growth factor-β (TGF-β) type I receptor determines the TGF-β intracellular signaling specificity. EMBO J 16:3912–3923.

Feng X-H, Zhang Y, Wu RY, Derynck R. 1998. The tumor suppressor Smad4/DPC4 and transcriptional adaptor CBP/p300 are coactivators for Smad3 in TGF-β-induced transcriptional activation. Gene Dev 12:2153–2163.

Feng X-H, Lin X, Derynck R. 2000. Smad2, Smad3 and Smad4 cooperate with Sp1 to induce p15*Ink4B* transcription in response to TGF-β. EMBO J 19:5178–5193.

Francis-West PH, Abdelfattah A, Chen P, Allen C, Parish J, Ladher R, Allen S, MacPherson S, Luyten FP, Archer CW. 1999. Mechanisms of GDF-5 action during skeletal development. Development 126:1305–1315.

Galloway SM, McNatty KP, Cambridge LM, Laitinen MP, Juengel JL, Jokiranta TS, McLaren RJ, Luiro K, Dodds KG, Montgomery GW, Beattie AE, Davis GH, Ritvos O. 2000. Mutations in an oocyte-derived growth factor gene (BMP15) cause increased ovulation rate and infertility in a dosage-sensitive manner. Nat Genet 25:279–283.

Germain S, Howell M, Esslemont GM, Hill CS. 2000. Homeodomain and winged-helix transcription factors recruit activated Smads to distinct promoter elements via a common Smad interaction motif. Gene Dev 14:435–451.

Gilboa L, Nohe A, Geissendorfer T, Sebald W, Henis YI, Knaus P. 2000. Bone morphogenetic protein receptor complexes on the surface of live cells: a new oligomerization mode for serine/threonine kinase receptors. Mol Biol Cell 11:1023–1035.

Goggins M, Shekher M, Turnacioglu K, Yeo CJ, Hruban RH, Kern SE. 1998. Genetic alterations of the transforming growth factor β receptor genes in pancreatic and biliary adenocarcinomas. Cancer Res 58:5329–5332.

Golub TR, Barker GF, Bohlander SK, Hiebert SW, Ward DC, Bray-Ward P, Morgan E, Raimondi SC, Rowley JD, Gilliland DG. 1995. Fusion of the TEL gene on 12p13 to the AML1 gene on 21q22 in acute lymphoblastic leukemia. Proc Natl Acad Sci USA 92:4917–4921.

Gong Y, Krakow D, Marcelino J, Wilkin D, Chitayat D, Babul-Hirji R, Hudgins L, Cremers CW, Cremers FP, Brunner HG, Reinker K, Rimoin DL, Cohn DH, Goodman FR, Reardon W, Patton M, Francomano CA, Warman ML. 1999. Heterozygous mutations in the gene encoding noggin affect human joint morphogenesis. Nat Genet 21:302–304.

Gouédard L, Chen Y-G, Thevenet L, Racine C, Borie S, Lamarre I, Josso N, Massagué J, di Clemente N. 2000. Engagement of bone morphogenetic protein type IB receptor and Smad1 signaling by anti-Müllerian hormone and its type II receptor. J Biol Chem 275:27973–27978.

Gripp KW, Wotton D, Edwards MC, Roessler E, Ades L, Meinecke P, Richieri-Costa A, Zackai EH, Massague J, Muenke M, Elledge SJ. 2000. Mutations in TGIF cause holoprosencephaly and link NODAL signalling to human neural axis determination. Nat Genet 25:205–208.

Grobet L, Martin LJ, Poncelet D, Pirottin D, Brouwers B, Riquet J, Schoeberlein A, Dunner S, Menissier F, Massabanda J, Fries R, Hanset R, Georges M. 1997. A deletion in the bovine myostatin gene causes the double-muscled phenotype in cattle. Nat Genet 17:71–74.

Gu Z, Reynolds EM, Song J, Lei H, Feijen A, Yu L, He W, MacLaughlin DT, van den Eijnden-van Raaij J, Donahoe PK, Li E. 1999. The type I serine/threonine kinase receptor ActRIA (ALK2) is required for gastrulation of the mouse embryo. Development 126:2551–2561.

Hahn SA, Hoque AT, Moskaluk CA, da Costa LT, Schutte M, Rozenblum E, Seymour AB, Weinstein CL, Yeo CJ, Hruban RH, Kern SE. 1996a. Homozygous deletion map at 18q21.1 in pancreatic cancer. Cancer Res 56:490–494.

Hahn SA, Schutte M, Hoque AT, Moskaluk CA, da Costa LT, Rozenblum E, Weinstein CL, Fischer A, Yeo CJ, Hruban RH, Kern SE. 1996b. DPC4, a candidate tumor suppressor gene at human chromosome 18q21.1. Science 271:350–353.

Hanai J-i, Chen LF, Kanno T, Ohtani-Fujita N, Kim WY, Guo WH, Imamura T, Ishidou Y, Fukuchi M, Shi MJ, Stavnezer J, Kawabata M, Miyazono K, Ito Y. 1999. Interaction and functional cooperation of PEBP2/CBF with Smads: Synergistic induction of the immunoglobulin germline Cα promoter. J Biol Chem 274:31577–31582.

Hata A, Seoane J, Lagna G, Montalvo E, Hemmati-Brivanlou A, Massagué J. 2000. OAZ uses distinct DNA- and protein-binding zinc fingers in separate BMP-Smad and Olf signaling pathways. Cell 100:229–240.

Heldin C-H, Miyazono K, ten Dijke P. 1997. TGF-β signalling from cell membrane to nucleus through SMAD proteins. Nature 390:465–471.

Howe JR, Roth S, Ringold JC, Summers RW, Jarvinen HJ, Sistonen P, Tomlinson IP, Houlston RS, Bevan S, Mitros FA, Stone EM, Aaltonen LA. 1998. Mutations in the SMAD4/DPC4 gene in juvenile polyposis. Science 280:1086–1088.

Hua X, Miller ZA, Wu G, Shi Y, Lodish HF. 1999. Specificity in transforming growth factor β-induced transcription of the plasminogen activator inhibitor-1 gene: interactions of promoter DNA, transcription factor μ E3, and Smad proteins. Proc Natl Acad Sci USA 96:13130–13135.

Ida K, Kitabayashi I, Taki T, Taniwaki M, Noro K, Yamamoto M, Ohki M, Hayashi Y. 1997. Adenoviral E1A-associated protein p300 is involved in acute myeloid leukemia with t(11;22)(q23;q13). Blood 90:4699–4704.

Ishikawa T, Yoshioka H, Ohuchi H, Noji S, Nohno T. 1995. Truncated type II receptor for BMP-4 induces secondary axial structures in *Xenopus* embryos. Biochem Biophys Res Commun 216:26–33.

Ito Y. 1999. Molecular basis of tissue-specific gene expression mediated by the Runt domain transcription factor PEBP2/CBF. Genes Cells 4:685–696.

Itoh S, Ericsson J, Nishikawa J, Heldin C-H, ten Dijke P. 2000. The transcriptional co-activator P/CAF potentiates TGF-β/Smad signaling. Nucleic Acids Res 28:4291–4298.

Izumoto S, Arita N, Ohnishi T, Hiraga S, Taki T, Tomita N, Ohue M, Hayakawa T. 1997. Microsatellite instability and mutated type II transforming growth factor-β receptor gene in gliomas. Cancer Lett 112:251–256.

Jakubowiak A, Pouponnot C, Berguido F, Frank R, Mao S, Massagué J, Nimer SD. 2000. Inhibition of the transforming growth factor β1 signaling pathway by the AML1/ETO leukemia-associated fusion protein. J Biol Chem 275:40282–40287.

Janssens K, Gershoni-Baruch R, Guanabens N, Migone N, Ralston S, Bonduelle M, Lissens W, Van Maldergem L, Vanhoenacker F, Verbruggen L, Van Hul W. 2000. Mutations in the gene encoding the latency-associated peptide of TGF- β1 cause Camurati-Engelmann disease. Nat Genet 26:273–275.

Jiang Y, Liang H, Guo W, Kottickal LV, Nagarajan L. 2000. Differential expression of a novel C-terminally truncated splice form of SMAD5 in hematopoietic stem cells and leukemia. Blood 95:3945–3950.

Johnson DW, Berg JN, Baldwin MA, Gallione CJ, Marondel I, Yoon SJ, Stenzel TT, Speer M, Pericak-Vance MA, Diamond A, Guttmacher AE, Jackson CE, Attisano L, Kucherlapati R, Porteous ME, Marchuk DA. 1996. Mutations in the activin receptor-like kinase 1

gene in hereditary haemorrhagic telangiectasia type 2. Nat Genet 13:189–195.
Kang Y, Reddi AH. 1996. Identification and cloning of a novel type I serine/threonine kinase receptor of the TGF-β/BMP superfamily in rat prostate. Biochem Mol Biol Int 40:993–1001.
Kang SH, Won K, Chung HW, Jong HS, Song YS, Kim SJ, Bang YJ, Kim NK. 1998. Genetic integrity of transforming growth factor β (TGF-β) receptors in cervical carcinoma cell lines: loss of growth sensitivity but conserved transcriptional response to TGF-β. Int J Cancer 77:620–625.
Kardassis D, Pardali K, Zannis VI. 2000. Smad proteins transactivate the human ApoCIII promoter by interacting physically and functionally with hepatocyte nuclear factor 4. J Biol Chem 275:41405–41414.
Kawabata M, Miyazono K. 2000. Bone morphogenetic proteins. In: Canalis E, editor. Skeletal Growth Factors. Philadelphia: Lippincott Williams & Wikins. p 269–290.
Kim IY, Ahn HJ, Zelner DJ, Shaw JW, Lang S, Kato M, Oefelein MG, Miyazono K, Nemeth JA, Kozlowski JM, Lee C. 1996a. Loss of expression of transforming growth factor β type I and type II receptors correlates with tumor grade in human prostate cancer tissues. Clin Cancer Res 2:1255–1261.
Kim IY, Ahn HJ, Zelner DJ, Shaw JW, Sensibar JA, Kim JH, Kato M, Lee C. 1996b. Genetic change in transforming growth factor β (TGF-β) receptor type I gene correlates with insensitivity to TGF-β1 in human prostate cancer cells. Cancer Res 56:44–48.
Kim RH, Wang D, Tsang M, Martin J, Huff C, de Caestecker MP, Parks WT, Meng X, Lechleider RJ, Wang T, Roberts AB. 2000. A novel Smad nuclear interacting protein, SNIP1, suppresses p300-dependent TGF-β signal transduction. Gene Dev 14:1605–1616.
Kimura N, Matsuo R, Shibuya H, Nakashima K, Taga T. 2000. BMP2-induced apoptosis is mediated by activation of the TAK1-p38 kinase pathway that is negatively regulated by Smad6. J Biol Chem 275:17647–17652.
Kinoshita A, Saito T, Tomita H, Makita Y, Yoshida K, Ghadami M, Yamada K, Kondo S, Ikegawa S, Nishimura G, Fukushima Y, Nakagomi T, Saito H, Sugimoto T, Kamegaya M, Hisa K, Murray JC, Taniguchi N, Niikawa N, Yoshiura K-i. 2000. Domain-specific mutations in *TGFB1* result in Camurati-Engelmann disease. Nat Genet 26:19–20.
Knaus PI, Lindemann D, DeCoteau JF, Perlman R, Yankelev H, Hille M, Kadin ME, Lodish HF. 1996. A dominant inhibitory mutant of the type II transforming growth factor β receptor in the malignant progression of a cutaneous T-cell lymphoma. Mol Cell Biol 16:3480–3489.
Kosaki K, Bassi MT, Kosaki R, Lewin M, Belmont J, Schauer G, Casey B. 1999. Characterization and mutation analysis of human *LEFTY A* and *LEFTY B*, homologues of murine genes implicated in left-right axis development. Am J Hum Genet 64:712–721.
Kosaki R, Gebbia M, Kosaki K, Lewin M, Bowers P, Towbin JA, Casey B. 1999. Left-right axis malformations associated with mutations in *ACVR2B*, the gene for human activin receptor type IIB. Am J Med Genet 82:70–76.
Kretzschmar M, Doody J, Timokhina I, Massagué J. 1999. A mechanism of repression of TGFβ/Smad signaling by oncogenic Ras. Genes Dev 13:804–816.
Kumar A, Novoselov V, Celeste AJ, Wolfman NM, ten Dijke P, Kuehn MR. 2001. Nodal signaling utilizes activin/TGF-β receptor regulated Smads. J Biol Chem 276:656–661.
Kurokawa M, Mitani K, Irie K, Matsuyama T, Takahashi T, Chiba S, Yazaki Y, Matsumoto K, Hirai H. 1998. The oncoprotein Evi-1 represses TGF-β signalling by inhibiting Smad3. Nature 394:92–96.
Labbé E, Silvestri C, Hoodless PA, Wrana JL, Attisano L. 1998. Smad2 and Smad3 positively and negatively regulate TGFβ-dependent transcription through the forkhead DNA-binding protein FAST2. Mol Cell 2:109–120.
Labbé E, Letamendia A, Attisano L. 2000. Association of Smads with lymphoid enhancer binding factor 1/T cell-specific factor mediates cooperative signaling by the transforming growth factor-β and Wnt pathways. Proc Natl Acad Sci USA 97:8358–8363.
Lane KB, Machado RD, Pauciulo MW, Thomson JR, Philips JA, Loyd JE, Nichols WC, Trembath RC. 2000. Heterozygous germline mutations in *BMPR2*, encoding a TGF-β receptor, cause familial primary pulmonary hypertension. Nat Genet 26:81–84.
Lau AL, Kumar TR, Nishimori K, Bonadio J, Matzuk MM. 2000. Activin βC and βE genes are not essential for mouse liver growth, differentiation, and regeneration. Mol Cell Biol 20:6127–6137.
Lebrun JJ, Vale WW. 1997. Activin and inhibin have antagonistic effects on ligand-dependent heteromerization of the type I and type II activin receptors and human erythroid differentiation. Mol Cell Biol 17:1682–1691.
Lee KS, Kim HJ, Li QL, Chi XZ, Ueta C, Komori T, Wozney JM, Kim EG, Choi JY, Ryoo HM, Bae SC. 2000. Runx2 is a common target of transforming growth factor β1 and bone morphogenetic protein 2, and cooperation between Runx2 and Smad5 induces osteoblast-specific gene expression in the pluripotent mesenchymal precursor cell line C2C12. Mol Cell Biol 20:8783–8792.
Lewis KA, Gray PC, Blount AL, MacConell LA, Wiater E, Bilezikjian LM, Vale W. 2000. Betaglycan binds inhibin and can mediate functional antagonism of activin signalling. Nature 404:411–414.
Li B, Khanna A, Sharma V, Singh T, Suthanthiran M, August P. 1999. TGF-β1 DNA polymorphisms, protein levels, and blood pressure. Hypertension 33:271–275.
Li DY, Sorensen LK, Brooke BS, Urness LD, Davis EC, Taylor DG, Boak BB, Wendel DP. 1999. Defective angiogenesis in mice lacking endoglin. Science 284:1534–1537.
Lin X, Liang M, Feng X-H. 2000. Smurf2 is a ubiquitin E3 ligase mediating proteasome-dependent degradation of Smad2 in TGF-β signaling. J Biol Chem 275:36818–36822.
Liu F, Massagué J, Ruiz i Altaba A. 1998. Carboxy-terminally truncated Gli3 proteins associate with Smads. Nat Genet 20:325–326.
Liu X, Elia AEH, Law SF, Golemis EA, Farley J, Wang T. 2000. A novel ability of Smad3 to regulate proteasomal degradation of a Cas family member HEF1. EMBO J 19:6759–6769.
Lopez-Rovira T, Chalaux E, Rosa JL, Bartrons R, Ventura F. 2000. Interaction and functional cooperation of NFkB with Smads. J Biol Chem 275:28937–28946.
Luo K, Stroschein SL, Wang W, Chen D, Martens E, Zhou S, Zhou Q. 1999. The Ski oncoprotein interacts with the Smad proteins to repress TGFβ signaling. Gene Dev 13:2196–2206.
Luyten FP, Kaplan FS, Shore EM. 2000. Clinical disorders associated with bone morphogenetic proteins In: Canalis E, editor. Skeletal Growth Factors. Philadelphia: Lippincott Williams & Wikins. p 323–334.
MacGrogan D, Pegram M, Slamon D, Bookstein R. 1997. Comparative mutational analysis of DPC4 (Smad4) in prostatic and colorectal carcinomas. Oncogene 15:1111–1114.
Macías-Silva M, Hoodless PA, Tang SJ, Buchwald M, Wrana JL. 1998. Specific activation of Smad1 signaling pathways by the BMP7 type I receptor, ALK2. J Biol Chem 273:25628–25636.
Markowitz S, Wang J, Myeroff L, Parsons R, Sun L, Lutterbaugh J, Fan RS, Zborowska E, Kinzler KW, Vogelstein B, et al. 1995. Inactivation of the type II TGF-β receptor in colon cancer cells with microsatellite instability. Science 268:1336–1338.
Massagué J. 1998. TGF-β signal transduction. Annu Rev Biochem 67:753–791.
Massagué J, Blain SW, Lo RS. 2000. TGFβ signaling in growth control, cancer, and heritable disorders. Cell 103:295–309.
Massagué J, Chen Y-G. 2000. Controlling TGF-β signaling. Genes Dev 14:627–644.
McAllister KA, Grogg KM, Johnson DW, Gallione CJ, Baldwin MA, Jackson CE, Helmbold EA, Markel DS, McKinnon WC, Murrell J. et al. 1994. Endoglin, a TGF-β binding protein of endothelial cells, is the gene for hereditary haemorrhagic telangiectasia type 1. Nat Genet 8:345–351.
McCaffrey TA, Du B, Consigli S, Szabo P, Bray PJ, Hartner L, Weksler BB, Sanborn TA, Bergman G, Bush HL Jr. 1997. Genomic instability in the type II TGF-β1 receptor gene in atherosclerotic and restenotic vascular cells. J Clin Invest 100:2182–2188.
McPherron AC, Lee SJ. 1997. Double muscling in cattle due to mutations in the myostatin gene. Proc Natl Acad Sci USA 94:12457–12461.
McPherron AC, Lawler AM, Lee SJ. 1997. Regulation of skeletal muscle mass in mice by a new TGF-β superfamily member. Nature 387:83–90.
Melhuish TA, Wotton D. 2000. The intraction of the carboxy terminus-binding protein with the Smad corepressor TGIF is disrupted by a holoprosencephaly mutation in TGIF. J Biol Chem 275:39762–39766.
Meno C, Gritsman K, Ohishi S, Ohfuji Y, Heckscher E, Mochida K, Shimono A, Kondoh H, Talbot WS, Robertson EJ, et al. 1999. Mouse Lefty2 and zebrafish antivin are feedback inhibitors of Nodal signaling during vertebrate gastrulation. Mol Cell 4:287–298.
Miura S, Takeshita T, Asao H, Kimura Y, Murata K, Sasaki Y, Hanai J-i, Beppu H, Tsukazaki T, Wrana JL, Miyazono K, Sugamura K. 2000. Hgs (Hrs), a FYVE domain protein, is involved in Smad signaling through cooperation with SARA. Mol Cell Biol 20:9346–9355.

Miyazono K, ten Dijke P, Ichijo H, Heldin C-H. 1994. Receptors for transforming growth factor-β. Adv Immunol 55:181–220.
Miyazono K. 2000. Positive and negative regulation of TGF-β signaling. J Cell Sci 113:1101–1109.
Miyazono K, ten Dijke P, Heldin C-H. 2000. TGF-β signaling by Smad proteins. Adv Immunol 75:115–157.
Miyazono K. 2001. Bone morphogenetic protein receptors and actions. In: Bilezikian JP, Raisz LG, Rodin G, editors. Principles of Bone Biology, 2nd ed: San Diego Academic Press. (in press).
Mulder KM. 2000. Role of Ras and Mapks in TGFβ signaling. Cytokines Growth Factor Rev 11:23–35.
Myeroff LL, Parsons R, Kim SJ, Hedrick L, Cho KR, Orth K, Mathis M, Kinzler KW, Lutterbaugh J, Park K, et al. 1995. A transforming growth factor β receptor type II gene mutation common in colon and gastric but rare in endometrial cancers with microsatellite instability. Cancer Res 55:5545–5547.
Nagatake M, Takagi Y, Osada H, Uchida K, Mitsudomi T, Saji S, Shimokata K, Takahashi T, Takahashi T. 1996. Somatic in vivo alterations of the DPC4 gene at 18q21 in human lung cancers. Cancer Res 56:2718–2720.
Nakamura K, Shirai T, Morishita S, Uchida S, Saeki-Miura K, Makishima F. 1999. p38 mitogen-activated protein kinase functionally contributes to chondrogenesis induced by growth/differentiation factor-5 in ATDC5 cells. Exp Cell Res 250:351–363.
Nakaoka T, Gonda K, Ogita T, Otawara-Hamamoto Y, Okabe F, Harii K, Miyazono K, Takuwa Y, Fujita T. 1997. Inhibition of rat vascular smooth muscle proliferation in vitro and in vivo by bone morphogenetic protein-2. J Clin Invest 100:2824–2832.
Nakashima K, Yanagisawa M, Arakawa H, Kimura N, Hisatsune T, Kawabata M, Miyazono K, Taga T. 1999. Synergistic signaling in fetal brain by STAT3-Smad1 complex bridged by p300. Science 284:479–482.
Nishihara A, Hanai J-i, Okamoto N, Yanagisawa J, Kato S, Miyazono K, Kawabata M. 1998. Role of p300, a transcriptional coactivator, in signalling of TGF-β. Genes Cells 3:613–623.
Nishihara A, Hanai J-i, Imamura T, Miyazono K, Kawabata M. 1999. E1A inhibits transforming growth factor-β signaling through binding to Smad proteins. J Biol Chem 274:28716–28723.
Nishita M, Hashimoto MK, Ogata S, Laurent MN, Ueno N, Shibuya H, Cho KWY. 2000. Interaction between Wnt and TGF-β signalling pathways during formation of Spemann's organizer. Nature 403:781–785.
Nishitoh H, Ichijo H, Kimura M, Matsumoto T, Makishima F, Yamaguchi A, Yamashita H, Enomoto S, Miyazono K. 1996. Identification of type I and type II serine/threonine kinase receptors for growth/differentiation factor-5. J Biol Chem 271:21345–21352.
Nishizuka S, Tamura G, Maesawa C, Sakata K, Suzuki Y, Iwaya T, Terashima M, Saito K, Satodate R. 1997. Analysis of the DPC4 gene in gastric carcinoma. Jpn J Cancer Res 88:335–339.
Nomura M, Li E. 1998. Smad2 role in mesoderm formation, left-right patterning and craniofacial development. Nature 393:786–790.
Nucifora G, Begy CR, Kobayashi H, Roulston D, Claxton D, Pedersen-Bjergaard J, Parganas E, Ihle JN, Rowley JD. 1994. Consistent intergenic splicing and production of multiple transcripts between AML1 at 21q22 and unrelated genes at 3q26 in (3;21)(q26;q22) translocations. Proc Natl Acad Sci USA 91:4004–4008.
Oh SP, Seki T, Goss KA, Imamura T, Yi Y, Donahoe PK, Li L, Miyazono K, ten Dijke P, Kim S, Li E. 2000. Activin receptor-like kinase 1 modulates transforming growth factor-β1 signaling in the regulation of angiogenesis. Proc Natl Acad Sci USA 97:2626–2631.
Onichtchouk D, Chen YG, Dosch R, Gawantka V, Delius H, Massagué J, Niehrs C. 1999. Silencing of TGF-β signalling by the pseudoreceptor BAMBI. Nature 401:480–485.
Pardali E, Xie XQ, Tsapogas P, Itoh S, Arvanitidis K, Heldin C-H, ten Dijke P, Grundstrom T, Sideras P. 2000. Smad and AML proteins synergistically confer transforming growth factor β1 responsiveness to human germ-line IgA genes. J Biol Chem 275:3552–3560.
Pardali K, Kurisaki A, Moren A, ten Dijke P, Kardassis D, Moustakas A. 2000. Role of Smad proteins and transcription factor Sp1 in $p21^{Waf-1/Cip-1}$. J Biol Chem 275:29244–29256.
Pece-Barbara N, Cymerman U, Vera S, Marchuk DA, Letarte M. 1999. Expression analysis of four endoglin missense mutations suggests that haploinsufficiency is the predominant mechanism for hereditary hemorrhagic telangiectasia type 1. Hum Mol Genet 8:2171–2181.
Pekarsky Y, Rynditch A, Wieser R, Fonatsch C, Gardiner K. 1997. Activation of a novel gene in 3q21 and identification of intergenic fusion transcripts with ecotropic viral insertion site I in leukemia. Cancer Res 57:3914–3919.
Petrij F, Giles RH, Dauwerse HG, Saris JJ, Hennekam RC, Masuno M, Tommerup N, van Ommen GJ, Goodman RH, Peters DJ, et al. 1995. Rubinstein-Taybi syndrome caused by mutations in the transcriptional co-activator CBP. Nature 376:348–351.
Polinkovsky A, Robin NH, Thomas JT, Irons M, Lynn A, Goodman FR, Reardon W, Kant SG, Brunner HG, van der Burgt I, Chitayat D, McGaughran J, Donnai D, Luyten FP, Warman ML. 1997. Mutations in CDMP1 cause autosomal dominant brachydactyly type C. Nat Genet 17:18–19.
Preudhomme C, Warot-Loze D, Roumier C, Grardel-Duflos N, Garand R, Lai JL, Dastugue N, Macintyre E, Denis C, Bauters F, Kerckaert JP, Cosson A, Fenaux P. 2000. High incidence of biallelic point mutations in the runt domain of the AML1/PEBP2αB gene in Mo acute myeloid leukemia and in myeloid malignancies with acquired trisomy 21. Blood 96:2862–2869.
Reddi AH. 1998. Role of morphogenetic proteins in skeletal tissue engineering and regeneration. Nat Biotechnol 16:247–252.
Romana SP, Mauchauffe M, Le Coniat M, Chumakov I, Le Paslier D, Berger R, Bernard OA. 1995. The t(12;21) of acute lymphoblastic leukemia results in a tel-AML1 gene fusion. Blood 85:3662–3670.
Roberts AB, Sporn MB. 1990. The transforming growth factor-βs. In: Sporn MB, Roberts AB, editors. Peptide Growth Factors and Their Receptors part I. Berlin: Springer-Verlag. p 419–472.
Rosenzweig BL, Imamura T, Okadome T, Cox GN, Yamashita H, ten Dijke P, Heldin C-H, Miyazono K. 1995. Cloning and characterization of a human type II receptor for bone morphogenetic proteins. Proc Natl Acad Sci USA 92:7632–7636.
Ryden M, Imamura T, Jornvall H, Belluardo N, Neveu I, Trupp M, Okadome T, ten Dijke P, Ibanez CF. 1996. A novel type I receptor serine-threonine kinase predominantly expressed in the adult central nervous system. J Biol Chem 271:30603–30609.
Sano Y, Harada J, Tashiro S, Gotoh-Mandeville R, Maekawa T, Ishii S. 1999. ATF-2 is a common nuclear target of Smad and TAK1 pathways in transforming growth factor-β signaling. J Biol Chem 274:8949–8957.
Scherer A, Graff JM. 2000. Calmodulin differentially modulates Smad1 and Smad2 signaling. J Biol Chem 275:41430–41438.
Schiemann WP, Pfeifer WM, Levi E, Kadin ME, Lodish HF. 1999. A deletion in the gene for transforming growth factor β type I receptor abolishes growth regulation by transforming growth factor β in a cutaneous T-cell lymphoma. Blood 94:2854–2861.
Schutte M. 1999. DPC4/SMAD4 gene alterations in human cancer, and their functional implications. Ann Oncol 10 (Suppl 4):56–59.
Shen MM, Schier AF. 2000. The EGF-CFC gene family in vertebrate development. Trends Genet 16:303–309.
Shi X, Yang X, Chen D, Chang Z, Cao X. 1999. Smad1 interacts with homeobox DNA-binding proteins in bone morphogenetic protein signaling. J Biol Chem 274:13711–13717.
Shi X, Bai S, Li L, Cao X. 2001. Hoxa-9 represses TGF-β-induced osteopontin gene transcription. J Biol Chem 276:850–885.
Shimizu A, Kato M, Nakao A, Imamura T, ten Dijke P, Heldin C-H, Kawabata M, Shimada S, Miyazono K. 1998. Identification of receptors and Smad proteins involved in activin signaling in a human epidermal keratinocyte cell line. Genes Cells 3:125–134.
Song CZ, Tian X, Gelehrter TD. 1999. Glucocorticoid receptor inhibits transforming growth factor-β signaling by directly targeting the transcriptional activation function of Smad3. Proc Natl Acad Sci USA 96:11776–11781.
Song WJ, Sullivan MG, Legare RD, Hutchings S, Tan X, Kufrin D, Ratajczak J, Resende IC, Haworth C, Hock R, Loh M, Felix C, Roy DC, Busque L, Kurnit D, Willman C, Gewirtz AM, Speck NA, Bushweller JH, Li FP, Gardiner K, Poncz M, Maris JM, Gilliland DG. 1999. Haploinsufficiency of CBFA2 causes familial thrombocytopenia with propensity to develop acute myelogenous leukaemia. Nat Genet 23:166–175.
Stroschein SL, Wang W, Zhou S, Zhou Q, Luo K. 1999. Negative feedback regulation of TGF-β signaling by the SnoN oncoprotein. Science 286:771–774.
Sun Y, Liu X, Ng-Eaton E, Lane WS, Lodish HF, Weinberg RA. 1999a. Interaction of the Ski oncoprotein with Smad3 regulates TGF-β signaling. Mol Cell 4:499–509.
Sun Y, Liu X, Ng-Eaton E, Lodish HF, Weinberg RA. 1999b. SnoN and Ski protooncoproteins are rapidly degraded in response to transforming growth factor-β signaling. Proc Natl Acad Sci USA 96:12442–12447.
Suthanthiran M, Li B, Song JO, Ding R, Sharma VK, Schwartz JE, August P. 2000. Transforming growth factor-β1 hyperexpression in African-American hypertensives: A novel mediator of hyper-

tension and/or target organ damage. Proc Natl Acad Sci USA 97:3479–3484.
Suzukawa K, Kodera T, Shimizu S, Nagasawa T, Asou H, Kamada N, Taniwaki M, Yokota J, Morishita K. 1999. Activation of EVI1 transcripts with chromosomal translocation joining the TCRVβ locus and the EVI1 gene in human acute undifferentiated leukemia cell line (Kasumi-3) with a complex translocation of der(3)t(3;7;8). Leukemia 13:1359–1366.
Takakura S, Okamoto A, Saito M, Yasuhara T, Shinozaki H, Isonishi S, Yoshimura T, Ohtake Y, Ochiai K, Tanaka T. 1999. Allelic imbalance in chromosome band 18q21 and SMAD4 mutations in ovarian cancers. Genes Chromosomes Cancer 24:264–271.
Taki T, Sako M, Tsuchida M, Hayashi Y. 1997. The t(11;16)(q23;p13) translocation in myelodysplastic syndrome fuses the MLL gene to the CBP gene. Blood 89:3945–3950.
Tanaka S, Mori M, Mafune K, Ohno S, Sugimachi K. 2000. A dominant negative mutation of transforming growth factor-β receptor type II gene in microsatellite stable oesophageal carcinoma. Br J Cancer 82:1557–1560.
ten Dijke P, Yamashita H, Sampath TK, Reddi AH, Estevez M, Riddle DL, Ichijo H, Heldin C-H, Miyazono K. 1994. Identification of type I receptors for osteogenic protein-1 and bone morphogenetic protein-4. J Biol Chem 269:16985–16988.
Thisse C, Thisse B. 1999. Antivin, a novel and divergent member of the TGFβ superfamily, negatively regulates mesoderm induction. Development 126:229–240.
Thomas JT, Lin K, Nandedkar M, Camargo M, Cervenka J, Luyten FP. 1996. A human chondrodysplasia due to a mutation in a TGF-β superfamily member. Nat Genet 12:315–317.
Thomas JT, Kilpatrick MW, Lin K, Erlacher L, Lembessis P, Costa T, Tsipouras P, Luyten FP. 1997. Disruption of human limb morphogenesis by a dominant negative mutation in *CDMP1*. Nat Genet 17:58–64.
Thomas M, Langley B, Berry C, Sharma M, Kirk S, Bass J, Kambadur R. 2000. Myostatin, a negative regulator of muscle growth, functions by inhibiting myoblast proliferation. J Biol Chem 275:40235–40243.
Thomson JR, Machado RD, Pauciulo MW, Morgan NV, Humbert M, Elliott GC, Ward K, Yacoub M, Mikhail G, Rogers P, Newman J, Wheeler L, Higenbottam T, Gibbs JS, Egan J, Crozier A, Peacock A, Allcock R, Corris P, Loyd JE, Trembath RC, Nichols WC. 2000. Sporadic primary pulmonary hypertension is associated with germline mutations of the gene encoding BMPR-II, a receptor member of the TGF-β family. J Med Genet 37:741–745.
Togo G, Toda N, Kanai F, Kato N, Shiratori Y, Kishi K, Imazeki F, Makuuchi M, Omata M. 1996. A transforming growth factor β type II receptor gene mutation common in sporadic cecum cancer with microsatellite instability. Cancer Res 56:5620–5623.
Tsuchida K, Sawchenko PE, Nishikawa S, Vale WW. 1996. Molecular cloning of a novel type I receptor serine/threonine kinase for the TGF-β superfamily from rat brain. Mol Cell Neurosci 7:467–478.
Tsukazaki T, Chiang TA, Davison AF, Attisano L, Wrana JL. 1998. SARA, a FYVE domain protein that recruits Smad2 to the TGFβ receptor. Cell 95:779–791.
Uchida K, Nagatake M, Osada H, Yatabe Y, Kondo M, Mitsudomi T, Masuda A, Takahashi T, Takahashi T. 1996. Somatic in vivo alterations of the JV18-1 gene at 18q21 in human lung cancers. Cancer Res 56:5583–5585.
Urano T, Yashiroda H, Muraoka M, Tanaka K, Hosoi T, Inoue S, Ouchi Y, Tanaka K, Toyoshima H. 1999. p57Kip2 is degraded through the proteasome in osteoblasts stimulated to proliferation by transforming growth factor β1. J Biol Chem 274:12197–12200.
Urness LD, Sorensen LK, Li DY. 2000. Arteriovenous malformations in mice lacking activin receptor-like kinase-1. Nat Genet 26:328–331.
Verschueren K, Remacle JE, Collart C, Kraft H, Baker BS, Tylzanowski P, Nelles L, Wuytens G, Su MT, Bodmer R, Smith JC, Huylebroeck D. 1999. SIP1, a novel zinc finger/homeodomain repressor, interacts with Smad proteins and binds to 5'-CACCT sequences in candidate target genes. J Biol Chem 274:20489–20498.
Vincent F, Hagiwara K, Ke Y, Stoner GD, Demetrick DJ, Bennett WP. 1996. Mutation analysis of the transforming growth factor β type II receptor in sporadic human cancers of the pancreas, liver, and breast. Biochem Biophys Res Commun 223:561–564.
Waldrip WR, Bikoff EK, Hoodless PA, Wrana JL, Robertson EJ. 1998. Smad2 signaling in extraembryonic tissues determines anterior-posterior polarity of the early mouse embryo. Cell 92:797–808.
Wang D, Kanuma T, Mizunuma H, Takama F, Ibuki Y, Wake N, Mogi A, Shitara Y, Takenoshita S. 2000. Analysis of specific gene mutations in the transforming growth factor-β signal transduction pathway in human ovarian cancer. Cancer Res 60:4507–4512.
Woodford-Richens K, Williamson J, Bevan S, Young J, Leggett B, Frayling I, Thway Y, Hodgson S, Kim JC, Iwama T, Novelli M, Sheer D, Poulsom R, Wright N, Houlston R, Tomlinson I. 2000. Allelic loss at SMAD4 in polyps from juvenile polyposis patients and use of fluorescence in situ hybridization to demonstrate clonal origin of the epithelium. Cancer Res 60:2477–2482.
Wotton D, Lo RS, Lee S, Massagué J. 1999. A Smad transcriptional corepressor. Cell 97:23–39.
Xiao Z, Liu X, Lodish HF. 2000. Importin β mediates nuclear translocation of Smad3. J Biol Chem 275:23425–23428.
Yagi K, Goto D, Hamamoto T, Takenoshita S, Kato M, Miyazono K. 1999. Alternatively spliced variant of Smad2 lacking exon 3: Comparison with wild-type Smad2 and Smad3. J Biol Chem 274:703–709.
Yahata T, de Caestecker MP, Lechleider RJ, Andriole S, Roberts AB, Isselbacher KJ, Shioda T. 2000. The MSG1 non-DNA-binding transactivator binds to the p300/CBP coactivators, enhancing their functional link to the Smad transcription factors. J Biol Chem 275:8825–8834.
Yakicier MC, Irmak MB, Romano A, Kew M, Ozturk M. 1999. Smad2 and Smad4 gene mutations in hepatocellular carcinoma. Oncogene 18:4879–4883.
Yamada Y, Miyauchi A, Goto J, Takagi Y, Okuizumi H, Kanematsu M, Hase M, Takai H, Harada A, Ikeda K. 1998. Association of a polymorphism of the transforming growth factor-β1 gene with genetic susceptibility to osteoporosis in postmenopausal Japanese women. J Bone Miner Res 13:1569–1576.
Yanagisawa J, Yanagi Y, Masuhiro Y, Suzawa M, Watanabe M, Kashiwagi K, Toriyabe T, Kawabata M, Miyazono K, Kato S. 1999. Convergence of transforming growth factor-β and vitamin D signaling pathways on SMAD transcriptional coactivators. Science 283:1317–1321.
Yang X, Castilla LH, Xu X, Li C, Gotay J, Weinstein M, Liu PP, Deng CX. 1999. Angiogenesis defects and mesenchymal apoptosis in mice lacking SMAD5. Development 126:1571–1580.
Yokota M, Ichihara S, Lin TL, Nakashima N, Yamada Y. 2000. Association of a T29→C polymorphism of the transforming growth factor-β1 gene with genetic susceptibility to myocardial infarction in Japanese. Circulation 101:2783–2787.
Yoshida Y, Tanaka S, Umemori H, Minowa M, Usui M, Ikematsu N, Hosoda E, Imamura T, Kuno J, Yamashita T, Miyazono K, Noda M, Noda T, Yamamoto T. 2000. Negative regulation of BMP/Smad signaling by Tob in osteoblasts. Cell 103:1085–1097.
Zhang Y, Feng X-H, Derynck R. 1998. Smad3 and Smad4 cooperate with c-Jun/c-Fos to mediate TGF-β-induced transcription. Nature 394:909–913.
Zhang Y, Derynck R. 2000. Transcriptional regulation of the transforming growth factor-β-inducible mouse germ line Ig α constant region gene by functional cooperation of Smad, CREB, and AML family members. J Biol Chem 275:16979–16985.
Zhang YW, Yasui N, Ito K, Huang G, Fujii M, Hanai J-i, Nogami H, Ochi T, Miyazono K, Ito Y. 2000. A *RUNX2 / PEBP2αA / CBFA1* mutation displaying impaired transactivation and Smad interaction in cleidocranial dysplasia. Proc Natl Acad Sci USA 97:10549–10554.
Zhou G, Chen Y, Zhou L, Thirunavukkarasu K, Hecht J, Chitayat D, Gelb BD, Pirinen S, Berry SA, Greenberg CR, Karsenty G, Lee B. 1999. CBFA1 mutation analysis and functional correlation with phenotypic variability in cleidocranial dysplasia. Hum Mol Genet 8:2311–2316.
Zhu H, Kavsak P, Abdollah S, Wrana JL, Thomsen GH. 1999. A SMAD ubiquitin ligase targerts the BMP pathway and affects embryonic pattern formation. Nature 400:687–693.